

A MATHEMATICAL MODEL FOR THE ELECTROCHEMICAL IMPEDANCE
RESPONSE OF A CONTINUOUS GLUCOSE SENSOR

By

MING GAO

A DISSERTATION PRESENTED TO THE GRADUATE SCHOOL
OF THE UNIVERSITY OF FLORIDA IN PARTIAL FULFILLMENT
OF THE REQUIREMENTS FOR THE DEGREE OF
DOCTOR OF PHILOSOPHY

UNIVERSITY OF FLORIDA

2020

© 2020 Ming Gao

This dissertation is dedicated to all the people I love in my life.

ACKNOWLEDGMENTS

I sincerely thank my advisor, Prof. Mark Orazem, who has always been supportive and encouraging during my doctoral research at University of Florida. I really appreciate that not only did he guide me in my research with his passion and knowledge, but also he set a role model to me in life. The experience in his research group not only trained me to be a mature chemical engineer, but also cultivated me to be a better person. I will benefit from his guidance for the rest of my life.

I would like to thank my lab mates for all the help and the memories we share during the years. Especially, I would like to thank my undergraduate mentees Sam Keiffer and Emerick Gilliams for their assistance with my research. I would like to thank former group members Morgan Hazelbaker, Arthur Dizon, Christopher Alexander and Katherine Davis for their warm help since I joined group and all the laughter they brought to those years. I would like to thank Chen You and Sam Jacobs for their support and company. Also, my work was supported by Medtronic Diabetes. I would like to thank my collaborators Rui Kong and Andrea Varsavsky from Medtronic Diabetes for their help and support with the project.

I would like to thank Prof. Ben Smith and Anuj Chauhan for the help during my department transfer process, which makes all the happy memories begin. I would like to thank Jennifer and Athéna for their caring about me like family. I would like to thank everyone who has helped me during these years to make my life easier.

My deepest gratitude goes to my parents for their continuous love and support throughout my life. I would like to thank Weihuang for being a partner, my best friend and my biggest supporter. I would like to thank my friends for their companionship and help.

TABLE OF CONTENTS

| | <u>page</u> |
|-----------------------------------------------------------------------------|-------------|
| ACKNOWLEDGMENTS | 4 |
| LIST OF TABLES | 8 |
| LIST OF FIGURES | 9 |
| LIST OF CODES | 13 |
| LIST OF SYMBOLS | 13 |
| ABSTRACT | 15 |
| CHAPTER | |
| 1 INTRODUCTION | 17 |
| 2 BACKGROUND | 20 |
| 2.1 The Continuous Glucose Sensor | 20 |
| 2.1.1 Diabetes | 20 |
| 2.1.2 Development of Glucose Biosensors | 20 |
| 2.1.3 Modeling Glucose Sensors | 22 |
| 2.1.4 The Continuous Glucose Monitor (CGM) | 25 |
| 2.2 Electrochemical Impedance Spectroscopy | 25 |
| 2.2.1 Concepts of Electrochemical Impedance Spectroscopy | 26 |
| 2.2.2 Modeling Electrochemical Impedance Spectroscopy | 27 |
| 2.2.2.1 Phenomenological model | 28 |
| 2.2.2.2 Mechanistic model | 28 |
| 2.2.3 Interpretation of Electrochemical Impedance Spectroscopy | 30 |
| 2.2.3.1 Graphical representation | 31 |
| 2.2.3.2 Error structure | 31 |
| 2.2.3.3 Kramers-Kronig relationship | 32 |
| 2.2.3.4 Measurement model | 32 |
| 2.2.3.5 Regression analysis | 33 |
| 2.2.4 Characteristic Frequency | 33 |
| 2.3 Numerical Methods | 34 |
| 2.3.1 Finite-Difference Method | 34 |
| 2.3.2 BAND Algorithm | 34 |
| 3 MODEL FOR UNBUFFERED CONTINUOUS GLUCOSE SENSOR | 36 |
| 3.1 Chemistry of Continuous Glucose Sensor | 36 |
| 3.1.1 Homogeneous Reactions | 36 |
| 3.1.2 Heterogeneous Reactions | 38 |
| 3.2 Mathematical Development | 39 |

| | | |
|---------|------------------------------------------------------------------------------------------------|----|
| 3.2.1 | Governing Equations | 40 |
| 3.2.2 | Boundary Conditions | 43 |
| 3.2.3 | Calculation of Impedance | 45 |
| 3.2.3.1 | Mathematical calculation of impedance | 45 |
| 3.2.3.2 | Equivalent circuit framework | 47 |
| 3.3 | Simulation Results | 48 |
| 3.3.1 | Polarization Curves | 48 |
| 3.3.2 | Sensor Response on the Mass-Transfer-Limited Plateau | 49 |
| 3.3.3 | Concentration and Reaction Profiles | 49 |
| 4 | MODEL FOR CONTINUOUS GLUCOSE SENSOR IN PHOSPHATE BUFFER | 52 |
| 4.1 | Mathematical Development | 52 |
| 4.1.1 | Governing Equation | 52 |
| 4.1.2 | Boundary Conditions | 53 |
| 4.1.3 | Calculation of Impedance | 55 |
| 4.1.3.1 | Mathematical calculation of impedance | 55 |
| 4.1.3.2 | Boundary conditions | 57 |
| 4.2 | Simulation Results | 57 |
| 5 | MODEL FOR CONTINUOUS GLUCOSE SENSOR IN BICARBONATE BUFFER | 70 |
| 5.1 | Governing Equations | 70 |
| 5.2 | Boundary Conditions | 71 |
| 5.3 | Calculation of Impedance | 73 |
| 5.3.1 | Mathematical Calculation of Impedance | 73 |
| 5.3.2 | Boundary Conditions | 74 |
| 6 | EXPERIMENTS | 76 |
| 6.1 | Experimental Setup | 76 |
| 6.2 | Electrochemical Approach | 76 |
| 6.3 | Experimental Results | 77 |
| 6.3.1 | Regression with Measurement Model | 77 |
| 6.3.2 | Regression with Process Model | 78 |
| 6.3.3 | Accuracy Contour Plot | 79 |
| 7 | DISCUSSION | 86 |
| 7.1 | Parameters | 86 |
| 7.1.1 | Dimension and Mesh | 87 |
| 7.1.2 | Initial Concentration and Diffusion Coefficients | 88 |
| 7.1.3 | Diffusion Coefficients and Partition Coefficients Associated with Film Properties | 90 |
| 7.1.4 | Homogeneous and Heterogeneous Reaction Rate Constants | 90 |
| 7.1.5 | Other Operation Parameters | 91 |

| | | |
|-------------------------------|----------------------------------------------------------------------------------------------------------------|-----|
| 7.2 | Parameters Associated with Sensor Failure Mechanism | 91 |
| 7.2.1 | Parameters Associated with Enzyme Deactivation | 94 |
| 7.2.2 | Parameters Associated with Oxygen Deficiency | 96 |
| 7.2.2.1 | Partial pressure of oxygen | 98 |
| 7.2.2.2 | Partition coefficient of oxygen | 104 |
| 7.2.3 | Parameters Associated with Encapsulation | 106 |
| 7.3 | Parameters Associated with Sensor Design | 107 |
| 7.3.1 | Glucose oxidase layer thickness | 108 |
| 7.3.2 | Glucose limiting membrane thickness | 109 |
| 7.4 | Summary of Influence on Steady-State Profiles and Impedance | 111 |
| 7.5 | The Influence of Hydrogen Peroxide-Oxygen Redox Couple | 114 |
| 7.5.1 | The Influence of $K_{H_2O_2}$ at 0.4 V | 115 |
| 7.5.2 | The Influence of $K_{H_2O_2}$ at 0.2 V | 116 |
| 7.5.3 | The Influence of Oxygen Partition Coefficient at 0.4 V | 121 |
| 8 | CONCLUSIONS | 126 |
| 9 | FUTURE WORK | 128 |
| 9.1 | 2-D or 3-D Models for Continuous Glucose Monitors | 128 |
| 9.2 | Experimental Measurement and Regression Analysis of EIS for Continuous Glucose Monitors | 128 |
| 9.3 | The Influence of Coupled Faradaic and Charging Currents on Electrochemical Impedance Spectroscopy | 129 |
| 9.3.1 | Physical Model | 130 |
| 9.3.2 | Governing Equations | 131 |
| 9.3.3 | Ionic Adsorption at Equilibrium | 133 |
| APPENDIX | | |
| A | CODES FOR UNBUFFERED CONTINUOUS GLUCOSE SENSOR | 136 |
| A.1 | Input File | 136 |
| A.2 | Code for Steady-State Calculation | 139 |
| A.3 | Code for Impedance Calculation | 196 |
| B | MATLAB GRAPHICAL USER INTERFACE | 256 |
| B.1 | Main Console | 256 |
| B.2 | Sub Console for the Specific Model | 257 |
| B.2.1 | Control Panel | 257 |
| B.2.2 | Input Parameters | 260 |
| B.2.3 | Other Functions | 260 |
| REFERENCES | | |
| BIOGRAPHICAL SKETCH | | 267 |

LIST OF TABLES

| <u>Table</u> | | <u>page</u> |
|-----------------------------------------------------------------------------------|--|-------------|
| 2-1 Comparison between Phenomenological Model and Mechanistic Model | | 28 |
| 4-1 Sensor Dimensions | | 57 |
| 4-2 Partation Coefficients | | 58 |
| 4-3 Diffusion Coefficients | | 59 |
| 4-4 Operation Parameters | | 60 |
| 4-5 Inicial Concentration of Species Model With PBS Buffer | | 60 |
| 4-6 Inicial Concentration of Species Model With BBS Buffer | | 61 |
| 4-7 Regression Parameters | | 68 |
| 6-1 Values of Fitting Parameters of Process Model with Wire Properties | | 83 |
| 6-2 Values of Fitting Parameters of Modified Process Model with Wire Properties . | | 85 |
| 7-1 Sensor Dimensions | | 87 |
| 7-2 Initial Concentration of Species | | 89 |
| 7-3 Diffusion Coefficients in Bulk | | 90 |
| 7-4 Partation Coefficients | | 90 |
| 7-5 Diffusion Coefficients in GOx and GLM for PBS Model | | 91 |
| 7-6 Rate Constants | | 92 |
| 7-7 Operation Parameters | | 92 |
| 7-8 Parameters Associated with Sensor Failure Mechanism | | 93 |
| 7-9 Parameters that Influence the Polarization Curve | | 112 |
| 7-10 Parameters that Influence the Oxygen Curve | | 114 |
| 7-11 Parameters that Influence the Impedance Response | | 114 |

LIST OF FIGURES

| <u>Figure</u> | | <u>page</u> |
|------------------------------------------------------------------------------------------------------------------------------------------|--|-------------|
| 2-1 Schematic Representation of Electrochemical Impedance Spectroscopy | | 26 |
| 2-2 Schematic Representation of Input-output Signals | | 27 |
| 2-3 Phenomenological Model of A Single Electrochemical Reaction in Bulk Electrolyte | | 29 |
| 2-4 Phenomenological Model of Coupling of One Electrochemical Reaction and One Homogeneous Reaction with Gerischer Assumptions | | 29 |
| 2-5 Mechanistic Model of Diffusion Through a Porous Film | | 30 |
| 2-6 A schematic representation of the measurement model. | | 33 |
| 2-7 Matrix defining BAND | | 35 |
| 3-1 Schematic presentation of one-dimensional model | | 40 |
| 3-2 Equivalent framework for modeling overall impedance of a glucose sensor with GOx and GLM layers | | 47 |
| 3-3 Simulated impedance response for the circuit presented in Figure 3-2 | | 47 |
| 3-4 Simplified circuit framework for modeling the overall impedance | | 48 |
| 3-5 Polarization Curve of Basic Model | | 49 |
| 3-6 Sensor Response Curve of Basic Model | | 50 |
| 3-7 Steady-State Concentration Profiles of Basic Model | | 51 |
| 4-1 Sensor Response Curves | | 62 |
| 4-2 Steady-State Concentration Profiles and Reaction Rate Distribution | | 64 |
| 4-3 Calculated Diffusion Impedance | | 65 |
| 4-4 Calculated Overall Impedance | | 66 |
| 4-5 Process Model for Regression | | 67 |
| 4-6 Impedance Response with Frequency from 1.6 MHz to 1 mHz | | 69 |
| 6-1 Schematic Representation of Experimental Setup | | 77 |
| 6-2 Regression with the Measurement Model in Nyquist Plot | | 78 |
| 6-3 Electrical Circuit of Process Model | | 78 |
| 6-4 Regression with Process Model in Nyquist Plot | | 79 |

| | | |
|------|-------------------------------------------------------------------------------------------------------------------------------|-----|
| 6-5 | Schematic Representation of Accuracy Contour Plot | 80 |
| 6-6 | Accuracy Contour Plot | 81 |
| 6-7 | Accuracy Contour Plot with 1% Error | 82 |
| 6-8 | Equivalent Circuit of Electrochemical System with Wires for Accuracy Contour Plot | 82 |
| 6-9 | Regression of Impedance Data for Sensor up to GOx Layer with Process Model with Wire Properties | 83 |
| 6-10 | Modified Process Model with Wires Properties | 84 |
| 6-11 | Regression of Impedance Data for Sensor up to GOx Layer with Modified Process Model with Wire Properties | 84 |
| 7-1 | Schematic presentation of one-dimensional model | 88 |
| 7-2 | Schematic presentation of the Parameters in Tissue | 88 |
| 7-3 | Enzyme Response Curve | 95 |
| 7-4 | Steady-State Concentration Profiles and Reaction Rate Distribution with Enzyme Concentration as a Parameter | 97 |
| 7-5 | Diffusion Impedance with Enzyme Concentration as a Parameter | 98 |
| 7-6 | Overall Impedance with Enzyme Concentration as a Parameter | 99 |
| 7-7 | Oxygen Curve | 100 |
| 7-8 | Oxygen Curve at Different Applied Potential | 101 |
| 7-9 | Polarization Curve with Oxygen Partial Pressure as a Parameter | 101 |
| 7-10 | Steady-State Profiles with with Oxygen Partial Pressure as a Parameter | 102 |
| 7-11 | Diffusion Impedance with Oxygen Partial Pressure as a Parameter | 103 |
| 7-12 | Overall Impedance with Oxygen Partial Pressure as a Parameter | 104 |
| 7-13 | Steady-State Concentration Profiles and Reaction Rate Distribution with Oxygen Partition Coefficient as a Parameter | 105 |
| 7-14 | Diffusion Impedance with Partition Coefficient of Oxygen as a Parameter | 106 |
| 7-15 | Overall Impedance with Partition Coefficient of Oxygen as a Parameter | 107 |
| 7-16 | Steady-State Concentration Profiles and Reaction Rate Distribution with Thickness of GOx Layer as a Parameter | 108 |

| | |
|------------------------------------------------------------------------------------------------------------------------|-----|
| 7-17 Diffusion Impedance with Thickness of GOx Layer as a Parameter | 109 |
| 7-18 Overall Impedance with Thickness of GOx Layer as a Parameter | 110 |
| 7-19 Polarization Curve with GLM Thickness as a Parameter | 111 |
| 7-20 Oxygen Curve with GLM Thickness as a Parameter | 112 |
| 7-21 Steady-State Concentration Profiles and Reaction Rate Distribution with GLM Thickness as a Parameter | 113 |
| 7-22 Polarization Curve with $K_{H_2O_2}$ as a Parameter | 115 |
| 7-23 Steady-State Profiles with $K_{H_2O_2}$ as a Parameter | 116 |
| 7-24 Diffusion Impedance with $K_{H_2O_2}$ as a Parameter | 117 |
| 7-25 Overall Impedance with $K_{H_2O_2}$ as a Parameter | 118 |
| 7-26 Steady-State Concentration Profiles and Reaction Rate Distribution | 119 |
| 7-27 Diffusion Impedance with $K_{H_2O_2}$ as a Parameter | 120 |
| 7-28 Overall Impedance with $K_{H_2O_2}$ as a Parameter | 121 |
| 7-29 Steady-State Concentration Profiles and Reaction Rate Distribution | 123 |
| 7-30 Diffusion Impedance with Oxygen Partition Coefficient as a Parameter | 124 |
| 7-31 Overall Impedance with Oxygen Partition Coefficient as a Parameter | 124 |
| 9-1 Schematic Representation of Electrochemical Double Layer | 130 |
| 9-2 Concentration of Adsorbed Ionic Species as a Function of Applied Potential. . . | 134 |
| 9-3 Charge of Species in Diffuse Double Layer as a Function of Applied Potential. . | 135 |
| B-1 The Initial Program Layout of the Graphical User Interface in Matlab®. | 257 |
| B-2 An example of the brief guide of the Basic Model opened by the tab [?]. | 258 |
| B-3 The Layout Of The Program After Clicking the Tab [Model With BBS Buffer]. | 259 |
| B-4 The program layout for a specific model. | 259 |
| B-5 The program layout of changing input parameters. | 260 |

LIST OF CODES

| | <u>page</u> |
|--------------------------------------------------------------------------------------------------|-------------|
| A.1 Input files for the Model of Unbuffered Continuous Glucose Sensor | 137 |
| A.2 FORTRAN Code for Steady-State Calculations of Unbuffered Continuous Glucose Sensor | 140 |
| A.3 Matlab code to create and plot polarization curve | 188 |
| A.4 Matlab code to plot results from steady-state solutions | 190 |
| A.5 Matlab code for Oxygen Curve Calculation | 194 |
| A.6 FORTRAN Code for Impedance Calculations | 197 |
| A.7 Matlab code to plot impedance response from impedance calculations | 249 |

LIST OF SYMBOLS

Roman

| | |
|-----------------------------------|---------------------------------------------------------------------------------------------------------------------------------------------------------|
| b | lumped apparent transfer coefficient, $b = \alpha_a nF/RT$ or $b = \alpha_c nF/RT$, depending on the apparent transfer coefficient α , V^{-1} |
| C_{dl} | double-layer capacitance, F/cm^2 or F ($1 F = 1 C/V$) |
| c_i | volumetric concentration of species i , mol/cm^3 |
| D_i | diffusion coefficient for species i , cm^2/s |
| F | Faraday's constant, $96,487\text{ C/equiv}$ |
| GA | gluconic acid |
| G | glucose including both of α and β anomers |
| GOx _{OX} | glucose oxidase enzyme, oxidized form |
| GOx-H ₂ O ₂ | intermediate complex participating in the second enzymatic regeneration step, in a continuous glucose monitor |
| GOx _{RED} | glucose oxidase enzyme, reduced form |
| GOx-GA | intermediate complex participating in the first enzymatic reaction, in a continuous glucose monitor |
| j | current density, mA/cm^2 |
| k_b | backward rate constant for a chemical reaction, s^{-1} |
| K_{eq} | equilibrium rate constant for a chemical reaction, $K_{eq} = k_f/k_b$ |
| k_f | forward rate constant for a chemical reaction, $cm^3/(mol s)$ or s^{-1} |
| $K_{H_2O_2}$ | heterogeneous rate constant for electrochemical H ₂ O ₂ oxidation reaction, $A\text{ cm/mol}$ |
| K_{O_2} | heterogeneous rate constant for electrochemical O ₂ reduction reaction, $A\text{ cm/mol}$ |
| K_{red} | heterogeneous rate constant for electrochemical H ₂ O ₂ reduction reaction, $A\text{ cm/mol}$ |
| R_e | ohmic resistance, $\Omega\text{ cm}^2$ |
| R_i | homogeneous reaction rate of species i , $mol/cm^3\text{ s}$ |

| | |
|-------|---------------------------------------------------------------------------------------------------------|
| R_t | charge-transfer resistance, $\Omega \text{ cm}^2$ |
| V | electrode potential referenced to a silver/silver-chloride electrode, V |
| V_0 | equilibrium potential for electrochemical reactions referenced to a silver/silver-chloride electrode, V |
| Z | impedance, $\Omega \text{ cm}^2$ |
| Z_D | diffusion impedance, $\Omega \text{ cm}^2$ |
| Z_F | faradaic impedance, $\Omega \text{ cm}^2$ |

Greek

| | |
|-----------------------|-------------------------------------------------------------------------------------------------------|
| $\alpha\text{-}G$ | α -D-glucose |
| $\beta\text{-}G$ | β -D-glucose |
| δ_{GOx} | immobilized enzyme layer thickness, cm |
| γ_i | partition coefficient for species i at the interface between outer bound of GLM and diffusion layer |

General Notation

| | |
|------------------|----------------------------------------------|
| $\text{Im}\{X\}$ | imaginary part of X |
| $\text{Re}\{X\}$ | real part of X |
| \overline{X} | steady-state or time-averaged part of $X(t)$ |

Abstract of Dissertation Presented to the Graduate School
of the University of Florida in Partial Fulfillment of the
Requirements for the Degree of Doctor of Philosophy

A MATHEMATICAL MODEL FOR THE ELECTROCHEMICAL IMPEDANCE
RESPONSE OF A CONTINUOUS GLUCOSE SENSOR

By

Ming Gao

August 2020

Chair: Mark E. Orazem

Major: Chemical Engineering

The continuous glucose sensor is used to measure the glucose concentration in interstitial fluids by means of a glucose oxidase enzyme that converts glucose into hydrogen peroxide, which can be detected electrochemically. A mathematical model was developed for the impedance response of glucose-oxidase based electrochemical biosensors [3]. The homogeneous reactions included anomerization between α -D-glucose and β -D-glucose, four reversible enzymatic catalytic reactions transforming β -D-glucose and oxygen into gluconic acid and hydrogen peroxide, weak acid dissociation equilibrium, two reactions accounting of the pH-dependence of enzymatic activity, and a series of reactions associated with the buffer system. The electroactive hydrogen peroxide was considered to be oxidized or reduced at the electrode. In addition, reduction of oxygen was considered as a potential cathodic reaction. The heterogeneous reactions were coupled by the concentration of hydrogen ions, which appear as reactants for the cathodic reactions and as a product of the anodic reaction. Thus, the faradaic impedances associated with the three heterogeneous reactions could not be considered independent.

The mathematical model was solved numerically by using the finite-difference method and Newman's BAND algorithm [4]. The model demonstrates how the coupled non-linear homogeneous reactions affect the diffusion impedance, which has broadened the scope of the Gerischer impedance. The model can be used to explore the influence of various system parameters on limiting current, reaction profiles, and diffusion impedance. The

system parameters, including interstitial glucose concentration, oxygen concentration, active enzyme concentration, diffusion coefficients, reaction rate constants and layer thickness, are related to various sensor working conditions such as body sugar level, inflammation, sensor degradation and sensor design.

CHAPTER 1 INTRODUCTION

The continuous glucose monitor (CGM) is a device to measure the glucose level in the interstitial fluid in real time. The CGM serves as an artificial pancreas for people with type I diabetes to manage their blood sugar level. The CGM comprises three parts, the continuous glucose sensor embedded under the skin, the transmitter and the computer with built-in insulin pump. The FDA-approved continuous glucose sensor can last about 28 days. But even within the implanted period, the sensor needs to be calibrated frequently with a finger-prick test. Electrochemical impedance spectroscopy (EIS) can be potentially applied for in-vivo sensor calibration, sensor failure analysis, and false reading detection.

The most common type of continuous glucose sensor is the enzyme-based amperometric sensor. Glucose oxidase is the enzyme immobilized in the sensor to oxidize the glucose into gluconic acid. Depending on the type of glucose sensor, the electroactive species can be either oxygen or hydrogen peroxide. While the material and biomedical research has been intensively studied, only a few mathematical models have been developed to study the sensor response at either steady-state or transient conditions. Model development is critical in prediction of the sensor response, optimization of sensor performance, analysis of sensor failure mechanism and design of the sensors. The background of the development of continuous glucose sensor and the mathematical modeling of glucose sensors can be found in Chapter 2.

This dissertation focuses on the research of fundamental electrochemical engineering and its application on glucose sensors. The work involves extensive mathematics and the basic principles of electrochemical thermodynamics, kinetics and mass transfer. It emphasizes the understanding and application of electrochemical impedance spectroscopy (EIS), which is a sensitive surface characterization technique. The fundamental knowledge

of EIS is introduced in Chapter 2. The work involves modeling and numerical simulation, experiments, parametric studies, regression and statistical analysis.

A series of one-dimensional mathematical models for continuous glucose sensors were developed. The modeling began with four simple irreversible enzymatic reactions and one hydrogen peroxide electrochemical oxidation reaction. Enzyme kinetics, complex homogeneous reactions and heterogeneous reactions and mass-transport effects are further developed. A subsequent one-dimensional mathematical model [1] considers two film layers, the GOx layer, where the glucose oxidase enzyme is immobilized, and GLM layer, where the diffusion of species is controlled by the physical properties of the film. Only four enzymatic reactions and the glucose anomerization reaction were considered and the electrochemical reaction was relatively simple. The electrochemical impedance response was calculated.

The present work builds on the preliminary glucose sensor models. Three advanced complex mathematical models are presented in Chapter 3, Chapter 4 and Chapter 5. The models account for the role of hydrogen ions in electrochemical reactions, as activity of the enzyme is very sensitive to pH. Therefore, it is necessary to include the buffering system. The present model is based on ping-pong kinetics and law of mass action instead of using the Michaelis-Menten approximation. The model includes more complicated transport and reaction, including pH-dependent enzyme activity and buffer. Both steady-state and the impedance response are calculated. With the advanced model, the parameters associated with physical properties of the sensor, sensor operation conditions and sensor failure can be explored.

An extensive and systematic parametric study was performed and is discussed in Chapter 7. The steady-state concentration profiles and impedance response associated with different working parameters are calculated and visualized. The simulation facilitates the understanding of sensor response in the failure condition and the interpretation of

impedance response. Based on the understanding, process models were developed and used in regression analysis to extract statistically significant parameter estimates.

Experimental electrochemical measurements were performed with three types of sensor provided by Medtronic Diabetes. The controlled variables included the glucose concentration, hydrogen peroxide concentration, built-in or external reference electrode, stirring condition, and buffering condition. The analysis of the experimental results is shown in Chapter 6.

A detailed suggestion for future work is presented in Chapter 9. Further exploration of the influence of electrode geometry need to be studied by building a multi-dimension model. With better experimental setup, more impedance measurements need to be performed with the glucose sensors. The influence of coupled faradaic and charging currents on electrochemical impedance spectroscopy was studied as a side project. Some preliminary mathematical development and simulation results are presented in Chapter 9.

A sample code of unbuffered continuous glucose sensor is shown in Appendix A. It includes the input file of parameters, FORTRAN code for steady-state and impedance calculations, and Matlab® code for visualisation of simulation results. A Graphical User Interface was written in Matlab® with Fortran executables. The console and function of the program is introduced in detail in Appendix B.

CHAPTER 2 BACKGROUND

2.1 The Continuous Glucose Sensor

Diabetes is a chronic metabolic disease, to which, in 2012, 1.5 million deaths worldwide were directly attributed [2]. Since the treatment requires frequent testing of blood glucose levels, the development of highly sensitive, pain-free, and low-cost glucose biosensors has attracted broad attention over the past five decades. The continuous glucose sensor is an advanced commercially-available device used to help people monitor their glucose level in real time and manage their diabetes.

2.1.1 Diabetes

Diabetes, also called diabetes mellitus, is a chronic metabolic disease, to which 1.5 million of deaths are directly attributed. Diabetes reduces the ability of the body to process sugar (glucose) such that the glucose concentration in the blood is increased, causing hyperglycemia.

There are two types of diabetes, type I and type II. Type II diabetes is more common, and limits the ability of the body to use insulin. Type II diabetes can be prevented or delayed with healthy life style, diet, weight management and active exercise. Unlike Type II diabetes, there is neither treatment nor cure for Type I diabetes. It occurs at any age, in people of any race, and of any shape and size. But Type I diabetes can be managed by testing the blood sugar level and injecting insulin as needed. Since the management requires frequent testing of blood glucose levels, the development of highly sensitive, pain-free and low-cost glucose biosensor has attracted broad attention over the past five decades.

2.1.2 Development of Glucose Biosensors

The research on glucose biosensors was pioneered by Clark and Lyons [3], who raised the concept of biosensors in 1962. Their work was followed by Updike and Hicks [4], who developed the first practical enzyme-based glucose sensor in 1967. Three generations of

glucose biosensors have been developed to date. The first-generation glucose biosensors were amperometric sensors based on the oxygen–hydrogen peroxide pair as a mediator. They either detected the consumption of oxygen by applying a negative potential [4] or monitored the production of hydrogen peroxide by applying a positive potential [5]. The second-generation glucose biosensors demonstrated during 1980s' were based on other mediators, such as ferrocene, ferricyanide, and methylene blue [6–9]. The third-generation glucose biosensors were proposed to be based on direct electron transfer between the enzyme and electrode without toxic mediators [10–13]; however, the mechanism is in dispute [14, 15].

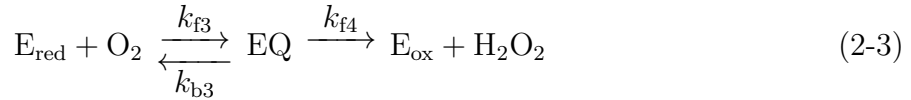
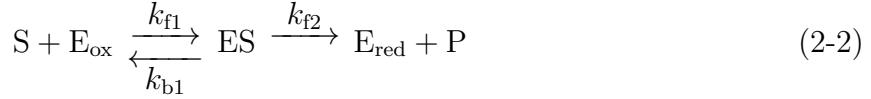
The enzymes hexokinase, glucose oxidase (GOx), and glucose-1-dehydrogenase (GDH) have been used for glucose sensing [16]. The enzyme most commonly used in glucose sensors is glucose oxidase, discovered by Müller [17] from *Aspergillus niger* and *Penicillium glaucum* in 1928. During 1960s to 1970s, a significant effort was expended to understand the physical characteristics and the kinetic mechanism for reactions associated with glucose oxidase. Glucose was found to have higher turnover than other sugars in the presence of glucose oxidase [18]. In addition, glucose oxidase was found to be very specific for β -D-glucose [18]. The α -D-glucose and β -D-glucose anomers are both stable and mutarotate following [19]



The equilibrium constant for reaction (2-1) favors the β -D-glucose anomer.

Nakamura and Ogura [20] and Bright and coworkers [21, 22] believed that glucose is reversibly oxidized by enzymatic reactions to D-gluconolactone, which can hydrolyze spontaneously to gluconic acid. The mechanism for the enzymatic reaction consuming

glucose and oxygen to produce hydrogen peroxide [18, 21–23] was proposed to be

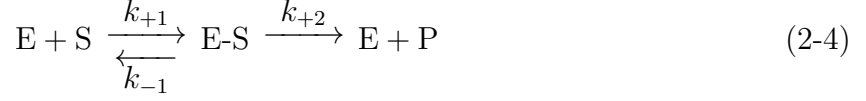


where S is the β -D-glucose substrate, E_{ox} is the oxidized form of glucose oxidase, ES is the first intermediate enzyme complex that is created by glucose and glucose oxidase, E_{red} is the reduced form of glucose oxidase, P is the gluconic acid product, and EQ is the second intermediate enzyme complex.

2.1.3 Modeling Glucose Sensors

Mathematical models have been developed to explore the influence of the complex homogeneous and heterogeneous reactions on sensor response. Bartlett and coworkers [24–27] developed a one-dimensional model for amperometric sensors in which the mechanism for enzymatic reactions was based on the Michaelis-Menten approximation. The assumptions in Michaelis-Menten kinetics are that the substrate concentration is very large and that reactions creating the complexes are equilibrated. Parker and Schwartz [28] showed that the Michaelis-Menten approximation works well only with excess oxygen and argued that, given the low solubility of oxygen in interstitial fluids, assumption of Michaelis-Menten kinetics is not appropriate for a CGM system. Gooding and Hall [29] further developed Parker and Schwartz's steady-state model [28] in which the homogeneous enzymatic reaction followed ping-pong kinetics and the laws of mass action. The electrochemical reduction of oxygen was assumed to be mass-transfer controlled. The mathematical modeling for enzyme-based amperometric glucose started with simplified modeling of general enzyme kinetics. The general enzyme-substrate interaction is Michaelis-Menten kinetics. In this model, the enzyme, E, and the substrate, S, combines reversibly to form the intermediate complex, E-S, which irreversibly decomposes into the

product, P, and the original enzyme, E. The reaction can be expressed as



where k_{+1} is the forward rate constant, k_{-1} is the reverse rate constant and k_{+2} is the catalytic reaction rate constant.

Michaelis and Menten [30] made assumptions of equilibrium approximation as

$$k_{+1}[E][S] = k_{+1}[E-S] \quad (2-5)$$

such that the reaction rate can be expressed as

$$\frac{d[P]}{dt} = \frac{V_{\max}[S]}{K_d + [S]} \quad (2-6)$$

The approximation is further modified by Briggsan and Haldane [31] to quasi-steady-state approximation, as

$$k_{+1}[E][S] = k_{+1}[E-S] + k_{+2}[E-S] \quad (2-7)$$

and the reaction rate becomes

$$\frac{d[P]}{dt} = \frac{V_{\max}[S]}{K_M + [S]} \quad (2-8)$$

where maximum reaction rate is $V_{\max} = k_2[E]_0$ and the Michaelis-Menten constant is $K_M = \frac{k_{-1}+k_2}{k_1}$.

Mell and Maloy [32] simulated the original Michaelis-Menten enzyme kinetics with diffusion through an membrane. The way they treated the enzymatic reaction is very simple. Bartlett and coworkers [24–27] further developed glucose oxidase enzyme kinetics and published a series of work regarding the numerical simulation based on immobilized enzyme layers with coupled diffusion-reaction physics. Leypoldt and Gough [33] modeled the glucose sensor based on detection of oxygen. In this model, two substrates were considered, oxygen and glucose. Based on the same mechanism and kinetics, Gough et al [34] further simulated a two-dimensional cylindrical glucose sensor with both steady-state

and transient simulations. Relatively modern modeling work has been done. Abdekhodaie and Wu [35] reported a theoretical modeling of a glucose-sensitive membrane, where the immobilized enzyme catalyze the glucose into gluconic acid and recycle the oxygen and hydrogen peroxide. They studied the steady state behavior of the membrane considering oxygen limitation and change in diffusivity caused by hydrogel swelling, but with no electrochemical detection.

All these previous works employed Michaelis-Menten kinetics with idealized and simplified assumptions. While the reaction rate expression can be modified to consider the transport phenomenon and oxygen concentration, the assumptions made for Michaelis-Menten kinetics fail in real cases, which makes Michaelis-Menten kinetics inappropriate for continuous glucose sensors. The enzymatic reactions in continuous glucose sensors, first reported by Bright and Gibson [18, 21–23], include two steps, the enzyme catalytic reactions are shown in Equation (2-2) and (2-3).

The enzymatic reactions for glucose oxidase are more complicated, including regeneration of enzyme. They are reversible but not at equilibrium at steady-state. The total amount of active enzyme is not constant and the substrates are not excessive compared with enzyme. The sensor response depends on the limitation of oxygen concentration. Even in the work reported Abdekhodaie and Wu [35], the oxygen concentration is still much more excessive than the real continuous glucose sensor.

Gao et al [1] previously published an one-dimensional mathematical model for continuous glucose sensors. In that model, two film layers were considered, the GOx layer, where the glucose oxidase enzyme is immobilized, and GLM layer, where the diffusion of species is controlled by the physical properties of the film. Only four enzymatic reactions and the glucose anomerization reaction were considered and the electrochemical reaction is relatively simple. The electrochemical impedance response was calculated. To better simulate the real sensor and study the sensor failure mechanism, more considerations were made in the present modeling work. The hydrogen ion is involved in electrochemical

reactions, the concentration distribution of hydrogen ion has a large variance within the sensor. The activity of the enzyme is very sensitive to pH. Therefore, it is necessary to include the buffering system. The present model is based on ping-pong kinetics and law of mass instead of Michaelis-Menten approximation. The model includes more complicated transport and reaction, including pH-dependence enzyme activity and buffer. Considering the mass-transfer of hydrogen ion, the coupled impedance response is calculated. With the advanced model, the parameters associated with physical properties of the sensor, sensor operation conditions and sensor failure can be explored. It will help understand the impedance response as well.

2.1.4 The Continuous Glucose Monitor (CGM)

Continuous glucose monitoring (CGM) can provide real-time testing of glucose levels, which makes it a promising tool for modern diabetes management. Continuous *ex vivo* glucose monitoring was developed in 1974 [36]; whereas, the first subcutaneous implantation was demonstrated by Shichiri in 1982 [37]. Although there were case studies showing that 14-day [38] or 28-day [39] wear periods of a subcutaneous CGM was achievable, commercially available subcutaneous CGM are generally changed every seven days to avoid unreliable results. Some reasons for failure include sensor degradation [40], formation of cell-based metabolic barriers such as macrophages that limit transport of glucose to the sensor [41], and formation of red blood cell clots or other metabolic sinks that consume glucose [42]. As electrochemical impedance spectroscopy is both nondestructive and sensitive to properties affecting electrochemical systems, it has been used to assess the condition of implanted biological sensors [43–45].

2.2 Electrochemical Impedance Spectroscopy

Electrochemical impedance spectroscopy (EIS) is sensitive surface characterization technique for electrochemical systems. It has broad application in studying surface adsorption-desorption, charging, diffusion and complicated electrochemical processes.

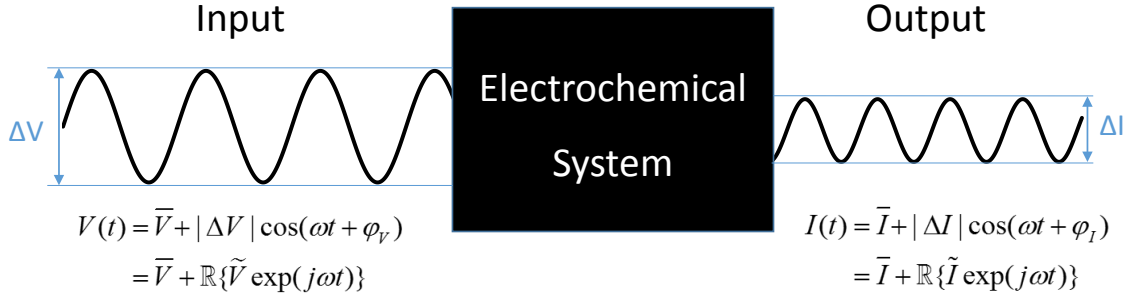


Figure 2-1. Schematic representation of electrochemical impedance spectroscopy (EIS), where a sinusoidal electric potential perturbation is applied to an electrochemical system and the sinusoidal current response is measured.

2.2.1 Concepts of Electrochemical Impedance Spectroscopy

The electrochemical impedance spectroscopy is a transfer function to describe the relationship between input and output signals. According to Figure 2-1, for an unknown electrochemical system, a sinusoidal potential perturbation with frequency ω is applied to the system and the corresponding current response is measured as an output signal. By analyzing the relationship between the input-output perturbations, the impedance can be calculated. Mathematically, the input sinusoidal potential input signal can be expressed as

$$V(t) = \bar{V} + |\Delta V| \cos(\omega t) \quad (2-9)$$

where \bar{V} is the steady-state potential, and $|\Delta V|$ represents the magnitude of the oscillating part of the potential. ω is the frequency at which the perturbation is oscillating. Similarly, the output sinusoidal current signal is shown as

$$I(t) = \bar{I} + |\Delta I| \cos(\omega t + \varphi) \quad (2-10)$$

The output signal can be measured oscillating at the same frequency ω but with a phase lag φ from the input signal. The relationship is represented in Figure 2-2. Alternatively, the input and out signal could be represented using Euler's formula as

$$V(t) = \bar{V} + \text{Re}\{\tilde{V} \exp(j\omega t)\} \quad (2-11)$$

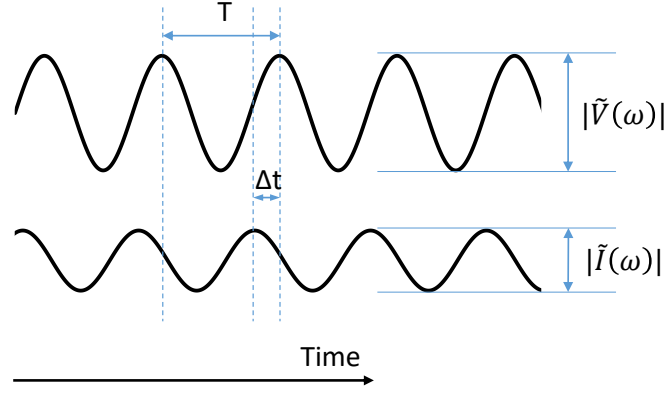


Figure 2-2. Schematic representation of the calculation of the transfer function for a sinusoidal input at frequency ω . The time lag between the two signals is δt and the period of the signals is T .

and

$$I(t) = \bar{I} + \operatorname{Re}\{\tilde{I} \exp(j\omega t)\} \quad (2-12)$$

where \tilde{V} and \tilde{I} are complex quantities that are functions of frequency but are independent of time. The impedance is also a function of frequency, which can be obtained by the relationship of input and output signal $\tilde{V}(\omega)$ and $\tilde{I}(\omega)$.

$$Z(\omega) = \frac{\tilde{V}(\omega)}{\tilde{I}(\omega)} \quad (2-13)$$

The impedance is a complex function, which can be separated into real and imaginary parts

$$Z(\omega) = Z_r(\omega) + jZ_i(\omega) \quad (2-14)$$

2.2.2 Modeling Electrochemical Impedance Spectroscopy

There are two types of model when it comes to modeling the electrochemical impedance spectroscopy. One type of model is phenomenological model, also called process model. The model is proposed based on the hypotheses involving charge transfer, mass transfer and physical phenomena, such as growth of films. These models are expressed in the form of equivalent electrical circuits. The other type of model is mechanistic model. This type of model is more complicated, which needs to consider the electrochemical

reactions, the chemical reactions, the mass transport and physical properties of the electrochemical systems specifically. These models are usually built mathematically with governing equations and solved numerically.

Table 2-1. Comparison between Phenomenological Model and Mechanistic Model

| Phenomenological Model | Mechanistic Model |
|-----------------------------------------------------------------------|------------------------------------------------------------------|
| •Used to fit data | •Used to gain insight into the physical and chemical processes |
| •Help explain existing data | •Requires inclusion of all relevant phenomena |
| •Has fewer parameters | •Has many parameters |
| •Less useful as a predictive tool to guide new designs or experiments | •Useful as a predictive tool to guide new designs or experiments |

2.2.2.1 Phenomenological model

As shown in Table 2-1, the phenomenological models are useful to fit the impedance data based on the understanding of the electrochemical system. It has fewer parameters and usually, these parameters are lumped parameters. The fitting parameters can help explain the data. However, because of the lumped parameters, these models are less useful as predictive tool. Sometimes, multiple phenological models might be able to be applied to the same electrochemical system.

Here are the examples of the phenomenological models for typical electrochemical systems. For an ideal electrochemical system with only one electrochemical reaction happening on the electrode. The electroactive species are sufficient in the bulk solution and they diffuse really fast to the electrode. The equivalent circuit is a charge-transfer resistance (R_t) in parallel with a double-layer capacitance (C_{dl}), which in series with an ohmic resistance of the electrolyte (R_e). By assuming the values of these parameters as $R_t = 10\Omega$, $C_{dl} = 20\mu F$ and $R_e = 10\Omega$, the impedance can be calculated, shown in Nyquist plot in Figure 2.2.2.1.

2.2.2.2 Mechanistic model

As shown in Table 2-1, the mechanistic models are used to gain insight into the consequence of the coupled behavior of physical and chemical processes. To build the

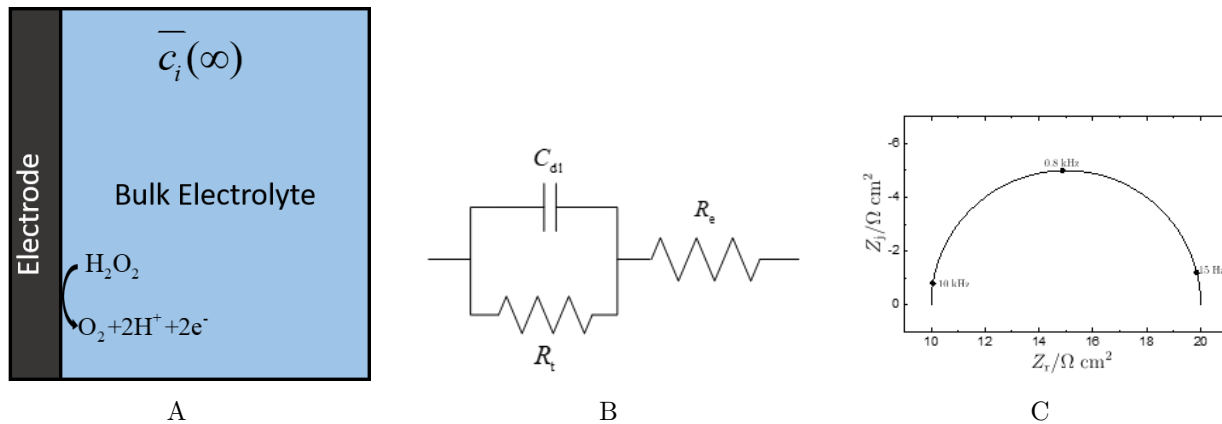


Figure 2-3. Phenomenological model of a single electrochemical reaction in bulk electrolyte. A) Schematic representation of an electrode placed in the bulk electrolyte with sufficient amount of electroactive species H_2O_2 ; B) Equivalent Circuit; C) The Nyquist plot of overall impedance

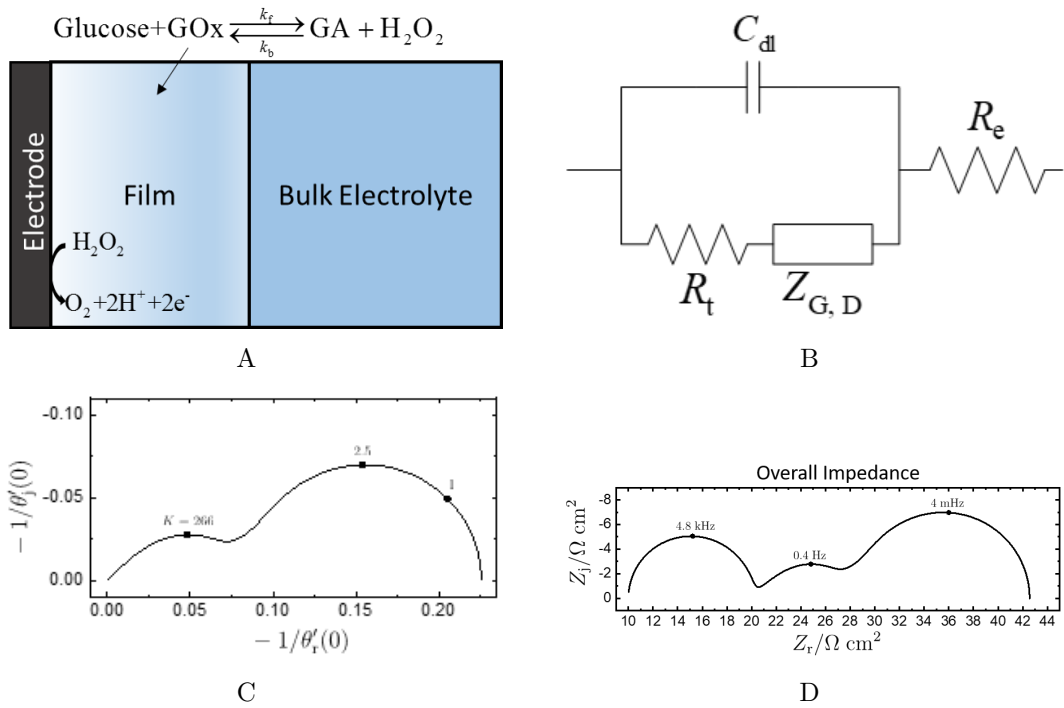


Figure 2-4. Phenomenological model of one electrochemical reaction and one homogeneous reaction with Gerischer assumptions. A) Schematic representation of an electrode placed in the bulk electrolyte with sufficient amount of electroactive species H_2O_2 ; B) Equivalent Circuit; C) The Nyquist plot of overall impedance

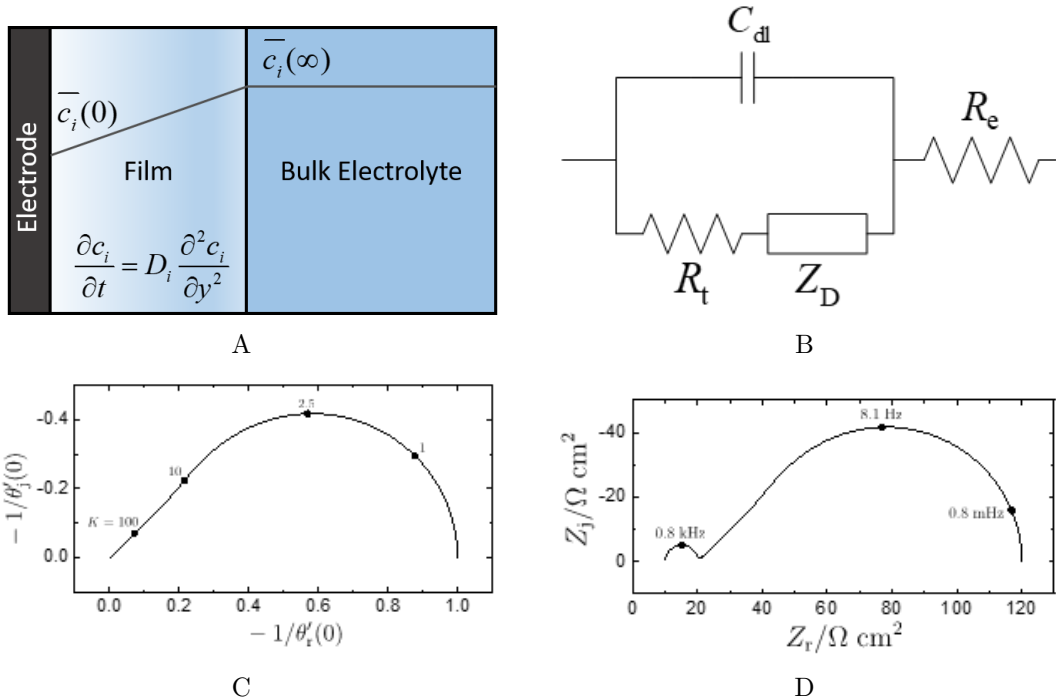


Figure 2-5. Mechanistic model of an electroactive species diffuses from bulk electrolyte through a stagnant film to the electrode. A) Schematic representation of diffusion through a stagnant film. The electroactive species is excessive in the bulk electrolyte; B) Equivalent Circuit; C) The dimensionless diffusion impedance calculated form the mechanistic model; D) The Nyquist plot of overall impedance

mechanistic models, it requires inclusion of all relevant phenomena, such as reactions, transport process, film properties and so on. The models may have many parameters. But the parameters are associated with physical meanings. Therefore, the mechanistic models are useful as a predictive tool to guide new designs or experiments.

2.2.3 Interpretation of Electrochemical Impedance Spectroscopy

To gain useful information from the electrochemical impedance spectroscopy, the impedance data need to be represented into graphical formats and analyzed by mathematical analysis.

2.2.3.1 Graphical representation

Graphical representation of the impedance data is an effective way to visualize and evaluate the data. There are mainly two types of the representation, Nyquist plots and Bode plots.

Nyquist plots The impedance data is usually represented in the Nyquist plots, where the imaginary part of the impedance is plotted versus the real part of the impedance in a complex plane, as shown in Figure 2.2.2.1.

Bode plots Bode plots are the representation of impedance in terms of magnitude and phase angle as functions of frequency on a logarithmic scale. The phase angle is expressed as

$$\varphi = \tan^{-1} \left(\frac{Z_j}{Z_r} \right) \quad (2-15)$$

The modulus of the impedance is

$$|Z| = \sqrt{(Z_r)^2 + (Z_j)^2} \quad (2-16)$$

To get rid of the influence of electrolyte ohmic resistance, the ohmic-resistance corrected phase angle is given by

$$\varphi_{\text{adj}} = \tan^{-1} \left(\frac{Z_j}{Z_r - R_e} \right) \quad (2-17)$$

2.2.3.2 Error structure

The impedance measurements usually consists of two types of errors: stochastic errors and experimental bias errors. The stochastic errors are frequency dependent. They are caused by the integration of time-domain signals that influenced by the noise from instrumental sources or the electrochemical systems. The identification of the stochastic errors is very critical in interpretation and regression analysis of the impedance data. The systematic experimental bias errors arise from the instrumental artifacts or nonstationary behavior. The impedance data with experimental bias errors is not trust-worthy to extrapolate useful information. In most of cases, due to that

the experimental errors caused by instrumental artifacts and nonstationary behavior is inconsistent with Kramers-Kronig relations, the Kramers-Kronig relations can serve as a useful tool to distinguish between stochastic and experimental bias errors. Therefore, to interpret impedance data, the first thing to do is to check the consistency with Kramers-Kronig relations to exclude the data points that flawed by instrumental artifacts and nonstationary behavior. The next thing is to perform fitting and statistical analysis to identify the error structure of the measurements, which can serve as a good weight strategy for the regression.

2.2.3.3 Kramers-Kronig relationship

The Kramers-Kronig relations are mathematical integral equations relates the real and imaginary parts of the complex quantities. The impedance measurements satisfy the Kramers-Kronig relations must be linear, causal, and stable, which means that the system respond linearly to the perturbations, the response do not proceed the perturbations and the perturbation applied to the system do not grow with time. The inconsistency of Kramers-Kronig relations of impedance measurements usually caused by experimental bias error. It serves as criterion to distinguishing between bias and stochastic errors.

2.2.3.4 Measurement model

Measurement model is a tool to apply Kramers-Kronig relations and quantitatively assess the stochastic errors and experimental errors. It is firstly applied to electrochemical impedance by Agarwal et al. [46–48]. The measurement model is a linear superposition of Voigt elements or RC circuits, as represented in Figure 2-6. The impedance of the measurement model can be expressed as

$$Z(\omega) = R_0 + \sum_k^N \frac{R_k}{1_j\omega\tau_k} \quad (2-18)$$

where R_0 , R_k and τ_k are the fitting parameters. The number of fitting parameters depends on the number of Voigt elements included in the regression.

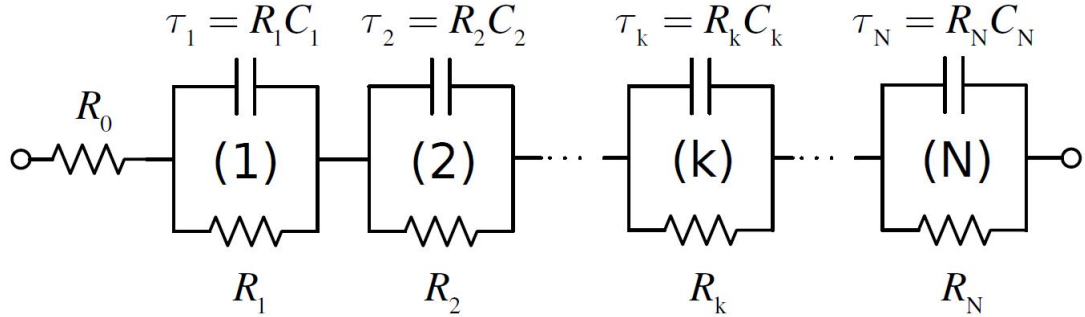


Figure 2-6. A schematic representation of the measurement model.

2.2.3.5 Regression analysis

The impedance data can be evaluated by the regression analysis with process model. The information can be obtained from the fitting procedures are the parameter values, confidence intervals and the statistic measure of the quality of the regression. [49] The regression algorithm used in the present work is Levenberg-Marquardt method.

2.2.4 Characteristic Frequency

For a surface distribution of time constants, the effective double-layer capacitance can be extracted by Brug formula, which is given as

$$C_{\text{eff,surf}} = Q^{1/\alpha} R_e^{(1-\alpha)/\alpha} \quad (2-19)$$

The characteristic frequency is

$$f_\delta = \frac{1}{2\pi (R_e Q)^{1/\alpha}} \quad (2-20)$$

For a normal distribution of time constants due to the growth oxide film, the effective capacitance can be extracted from the (Constant-Phase Elements) CPE values by the Power-Law model, which is given as

$$C_{\text{eff,PL}} = gQ (\rho_\delta \epsilon \epsilon_0)^{1-\alpha} \quad (2-21)$$

The characteristic frequency is

$$f_\delta = \frac{1}{2\pi \rho_\delta \epsilon \epsilon_0} \quad (2-22)$$

2.3 Numerical Methods

The set of coupled nonlinear ordinary differential equations corresponding to the steady-state condition was solved numerically by a finite difference method implemented in the FORTRAN language. The code employed the BAND algorithm developed by Newman,[50] and a Newton–Raphson iterative scheme was employed to achieve quadratic convergence.

2.3.1 Finite-Difference Method

The set of coupled nonlinear ordinary differential equations were linearized by central finite-difference method. The first-order derivative and second-order derivatives can be expressed as

$$\frac{dc}{dy} = \frac{c(y_j + h) - c(y_j - h)}{2h} + \mathcal{O}(h^2) \quad (2-23)$$

and

$$\frac{d^2c}{dy^2} = \frac{c(y_j + h) - 2c(y_j) + c(y_j - h)}{h^2} + \mathcal{O}(h^2) \quad (2-24)$$

where the second-order derivative of c is evaluated at y_j , h is the step size and the accuracy is on the second order of the mesh size.

2.3.2 BAND Algorithm

The numerical technique of solving coupled, non-linear ordinary differential equations is called BAND and presented by Newman. [50]

A set of coupled, second-order non-linear ordinary differential equations can be linearizing using finite-difference method in Equations (2-23) and (2-24), and written in a more general form

$$\sum_{k=1}^n A_{i,k}(J)C_k(J-1) + B_{i,k}(J)C_k(J) + D_{i,k}(J)C_k(J+1) = G_i(j) \quad (2-25)$$

which is evaluated at position x_j . $A_{i,k}(j)$, $B_{i,k}(j)$ and $D_{i,k}(j)$ are the coefficients of equation i and variable c_k at the mesh points x_{j-1} , x_j and x_{j+1} .

$$\begin{bmatrix} B(1) & & & & \\ A(2) & B(2) & D(2) & & \\ \vdots & \vdots & \vdots & & \\ & A(J) & B(J) & D(J) & \\ & & \vdots & \vdots & \vdots \\ & & & & B(NJ) \end{bmatrix} \times \begin{bmatrix} C(1) \\ C(2) \\ \vdots \\ C(J) \\ \vdots \\ C(NJ) \end{bmatrix} = \begin{bmatrix} G(1) \\ G(2) \\ \vdots \\ G(J) \\ \vdots \\ G(NJ) \end{bmatrix}$$

Figure 2-7. Matrix defining BAND.

The boundary condition for the first mesh point, at $J = 1$, can be written

$$\sum_{k=1}^n B_{i,k}(1)C_k(1) = G_i(1) \quad (2-26)$$

and the last mesh point, at $J = NJ$, can be written

$$\sum_{k=1}^n B_{i,k}(NJ)C_k(NJ) = G_i(NJ) \quad (2-27)$$

These governing difference equations, equations (2-25), (2-26), and (2-27), can be written conveniently in matrix form (see Figure 2-7).

By an iterative computation, the variable c_k at all the mesh points can be obtained when they satisfy the convergence criteria.

CHAPTER 3

MODEL FOR UNBUFFERED CONTINUOUS GLUCOSE SENSOR

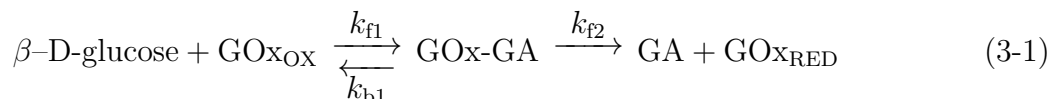
This chapter describes a basic mathematical model for continuous glucose sensor, which includes the enzymatic reactions that convert β -glucose to electroactive hydrogen peroxide, the weak acid dissociation equilibrium and the pH-dependence of the enzyme activity as homogeneous reactions. The electroactive hydrogen peroxide is considered to be both oxidized and reduced at the electrode surface to contribute in either anodic or cathodic current depending on the applied potential. The detailed chemistry of the basic model for continuous glucose sensor is explained. The convective-diffusion governing equation and boundary conditions are shown in detail. The model is calculated at both steady state and oscillating state. The steady-state results show the concentration distributions of species and reaction rate distributions at steady state to help understand the reaction mechanism. The output results are used for oscillating-state model to calculate the phasor of concentrations, which is used for impedance calculation. The mathematical development of impedance is also shown in detail. Some preliminary results are shown and explained from the calculation of the model.

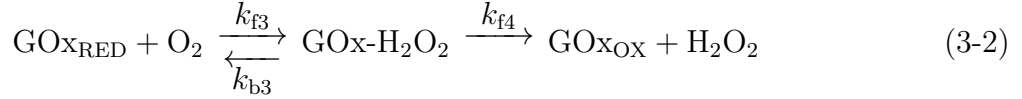
3.1 Chemistry of Continuous Glucose Sensor

The chemistry of continuous glucose sensor contains two parts, the homogeneous reactions and the heterogeneous reactions. The homogeneous reactions are the reactions happening in the electrolyte or in the films of the sensor while the species transport within the sensor. The heterogenous reactions are the electrochemical reactions at the electrode surface. The reactions accounted in the model are explained below.

3.1.1 Homogeneous Reactions

There are four enzymatic reactions to convert β -D-glucose into electro-active hydrogen peroxide following





where GOx_{OX} is the oxidized form of glucose oxidase, GOx-GA is the complex intermediate of the reaction of glucose and GOx_{OX} , GOx_{RED} is the reduced form of glucose oxidase, GA is gluconic acid, and $\text{GOx-H}_2\text{O}_2$ is the complex intermediate of the reaction of GOx_{RED} and oxygen. The glucose oxidase that is reduced by reaction (7-1) is regenerated by reaction (7-2).

In interstitial fluids, D-glucose exists as a mixture of α and β anomers. The anomeration reaction was assumed to follow



To include the pH-dependence of the enzyme activity, the water dissociation, gluconic acid dissociation and the enzyme-complex equilibrium are considered as following,

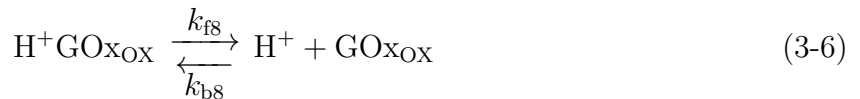


for water dissociation,



for gluconic acid dissociation.

The pH dependence of enzyme activity was treated following Bright and Appleby.[22] The hydrogen ion and oxidized enzyme GOx_{OX} formed an inactive complex species $\text{H}^+\text{GOx}_{\text{OX}}$



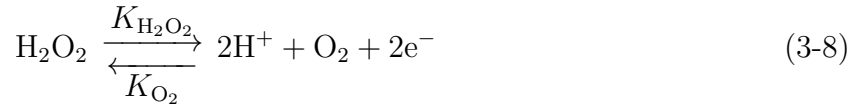
The reduced enzyme GOx_{RED} dissociated hydrogen ion at high pH to form an inactive species GOx_{RED}⁻



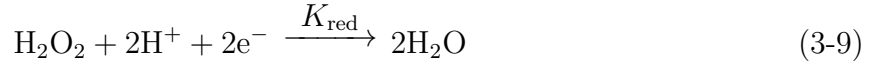
Reaction (3-6) and (3-7) provide for reversible enzyme deactivation at both high and low pH.

3.1.2 Heterogeneous Reactions

Hydrogen peroxide is electro-active and was assumed to be consumed at the electrode. To make the model applicable to a broader potential range, the cathodic oxygen reduction reaction was also considered. The electrochemical reaction was therefore expressed as



The reduction of hydrogen peroxide to water was considered to follow



The current density for the hydrogen peroxide oxidation reaction was expressed as

$$j_{\text{H}_2\text{O}_2} = K_{\text{H}_2\text{O}_2} c_{\text{H}_2\text{O}_2}(0) \exp(b_{\text{H}_2\text{O}_2} V) \quad (3-10)$$

where the concentration $c_{\text{H}_2\text{O}_2}(0)$ is evaluated at the electrode–GOx interface, V represents the electrode potential referenced to a silver/silver-chloride electrode, $b_{\text{H}_2\text{O}_2} = \alpha_{\text{H}_2\text{O}_2} F/RT$, and $\alpha_{\text{H}_2\text{O}_2}$ is the apparent transfer coefficient for the hydrogen peroxide oxidation reaction.

The current density of the oxygen reduction reaction was

$$j_{\text{O}_2} = -K_{\text{O}_2} c_{\text{O}_2}(0) c_{\text{H}}^2(0) \exp(-b_{\text{O}_2} V) \quad (3-11)$$

and the current density of the hydrogen peroxide reduction reaction was

$$j_{\text{red}} = -K_{\text{red}} c_{\text{H}_2\text{O}_2}(0) c_{\text{H}}^2(0) \exp(-b_{\text{red}} V) \quad (3-12)$$

where $b_{O_2} = \alpha_{O_2}F/RT$, $b_{\text{red}} = \alpha_{\text{red}}F/RT$, and α_{O_2} and α_{red} are the apparent transfer coefficients for the oxygen reduction reaction and the hydrogen peroxide reduction reaction, respectively.

The corresponding total faradaic current for all the heterogeneous reactions included was expressed as

$$\begin{aligned} j_F &= K_{H_2O_2}c_{H_2O_2}(0) \exp(b_{H_2O_2}V) \\ &\quad - K_{O_2}c_{O_2}(0)c_H^2(0) \exp(-b_{O_2}V) \\ &\quad - K_{\text{red}}c_{H_2O_2}(0)c_H^2(0) \exp(-b_{\text{red}}V) \end{aligned} \quad (3-13)$$

where $K_{H_2O_2}$, K_{O_2} and K_{red} are the effective heterogeneous rate constants. Following Orazem and Tribollet [49], the effective heterogeneous rate constants incorporated interfacial equilibrium potentials, i.e.,

$$K_{H_2O_2} = nFK_{H_2O_2}^* \exp(-b_{H_2O_2}V_{0,H_2O_2}) \quad (3-14)$$

$$K_{O_2} = nFK_{O_2}^* \exp(b_{O_2}V_{0,O_2}) \quad (3-15)$$

and

$$K_{\text{red}} = nFK_{\text{red}}^* \exp(b_{\text{red}}V_{0,\text{red}}) \quad (3-16)$$

where $K_{H_2O_2}^*$, $K_{O_2}^*$ and K_{red}^* are the intrinsic heterogeneous rate constants and V_{0,H_2O_2} , V_{0,O_2} and $V_{0,\text{red}}$ are the equilibrium potentials corresponding to each heterogeneous reactions respectively. The effective rate constants for the peroxide oxidation and reduction reactions were chosen to yield polarization curves that matched current-voltage curves of a commercial glucose sensor.

3.2 Mathematical Development

The glucose sensor is modeled one-dimensionally as shown in Figure 7-1. The mesh size was refined in regions in which homogeneous reactions led to large concentration derivatives. A subroutine was developed that coupled regions of differing mesh size while

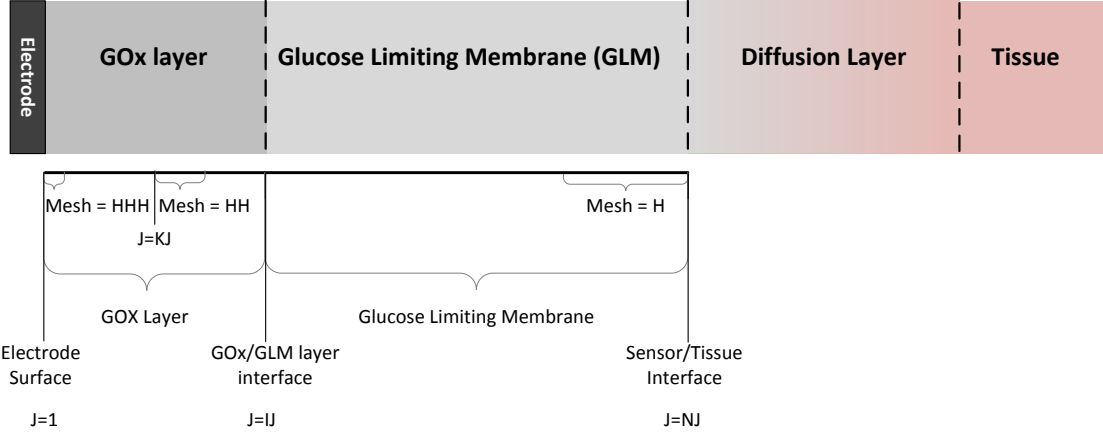


Figure 3-1. One-dimensional schematic representation of the glucose sensor showing three dissimilar mesh sizes. The finest mesh size HHH is near the electrode surface ($J = 1$), a slightly larger mesh size HH was used in the remainder of the GOx layer, and the coarsest mesh size H was used in the GLM layer. The GOx–GLM interface was located at $J = IJ$, and the outer limit of the GLM layer was located at $J = NJ$. There is a diffusion layer at the outer bound of GLM layer in the tissue.

maintaining finite difference accuracy on the order of the square of the mesh size. The same approach was used to solve the set of coupled linear ordinary differential equations corresponding to the impedance calculations.

3.2.1 Governing Equations

The general conservation equation for each species was expressed in the form

$$\frac{\partial c_i}{\partial t} = D_i \frac{\partial^2 c_i}{\partial y^2} + R_i \quad (3-17)$$

where R_i is the reaction rate of generation of species i by homogeneous reactions, D_i is the effective diffusion coefficient of species i in corresponding layer.

According to the homogeneous reactions, the reaction rates can be expressed out following the laws of mass action.

The rates of homogeneous reactions (7-1), (7-2) and (3-3) were expressed as

$$R_1 = k_{f1} c_{\beta-G}(y) c_{GOx_OX}(y) - k_{b1} c_{GOx-GA}(y) \quad (3-18)$$

for the reversible production of the complex intermediate GOx-GA by the reaction of the β -D-glucose anomer and the oxidized form of glucose oxidase,

$$R_2 = k_{f2} c_{\text{GOx-GA}}(y) \quad (3-19)$$

for the irreversible conversion of the intermediate GOx-GA to gluconic acid and the reduced form of glucose oxidase,

$$R_3 = k_{f3} c_{\text{O}_2}(y) c_{\text{GOx-RED}}(y) - k_{b3} c_{\text{GOx-H}_2\text{O}_2}(y) \quad (3-20)$$

for the reversible production of the complex intermediate GOx-H₂O₂ by the reaction of dissolved oxygen and the reduced form of glucose oxidase,

$$R_4 = k_{f4} c_{\text{GOx-H}_2\text{O}_2}(y) \quad (3-21)$$

for the irreversible conversion of the intermediate GOx-H₂O₂ to hydrogen peroxide and the oxidized form of glucose oxidase, and

$$R_5 = k_{f5} c_{\alpha\text{-G}}(y) - k_{b5} c_{\beta\text{-G}}(y) \quad (3-22)$$

for the inter-conversion between α and β anomers of D-glucose.

The reaction rates of homogeneous reactions accounting pH-dependence of enzyme activity (3-4),(3-5),(3-6) and (3-7) were assumed much faster than other reactions. Therefore, the water dissociation, gluconic acid dissociation, the complex between H⁺, OH⁻ and enzymes were assumed equilibrated. For the models including biological buffer systems, the reactions involving dissociation of buffer species were also assumed equilibrated.

For the model without buffer, the corresponding conservation equation for each species was written as

$$\frac{\partial c_{\beta\text{-G}}}{\partial t} = D_{\beta\text{-G}} \frac{\partial^2 c_{\beta\text{-G}}}{\partial y^2} - R_1 + R_5 \quad (3-23)$$

for β -D-glucose (β -G),

$$\frac{\partial c_{GA}}{\partial t} = D_{GA} \frac{\partial^2 c_{GA}}{\partial y^2} + R_2 - R_7 \quad (3-24)$$

for the gluconic acid (GA) product,

$$\frac{\partial c_{O_2}}{\partial t} = D_{O_2} \frac{\partial^2 c_{O_2}}{\partial y^2} - R_3 \quad (3-25)$$

for oxygen (O_2),

$$\frac{\partial c_{H_2O_2}}{\partial t} = D_{H_2O_2} \frac{\partial^2 c_{H_2O_2}}{\partial y^2} + R_4 \quad (3-26)$$

for hydrogen peroxide (H_2O_2), and

$$\frac{\partial c_{\alpha-G}}{\partial t} = D_{\alpha-G} \frac{\partial^2 c_{\alpha-G}}{\partial y^2} - R_5 \quad (3-27)$$

for α -D-glucose (α -G). The enzymatic species were assumed to be immobilized and to exist only in the GOx layer. The corresponding balances were written as

$$\frac{\partial c_{GOx_{OX}}}{\partial t} = -R_1 + R_4 + R_8 \quad (3-28)$$

for glucose oxidase (GOx_{OX}) in oxidized form,

$$\frac{\partial c_{GOx-GA}}{\partial t} = R_1 - R_2 \quad (3-29)$$

for the first intermediate complex (GOx-GA) formed by oxidation of glucose,

$$\frac{\partial c_{GOx_{RED}}}{\partial t} = -R_3 + R_2 - R_9 \quad (3-30)$$

for reduced glucose oxidase (GOx_{RED}), and

$$\frac{\partial c_{GOx-H_2O_2}}{\partial t} = R_3 - R_4 \quad (3-31)$$

for the second intermediate complex ($\text{GOx-H}_2\text{O}_2$) formed by reaction of oxygen and reduced glucose oxidase. The conservation equations for the species involved in pH-dependence of enzyme activity were expressed as

$$\frac{\partial c_{\text{H}^+}}{\partial t} = D_{\text{H}^+} \frac{\partial^2 c_{\text{H}^+}}{\partial y^2} + R_6 + R_7 + R_8 + R_9 \quad (3-32)$$

for hydrogen ion,

$$\frac{\partial c_{\text{OH}^-}}{\partial t} = D_{\text{OH}^-} \frac{\partial^2 c_{\text{OH}^-}}{\partial y^2} + R_6 \quad (3-33)$$

for hydroxide ion,

$$\frac{\partial c_{\text{A}^-}}{\partial t} = D_{\text{A}^-} \frac{\partial^2 c_{\text{A}^-}}{\partial y^2} + R_7 \quad (3-34)$$

for gluconate ion,

$$\frac{\partial c_{\text{H}^+\text{GOx(ox.)}}}{\partial t} = -R_8 \quad (3-35)$$

for the deactivated enzyme complex ($\text{H}^+\text{GOx(ox.)}$) in oxidized form, and

$$\frac{\partial c_{\text{GOx}^-(\text{red.})}}{\partial t} = R_9 \quad (3-36)$$

for the deactivated enzyme ($\text{GOx}^-(\text{red.})$) in reduced form.

Due to that the reaction rates through R_6 to R_9 were unknown, the conservation equations were added up or subtracted from each other to cancel the terms of reaction rates $R_6 - R_9$.

3.2.2 Boundary Conditions

The boundary conditions at the electrode surface for the species not involved in electrochemical reactions were

$$\left. \frac{\partial c_i}{\partial y} \right|_{y=0} = 0 \quad \text{at} \quad y = 0 \quad (3-37)$$

The boundary conditions at the electrode surface for the electroactive species, hydrogen peroxide and oxygen, were

$$2FD_{H_2O_2} \frac{\partial c_{H_2O_2}}{\partial y} \Big|_{y=0} = j_{H_2O_2} + j_{O_2} - j_{\text{red}} \quad \text{at } y = 0 \quad (3-38)$$

and

$$2FD_{O_2} \frac{\partial c_{O_2}}{\partial y} \Big|_{y=0} = -j_{H_2O_2} - j_{O_2} \quad \text{at } y = 0 \quad (3-39)$$

respectively. Continuity of concentration and flux were assumed to apply at the GOx–GLM interface.

At the interface between GLM layer and tissue, it was assumed that there is a diffusion layer as a stagnant film with layer thickness δ . The flux of the mobile species in the diffusion layer were expressed as

$$N_i = k_i \left(\frac{c_i|_{y=NJ}}{\gamma_i} - c_i(\infty) \right) \quad (3-40)$$

where γ_i is the partition coefficient for each species between the interstitial fluid and the GLM. k_i is the mass-transfer coefficient of species i in the diffusion layer in tissue close to GLM layer. $c_i|_{y=NJ}$ is the concentration of species i at the interface between GLM layer and diffusion layer ($y = NJ$). $c_i(\infty)$ is the bulk concentration of species i in tissue. Therefore, the boundary condition at the interface of GLM layer and diffusion layer ($y = NJ$) is flux balance, which was expressed as

$$-D_{i,GLM} \frac{\partial c_i}{\partial y} \Big|_{y=NJ} = k_i \left(\frac{c_i|_{y=NJ}}{\gamma_i} - c_i(\infty) \right) \quad (3-41)$$

The boundary conditions at the outer limit of GLM for the immobile species, the enzymes and enzyme complexes, as well as the associated reaction rates were

$$c_i = 0 \quad \text{at } y = NJ \quad (3-42)$$

and

$$R_i = 0 \quad \text{at } y = NJ \quad (3-43)$$

respectively.

3.2.3 Calculation of Impedance

The set of governing equations were solved for both the steady-state condition and the frequency domain. Due to the nonlinear expressions for homogeneous reactions, the steady-state set of equations required iterative solution. The set of equations for faradaic impedance response developed in this section involves steady-state concentrations and therefore requires solution of the steady-state equation. The expressions for sensor impedance were obtained following an electrical circuit which provided a framework for the sensor impedance response [1](see Chapter 9 in reference [49]).

3.2.3.1 Mathematical calculation of impedance

Each variable was represented in terms of steady-state and oscillating terms as [49]

$$X_i = \bar{X}_i + \text{Re} \left\{ \tilde{X}_i \exp(j\omega t) \right\} \quad (3-44)$$

Thus, the generic expression (3-17) can be expressed as a complex equation

$$j\omega \tilde{c}_i = \sigma_{i,j} D_i \frac{\partial^2 \tilde{c}_i}{\partial y^2} + \tilde{R}_i \quad (3-45)$$

The real and imaginary parts of equations of the form of equation (3-45) were solved simultaneously.

The faradaic impedance can be expressed in terms of the charge transfer resistance R_t and the diffusion impedance Z_d as

$$Z_F = R_t + Z_d \quad (3-46)$$

Following the general mathematical derivation framework in Orazem and Tribollet[49], the charge transfer resistances can be calculated as

$$\begin{aligned} R_t &= 1/(K_{\text{H}_2\text{O}_2} b_{\text{H}_2\text{O}_2} \bar{c}_{\text{H}_2\text{O}_2}(0) \exp(b_{\text{H}_2\text{O}_2} \bar{V}) \\ &\quad + K_{\text{O}_2} b_{\text{O}_2} \bar{c}_{\text{O}_2}(0) \bar{c}_{\text{H}^+}^2(0) \exp(-b_{\text{O}_2} \bar{V}) \\ &\quad + K_{\text{red}} b_{\text{red}} \bar{c}_{\text{H}_2\text{O}_2}(0) \bar{c}_{\text{H}^+}^2(0) \exp(-b_{\text{red}} \bar{V})) \end{aligned} \quad (3-47)$$

The diffusion impedance can be calculated as

$$\begin{aligned} Z_D &= R_t [K_{\text{H}_2\text{O}_2} \exp(b_{\text{H}_2\text{O}_2} \bar{V}) - K_{\text{red}} \bar{c}_{\text{H}^+}^2(0) \exp(-b_{\text{red}} \bar{V})] \left(\frac{\tilde{c}_{\text{H}_2\text{O}_2}(0)}{\text{FD}_{\text{H}^+} \frac{d\tilde{c}_{\text{H}^+}}{dy} \Big|_{y=0}} \right) \\ &\quad + R_t K_{\text{O}_2} \bar{c}_{\text{H}^+}^2(0) \exp(-b_{\text{O}_2} \bar{V}) \left(-\frac{\tilde{c}_{\text{O}_2}(0)}{\text{FD}_{\text{H}^+} \frac{d\tilde{c}_{\text{H}^+}}{dy} \Big|_{y=0}} \right) \\ &\quad + R_t [2K_{\text{O}_2} \bar{c}_{\text{O}_2}(0) \bar{c}_{\text{H}^+}(0) \exp(-b_{\text{O}_2} \bar{V}) + 2K_{\text{red}} \bar{c}_{\text{H}_2\text{O}_2} \bar{c}_{\text{H}^+}(0) \exp(-b_{\text{red}} \bar{V})] \left(-\frac{\tilde{c}_{\text{H}^+}(0)}{\text{FD}_{\text{H}^+} \frac{d\tilde{c}_{\text{H}^+}}{dy} \Big|_{y=0}} \right) \end{aligned} \quad (3-48)$$

and the dimensionless diffusion impedance expressions for H_2O_2 , O_2 and H^+ are given by

$$\frac{-1}{\theta'_{\text{H}_2\text{O}_2}(K)} = \frac{1}{\delta_{\text{GOx}}} \left(-\frac{\tilde{c}_{\text{H}_2\text{O}_2}(0)}{\frac{d\tilde{c}_{\text{H}_2\text{O}_2}}{dy} \Big|_{y=0}} \right) \quad (3-49)$$

$$\frac{-1}{\theta'_{\text{O}_2}(K)} = \frac{1}{\delta_{\text{GOx}}} \left(-\frac{\tilde{c}_{\text{O}_2}(0)}{\frac{d\tilde{c}_{\text{O}_2}}{dy} \Big|_{y=0}} \right) \quad (3-50)$$

and

$$\frac{-1}{\theta'_{\text{H}^+}(K)} = \frac{1}{\delta_{\text{GOx}}} \left(-\frac{\tilde{c}_{\text{H}^+}(0)}{\frac{d\tilde{c}_{\text{H}^+}}{dy} \Big|_{y=0}} \right) \quad (3-51)$$

respectively, where δ_{GOx} is the GOx layer thickness.

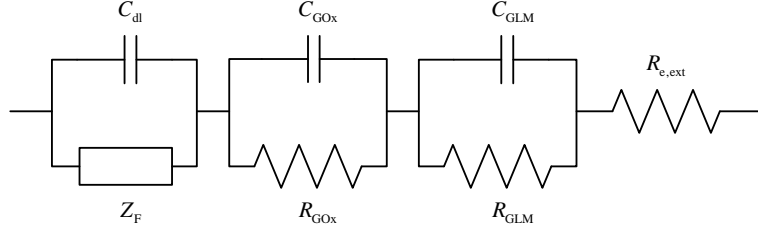


Figure 3-2. Proposed equivalent circuit framework for modeling overall impedance of a glucose sensor with GOx and GLM layers on the electrode surface.

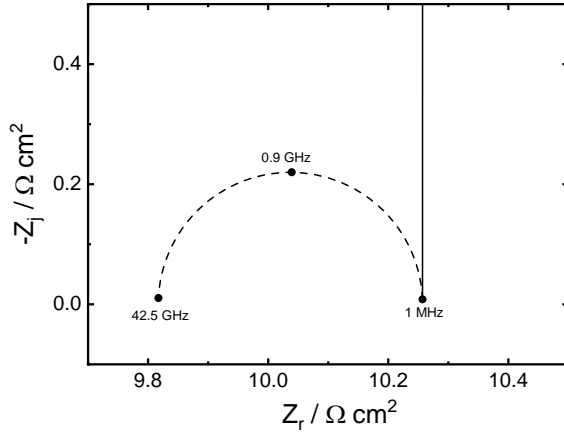


Figure 3-3. Impedance response for the circuit presented in Figure 3-2. The effective ohmic resistance R_e can be expressed as the sum of contributions from the interstitial fluid and the GOx and GLM layers.

3.2.3.2 Equivalent circuit framework

The overall impedance was represented by the proposed equivalent circuit framework shown in Figure 3-2, where the GOx and GLM layers are expected to provide a dielectric response in series with the interfacial impedance and the ohmic resistance of the interstitial fluid. Under the assumptions that the dielectric constant for the GOx and GLM layers has values of 10 and that the corresponding resistivity has value of $200 \Omega \text{ cm}$, the characteristic frequency of the layers would have a value of

$$f_c = \frac{1}{2\pi\varepsilon\varepsilon_0\rho} = 8.5 \text{ GHz} \quad (3-52)$$

which is outside the typical frequency range for impedance measurements. The corresponding impedance response, presented in Figure 3-3, shows that the effective ohmic resistance

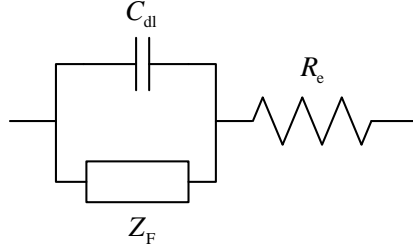


Figure 3-4. Simplified circuit framework for modeling the overall impedance of a glucose sensor in which the contribution of the GOx and GLM layers is represented by an effective ohmic resistance $R_e = R_{e,\text{ext}} + R_{\text{GOx}} + R_{\text{GLM}}$.

for the experimentally observable impedance can be expressed as the sum of contributions from the interstitial fluid and the GOx and GLM layers. Therefore, the circuit framework can be simplified as shown in Figure 3-4. The overall impedance may be expressed as

$$Z(\omega) = R_e + \frac{Z_F(\omega)}{1 + j\omega Z_F(\omega)C_{\text{dl}}} \quad (3-53)$$

where the capacitance was assumed to correspond to the electrode–GOx interface.^[1]

3.3 Simulation Results

The mathematical model generates plots to visualize the steady-state sensor response and impedance response. The steady-state sensor response includes polarization curves, sensor response curves at a specific applied potential, and the corresponding concentration and reaction profiles. The impedance response includes the dimensionless diffusion impedance associated with each heterogeneous reactions, the diffusion impedance and the overall impedance based on the mathematical development.

3.3.1 Polarization Curves

The calculated polarization curve is presented in Figure 3.3.1 with interstitial glucose concentration as a parameter.

The current density increased with increasing applied potential until it reached a diffusion-controlled plateau. This limiting current density for oxidation of hydrogen peroxide was a strong function of total interstitial glucose concentration. The enzyme was assumed to be specific to β -D-glucose and the anomeration reaction between

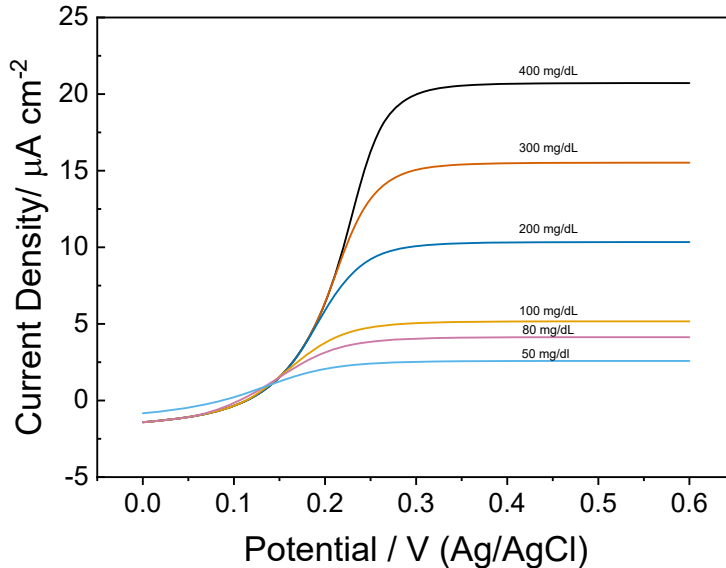


Figure 3-5. Calculated current density as a function of applied potential at an active glucose oxidase concentration of 356 nmol/cm^3 with glucose concentration as a parameter.

α -D-glucose and β -D-glucose was considered in the model. Maximum sensitivity to glucose concentration was found on the mass-transfer-limited plateau.

The mass-transfer-limited plateau is associated with transport of electroactive species to the electrode, where the surface concentration of the reacting species tends toward zero [51]. In the present case, on the anodic plateau, the electroactive species is hydrogen peroxide. Thus, the mass-transfer-limited plateau is associated only indirectly with the concentration of glucose, as the flux of hydrogen peroxide to the electrode surface is related to the interstitial glucose concentration.

3.3.2 Sensor Response on the Mass-Transfer-Limited Plateau

The sensor response curves calculated in the subsequent section were, therefore, obtained at an applied potential on the mass-transfer-limited plateau, shown in Figure 3.3.2.

3.3.3 Concentration and Reaction Profiles

The calculated concentration and reaction profiles are shown in Figure 3-7

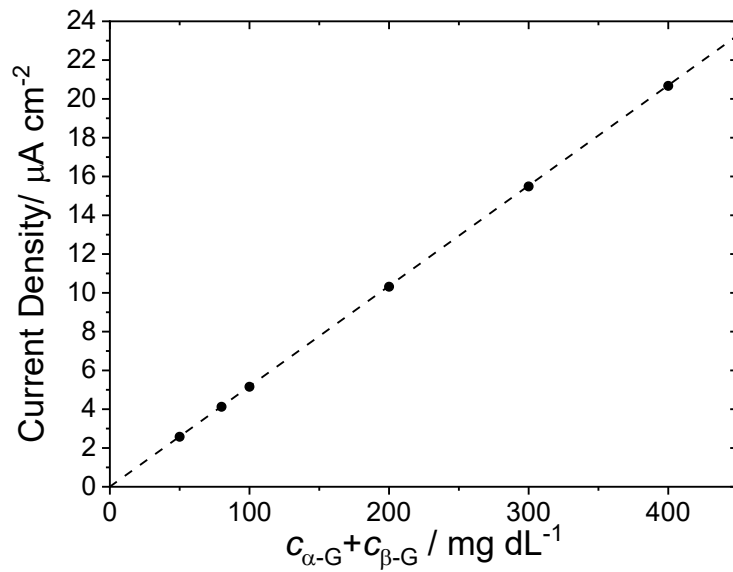


Figure 3-6. Calculated sensor response curve at an active glucose oxidase concentration of 356 nmol/cm³ as a function of total glucose concentration

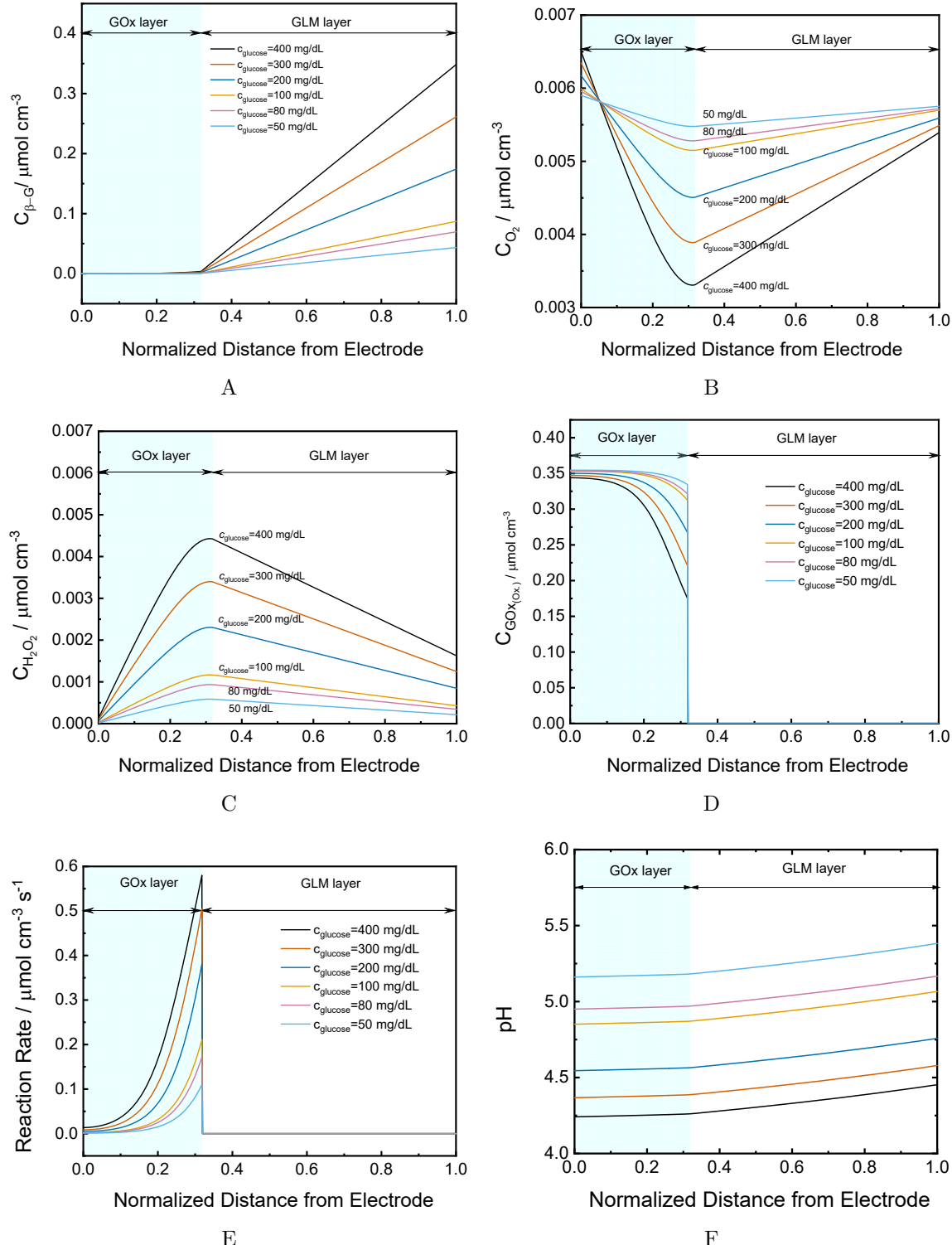


Figure 3-7. Calculated steady-state concentration profiles and reaction rate distribution as a function of distance to the electrode with glucose concentration as a parameter: (a) Beta-glucose concentration profile (b) Oxygen concentration profile (c) Hydrogen peroxide concentration profile (d) Enzymatic reaction rate distribution (e) Oxidized-form glucose oxidase concentration profile (e) pH distribution.

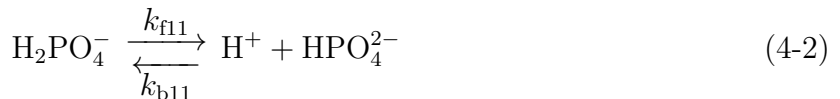
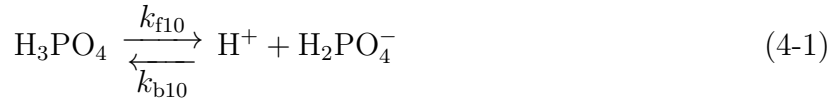
CHAPTER 4

MODEL FOR CONTINUOUS GLUCOSE SENSOR IN PHOSPHATE BUFFER

This chapter introduces the model with Phosphate Buffer Saline (PBS) as the biological buffer to the system. The hydrogen ion is involved in electrochemical reactions, the concentration distribution of hydrogen ion has a large variance within the sensor. The activity of the enzyme is very sensitive to pH. Therefore, it is necessary to include the buffering system. Experimentally, for *in – vito* conditions, the common biological buffer is phosphate buffer saline (PBS). This model provides simulation results for in-vitro experimental conditions.

4.1 Mathematical Development

In PBS, there are mainly 4 ionic species in balance, the phosphate ion PO_4^{3-} , the hydrogen phosphate ion HPO_4^{2-} , the dihydrogen phosphate ion H_2PO_4^- and the trihydrogen phosphate or phosphoric acid H_3PO_4 . More specifically, considering three equilibrium reactions as follow:



4.1.1 Governing Equation

For the model with phosphate buffer saline (PBS), the corresponding conservation equation for each species remained the same as the basic model without buffer, except the conservation equation for hydrogen ion, which was changed to

$$\frac{\partial c_{\text{H}^+}}{\partial t} = D_{\text{H}^+} \frac{\partial^2 c_{\text{H}^+}}{\partial y^2} + R_6 + R_7 + R_8 + R_9 + R_{10} + R_{11} + R_{12} \quad (4-4)$$

There are four major species in phosphate buffer saline (PBS), which are H_3PO_4 , H_2PO_4^- , HPO_4^{2-} and PO_4^{3-} . The conservation equations for these species were

$$\frac{\partial c_{\text{H}_3\text{PO}_4}}{\partial t} = D_{\text{H}_3\text{PO}_4} \frac{\partial^2 c_{\text{H}_3\text{PO}_4}}{\partial y^2} - R_{10} \quad (4-5)$$

for phosphoric acid (H_3PO_4),

$$\frac{\partial c_{\text{H}_2\text{PO}_4^-}}{\partial t} = D_{\text{H}_2\text{PO}_4^-} \frac{\partial^2 c_{\text{H}_2\text{PO}_4^-}}{\partial y^2} + R_{10} - R_{11} \quad (4-6)$$

for dihydrogen phosphate ion (H_2PO_4^-),

$$\frac{\partial c_{\text{HPO}_4^{2-}}}{\partial t} = D_{\text{HPO}_4^{2-}} \frac{\partial^2 c_{\text{HPO}_4^{2-}}}{\partial y^2} + R_{11} - R_{12} \quad (4-7)$$

for hydrogen phosphate ion (HPO_4^{2-}), and

$$\frac{\partial c_{\text{PO}_4^{3-}}}{\partial t} = D_{\text{PO}_4^{3-}} \frac{\partial^2 c_{\text{PO}_4^{3-}}}{\partial y^2} + R_{12} \quad (4-8)$$

for phosphate ion (PO_4^{3-}).

Due to that the reaction rates through R_6 to R_{12} were unknown, the conservation equations were added up or subtracted from each other to cancel the terms of reaction rates $R_6 - R_{12}$.

4.1.2 Boundary Conditions

At the electrode surface, the steady-state boundary conditions for the species not involved in electrochemical reactions are

$$\left. \frac{\partial \bar{c}_i}{\partial y} \right|_{y=0} = 0 \quad \text{at} \quad y = 0 \quad (4-9)$$

The boundary conditions at the electrode surface for the electroactive species are the flux to the electrode is equal to the faradaic current density, respectively. There are 4 electrochemical reactions and 3 electroactive species involved, hydrogen peroxide, oxygen

and hydrogen ion. Specifically, the boundary conditions for hydrogen peroxide is

$$2FD_{H_2O_2} \frac{\partial \bar{c}_{H_2O_2}}{\partial y} \Big|_{y=0} = \bar{j}_{H_2O_2} + \bar{j}_{O_2} - \bar{j}_{red} \quad \text{at } y = 0 \quad (4-10)$$

for oxygen is

$$2FD_{O_2} \frac{\partial \bar{c}_{O_2}}{\partial y} \Big|_{y=0} = -\bar{j}_{H_2O_2} - \bar{j}_{O_2} \quad \text{at } y = 0 \quad (4-11)$$

and for hydrogen ion is

$$FD_H \frac{\partial \bar{c}_H}{\partial y} \Big|_{y=0} = \bar{j}_{H_2O_2} + \bar{j}_{O_2} + \bar{j}_{red} + \bar{j}_{H_2} \quad \text{at } y = 0 \quad (4-12)$$

Continuity of concentration and flux were assumed to apply at the GOx–GLM interface.

At the interface between GLM layer and tissue, it was assumed that there is a diffusion layer as a stagnant film with layer thickness δ . The flux of the mobile species in the diffusion layer were expressed as

$$\bar{N}_i = k_i \left(\frac{\bar{c}_i|_{y=NJ}}{\gamma_i} - \bar{c}_i(\infty) \right) \quad (4-13)$$

where γ_i is the partition coefficient for each species between the interstitial fluid and the GLM. k_i is the mass-transfer coefficient of species i in the diffusion layer in tissue close to GLM layer. $c_i|_{y=NJ}$ is the concentration of species i at the interface between GLM layer and diffusion layer ($y = NJ$). $c_i(\infty)$ is the bulk concentration of species i in tissue. Therefore, the boundary condition at the interface of GLM layer and diffusion layer ($y = NJ$) is flux balance, which was expressed as

$$-D_{i,GLM} \frac{\partial \bar{c}_i}{\partial y} \Big|_{y=NJ} = k_i \left(\frac{\bar{c}_i|_{y=NJ}}{\gamma_i} - \bar{c}_i(\infty) \right) \quad (4-14)$$

The boundary conditions at the outer limit of GLM for the immobile species, the enzymes and enzyme complexes, as well as the associated homogeneous reaction rates were

$$\bar{c}_i = 0 \quad \text{at } y = NJ \quad (4-15)$$

and

$$\bar{R}_i = 0 \quad \text{at} \quad y = NJ \quad (4-16)$$

respectively. The anomeration reaction rate, the homogeneous reaction rates associated with weak acid, and the homogeneous reaction rates associated with buffering species are not zero.

4.1.3 Calculation of Impedance

The set of governing equations are solved for both the steady-state condition and the frequency domain. Due to the nonlinear expressions for homogeneous reactions, the steady-state set of equations required iterative solution. The set of equations for faradaic impedance response developed in this section involves steady-state concentrations and therefore requires solution of the steady-state equation. The expressions for sensor impedance were obtained following an electrical circuit which provided a framework for the sensor impedance response [1](see Chapter 9 in reference [49]).

4.1.3.1 Mathematical calculation of impedance

Under the sinusoidal perturbation, the generic expression (3-17) can be simplified by eliminating the explicit dependence on time and expressed as

$$j\omega \tilde{c}_i = D_i \frac{\partial^2 \tilde{c}_i}{\partial y^2} + \tilde{R}_i \quad (4-17)$$

The real and imaginary parts of equations of the form of equation (4-17) were solved simultaneously.

The faradaic impedance can be expressed in terms of the charge transfer resistance R_t and the diffusion impedance Z_d as

$$Z_F = R_t + Z_d \quad (4-18)$$

Following the general mathematical derivation framework in Orazem and Tribollet[49], the charge transfer resistances can be calculated as

$$\begin{aligned}
R_t &= \left(K_{H_2O_2} b_{H_2O_2} \bar{c}_{H_2O_2}(0) \exp(b_{H_2O_2} \bar{V}) \right. \\
&\quad + K_{O_2} b_{O_2} \bar{c}_{O_2}(0) \bar{c}_{H^+}^2(0) \exp(-b_{O_2} \bar{V}) \\
&\quad + K_{red} b_{red} \bar{c}_{H_2O_2}(0) \bar{c}_{H^+}^2(0) \exp(-b_{red} \bar{V}) \\
&\quad \left. + K_H b_H \bar{c}_{H^+}^2(0) \bar{c}_{H^+}^2(0) \exp(-b_H \bar{V}) \right)^{-1}
\end{aligned} \tag{4-19}$$

The diffusion impedance can be calculated as

$$\begin{aligned}
Z_D &= R_t \left[K_{H_2O_2} \exp(b_{H_2O_2} \bar{V}) - K_{red} \bar{c}_{H^+}^2(0) \exp(-b_{red} \bar{V}) \right] \left(\frac{\bar{c}_{H_2O_2}(0)}{FD_{H^+} \frac{d\bar{c}_{H^+}}{dy} \Big|_{y=0}} \right) \\
&\quad + R_t K_{O_2} \bar{c}_{H^+}^2(0) \exp(-b_{O_2} \bar{V}) \left(-\frac{\bar{c}_{O_2}(0)}{FD_{H^+} \frac{d\bar{c}_{H^+}}{dy} \Big|_{y=0}} \right) \\
&\quad + R_t [2K_{O_2} \bar{c}_{O_2}(0) \bar{c}_{H^+}(0) \exp(-b_{O_2} \bar{V}) + 2K_{red} \bar{c}_{H_2O_2}(0) \bar{c}_{H^+}(0) \exp(-b_{red} \bar{V}) + 2K_H \bar{c}_{H^+}(0) \exp(-b_H \bar{V})] \\
&\quad \left(-\frac{\bar{c}_{H^+}(0)}{FD_{H^+} \frac{d\bar{c}_{H^+}}{dy} \Big|_{y=0}} \right)
\end{aligned} \tag{4-20}$$

and the dimensionless diffusion impedance expressions for H_2O_2 , O_2 and H^+ are given by

$$\frac{-1}{\theta'_{H_2O_2}(K)} = \frac{1}{\delta_{GOx}} \left(-\frac{\bar{c}_{H_2O_2}(0)}{\frac{d\bar{c}_{H_2O_2}}{dy} \Big|_{y=0}} \right) \tag{4-21}$$

$$\frac{-1}{\theta'_{O_2}(K)} = \frac{1}{\delta_{GOx}} \left(-\frac{\bar{c}_{O_2}(0)}{\frac{d\bar{c}_{O_2}}{dy} \Big|_{y=0}} \right) \tag{4-22}$$

and

$$\frac{-1}{\theta'_{H^+}(K)} = \frac{1}{\delta_{GOx}} \left(-\frac{\bar{c}_{H^+}(0)}{\frac{d\bar{c}_{H^+}}{dy} \Big|_{y=0}} \right) \tag{4-23}$$

Table 4-1. Sensor dimensions

| Layers | Thickness |
|-----------------|-------------|
| GOx layer | 10 μm |
| GLM layer | 30 μm |
| Diffusion layer | 100 μm |

respectively, where δ_{GOx} is the GOx layer thickness.

4.1.3.2 Boundary conditions

For the phasor of oscillating concentrations, the boundary conditions far away from the electrode (at $J = NJ$) are

$$\tilde{c}_i = 0 \quad \text{at} \quad y = NJ \quad (4-24)$$

At the electrode, the boundary conditions for the species not involving the electrochemical reactions are

$$\left. \frac{\partial \tilde{c}_i}{\partial y} \right|_{y=0} = 0 \quad \text{at} \quad y = 0 \quad (4-25)$$

for the electroactive species, the boundary condition for hydrogen peroxide is

$$\tilde{c}_{H_2O_2} = 1 \quad \text{at} \quad y = 0 \quad (4-26)$$

and the boundary conditions for hydrogen ion and oxygen are the phasor of the flux is related to the phasor of the current density.

4.2 Simulation Results

The complex mechanism and physical properties of the sensor were considered in the advanced mathematical model. The simulation results show the calculated results based on the provided parameters and illustrates that the impedance response can be potentially utilized to differentiate the cases when the sensors operated under oxygen deficiency and enzyme deactivation conditions can provide false reading same as normal working sensors.

The parameter in the model can be divided into five main categories. The first category of the parameters associated with sensor dimensions as in Table 7-1. The physical properties of the biofilms including the enzyme-immobilized GOx layer and glucose limiting membrane (GLM layer) are associated with the partition coefficients and

Table 4-2. Partation coefficients of species at the interface of diffusion layer and GLM layer of the sensor.

| Species | Partition Coeffients |
|---------------------------------------------|----------------------|
| Glucose, gluconic acid and gluconate ion | 0.014 |
| Hydrogen peroxide | 0.11 |
| Oxygen | 0.32 |
| Hydrogen ion, hydroxide ion and buffer ions | 0.2 |

porosity factors. The partition coefficients of species in GLM layer are listed in Table 7-4. The porosity factors are used for modifying the diffusion coefficients of the species within different layers based on the Bruggeman Equation [52]. The diffusion coefficients of species within each layers are listed in Table 4-3.

Table 4-3. Diffusion coefficients of species in the bulk electrolyte, GOx layer and GLM layer of the sensor.

| Species | $D_{\text{bulk},i} \times 10^5 (\text{cm}^2/\text{s})$ | $D_{\text{GOx},i} \times 10^5 (\text{cm}^2/\text{s})$ | $D_{\text{GLM},i} \times 10^5 (\text{cm}^2/\text{s})$ |
|----------------------------------------------------|--------------------------------------------------------|-------------------------------------------------------|-------------------------------------------------------|
| Glucose, gluconic acid and gluconate ion | 0.72 | 0.576 | 0.122 |
| Glucose oxidase enzyme | 0 | 0 | 0 |
| Oxygen O_2 | 2.46 | 1.97 | 1.03 |
| Hydrogen peroxide H_2O_2 | 1.83 | 0.732 | 1.098 |
| Hydrogen ion H^+ | 9.30 | 7.44 | 3.91 |
| Hydroxide ion OH^- | 5.30 | 4.24 | 2.23 |
| Phosphoric acid H_3PO_4 | 0.90 | 0.180 | 0.378 |
| Dihydrogen phosphate ion H_2PO_4^- | 0.959 | 0.1918 | 0.403 |
| Hydrogen phosphate ion HPO_4^{2-} | 0.759 | 0.1518 | 0.319 |
| Phosphate ion PO_4^{3-} | 0.824 | 0.1648 | 0.346 |
| Carbon dioxide CO_2 | 2.49 | 2.23 | 1.61 |
| Carbonic acid H_2CO_3 | 1.30 | 1.16 | 0.842 |
| Bicarbonate ion HCO_3^- | 1.84 | 1.65 | 1.19 |
| Carbonate ion CO_3^{2-} | 0.92 | 0.823 | 0.596 |

Table 4-4. Sensor operation parameters

| Parameter | Value |
|-------------------------|--------------------------------------------|
| Potential | 0.4 V |
| pH | 7.4 |
| CPE value, Q | 2.61×10^{-5} F/s ^(1-a) |
| CPE value, α | 0.85 |
| Ohmic resistance, R_e | 10 Ω |

Table 4-5. Initial concentrations of species for model with PBS buffer

| Species | $c_{\text{bulk},i}$ or $p_{\text{bulk},i}$ |
|----------------------------------------------------------------------|--------------------------------------------|
| Glucose(both α and β anomers) | varied |
| Glucose oxidase enzyme (maximum) | 3.56×10^{-7} molcm ⁻³ |
| Oxygen O ₂ (partial pressure) | varied |
| Hydrogen peroxide H ₂ O ₂ | 1×10^{-20} molcm ⁻³ |
| Hydrogen ion H ⁺ | calculated based on pH |
| Hydroxide ion OH ⁻ | calculated based on pH |
| Phosphoric acid H ₃ PO ₄ | 3.63×10^{-11} molcm ⁻³ |
| Dihydrogen phosphate ion H ₂ PO ₄ ⁻ | 9.2×10^{-6} molcm ⁻³ |
| Hydrogen phosphate ion HPO ₄ ²⁻ | 4.02×10^{-5} molcm ⁻³ |
| Phosphate ion PO ₄ ³⁻ | 1.86×10^{-9} molcm ⁻³ |

The rate constants of the homogeneous and heterogenous reactions are chosen based on Gao et al. [1] and matching with experimental polarization curves. The sensor operation conditions can vary with parameters including applied potential, pH in the bulk, values of Constant-Phase Element(CPE) and ohmic resistance, listed in Table 7-7 and initial concentrations of the species in Table 4-5 for PBS model and in Table 4-6 for BBS model.

The sensor response curves for a sensor with 10 μm of GOx layer and 30 μm of GLM layer was calculated. The current density is linearly related to the glucose concentration, shown in Figure 4-1A. The normal glucose level in human tissue is around 100 mg/dL. The current density corresponding to 100 mg/dL of glucose in this case is $4.18 \mu A cm^{-2}$. The same current density can be read with higher glucose concentration but with enzyme deactivation and oxygen deficiency. Figure 7-7 shows the current density as function of partial pressure of oxygen with 200 mg/dL of glucose and 100% of enzyme concentration. With oxygen partial pressure decreasing, the current density maintains at a plateau then

Table 4-6. Initial concentrations of species for model with BBS buffer

| Species | $c_{\text{bulk},i}$ or $p_{\text{bulk},i}$ |
|--------------------------------------------|--------------------------------------------|
| Glucose(both α and β anomers) | varied |
| Glucose oxidase enzyme (maximum) | $3.56 \times 10^{-7} \text{ molcm}^{-3}$ |
| Oxygen O_2 (partial pressure) | varied |
| Hydrogen peroxide H_2O_2 | $1 \times 10^{-20} \text{ molcm}^{-3}$ |
| Hydrogen ion H^+ | calculated based on pH |
| Hydroxide ion OH^- | calculated based on pH |
| Carbon dioxide CO_2 (partial pressure) | 5% |
| Carbonic acid H_2CO_3 | $1.68 \times 10^{-9} \text{ molcm}^{-3}$ |
| Bicarbonate ion HCO_3^- | $2.37 \times 10^{-5} \text{ molcm}^{-3}$ |
| Carbonate ion CO_3^{2-} | $1.01 \times 10^{-7} \text{ molcm}^{-3}$ |

slight increases to a peak and then decreases dramatically. The sensor response curve indicates that within the normal range of oxygen partial pressure in tissue, which is 2% \sim 5%, the current density is not limited by the amount of oxygen. However, with further oxygen deficiency, which might be caused by biofouling, the current density is affected by oxygen deficiency. This is one of the case that sensor failure may give false reading. $4.18 \mu A cm^{-2}$ of current density is corresponding to 0.5% of oxygen partial pressure. The other case associated with sensor failure is the enzyme deactivation, shown in Figure 7-3. The current density shows similar trends as function of enzyme concentration with 200 mg/dL of glucose and 5% of oxygen partial pressure. With enzyme activity below 10% of the maximum, the current density decreases with further enzyme deactivation. $4.18 \mu A cm^{-2}$ of current density is corresponding to 3% of maximum enzyme activity. Therefore, the three cases give the same current density.

The steady state profiles can be calculated and help with understanding the reaction mechanism. The concentration distribution of glucose is shown in Figure 4-2A. For the normal glucose level case, 100 mg/dL in the bulk can be consumed completely. However, for the cases of enzyme deactivation and oxygen deficiency with higher glucose level, 200 mg/dL of glucose in the bulk can not be oxidized by the glucose oxidase enzyme within the sensor. That is the reason why the current density appears as the same. The concentration distribution of oxygen and hydrogen peroxide in Figure 4-2B and 4-2C

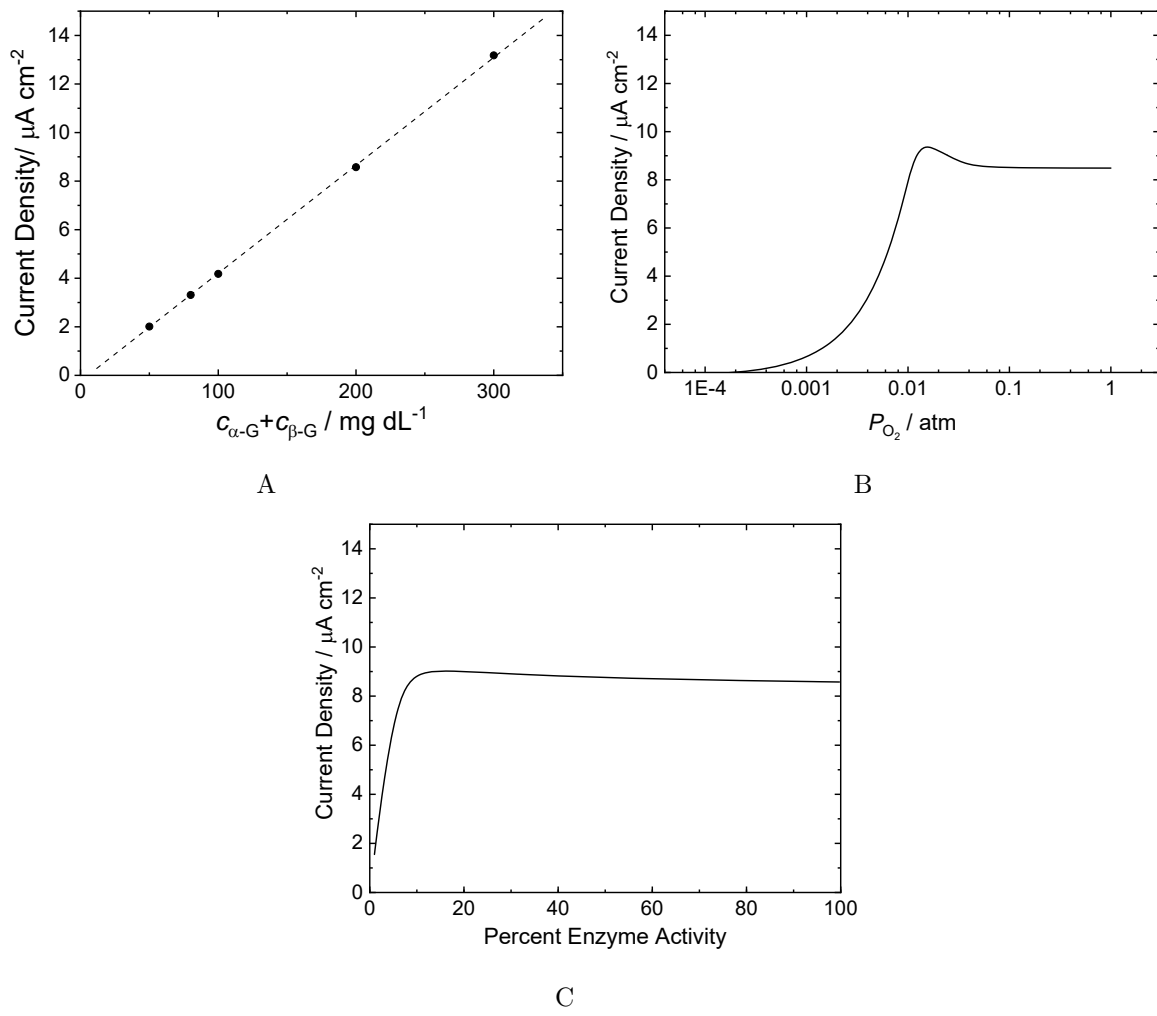


Figure 4-1. Calculated current density as a function of concentration of targeting species:
 (a) Sensor response curve with glucose concentration as a parameter, 5% of oxygen partial pressure and 100% of enzyme concentration (b) Sensor response curve with oxygen partial pressure as a parameter, 200 mg/dL of glucose and 100% of enzyme concentration (c) Sensor response curve with glucose oxidase enzyme (GOx) concentration as a parameter, 200 mg/dL of glucose and 5% of oxygen partial pressure.

support the same explanation. The flux of hydrogen peroxide to the electrode surface is proportional to the current density at 0.4V(Ag/AgCl) applied potential. Although the slope of the hydrogen peroxide concentration profile look different in Figure 4-2C, the distance of where the most of hydrogen peroxide is generated to the electrode balance difference. So the fluxes of hydrogen peroxide to the electrode of the three cases are the same. The enzymatic reaction rate distribution is shown in Figure 4-2D. For normal glucose concentration, the most amount of glucose is oxidized near the interface between GOx and GLM because of sufficient amount of enzyme and oxygen. For the oxygen deficiency case, there are not enough oxygen diffusing from the tissue to help recycle the enzyme. So the maxima of enzymatic reaction happens near the electrode surface, where the oxygen is generated by the electrochemical oxidation of hydrogen peroxide. For the enzyme deactivation case, the enzymatic reaction rate distributes uniformly as glucose diffuses to through the GOx layer.

As the transport-reaction mechanism is different for the three cases and explained by the steady-state profiles, the impedance response is expected to be different. The calculated diffusion impedance is shown in Figure 4-3. The diffusion impedance appears as merge of two loops. The high-frequency loop is the Gerischer impedance with a straight line towards higher frequencies. It provides information of the coupling between the homogeneous reactions and the heterogeneous reactions. The low-frequency capacitive loop is a semicircle corresponding to the mass-transfer impedance of the electroactive species. The further away from the electrode where hydrogen peroxide is generated, the larger in size the low frequency loop is. For the normal glucose concentration case, the enzymatic reaction primarily happen near the GOx–GLM interface, the low-frequency mass-transfer semicircle is largest in size and the characteristic frequency is the lowest (0.14 Hz). For the enzyme deactivation case, the enzymatic reaction distributed uniformly across the GOx layer, the major electroactive species hydrogen peroxide is produced closer to the electrode. Therefore, the low-frequency capacitive loop decreases in size and the

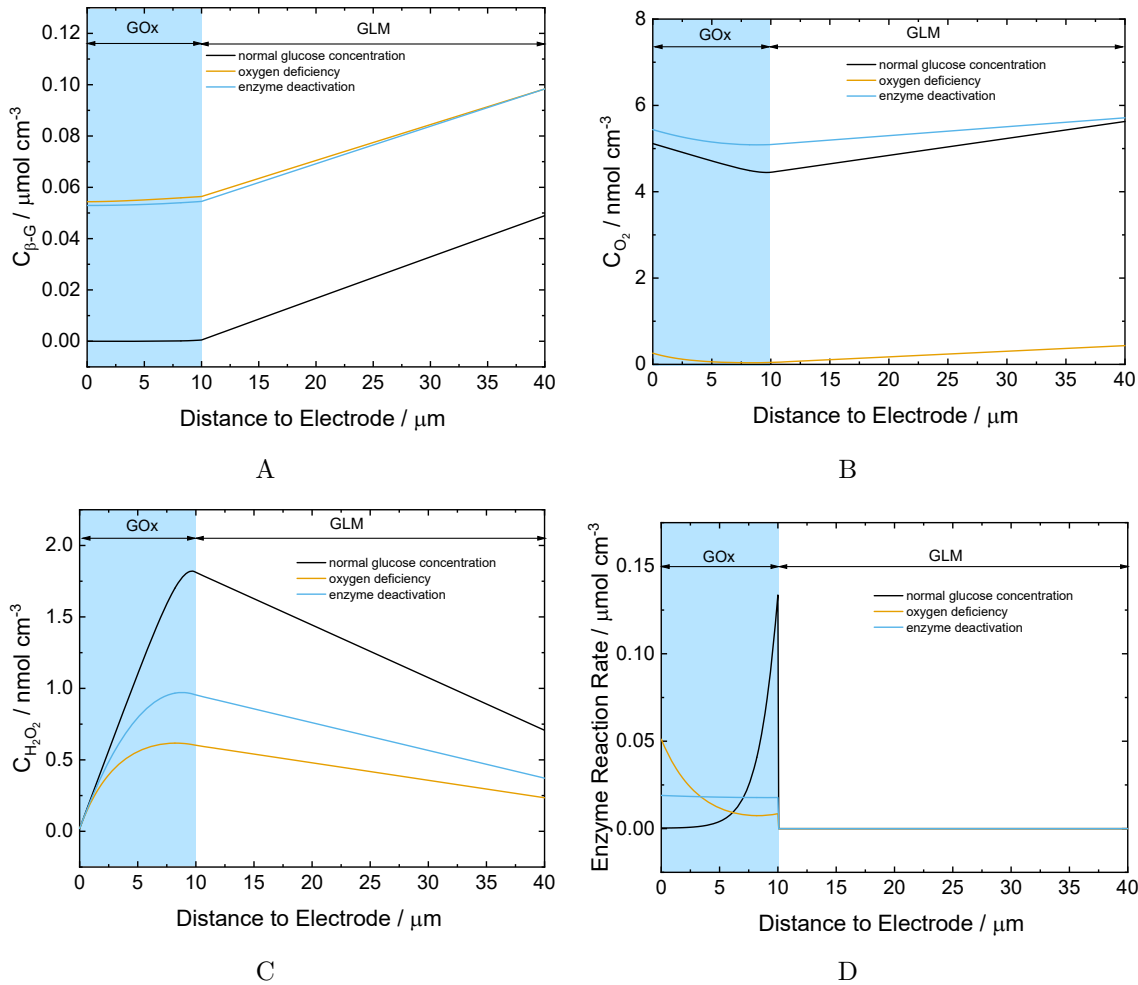


Figure 4-2. Calculated steady-state concentration profiles and reaction rate distribution as a function of distance to the electrode: (a) Beta-glucose concentration profile (b) Oxygen concentration profile (c) Hydrogen peroxide concentration profile (d) Enzymatic reaction rate distribution. The black line is corresponding to the case of normal glucose concentration with 100 mg/dL of glucose, 5 % of oxygen and 100 % of enzyme; the orange line is corresponding to the case of oxygen deficiency with 200 mg/dL of glucose, 0.5 % of oxygen and 100 % of enzyme; and the blue line is corresponding to the case of enzyme deactivation with 200 mg/dL of glucose, 5 % of oxygen and 3 % of enzyme.

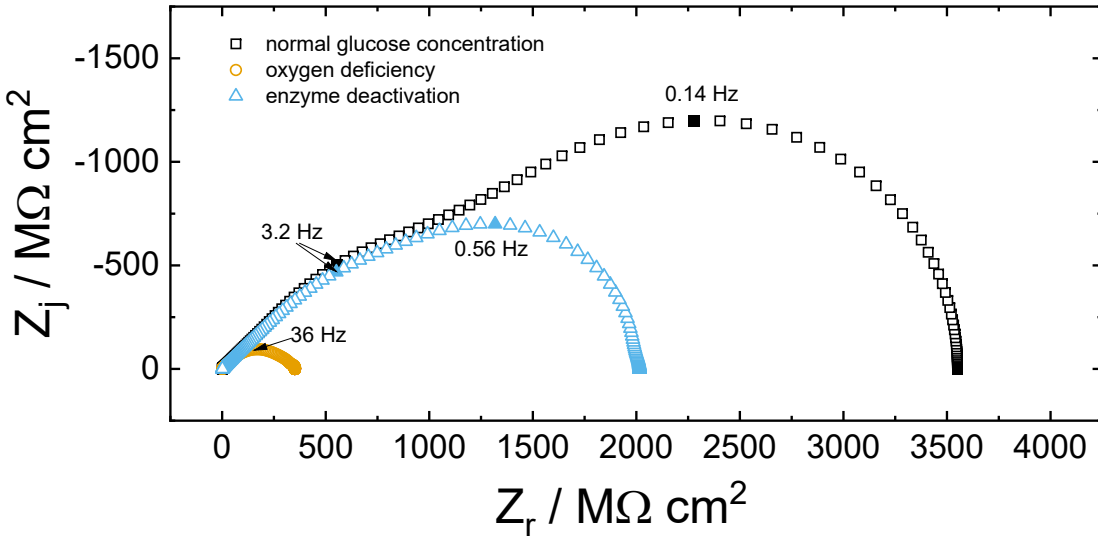


Figure 4-3. Calculated diffusion impedance for the three cases: (1) normal glucose concentration with 100 mg/dL of glucose, 5 % of oxygen and 100 % of enzyme; (2) oxygen deficiency with 200 mg/dL of glucose, 0.5 % of oxygen and 100 % of enzyme; (3) enzyme deactivation with 200 mg/dL of glucose, 5 % of oxygen and 3 % of enzyme.

characteristic frequency is higher (0.56 Hz). The high-frequency Gerischer impedance of both cases are approximately the same. For the case of oxygen deficiency, the enzymatic reaction mainly happen near the electrode surface, thus, the mass-transfer of hydrogen peroxide to the electrode surface is fast. Thus, the low-frequency semicircle shrinks and merges with the high-frequency loop and the impedance is dominated by the Gerischer impedance. The magnitudes of the diffusion impedance of the three cases providing same current density are obviously different.

Based on the diffusion impedance, the overall impedance is calculated, shown in Figure 4-4. In the simulation, the calculated frequency range is wide, from 1.6 μHz to 1.6 MHz. The shape of the Nyquist plot is part of the depressed semicircle, which is the same for the three cases. But the diameter of the semicircles are different. As the discussion by Gao et al [1], the diameter of the capacitive loop is attributed to the diffusion resistance.

A process model in Equation 4-27 was developed to regress the impedance response and extrapolate values of the diffusion resistance. The equivalent circuit of the process

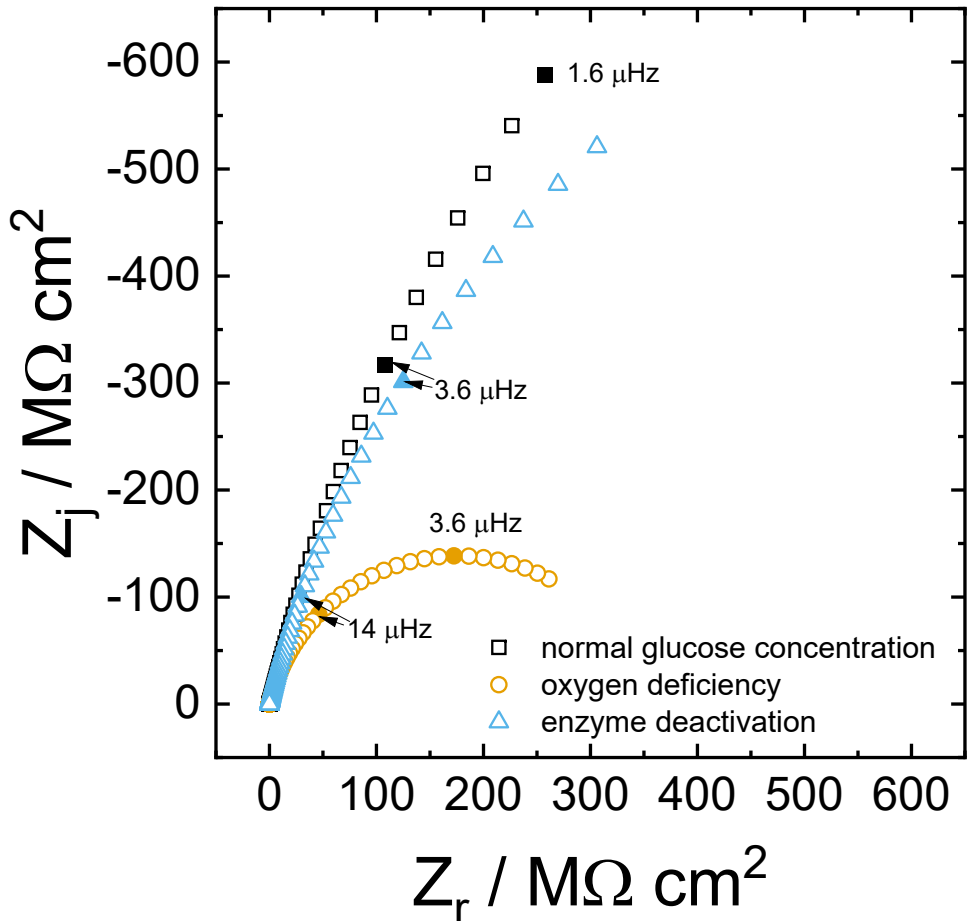


Figure 4-4. Calculated overall impedance following Equation 3-53 for the three cases: (1) normal glucose concentration with 100 mg/dL of glucose, 5 % of oxygen and 100 % of enzyme; (2) oxygen deficiency with 200 mg/dL of glucose, 0.5 % of oxygen and 100 % of enzyme; (3) enzyme deactivation with 200 mg/dL of glucose, 5 % of oxygen and 3 % of enzyme..

model is shown in Figure 4-5. There are 4 fitting parameters can be extrapolated from regression: the ohmic resistance R_e , the diffusion resistance R_d and the α and Q associated with the constant-phase element.

$$Z(\omega) = R_e + \frac{R_d}{1 + (j\omega)^\alpha R_d Q} \quad (4-27)$$

Figure 4-6A shows the impedance with frequency range scaled to the experimental measurable range from 1 mHz to 1.6 MHz. The overall impedance response for the three cases are not obviously different. By regression of the impedance response with

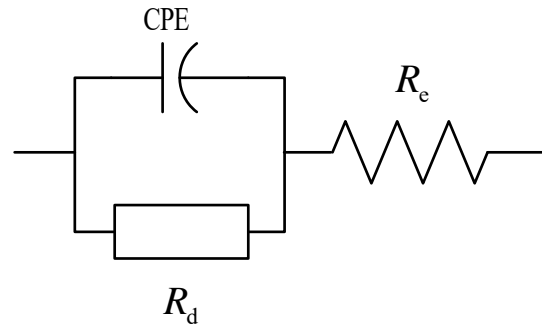


Figure 4-5. The process model developed for the regression of the impedance response of a continuous glucose sensor with the applied potential at mass-transfer limiting plateau. R_e is the ohmic resistance, R_d is the diffusion resistance and CPE is the constant-phase element.

frequency range from 1 mHz to 1.6 MHz, the fitting parameters can be extrapolated and are statistically significant, as in Table 4-7.

Table 4-7. Regression parameters and standard error for impedance response with frequency range from 1 mHz to 1.6 MHz

| | normal glucose concentration | | oxygen deficiency | | enzyme deactivation | |
|------------------------------------------|------------------------------|------------------------|-----------------------|------------------------|-----------------------|------------------------|
| | Value | Standard Error | Value | Standard Error | Value | Standard Error |
| R_e , W cm ² | 10 | 1.3×10^{-6} | 10 | 8.8×10^{-7} | 10 | 7.4×10^{-7} |
| R_d , MW cm ² | 3570 | 1.9 | 351 | 0.012 | 2018 | 0.34 |
| α | 0.85 | 2.0×10^{-8} | 0.85 | 1.3×10^{-8} | 0.85 | 1.13×10^{-8} |
| Q , F/cm ² s ^{1-a} | 2.61×10^{-5} | 2.56×10^{-12} | 2.61×10^{-5} | 1.67×10^{-12} | 2.61×10^{-5} | 1.41×10^{-12} |

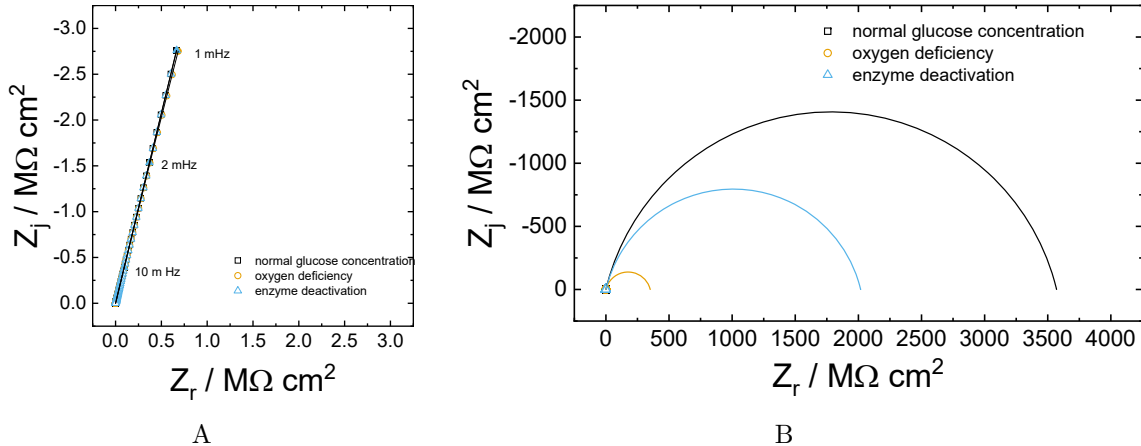


Figure 4-6. Impedance response with frequency from 1.6 MHz to 1 mHz (a) Impedance response with regression, the line is the regression results based on the process model. (b) Extrapolation results based on the fitting parameters in Table 4-7. The black line is corresponding to the case of normal glucose concentration with 100 mg/dL of glucose, 5 % of oxygen and 100 % of enzyme; the orange line is corresponding to the case of oxygen deficiency with 200 mg/dL of glucose, 0.5 % of oxygen and 100 % of enzyme; and the blue line is corresponding to the case of enzyme deactivation with 200 mg/dL of glucose, 5 % of oxygen and 3 % of enzyme.

Figure 4-6B shows the extrapolation of the full capacitive loop based on the fitting parameters Table 4-7. The diameter of the semicircles match with the magnitude of diffusion impedance in Figure 4-3.

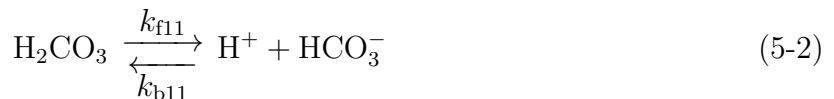
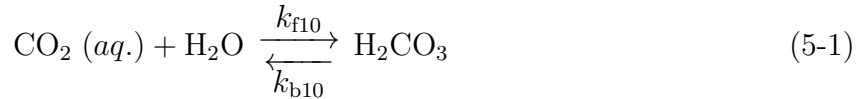
So far, the diffusion resistance from regression of impedance response is shown more sensitive than the current density, which is indicating that the impedance can be potentially used for differentiating the sensor failure cases and sensor calibration. However, further parametric study and developing the process model is necessary to understand the physical correlation between the regression parameters and the actual sensor failure mechanism.

CHAPTER 5

MODEL FOR CONTINUOUS GLUCOSE SENSOR IN BICARBONATE BUFFER

This chapter introduces the model with Bicarbonate Buffer Saline (BBS) as the biological buffer to the system. The bicarbonate buffer system is the primary buffering system in blood and tissue to maintain the pH. The carbon dioxide generated by respiration of human body hydrates to produce bicarbonate ion. The mathematical model for continuous glucose sensor with bicarbonate buffer provide better physical simulation of the concentration of the buffer species in the bulk, the diffusion of the buffer species through the bio-films of the sensor and the local change of the pH near the electrode surface.

In BBS, there are mainly 4 species in balance, the carbon dioxide CO_2 , the carbonic acid H_2CO_3 , the bicarbonate ion HCO_3^- and the carbonate ion CO_3^{2-} . More specifically, considering three equilibrium reactions as follow:



5.1 Governing Equations

For the model with bicarbonate buffer saline (BBS), the corresponding conservation equation for each species remained the same as the model with PBS buffer.

There are four major species in BBS, which are CO_2 , H_2CO_3 , HCO_3^- and CO_3^{2-} . The conservation equations for these species were

$$\frac{\partial c_{\text{CO}_2}}{\partial t} = D_{\text{CO}_2} \frac{\partial^2 c_{\text{CO}_2}}{\partial y^2} - R_{10} \quad (5-4)$$

for carbon dioxide (CO_2),

$$\frac{\partial c_{\text{H}_2\text{CO}_3}}{\partial t} = D_{\text{H}_2\text{CO}_3} \frac{\partial^2 c_{\text{H}_2\text{CO}_3}}{\partial y^2} + R_{10} + R_{11} \quad (5-5)$$

for carbonic acid (H_2CO_3^-),

$$\frac{\partial c_{\text{HCO}_3^-}}{\partial t} = D_{\text{HCO}_3^-} \frac{\partial^2 c_{\text{HCO}_3^-}}{\partial y^2} + R_{11} + R_{12} \quad (5-6)$$

for bicarbonate ion (HCO_3^{2-}), and

$$\frac{\partial c_{\text{CO}_3^{2-}}}{\partial t} = D_{\text{CO}_3^{2-}} \frac{\partial^2 c_{\text{CO}_3^{2-}}}{\partial y^2} + R_{12} \quad (5-7)$$

for carbonate ion (CO_3^{2-}). As the reaction rates through R_6 to R_{12} were unknown, the conservation equations were added up or subtracted from each other to cancel the terms of reaction rates $R_6 - R_{12}$.

5.2 Boundary Conditions

The boundary conditions at steady state are mostly similar to the model with PBS buffer shown in Chapter 4. The difference is the initial input of carbon dioxide is in gas phase and in the unit of partial pressure. The concentration of carbon dioxide dissolved in bulk electrolyte is calculated using Henry's Law.

At the electrode surface, the steady-state boundary conditions for the species not involved in electrochemical reactions are

$$\left. \frac{\partial \bar{c}_i}{\partial y} \right|_{y=0} = 0 \quad \text{at} \quad y = 0 \quad (5-8)$$

The boundary conditions at the electrode surface for the electroactive species are the flux to the electrode is equal to the faradaic current density, respectively. There are 4 electrochemical reactions and 3 electroactive species involved, hydrogen peroxide, oxygen and hydrogen ion. Specifically, the boundary conditions for hydrogen peroxide is

$$2FD_{\text{H}_2\text{O}_2} \left. \frac{\partial \bar{c}_{\text{H}_2\text{O}_2}}{\partial y} \right|_{y=0} = \bar{j}_{\text{H}_2\text{O}_2} + \bar{j}_{\text{O}_2} - \bar{j}_{\text{red}} \quad \text{at} \quad y = 0 \quad (5-9)$$

for oxygen is

$$2FD_{O_2} \frac{\partial \bar{c}_{O_2}}{\partial y} \Big|_{y=0} = -\bar{j}_{H_2O_2} - \bar{j}_{O_2} \quad \text{at } y = 0 \quad (5-10)$$

and for hydrogen ion is

$$FD_H \frac{\partial \bar{c}_H}{\partial y} \Big|_{y=0} = \bar{j}_{H_2O_2} + \bar{j}_{O_2} + \bar{j}_{red} + \bar{j}_{H_2} \quad \text{at } y = 0 \quad (5-11)$$

Continuity of concentration and flux were assumed to apply at the GOx–GLM interface.

At the interface between GLM layer and tissue, it was assumed that there is a diffusion layer as a stagnant film with layer thickness δ . The flux of the mobile species in the diffusion layer were expressed as

$$\bar{N}_i = k_i \left(\frac{\bar{c}_i|_{y=NJ}}{\gamma_i} - \bar{c}_i(\infty) \right) \quad (5-12)$$

where γ_i is the partition coefficient for each species between the interstitial fluid and the GLM. k_i is the mass-transfer coefficient of species i in the diffusion layer in tissue close to GLM layer. $c_i|_{y=NJ}$ is the concentration of species i at the interface between GLM layer and diffusion layer ($y = NJ$). $c_i(\infty)$ is the bulk concentration of species i in tissue. Therefore, the boundary condition at the interface of GLM layer and diffusion layer ($y = NJ$) is flux balance, which was expressed as

$$- D_{i,GLM} \frac{\partial \bar{c}_i}{\partial y} \Big|_{y=NJ} = k_i \left(\frac{\bar{c}_i|_{y=NJ}}{\gamma_i} - \bar{c}_i(\infty) \right) \quad (5-13)$$

The boundary conditions at the outer limit of GLM for the immobile species, the enzymes and enzyme complexes, as well as the associated reaction rates were

$$\bar{c}_i = 0 \quad \text{at } y = NJ \quad (5-14)$$

and

$$\bar{R}_i = 0 \quad \text{at } y = NJ \quad (5-15)$$

respectively.

5.3 Calculation of Impedance

The set of governing equations are solved for both the steady-state condition and the frequency domain. Due to the nonlinear expressions for homogeneous reactions, the steady-state set of equations required iterative solution. The set of equations for faradaic impedance response developed in this section involves steady-state concentrations and therefore requires solution of the steady-state equation. The expressions for sensor impedance were obtained following an electrical circuit which provided a framework for the sensor impedance response [1](see Chapter 9 in reference [49]).

5.3.1 Mathematical Calculation of Impedance

Under the sinusoidal perturbation, the convective-diffusion equation can be expressed as

$$j\omega \tilde{c}_i = D_i \frac{\partial^2 \tilde{c}_i}{\partial y^2} + \tilde{R}_i \quad (5-16)$$

The real and imaginary parts of equations of the form of equation (5-16) were solved simultaneously.

The faradaic impedance can be expressed in terms of the charge transfer resistance R_t and the diffusion impedance Z_d as

$$Z_F = R_t + Z_d \quad (5-17)$$

Following the general mathematical derivation framework in Orazem and Tribollet[49], the charge transfer resistances can be calculated as

$$\begin{aligned} R_t &= (K_{H_2O_2} b_{H_2O_2} \bar{c}_{H_2O_2}(0) \exp(b_{H_2O_2} \bar{V}) \\ &\quad + K_{O_2} b_{O_2} \bar{c}_{O_2}(0) \bar{c}_{H^+}^2(0) \exp(-b_{O_2} \bar{V}) \\ &\quad + K_{red} b_{red} \bar{c}_{H_2O_2}(0) \bar{c}_{H^+}^2(0) \exp(-b_{red} \bar{V}))^{-1} \\ &\quad + K_H b_H \bar{c}_{H^+}^2(0) \bar{c}_{H^+}^2(0) \exp(-b_H \bar{V}))^{-1} \end{aligned} \quad (5-18)$$

The diffusion impedance can be calculated as

$$\begin{aligned}
Z_D = & R_t [K_{H_2O_2} \exp(b_{H_2O_2} \bar{V}) - K_{red} \bar{c}_{H^+}^2(0) \exp(-b_{red} \bar{V})] \left(\frac{\bar{c}_{H_2O_2}(0)}{FD_{H^+} \frac{d\bar{c}_{H^+}}{dy} \Big|_{y=0}} \right) \\
& + R_t K_{O_2} \bar{c}_{H^+}^2(0) \exp(-b_{O_2} \bar{V}) \left(- \frac{\bar{c}_{O_2}(0)}{FD_{H^+} \frac{d\bar{c}_{H^+}}{dy} \Big|_{y=0}} \right) \\
& + R_t [2K_{O_2} \bar{c}_{O_2}(0) \bar{c}_{H^+}(0) \exp(-b_{O_2} \bar{V}) + 2K_{red} \bar{c}_{H_2O_2}(0) \bar{c}_{H^+}(0) \exp(-b_{red} \bar{V}) + 2K_H \bar{c}_{H^+}(0) \exp(-b_H \bar{V})] \\
& \left(- \frac{\bar{c}_{H^+}(0)}{FD_{H^+} \frac{d\bar{c}_{H^+}}{dy} \Big|_{y=0}} \right)
\end{aligned} \tag{5-19}$$

and the dimensionless diffusion impedance expressions for H_2O_2 , O_2 and H^+ are given by

$$\frac{-1}{\theta'_{H_2O_2}(K)} = \frac{1}{\delta_{GOx}} \left(- \frac{\bar{c}_{H_2O_2}(0)}{\frac{d\bar{c}_{H_2O_2}}{dy} \Big|_{y=0}} \right) \tag{5-20}$$

$$\frac{-1}{\theta'_{O_2}(K)} = \frac{1}{\delta_{GOx}} \left(- \frac{\bar{c}_{O_2}(0)}{\frac{d\bar{c}_{O_2}}{dy} \Big|_{y=0}} \right) \tag{5-21}$$

and

$$\frac{-1}{\theta'_{H^+}(K)} = \frac{1}{\delta_{GOx}} \left(- \frac{\bar{c}_{H^+}(0)}{\frac{d\bar{c}_{H^+}}{dy} \Big|_{y=0}} \right) \tag{5-22}$$

respectively, where δ_{GOx} is the GOx layer thickness.

5.3.2 Boundary Conditions

For the phasor of oscillating concentrations, the boundary conditions far away from the electrode (at $J = NJ$) are

$$\tilde{c}_i = 0 \quad \text{at} \quad y = NJ \tag{5-23}$$

At electrode, the boundary conditions for the species not involving the electrochemical reactions are

$$\left. \frac{\partial \tilde{c}_i}{\partial y} \right|_{y=0} = 0 \quad \text{at} \quad y = 0 \quad (5-24)$$

for the electroactive species, the boundary condition for hydrogen peroxide is

$$\tilde{c}_{H_2O_2} = 1 \quad \text{at} \quad y = 0 \quad (5-25)$$

and the boundary conditions for hydrogen ion and oxygen are the phasor of the flux is related to the phasor of the current density.

CHAPTER 6 EXPERIMENTS

This chapter introduces the experimental work performed with the continuous glucose sensor provided by Medtronic Diabetes for research purpose only. There are three kinds of sensor: the full sensor with GOx and GLM layers, the sensor up to the GOx layer without the GLM, and the bare platinum sensor. The experimental data were analyzed with the measurement model[53] to get the error structure of the data, which is used for the regression analysis with a process model. The ohmic resistance, effective capacitance and diffusion resistance can be extrapolated from the regression results. The characteristic frequency for geometry-induced frequency dispersion can be estimated. The surface roughness factor can also be evaluated.

6.1 Experimental Setup

The experimental measurement of the Electrochemical Impedance Spectroscopy (EIS) were performed with a 3-electrode system. The sensor served as the working electrode. Depending upon the experimental condition, the counter electrode and reference electrode could be the built-in electrodes integrated with the sensor or the external electrodes. For external electrodes, the counter electrode was a platinum foil and the reference electrode was Ag/AgCl. The electrolyte was a glucose solution with concentration ranging from 100-400 mg/dL and with/without PBS buffer. The schematic experimental setup is shown in Figure 6-1.

6.2 Electrochemical Approach

The electrochemical measurement was performed with a Gamry Reference 600+ or a Gamry Reference 3000 Potentiostat at room temperature. Three kinds of electrochemical characterization approach were performed: open circuit potential (OCP), step-potential chronoamperometry, and potentiostatic EIS.

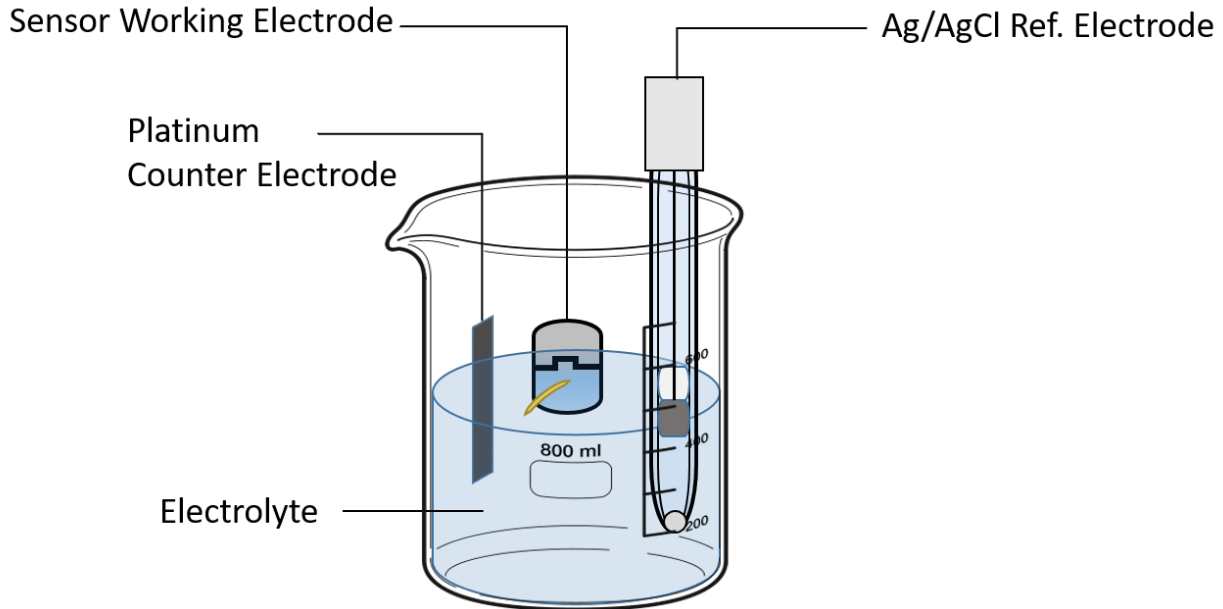


Figure 6-1. Schematic representation of the experimental setup for a three-electrode system to measure the impedance of a glucose sensor. The working electrode is the glucose sensor, the counter electrode is the platinum film and the reference electrode is the Ag/AgCl reference electrode.

6.3 Experimental Results

The impedance data were analyzed with the measurement model to check the Kramers-Kronig consistency and to get the error structure of the measurements. The Kramers-Kronig consistent impedance spectra were then regressed with proposed process models to get the value and confidence interval of fitting parameters, from which the effective capacitance, characteristic frequency and ohmic resistance can be evaluated.

6.3.1 Regression with Measurement Model

The impedance of a glucose sensor with only a GOx layer is presented in Figure 6-2. The electrolyte was 400 mg/dL of glucose in a PBS buffer, the applied potential was 0.4 V (Ag/AgCl), the perturbation amplitude was 20 mV, and the frequency range was from 100 kHz to 0.1 Hz. The impedance data were the regressed with the measurement model with error structure weighting. The error structure of the measurement can be expressed as

$$\sigma = 2.5321 \times 10^{-4} \times |Z_j| + 3.0089 \times 10^{-8} \times |Z|^2 + 4.5543 \times 10^{-1} \quad (6-1)$$

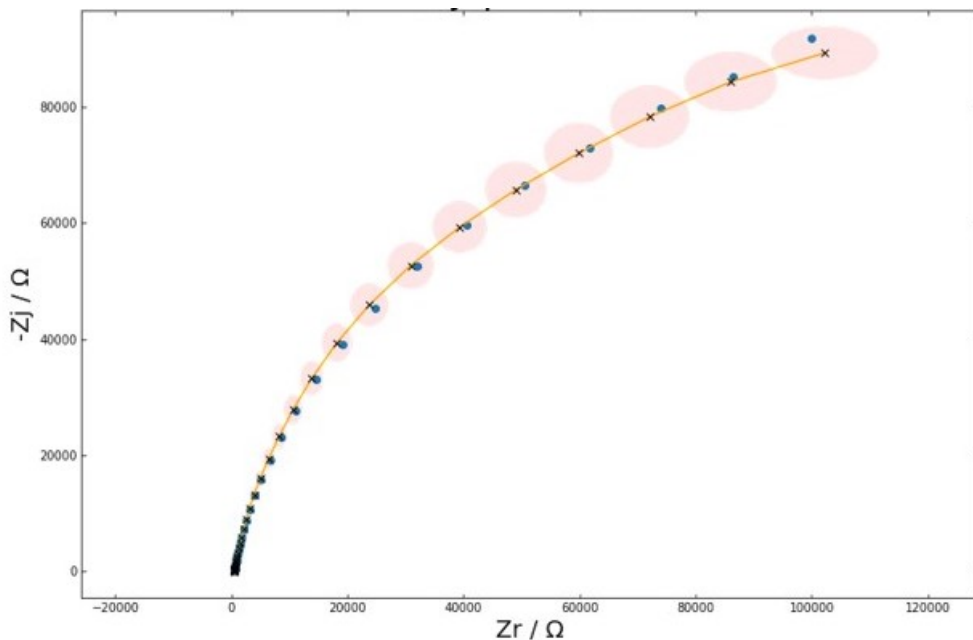


Figure 6-2. Regression with the measurement model in Nyquist plot for sensor from Medtronic with only GOx layer at 0.4 V (Ag/AgCl) applied potential.

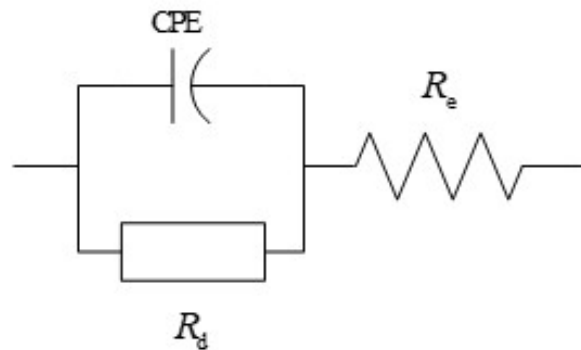


Figure 6-3. Electrical circuit of process model

The first measured frequency and the data within 5 Hz of the line frequency were eliminated. The rest of the data fell within the confidence interval of the fitting model, showing that the data in Figure 6-2 were Kramers-Kronig consistent.

6.3.2 Regression with Process Model

A process model was proposed on based on our understanding of the system, shown in Figure 6-3. The process model consists of a constant-phase element (CPE) in parallel with a diffusion resistance (R_d), which in series with an ohmic resistance (R_e). The overall

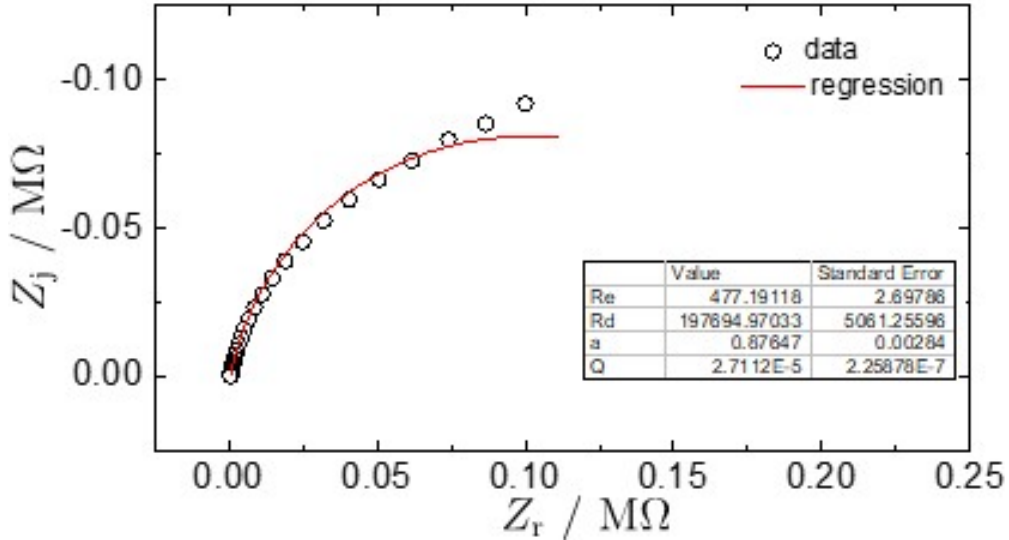


Figure 6-4. Regression with process model in Nyquist plot for sensor from Medtronic with only GOx layer, in 400 mg/dL of glucose and PBS buffer at 0.4 V (Ag/AgCl) applied potential.

impedance can be expressed as

$$Z = R_e + \frac{1}{1 + (j\omega)^\alpha R_d Q} \quad (6-2)$$

There are four fitting parameters: the values α and Q associated with the CPE, the diffusion resistance R_d , and the ohmic resistance R_e . The regression results for the sensor with only GOx layer are shown in Figure 6-4.

6.3.3 Accuracy Contour Plot

The high-frequency capacitive loop is Kramers-Kronig consistent, but it can be caused by the impedance of the wires. To explore the origin of the high-frequency capacitive loop, the accuracy contour plot of the potentiostat of the measurements is presented. The accuracy contour plot[54] is a useful way to learn the limits of a particular potentiostat and experimental setup, as shown in Figure 6-5. The lines A and E are determined by the minimum and maximum measurable current limits. The line C is determined by the maximum frequency capability of the instrument. The line of B and D are determined by the wire capacitance and wire inductance, respectively.

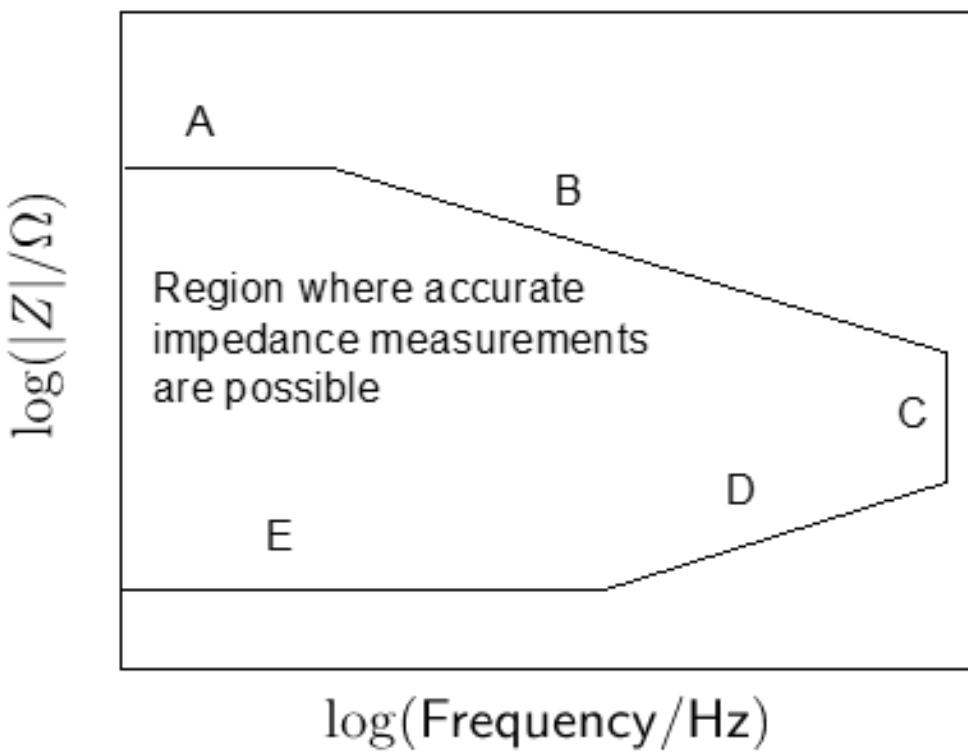


Figure 6-5. Schematic representation of accuracy contour plot: (A) Minimum current resolution; (B) Wire capacitance; (C) Maximum frequency capability of the instrument; (D) Wire inductance; (E) Maximum measurable current

The accuracy contour plot measured for the Gamry Reference 600+ potentiostat is shown in Figure 6-6. The maximum impedance for a 10 mV applied amplitude was on the order of $10^9 \Omega$. Based on linear regression and calculation, the wire capacitance was $1.04 \times 10^{-10} \text{ F}$. The wire resistance was about 1.9Ω , and the wire inductance was about 1.2 H .

As shown in Figure 6-7, the region for which the systematic error of the impedance measurement is less than 1% is smaller than the region shown in Figure 6-6. For the data with sensor up to GOx, the high-frequency part above 10^4 Hz was beyond the region for which the modulus of the impedance has more than 1% error. These results show that the high-frequency loop was influenced by the wires.

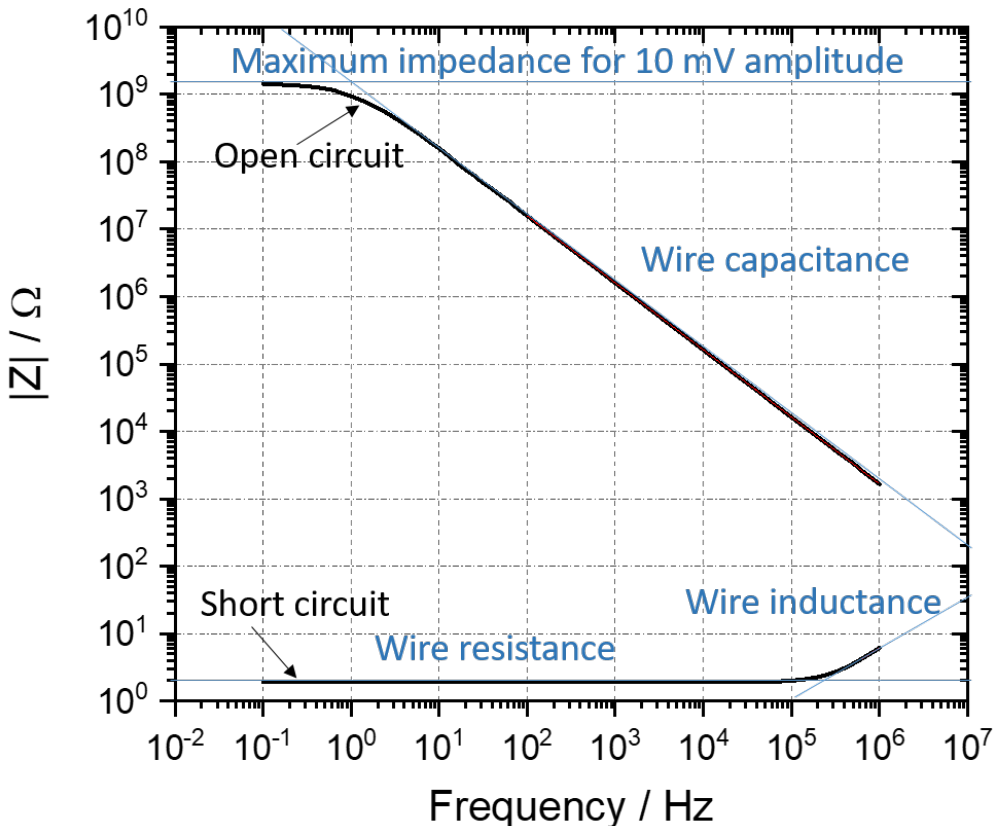


Figure 6-6. Accuracy contour plot for Gamry Reference 600+ potentiostat.

The equivalent circuit of the experimental cell with wires is shown in Figure 6-8. The wire resistance and wire inductance are in series with experimental electrochemical system, and the series combination is in parallel with the wire capacitance.

By replacing the impedance of the experimental cell Z_{cell} with the process model of the glucose sensor shown in Figure 6-3, the overall impedance could be expressed as

$$Z = \left(j\omega C_{\text{wire}} + \frac{1}{Z_{\text{wire}}} \right)^{-1} \quad (6-3)$$

where the wire resistance R_{wire} is lumped with the ohmic resistance of the cell R_e . The wire inductance was negligible. The cell impedance is expressed as

$$Z_{\text{cell}} = R_e + \frac{1}{1 + (j\omega)^\alpha R_d Q}$$

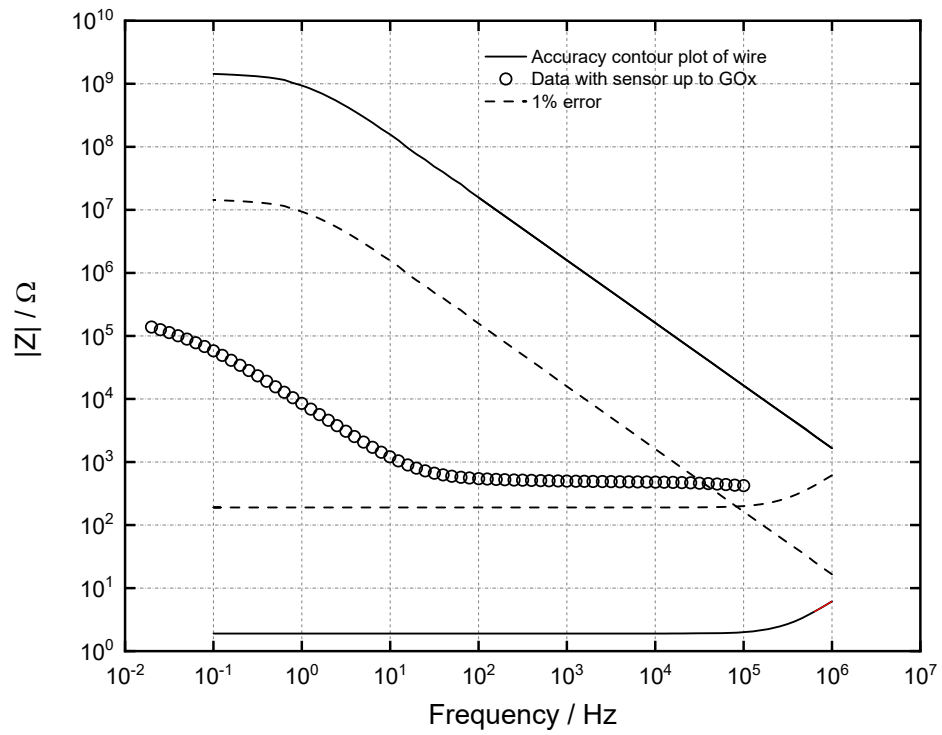


Figure 6-7. Accuracy contour plot with 1% error for impedance measurements of glucose sensor with only GOx layer. The region within the dashed lines is the measured modulus of the impedance will have an error less than or equal to 1 %.

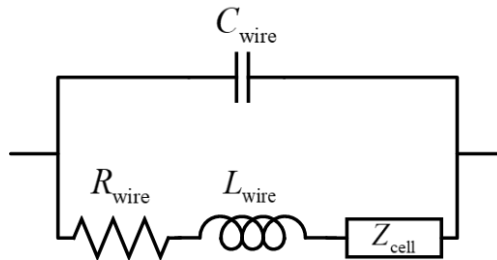


Figure 6-8. Equivalent circuit of electrochemical system with wires for accuracy contour plot. The wire resistance and wire inductance is in series with studied electrochemical system and in parallel with wire capacitance.

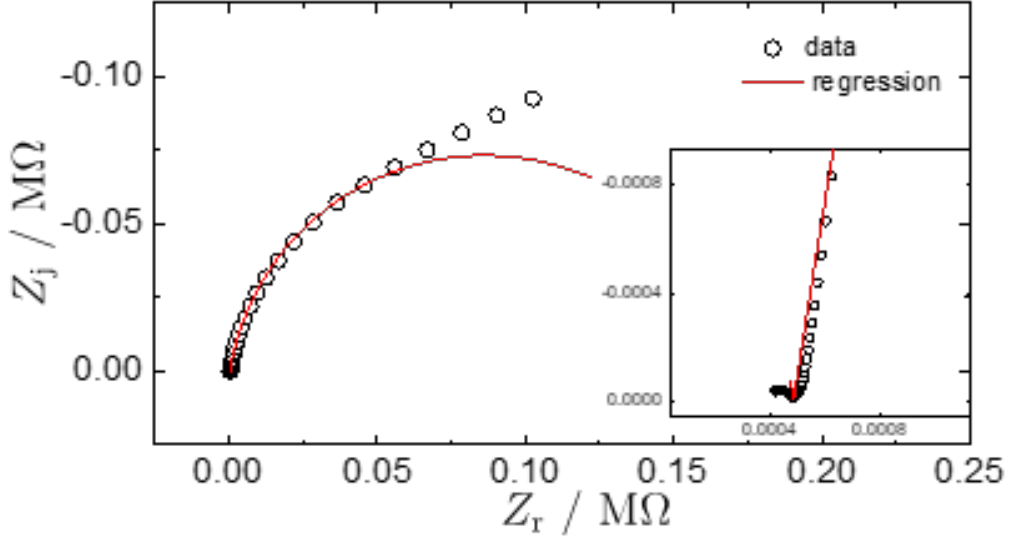


Figure 6-9. Regression of impedance data for sensor up to gox layer with process model with wire properties.

Table 6-1. Values of fitting parameters with wire properties for the impedance data with sensor up to GOx layer at 400 mV (Ag/AgCl) applied potential.

| | Value | Standard Error |
|-----------------------|----------|----------------|
| R_e, Ω | 485.588 | 2.38596 |
| R_d, Ω | 171454.6 | 8080.56196 |
| α | 0.90478 | 0.00236 |
| $Q, F/s^{(1-\alpha)}$ | 2.26E-05 | 1.73E-07 |
| C_{wire}, F | 5.74E-10 | 5.94E-11 |

Therefore, the fitting parameters are the ohmic resistance R_e , diffusion resistance R_d , CPE values α and Q and the wire capacitance C_{wire} . By fitting the data with sensor up to GOx layer, Figure 6-9 showed that the process model accounted for the high-frequency loop but did not fit the data very well.

The values of the fitting parameters were statistically significant and are shown in Table 6-1. To better capture the high-frequency feature, the wire capacitance was modified to a constant-phase element, as shown in Figure 6-10. The overall impedance can be expressed as

$$Z = \left((j\omega)^{\alpha_{\text{wire}}} Q_{\text{wire}} + \frac{1}{Z_{\text{wire}}} \right)^{-1} \quad (6-4)$$

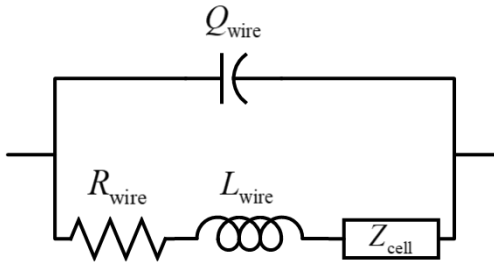


Figure 6-10. Modified process model with wires properties. The wire resistance and wire inductance is in series with studied electrochemical system and in parallel with wire CPE.

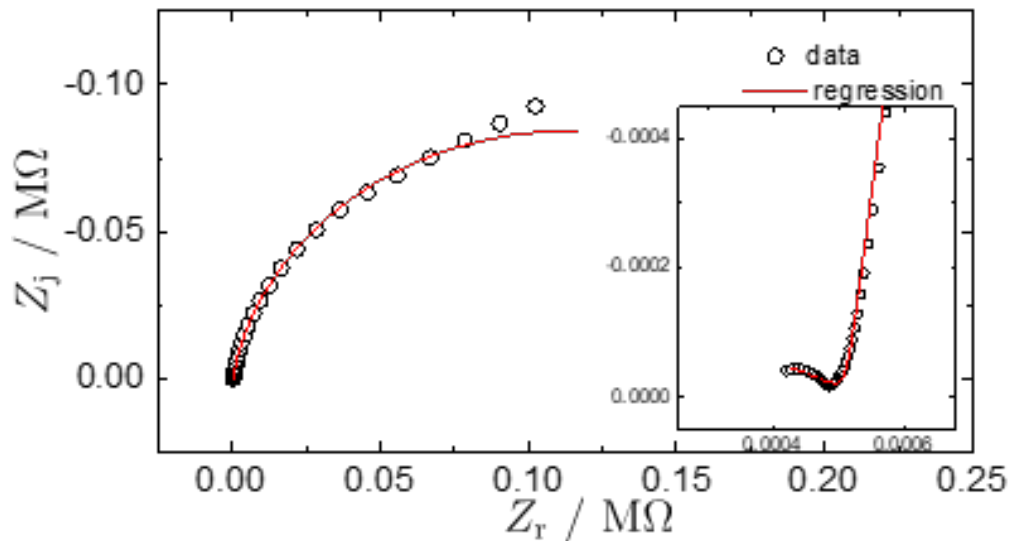


Figure 6-11. Regression of impedance data for sensor up to gox layer with modified process model with wire properties.

The fitting parameters are the ohmic resistance R_e , diffusion resistance R_d , CPE values α and Q of the studied electrochemical cell, and the CPE values α_{wire} and Q_{wire} of wires.

After modifying the process model with the wire CPE, the regression model fit the impedance data better, as shown in Figure 6-11. The values of the fitting parameters were statistically significant and are shown in Table 6-2.

The effective capacitance of the wire was calculated using the CPE values α_{wire} and Q_{wire} based on Brug formula (2-19). The wire capacitance was $6 \times 10^{-11}\text{F}$, which is on the same order of the wire capacitance extrapolated from the accuracy contour plot of $1 \times 10^{-10}\text{F}$.

Table 6-2. Values of fitting parameters of modified process model with wire properties for the impedance data with sensor up to GOx layer at 400 mV (Ag/AgCl) applied potential.

| | Value | Standard Error |
|-------------------------------------|----------|----------------|
| R_e, Ω | 523.7383 | 1.27467 |
| R_d, Ω | 288129.1 | 17343.79155 |
| α | 0.92716 | 0.00122 |
| $Q, F/s^{(1-\alpha)}$ | 2.04E-05 | 1.10E-07 |
| α_{wire} | 0.3514 | 0.0049 |
| $Q_{\text{wire}}, F/s^{(1-\alpha)}$ | 4.42E-06 | 2.95E-07 |

The effective capacitance of the sensor was calculated using the ohmic resistance R_e , and CPE values α and Q in Table 6-2. The sensor superficial capacitance was $1.43 \times 10^{-5} F$. The superficial area of the sensor was estimated to 0.0034 cm^2 . Thus, the sensor superficial capacitance was equal to $4.2 \times 10^{-3} F \text{ cm}^{-2}$. If the double layer capacitance was assumed to be $20 \mu F \text{ cm}^{-2}$, the surface roughness factor could be calculated as the ratio of the superficial capacitance to the double layer capacitance. The surface roughness factor was 210. The characteristic frequency was 42 Hz based on Equation (2-20).

In conclusion, process models were proposed to facilitate quantitative interpretation of impedance spectra. The fitting parameters included the CPE parameters, ohmic resistance, and diffusion resistance. The Brug formula was used to extract capacitance from CPE parameters. Capacitance yields consistent roughness factor on the order of 200. Frequency dispersion expected above 40 Hz. The impedance spectra influenced by frequency dispersion are eliminated. A fewer data points can be used for regression analysis. Therefore, interpretation of Gerischer parameters requires more work.

CHAPTER 7

DISCUSSION

There are multiple parameters in the model associated with the physics and chemistry of the sensor. The discussion of parameters is organized according to impact on sensor failure mechanism. Based on the calculation results of the model, the influence of the model parameters is summarized.

7.1 Parameters

There are many parameters in the model. The parameters all have physical meaning. The treatments of the values are based on the literature research, matching with experimental results, and modification to reasonable ranges associated with the continuous glucose sensor. The enzymatic reaction rate constants were based on both experimental studies and modeling studies from literature [21, 28, 29, 55–59]. The heterogeneous reaction rate constants were calculated based on the equilibrium potential, exchange currents and Tafel slopes of the electrochemical reactions on platinum electrodes from literature [60–63], and then optimized based on experimental polarization curves. The operation parameters include the glucose concentration, oxygen concentration and enzyme activity, and applied potential. The effective diffusion coefficients of the species within different layers of the sensor depend on the physical property of the film and are experimentally measurable. In the model, they are calculated based on diffusion coefficients at standard condition in dilute solution and modified with porosity factors. The operation parameters provide degrees of freedom in operating the sensor conditions and simulations.

In treatment of biological buffers, the activity coefficients of ionic species depending upon both its charge and the ionic strength of species are considered, and the equilibrium constants are modified accordingly. The initial input concentration of the buffering species are precalculated in a model for batched buffer solution. The model was built in Matlab[®]

Table 7-1. Sensor dimensions

| Layers | Thickness |
|-----------------|-------------------|
| GOx layer | 10 μm |
| GLM layer | 30 μm |
| Diffusion layer | 100 μm |

using the concentration of buffer species of the experimental recipes and the apparent equilibrium constants.

A systematic parametric study was performed to explore the parameter space and to match with experimental data. The model parameters are characterized and introduced below.

7.1.1 Dimension and Mesh

The one-dimensional model accounts for the dimension from the electrode surface to the tissue, as introduced in detail in Gao et al.'s modeling paper[1]. The dimension is tied to the sensor design and encapsulation layer on the sensor. From the electrode surface, there are the GOx layer with thickness of δ_{GOx} , GLM layer with thickness of δ_{GLM} , and the diffusion layer in the tissue with thickness of δ_{Diff} . An example of the thickness of the layer is shown in Table 7-1. The influence of layer thickness on steady-state profiles and impedance response was studied in this work.

The model was calculated by use of finite-difference numerical method and Newman's BAND algorithm[64]. The one-dimensional model was divided into three regime with different number of nodes and different mesh size. The mesh size was refined near the electrode surface due to the large concentration derivatives lead by electrochemical reactions. The details are shown in Figure 7-1. In the GOx layer, there are two domains, one with mesh size HHH from the electrode surface ($J = 1$) to the interface ($J = KJ$), and the other with mesh size HH from the interface ($J = KJ$) to GOx–GLM interface ($J = IJ$). The mesh size in GLM layer is H . The choice of the number of mesh points directly is associated with speed of convergence, accuracy and round-off errors. The

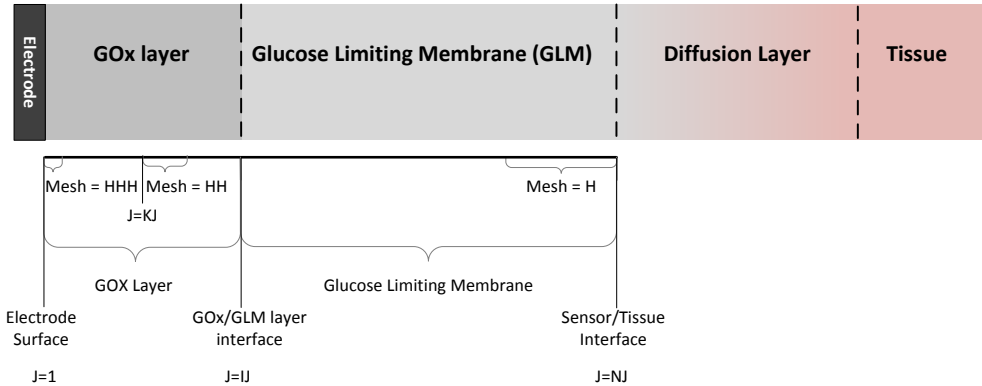


Figure 7-1. One-dimensional schematic representation of the glucose sensor showing three dissimilar mesh sizes. The finest mesh size HHH is near the electrode surface ($J = 1$), a slightly larger mesh size HH was used in the remainder of the GOx layer, and the coarsest mesh size H was used in the GLM layer. The GOx–GLM interface was located at $J = IJ$, and the outer limit of the GLM layer was located at $J = NJ$. There is a diffusion layer at the outer bound of GLM layer in the tissue.

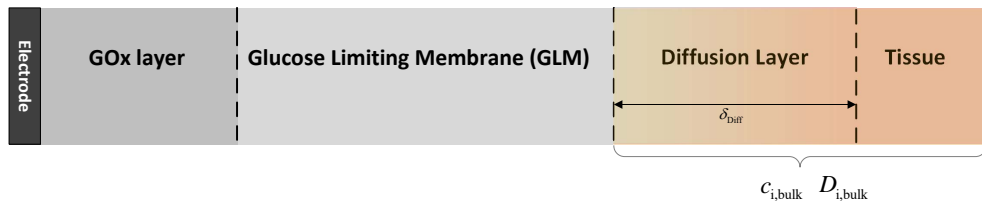


Figure 7-2. Parameters in the diffusion layer and tissue based on the one-dimensional schematic representation of the glucose sensor.

default values of the number of points of each domain were chosen to achieve reasonable calculation speed and accuracy.

7.1.2 Initial Concentration and Diffusion Coefficients

Treatment of the diffusion layer and tissue outside of the sensor serves as a boundary condition for the one-dimensional model. The parameters associated with tissue are the diffusion layer thickness, the initial concentration of species in the tissue and the corresponding diffusion coefficients in bulk electrolyte, represented in Figure 7-2.

The concentration of the species are initialized to the concentration in the bulk tissue. The glucose exists in two forms, $\alpha - D - \text{glucose}$ and $\beta - D - \text{glucose}$. The anomeration reaction between the two forms of glucose was considered as a homogeneous

Table 7-2. Initial concentrations of species

| Species | $C_{\text{bulk},i}$ or $p_{\text{bulk},i}$ |
|--------------------------------------------|--------------------------------------------|
| Glucose(both α and β anomers) | varied |
| Glucose oxidase enzyme (maximum) | $3.56 \times 10^{-7} \text{ molcm}^{-3}$ |
| Oxygen O_2 (partial pressure) | varied |
| Hydrogen peroxide H_2O_2 | $1 \times 10^{-20} \text{ molcm}^{-3}$ |
| Hydrogen ion H^+ | calculated based on pH |
| Hydroxide ion OH^- | calculated based on pH |
| Phosphoric acid H_3PO_4 | $3.63 \times 10^{-11} \text{ molcm}^{-3}$ |
| Dihydrogen phosphate ion $H_2PO_4^-$ | $9.2 \times 10^{-6} \text{ molcm}^{-3}$ |
| Hydrogen phosphate ion HPO_4^{2-} | $4.02 \times 10^{-5} \text{ molcm}^{-3}$ |
| Phosphate ion PO_4^{3-} | $1.86 \times 10^{-9} \text{ molcm}^{-3}$ |
| Carbon dioxide CO_2 (partial pressure) | 5% |
| Carbonic acid H_2CO_3 | $1.68 \times 10^{-9} \text{ molcm}^{-3}$ |
| Bicarbonate ion HCO_3^- | $2.37 \times 10^{-5} \text{ molcm}^{-3}$ |
| Carbonate ion CO_3^{2-} | $1.01 \times 10^{-7} \text{ molcm}^{-3}$ |

reaction that took place throughout the sensor. The total concentration is the input.

The glucose oxidase enzyme was immobilized only in the GOx layer, existing in 6 forms: oxidized glucose oxidase (GOx_{OX}), reduced glucose oxidase (GOx_{RED}), the intermediate enzyme complex species (GOx-GA and GOx- H_2O_2), and the pH-deactivated enzyme complex species (H^+GOx_{OX} and GOx_{RED}^-). The total amount of enzyme was the initial concentrations were divided equally into the 6 forms of enzyme. Hydrogen peroxide is toxic, and the GLM layer should prevent the diffusion of hydrogen peroxide. In tissue, the concentration of hydrogen peroxide was set to a small number closed to zero. The concentrations of hydrogen ion and hydroxide ion were based on the input pH. The initial concentration of buffer species corresponding to different model were based on buffer recipes.

The diffusion coefficient is the physical property associated with diffusivity of the species under the driving force of diffusion. The diffusion coefficients of species at infinite dilute in water at $25^\circ C$ are chosen as initial input in bulk, shown in Table 7-3.

Table 7-3. Diffusion coefficients of species in bulk.

| Species | $D_{\text{bulk},i} \times 10^5 (\text{cm}^2/\text{s})$ |
|----------------------------------------------------|--------------------------------------------------------|
| Glucose, gluconic acid and gluconate ion | 0.72 |
| Glucose oxidase enzyme | 0 |
| Oxygen O_2 | 2.46 |
| Hydrogen peroxide H_2O_2 | 1.83 |
| Hydrogen ion H^+ | 9.30 |
| Hydroxide ion OH^- | 5.30 |
| Phosphoric acid H_3PO_4 | 0.90 |
| Dihydrogen phosphate ion H_2PO_4^- | 0.959 |
| Hydrogen phosphate ion HPO_4^{2-} | 0.759 |
| Phosphate ion PO_4^{3-} | 0.824 |
| Carbon dioxide CO_2 | 2.49 |
| Carbonic acid H_2CO_3 | 1.30 |
| Bicarbonate ion HCO_3^- | 1.84 |
| Carbonate ion CO_3^{2-} | 0.92 |

Table 7-4. Partition coefficients of species at the interface of diffusion layer and GLM layer of the sensor.

| Species | Partition Coefficients |
|---------------------------------------------|------------------------|
| Glucose, gluconic acid and gluconate ion | 0.014 |
| Hydrogen peroxide | 0.11 |
| Oxygen | 0.32 |
| Hydrogen ion, hydroxide ion and buffer ions | 0.2 |

7.1.3 Diffusion Coefficients and Partition Coefficients Associated with Film Properties

The physical properties of the biofilm, including the enzyme-immobilized GOx layer and glucose limiting membrane (GLM layer), are associated with the partition coefficients and porosity factors. The partition coefficients of species in GLM layer are listed in Table 7-4. The porosity factors were used for modifying the diffusion coefficients of the species within different layers based on the Bruggeman Equation [65]. The diffusion coefficients of species within each layers are listed in Table 4-3.

7.1.4 Homogeneous and Heterogeneous Reaction Rate Constants

The rate constants of the homogeneous and heterogeneous reactions are chosen based on Gao et al. [1] and matching with experimental polarization curves. One example of the default reaction rate constants for model with PBS buffer is shown in Table 7-6. The

Table 7-5. Diffusion coefficients of species in GOx layer and GLM layer of the sensor for PBS model.

| Species | $D_{GOx,i} \times 10^5 (\text{cm}^2/\text{s})$ | $D_{GLM,i} \times 10^5 (\text{cm}^2/\text{s})$ |
|------------------------------------------|------------------------------------------------|------------------------------------------------|
| Glucose, gluconic acid and gluconate ion | 0.576 | 0.122 |
| Glucose oxidase enzyme | 0 | 0 |
| Oxygen O_2 | 1.97 | 1.03 |
| Hydrogen peroxide H_2O_2 | 0.732 | 1.098 |
| Hydrogen ion H^+ | 7.44 | 3.91 |
| Hydroxide ion OH^- | 4.24 | 2.23 |
| Phosphoric acid H_3PO_4 | 0.180 | 0.378 |
| Dihydrogen phosphate ion $H_2PO_4^-$ | 0.1918 | 0.403 |
| Hydrogen phosphate ion HPO_4^{2-} | 0.1518 | 0.319 |
| Phosphate ion PO_4^{3-} | 0.1648 | 0.346 |

equilibrium constants of PBS buffer was modified based on solution activity and ionic strength. The concentrations of the buffer species and equilibrated pH match with the experimental conditions.

7.1.5 Other Operation Parameters

The sensor operation conditions can vary with parameters including applied potential, pH in the bulk, values of Constant-Phase Element(CPE) and ohmic resistance, listed in Table 7-7 and initial concentrations of the species in Table 7.1.2.

7.2 Parameters Associated with Sensor Failure Mechanism

There are many reasons can cause sensor failure and provide inaccurate reading, such as enzyme deactivation, biofouling, oxygen deficiency, electrode poisoning, interfering species and membrane deteriorating. The parameters in the model can be used to study the sensor failure mechanism are listed in Table 7-8.

Table 7-6. Homogeneous and Heterogeneous Rate Constants for One-Dimensional Mathematical Model for Continuous Glucose Monitor with Phosphate Buffer Saline.

| Parameter | Symbol | Value | Units |
|------------------------------------------------------------------|----------------------------|------------------------|------------------------------|
| Homogeneous rate constant 1 | k_{f1} | 10^9 | $\text{cm}^3/\text{mol s}$ |
| Homogeneous equilibrium constant 1 | K_{eq1} | 10^7 | cm^3/mol |
| Homogeneous rate constant 2 | k_{f2} | 10^3 | s^{-1} |
| Homogeneous rate constant 3 | k_{f3} | 10^9 | $\text{cm}^3/\text{mol s}$ |
| Homogeneous equilibrium constant 3 | K_{eq3} | 10^7 | cm^3/mol |
| Homogeneous rate constant 4 | k_{f4} | 10^9 | s^{-1} |
| Homogeneous rate constant 5 | k_{f5} | 6×10^{-3} | s^{-1} |
| Homogeneous equilibrium constant 5 | K_{eq5} | 1.74 | dimensionless |
| Homogeneous rate constant 6 | k_{f6} | 3.32×10^{-6} | $\text{cm}^3/\text{mol s}$ |
| Homogeneous equilibrium constant 6 | K_{eq6} | 2.37×10^{-20} | s^{-1} |
| Homogeneous equilibrium constant 7 | K_{eq7} | 2×10^{-4} | $(\text{mol}/\text{cm}^3)^2$ |
| Homogeneous equilibrium constant 8 | K_{eq8} | 2×10^{-6} | mol/cm^3 |
| Homogeneous equilibrium constant 9 | K_{eq9} | 3.95×10^{-11} | mol/cm^3 |
| Homogeneous equilibrium constant 10 | K_{eq10} | 1.2×10^{-5} | mol/cm^3 |
| Homogeneous equilibrium constant 11 | K_{eq11} | 2.05×10^{-10} | mol/cm^3 |
| Homogeneous equilibrium constant 12 | K_{eq12} | 2.16×10^{-15} | mol/cm^3 |
| Heterogeneous rate constant for H_2O_2 oxidation | $K_{\text{H}_2\text{O}_2}$ | 20 | A cm/mol |
| Heterogeneous coefficient for H_2O_2 oxidation | $b_{\text{H}_2\text{O}_2}$ | 20.4 | V^{-1} |
| Heterogeneous rate constant for O_2 reduction | K_{O_2} | 5×10^{-6} | A cm/mol |
| Heterogeneous coefficients for O_2 reduction | b_{O_2} | 38.4 | V^{-1} |
| Heterogeneous rate constant for H_2O_2 reduction | K_{red} | 5×10^4 | A cm/mol |
| Heterogeneous coefficients for H_2O_2 reduction | b_{red} | 32 | V^{-1} |

Table 7-7. Sensor operation parameters

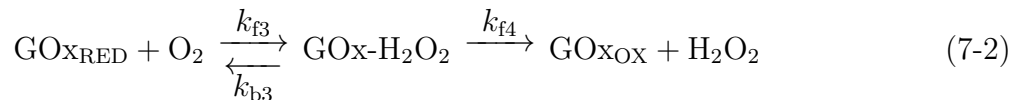
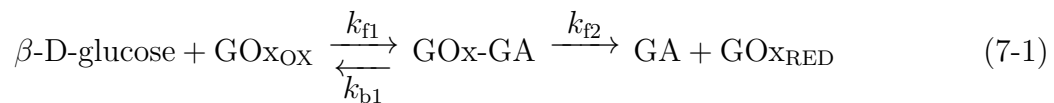
| Parameter | Value |
|-------------------------|-------------------------------------------|
| Potential | 0.4 V |
| pH | 7.4 |
| CPE value, Q | $2.61 \times 10^{-5} \text{ F/s}^{(1-a)}$ |
| CPE value, α | 0.85 |
| Ohmic resistance, R_e | 10 Ω |

Table 7-8. Parameters Associated with Sensor Failure Mechanism

| Enzyme Deactivation | Oxygen deficiency | Encapsulation or biofouling |
|---------------------------------------|------------------------------------------------------------------|--------------------------------|
| Total enzyme concentration | Oxygen partial pressure | Diffusion coefficients in bulk |
| pH-dependent enzyme activity | Oxygen solubility | Partition coefficients |
| Temperature-dependent enzyme activity | Oxygen partition coefficient Diffusion coefficients of oxygen | Diffusion layer thickness |
| Electrode poisoning | Interfering Species | Membrane Deteriorating |
| Heterogeneous rate constants | Active surface area | Diffusion coefficients in GLM |
| Tafel b values | Heterogeneous rate constants | Partition coefficients |
| Active surface area | Surface concentration | |

7.2.1 Parameters Associated with Enzyme Deactivation

In common CGMs, there are two primary layers on the electrode surface[1], the GOx layer and the GLM layer. In the GOx layer of the sensor, the glucose oxidase (GOx) enzyme is immobilized by organic crosslinkers. The glucose oxidase enzyme exists in two forms, the oxidized form (GOx_{OX}) and the reduced form (GOx_{RED}), as shown in Equation 7-1 and 7-2. The catalytic enzymatic reaction within GOx layer recycles the two forms of enzyme by redox reactions with oxygen and hydrogen peroxide.



where GOx_{OX} is the oxidized form of glucose oxidase, GOx-GA is the complex intermediate of the reaction of glucose and GOx_{OX} , GOx_{RED} is the reduced form of glucose oxidase, GA is gluconic acid, and $\text{GOx-H}_2\text{O}_2$ is the complex intermediate of the reaction of GOx_{RED} and oxygen. The glucose oxidase that is reduced by reaction (7-1) is regenerated by reaction (7-2).

There are many reasons to cause enzyme deactivation, such as pH, temperature and hydrogen peroxide poisoning. The most direct cause is that it will change the total amount of enzyme within the GOx layer. The temperature also influences the enzyme activity, which leads to decrease of reaction kinetics. The input model parameters associated with enzyme deactivation are total enzyme concentration, pH-dependent enzyme concentration and temperature-dependent enzymatic reaction rate constants.

The enzyme in the sensor exists in 6 forms, the oxidized glucose oxidase (GOx_{OX}), reduced glucose oxidase (GOx_{RED}), the intermediate enzyme complex species (GOx-GA and $\text{GOx-H}_2\text{O}_2$), and the pH-deactivated enzyme complex species ($\text{H}^+\text{GOx}_{\text{OX}}$ and $\text{GOx}_{\text{RED}}^-$). The initial input of the total enzyme concentration is distributed equally into

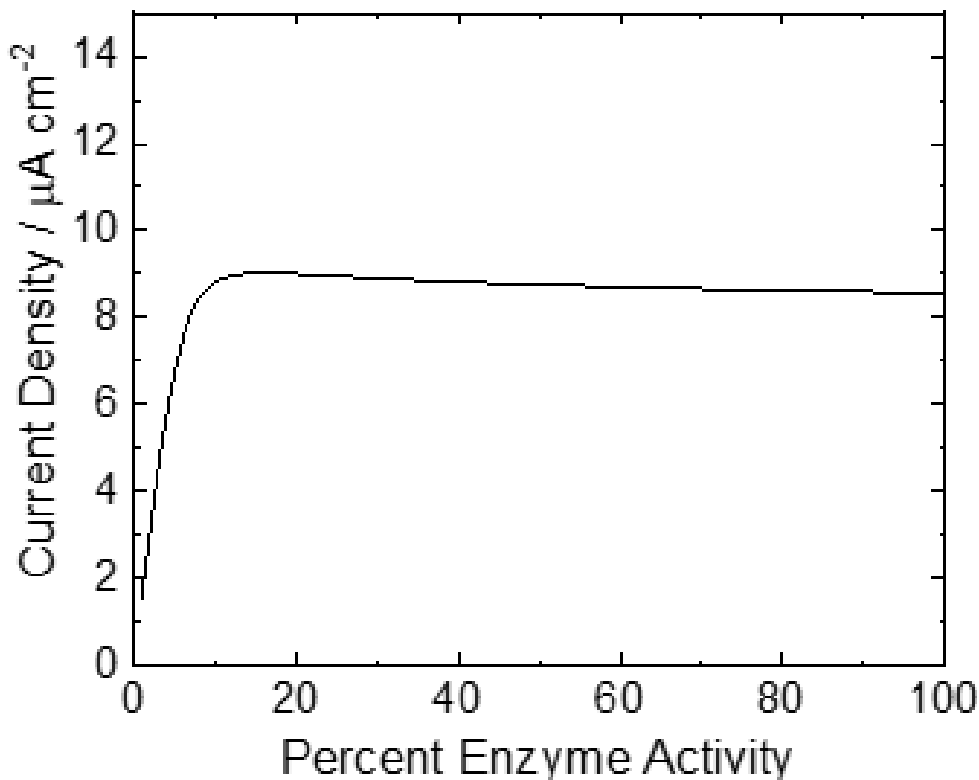


Figure 7-3. Sensor response curve with glucose oxidase enzyme (GOx) concentration as a parameter, 200 mg/dL of glucose and 5% of oxygen partial pressure.

these 6 forms and the concentration distribution of each forms at steady state can be calculated by the model.

The default value of the maximum amount of enzyme concentration is $3.56 \times 10^{-7} \text{ mol cm}^{-3}$ based on GOx activie 20000U/mL, GOx specific activity 350 U/mg protein, GOx concentration 0.0057 g/ml and molecular weight 160000 Da.

Figure 7-3 shows the current density as a function of enzyme concentration. With enzyme concentration decreasing, the current density initially maintains a plateau with slight rising to a peak current density, and then drop dramatically due to further enzyme deactivation.

The enzyme concentrations associated with current density decrease were chosen to explore the steady-state profiles, in Figure 7-4. According to the glucose concentration profile at steady-state, in Figure 7-4A, with enzyme concentration deactivated to 10%

of the maximum amount, the glucose diffused into the sensor can not be completely consumed. So the current density drop was associated with the decrease in consumption of glucose in the GOx layer. The concentration profile of the active oxidized GOx is shown in Figure 7-4C. Even with sufficient amount of oxygen in the GOx helping recycle the enzyme, the concentration of GO_xO_x in GOx layer was very low with total enzyme concentration decreasing. The enzymatic reaction rate also decreased as the total amount of enzyme decreasing. The maximum distribution of the reaction rate profile shifted from interface of the GOx and GLM layers to the electrode surface.

The diffusion impedance is shown in Figure 7-5. The diffusion impedance with maximum amount of enzyme (black) appeared as two loops, the high-frequency Gerischer impedance and the low-frequency semicircle associated with mass transfer. The low-frequency diffusion impedance associated with the mass-transfer of hydrogen peroxide dominated, due to the reaction mostly happened at the interface of GOx and GLM layers. With enzyme deactivation, the low-frequency loop shrank and merges with the Gerishcer impedance. With further enzyme deactivation, the diffusion impedance increased in size.

The overall impedance is partial capacitive loop in Figure 7-6. The overall impedance decreased and then increased in size with enzyme deactivation. This was due to initially, the overall impedance was dominated by the low-frequency diffusion impedance, which decreased in size as reactions shift towards the electrode with enzyme deactivation. With further enzyme deactivation, the overall impedance was dominated by the high-frequency Gerischer impedance, which increased in size as further enzyme deactivated.

7.2.2 Parameters Associated with Oxygen Deficiency

The oxygen plays an important role in the chemistry and physics of CGM. In the enzymatic reactions, the oxygen oxidized the reduced form of glucose oxidase to recycle the enzyme. The oxygen mainly diffused into the sensor from the tissue through GLM layer. The oxygen was also generated electrochemically by oxidation reaction of hydrogen

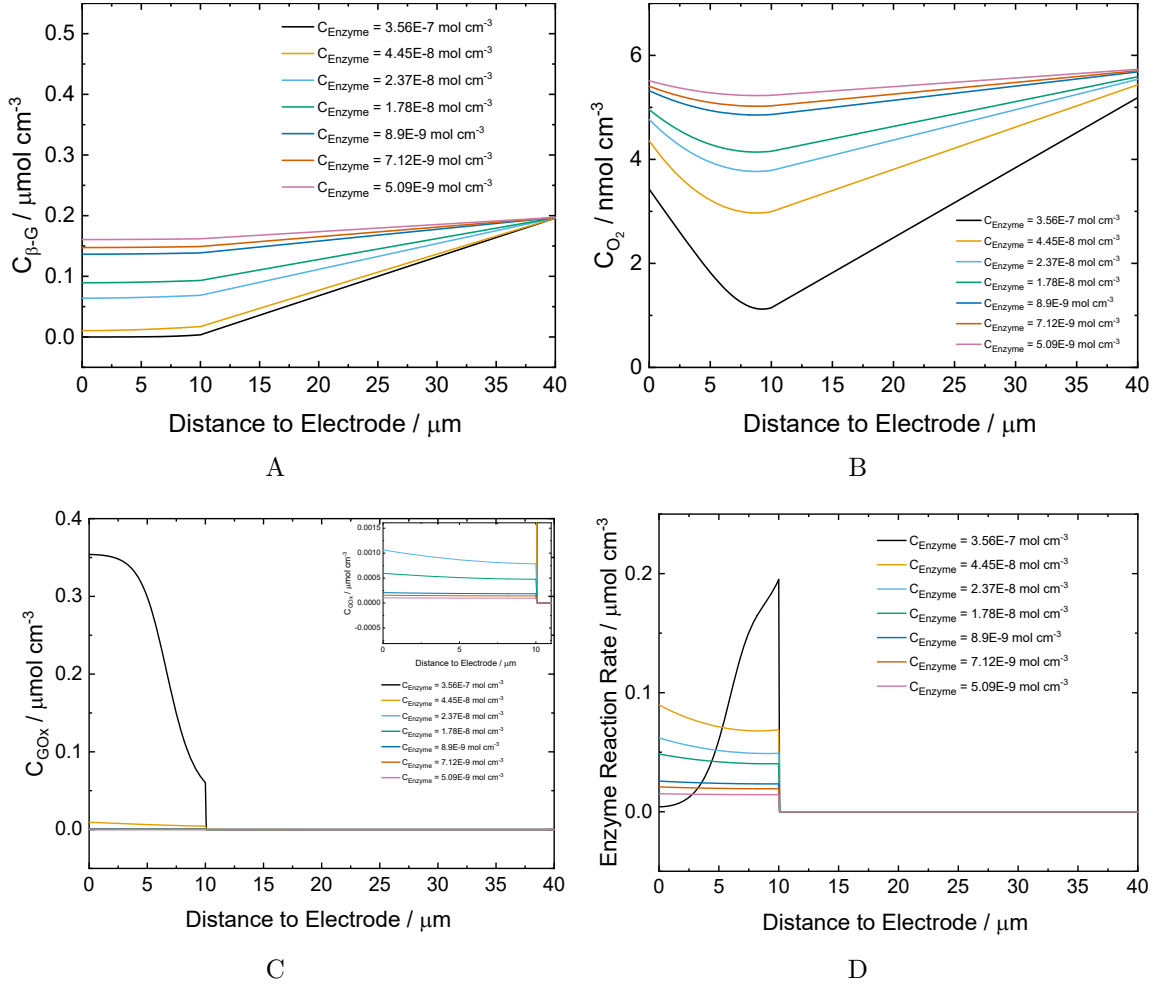


Figure 7-4. Calculated steady-state concentration profiles and reaction rate distribution as a function of distance to the electrode with enzyme concentration as a parameter: (a) Beta-glucose concentration profile (b) Oxygen concentration profile (c) Oxidized glucose oxidase concentration profile (d) Enzymatic reaction rate distribution.

peroxide. When the oxygen diffused into the sensor was sufficient, the enzymatic reactions happened near the interface between the GOx and GLM layers. However, if there was oxygen deficiency, then the enzymatic reaction depends on the electrochemical generated oxygen. The enzymatic reaction rate profile maximizes near the electrode surface. The corresponding impedance responses were different. Therefore, the oxygen in the sensor determined the reaction mechanism and reading accuracy of the sensor.

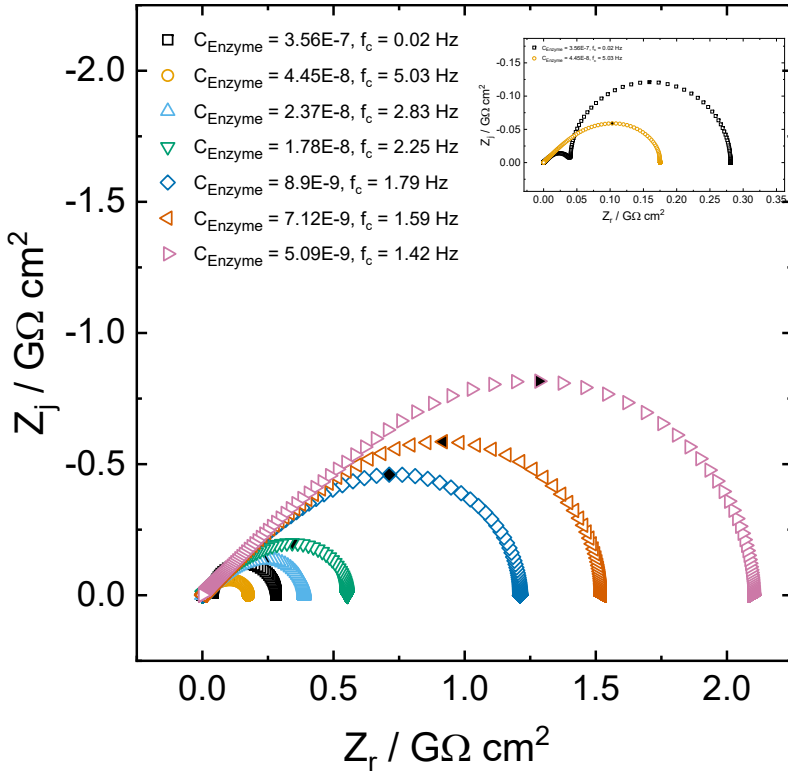


Figure 7-5. Diffusion impedance with enzyme concentration as a parameter, 400 mg/dL of glucose and 5% of oxygen partial pressure.

In the human body, depending on the sensor location and the individual variability, the oxygen partial pressure could vary between 1% ~ 5% (atm). Due to the foreign body response to the implanted sensor, an encapsulation layer could grow on the sensor. This encapsulation may also cause oxygen deficiency. The physical properties of the sensor films may also influence the amount of oxygen diffuses into the sensor.

In Figure 7-7, the current density was a function of oxygen partial pressure. At 0.4 V applied potential, as oxygen partial pressure decreases, the current density maintained at a plateau at first, increased to a peak, then dropped as further oxygen partial pressure decreases.

7.2.2.1 Partial pressure of oxygen

It is shown in Figure 7-8, the oxygen curve depended on applied potential. At 0.4V applied potential, the current density was affected by the amount of oxygen when the

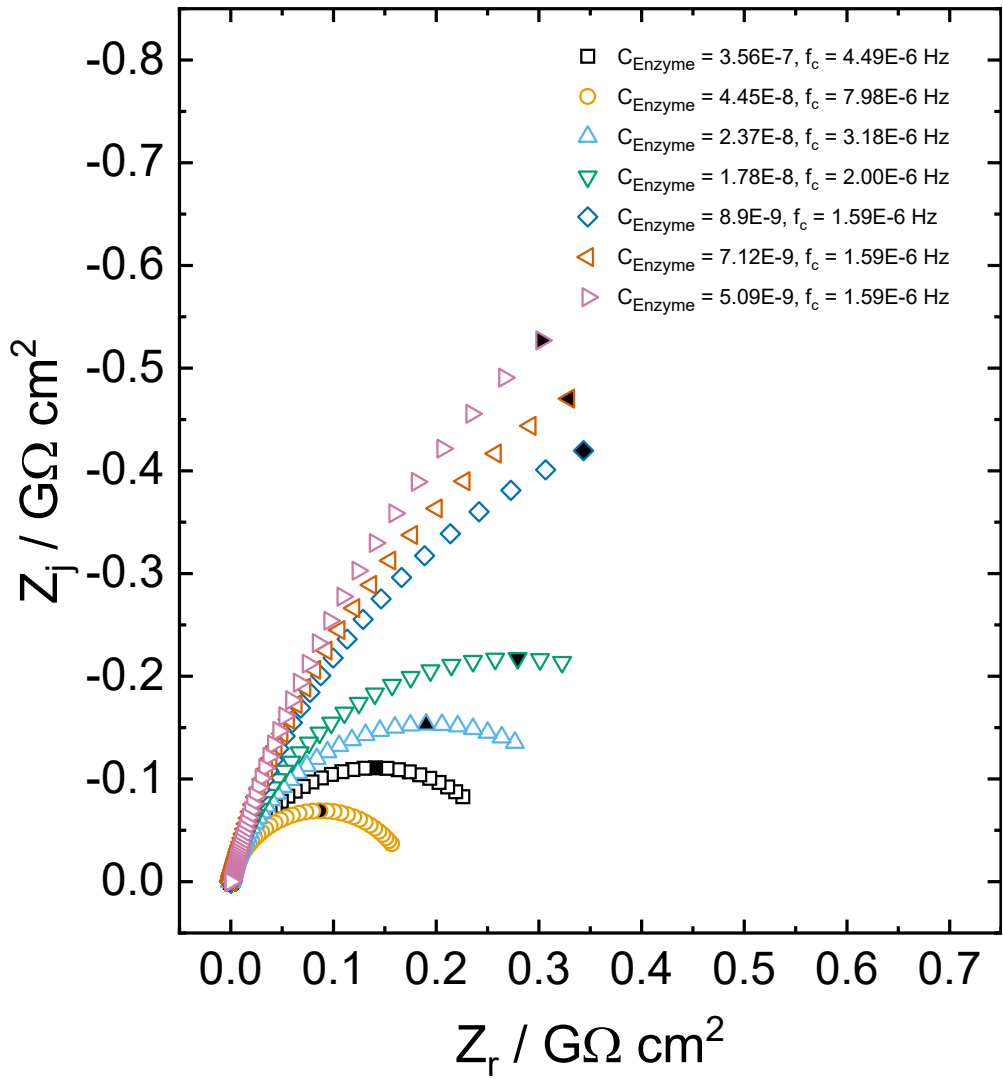


Figure 7-6. Overall impedance with enzyme concentration as a parameter, 400 mg/dL of glucose and 5% of oxygen partial pressure.

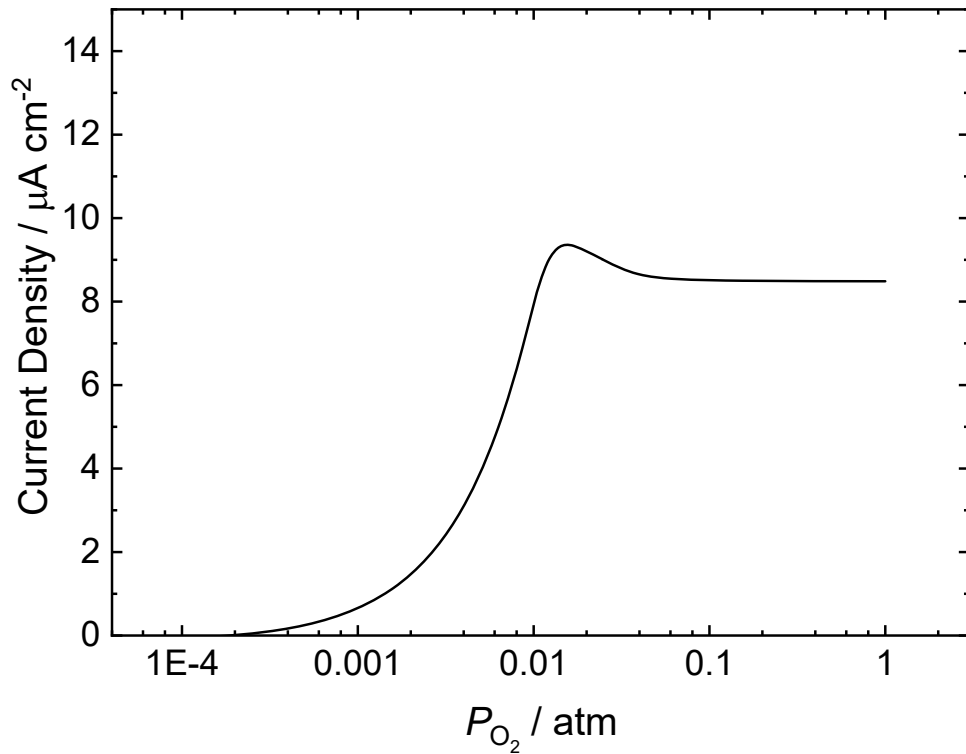


Figure 7-7. Sensor response curve with oxygen partial pressure as a parameter, 200 mg/dL of glucose and 100% of enzyme concentration.

partial pressure was below 0.01 atm. The current density was more sensitive with respect to partial pressure of O₂ at 0.2 V applied potential. Current density was affected by the partial pressure of oxygen. The sensitivity to oxygen depended on applied potential.

The polarization curve, which was the current density as function of applied potential, is shown in Figure 7-9. Decreasing the partial pressure of oxygen from 0.06 atm to 0.01 atm only affected the current density below the mass-transfer limited plateau. Further decreasing the partial pressure of O₂ from 0.01 atm to 0.001 atm decreased the limiting current density.

The steady-state simulation help us to understand the reaction mechanism. The location of maximum homogeneous reaction rate shifted towards the electrode surface as oxygen partial pressure decreased.

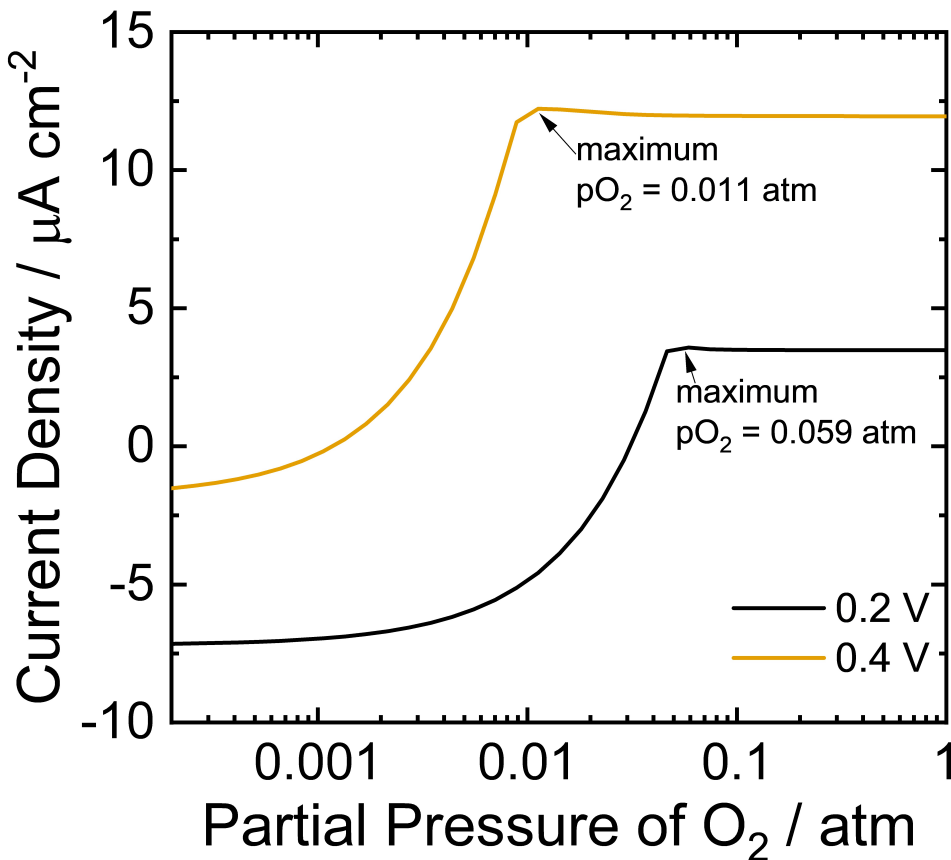


Figure 7-8. Sensor response curve with oxygen partial pressure as a parameter, 400 mg/dL of glucose and 100% of enzyme concentration, at 0.4 V applied potential (orange) and 0.2 V applied potential (0.2 V).

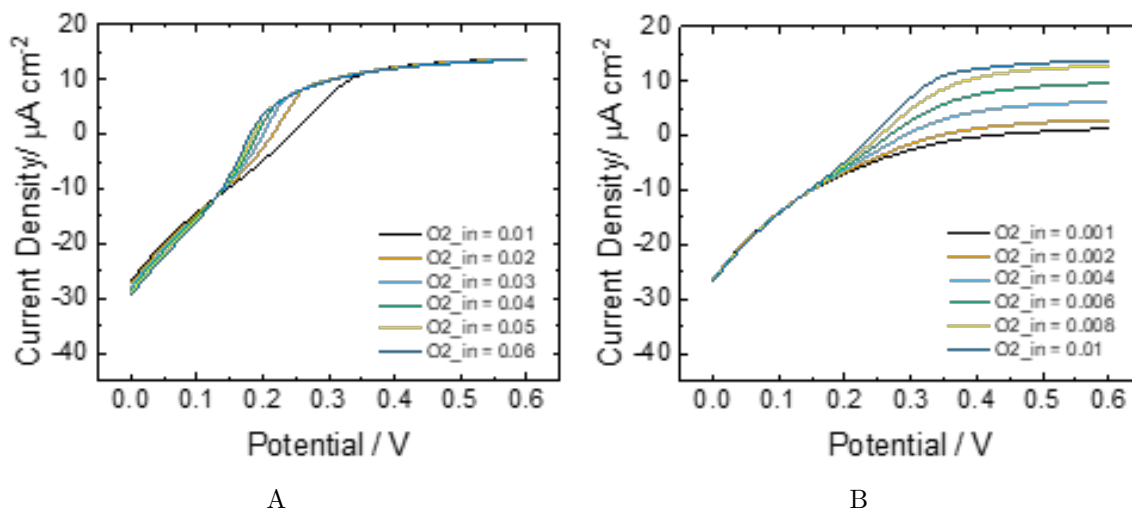


Figure 7-9. Calculated polarization curve with oxygen partial as a parameter: (a) Decreasing partial pressure of oxygen from 0.06 atm to 0.01 atm (b) Decreasing partial pressure of oxygen from 0.01 atm to 0.001 atm.

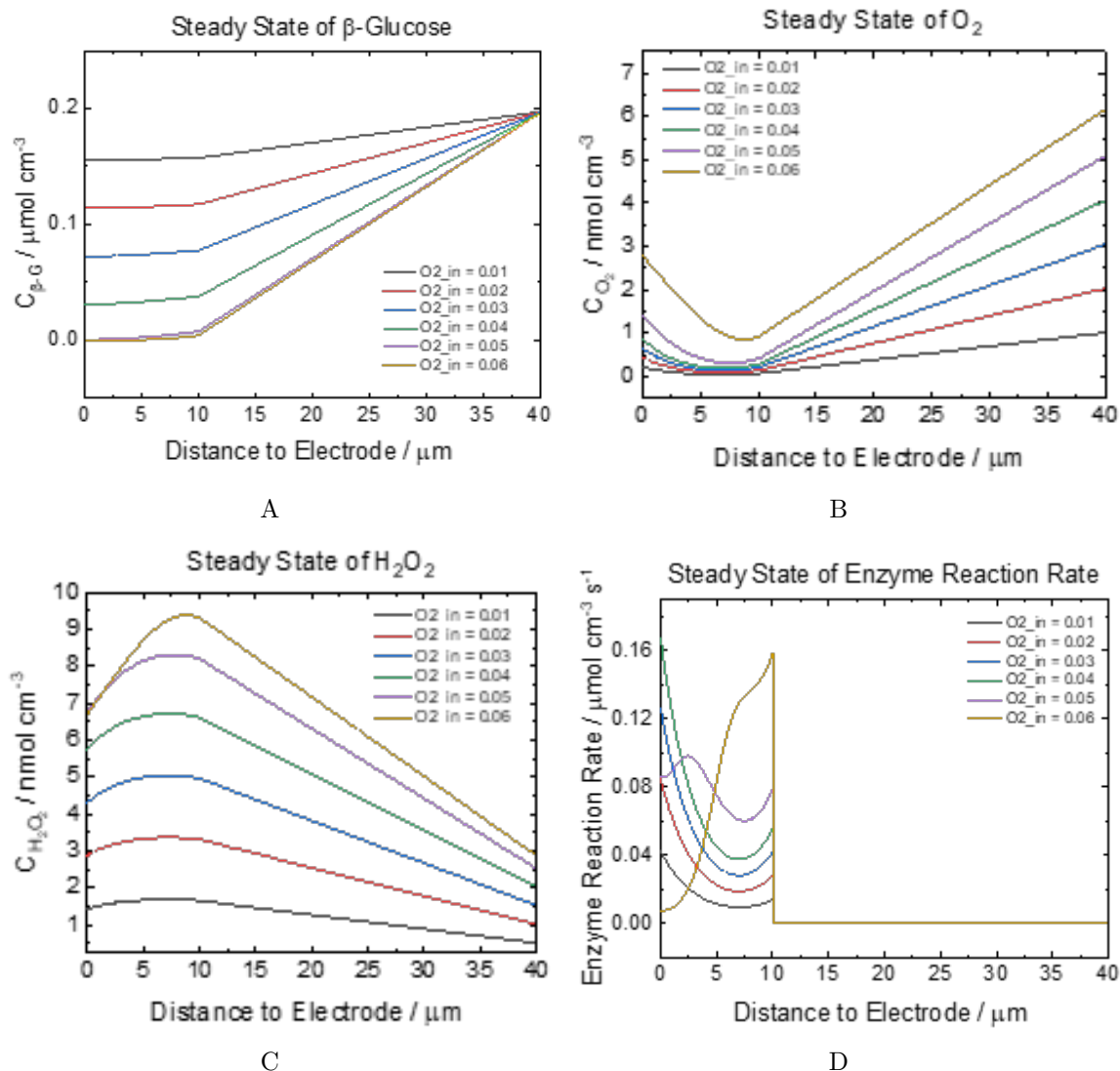


Figure 7-10. Calculated steady-state concentration profiles and reaction rate distribution as a function of distance to the electrode with oxygen partial pressure as a parameter: (a) Beta-glucose concentration profile (b) Oxygen concentration profile (c) Hydrogen peroxide concentration profile (d) Enzymatic reaction rate distribution.

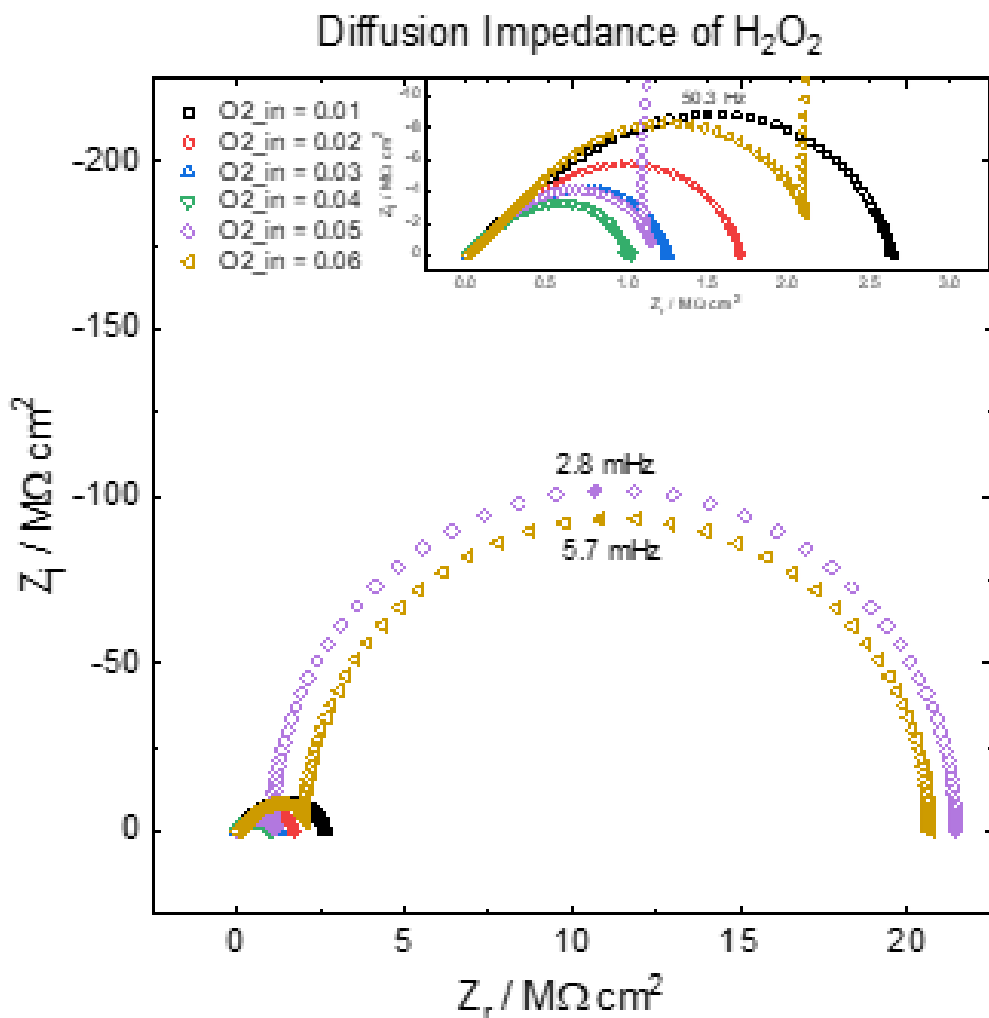


Figure 7-11. Diffusion impedance with oxygen partial pressure as a parameter, 400 mg/dL of glucose and 100% of enzyme concentration at 0.2 V applied potential.

The diffusion impedance with oxygen partial pressure as a parameter is shown in Figure 7-11. The diffusion impedance appears as two loops, the high-frequency Gerischer impedance and the low-frequency semicircle associated with mass transfer. The low-frequency diffusion impedance associated with the mass-transfer of hydrogen peroxide dominated, due to the reaction mostly happened at the interface of GOx and GLM layer. With oxygen deficiency, the low-frequency loop shrank and merged with the Gerishcer impedance. With further oxygen partial pressure decreasing, the diffusion impedance increased in size.

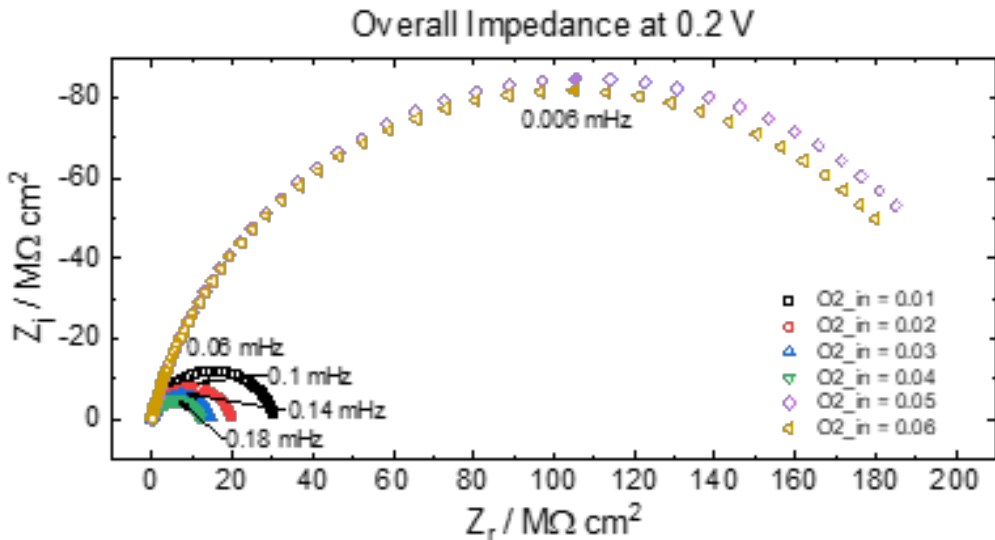


Figure 7-12. Overall impedance with oxygen partial pressure as a parameter, 400 mg/dL of glucose and 100% of enzyme concentration at 0.2 V applied potential.

The overall impedance is partial depressed semicircle, shown in Figure 7-12. The overall impedance increases in size with oxygen partial pressure decreases and then drops to a smaller magnitude. At high oxygen partial pressure, the overall impedance was dominated by the low-frequency diffusion impedance, which decreased in size as reactions shifted towards the electrode with oxygen partial pressure decreasing. With further oxygen partial pressure decreasing, the overall impedance was dominated by the high-frequency Gerischer impedance, which increased in size as further oxygen partial pressure decreasing.

The characteristic frequency of overall impedance at lower applied potential can help us determine if the impedance is dominated by diffusion impedance or by the Gerischer impedance, which can help differentiate the case of oxygen deficiency.

7.2.2.2 Partition coefficient of oxygen

The diffusion impedance with partition coefficient of oxygen as a parameter is shown in Figure 7-14. The diffusion impedance appears as two loops, the high-frequency Gerischer impedance and the low-frequency semicircle associated with mass transfer. The low-frequency diffusion impedance associated with the mass-transfer of hydrogen peroxide

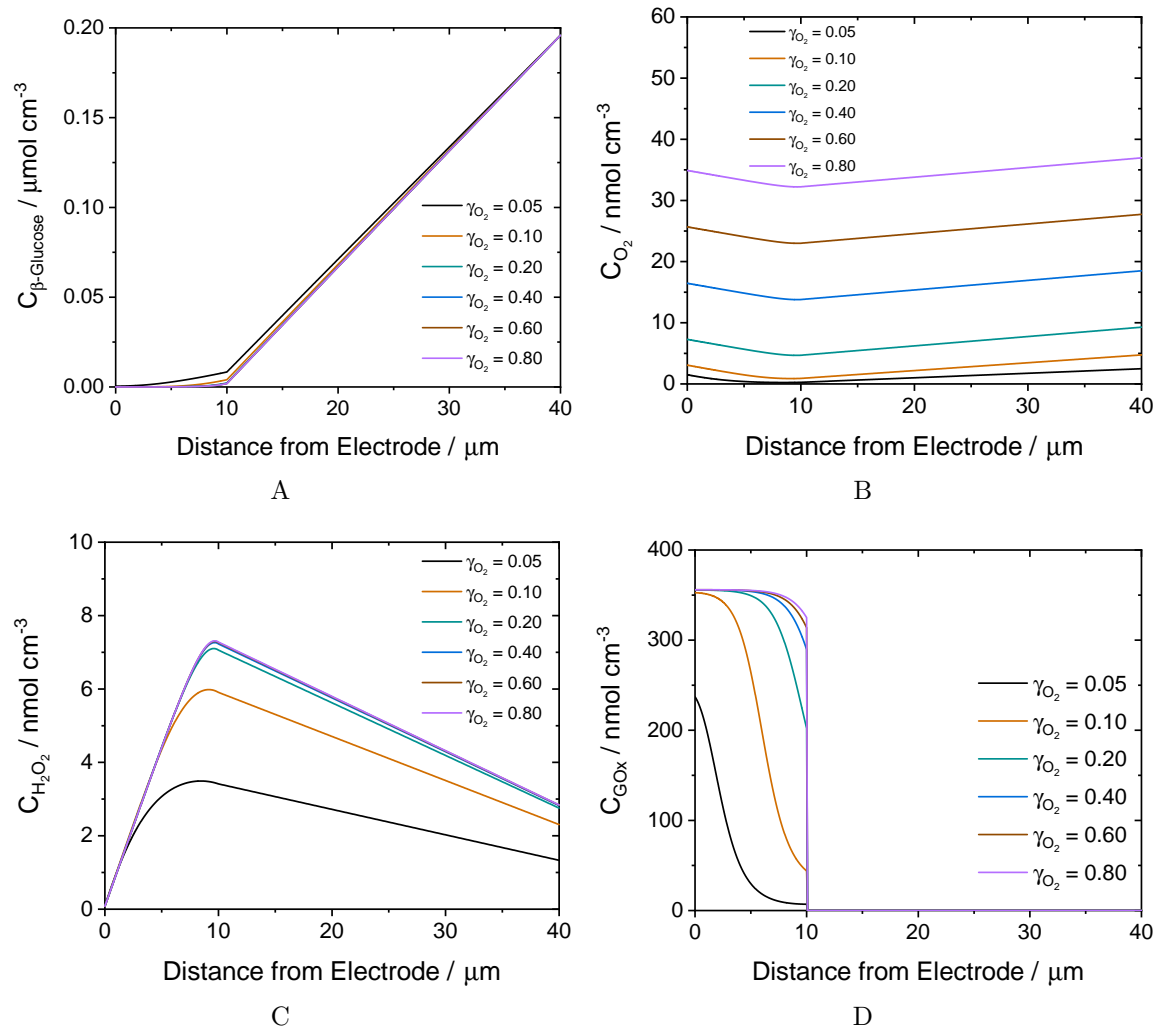


Figure 7-13. Calculated steady-state concentration profiles and reaction rate distribution as a function of distance to the electrode with oxygen partition coefficient as a parameter: (a) Beta-glucose concentration profile (b) Oxygen concentration profile (c) Hydrogen peroxide concentration profile (d) Enzymatic reaction rate distribution.

dominant, due to the reaction mostly happen at the interface of GOx and GLM layer.

With oxygen deficiency, the low-frequency loop shrinks and merges with the Gerishcer impedance. With further oxygen partial pressure decreasing, the diffusion impedance increases in size.

The overall impedance is partial depressed semicircle in Figure 7-15. The overall impedance increases in size with oxygen partial pressure decreases and then drops to a

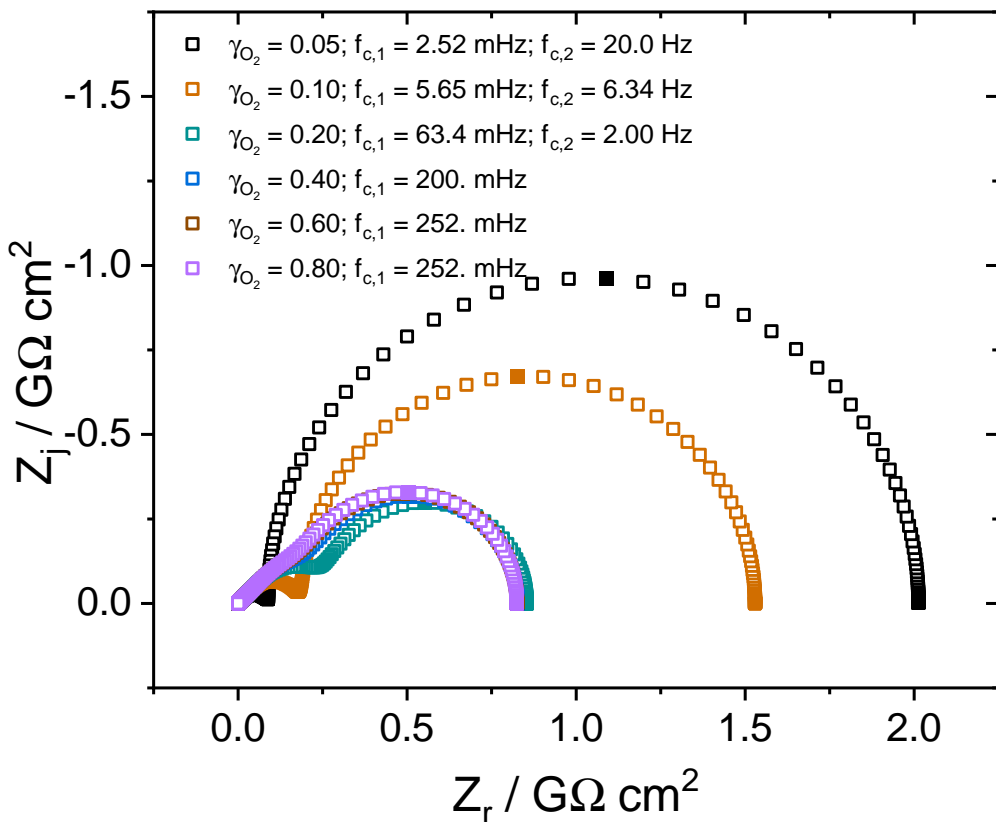


Figure 7-14. Diffusion impedance with partition coefficient of oxygen as a parameter, 400 mg/dL of glucose and 100% of enzyme concentration at 0.4 V applied potential.

smaller magnitude. This is due to initially, the overall impedance is dominated by the low-frequency diffusion impedance, which decreases in size as reactions shift towards the electrode with oxygen partial pressure decreasing. With further oxygen partial pressure decreasing, the overall impedance is dominated by the high-frequency Gerischer impedance, which increases in size as further oxygen partial pressure decreasing.

7.2.3 Parameters Associated with Encapsulation

Due to the foreign body response, biofouling occur after the implantation of sensor in the subcutaneous tissue. An encapsulation layer containing micro phages, blood vessels, proteins and so on grows on the sensor after a few days of implantation. This encapsulation layer may consume or inhibit the diffusion of glucose and oxygen from subcutaneous fluid into the sensor. In the present mathematical model of the continuous

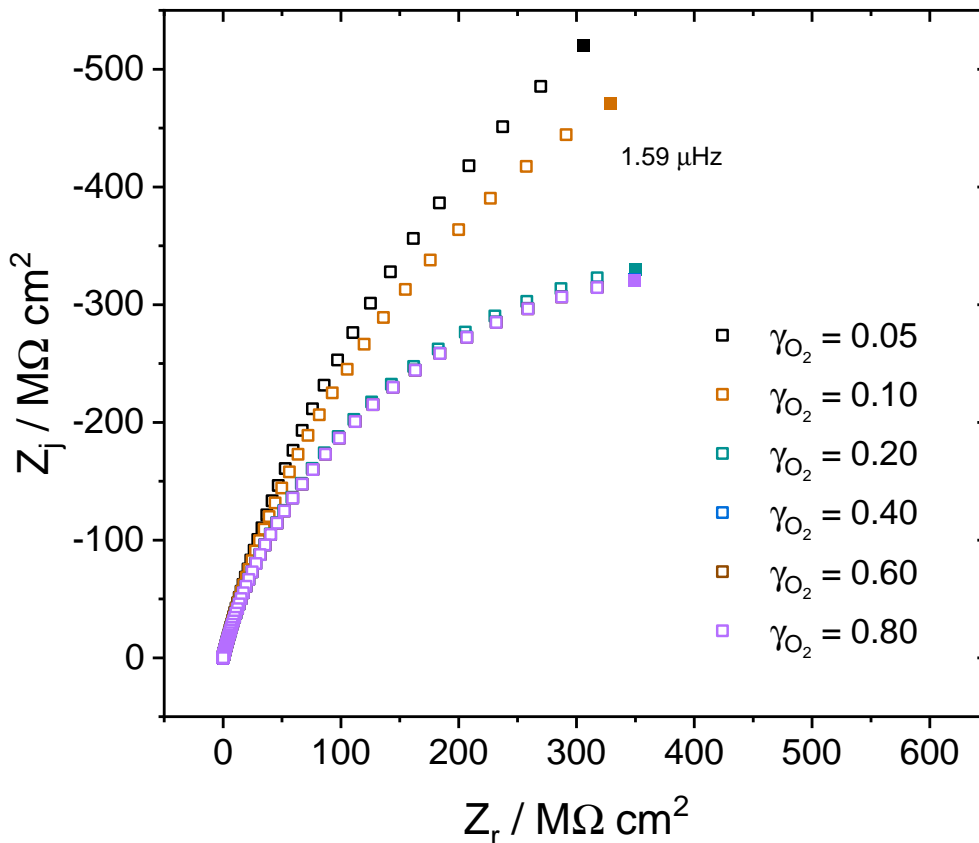


Figure 7-15. Overall impedance with partition coefficient of oxygen as a parameter, 400 mg/dL of glucose and 100% of enzyme concentration at 0.4 V applied potential.

glucose monitor, two kinds of parameters are associated encapsulation layer and may describe the sensor failure mechanism due to biofouling to some extent. The parameters are the thickness of the diffusion layer in tissue and the diffusion coefficients of relevant species in bulk.

7.3 Parameters Associated with Sensor Design

The presented mathematical model is one-dimensional. The system parameters associated with sensor design are the thickness of the glucose oxidase layer and glucose limiting membrane. To study the influence of geometry of the electrode on impedance, a 2-D or 3-D model need to be further developed.

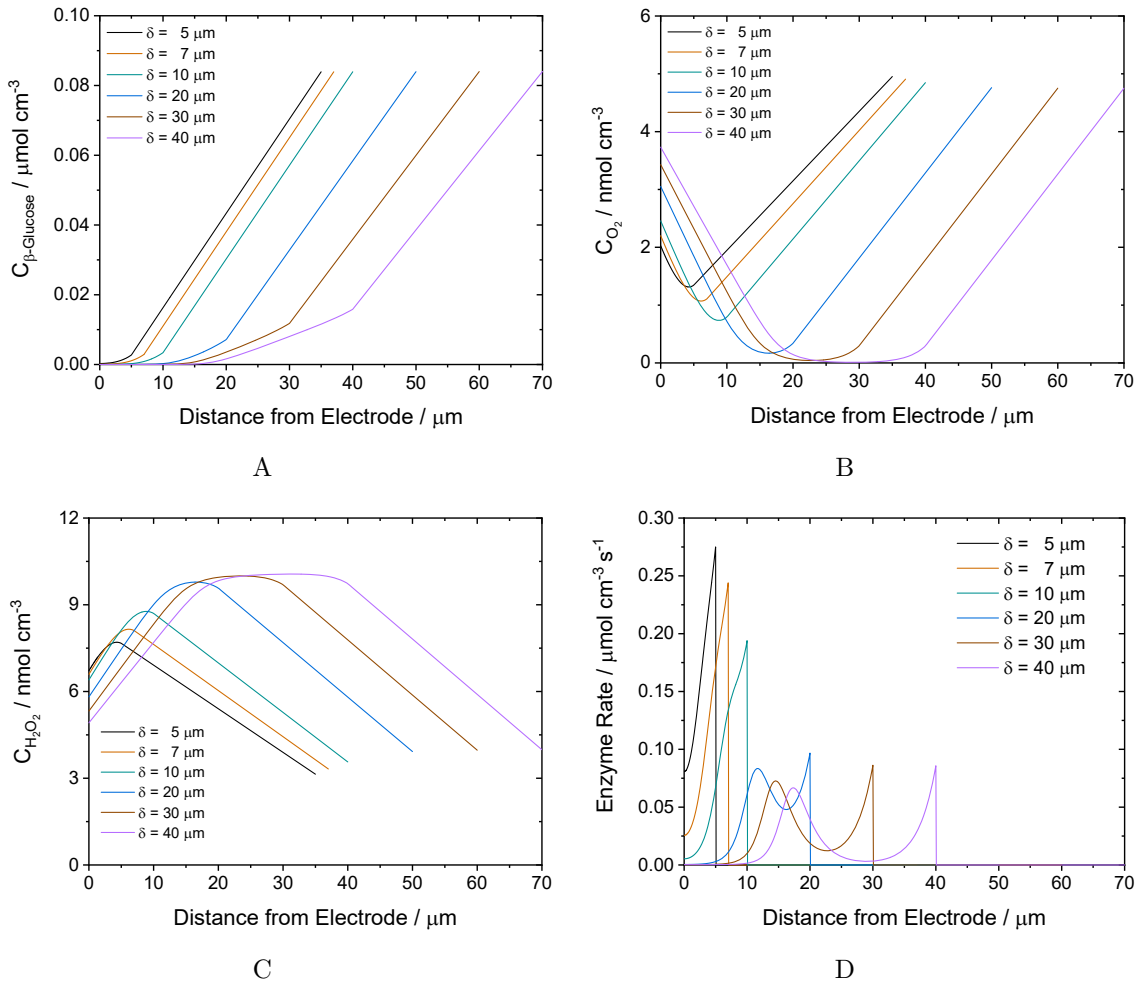


Figure 7-16. Calculated steady-state concentration profiles and reaction rate distribution as a function of distance to the electrode with thickness of GOx layer as a parameter: (a) Beta-glucose concentration profile (b) Oxygen concentration profile (c) Hydrogen peroxide concentration profile (d) Enzymatic reaction rate distribution.

7.3.1 Glucose oxidase layer thickness

The diffusion impedance with thickness of GOx layer as a parameter is shown in Figure 7-17. The diffusion impedance appears as two loops, the high-frequency Gerischer impedance and the low-frequency semicircle associated with mass transfer. The low-frequency diffusion impedance associated with the mass-transfer of hydrogen peroxide dominant, due to the reaction mostly happen at the interface of GOx and GLM layer. With oxygen deficiency, the low-frequency loop shrinks and merges with

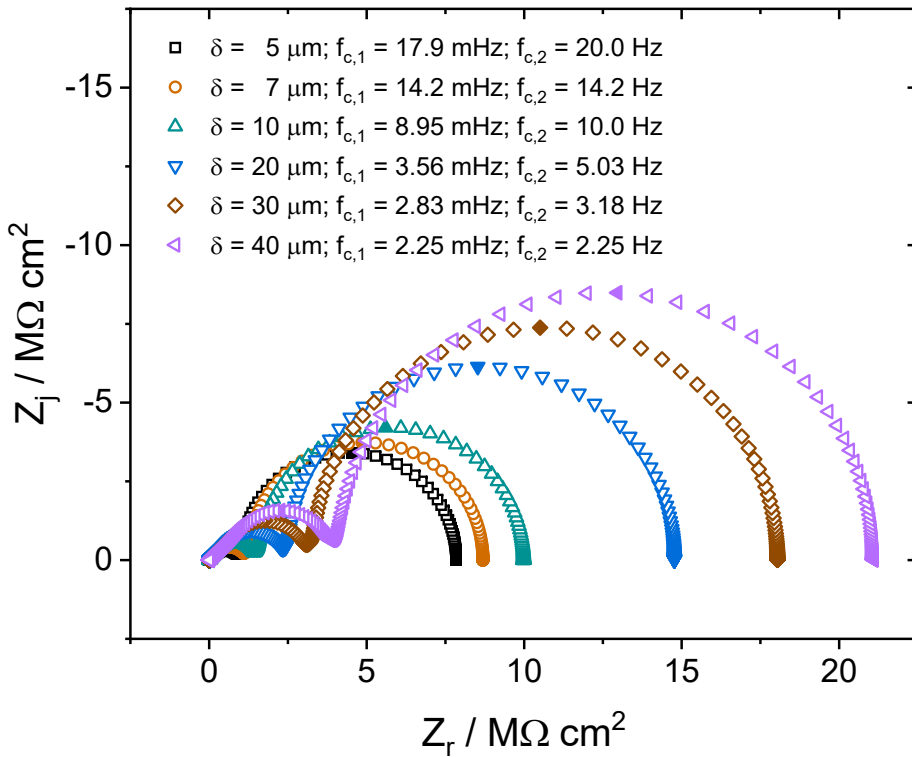


Figure 7-17. Diffusion impedance with thickness of GOx layer as a parameter, 400 mg/dL of glucose and 100% of enzyme concentration at 0.4 V applied potential.

the Gerishcer impedance. With further oxygen partial pressure decreasing, the diffusion impedance increases in size.

The overall impedance is partial depressed semicircle in Figure 7-18. The overall impedance increases in size with oxygen partial pressure decreases and then drops to a smaller magnitude. This is due to initially, the overall impedance is dominated by the low-frequency diffusion impedance, which decreases in size as reactions shift towards the electrode with oxygen partial pressure decreasing. With further oxygen partial pressure decreasing, the overall impedance is dominated by the high-frequency Gerischer impedance, which increases in size as further oxygen partial pressure decreasing.

7.3.2 Glucose limiting membrane thickness

The thickness of glucose limiting membrane (GLM) is an essential parameter associated with sensor design. If GLM layer is too thin, too much glucose diffuses into

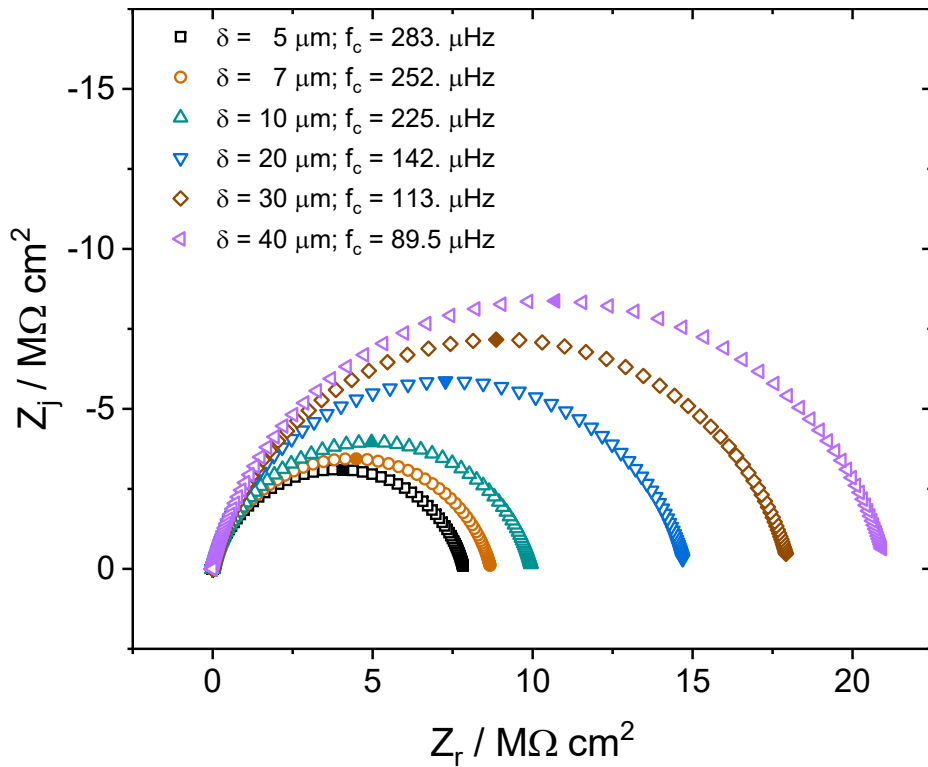


Figure 7-18. Overall impedance with thickness of GOx layer as a parameter, 400 mg/dL of glucose and 100% of enzyme concentration at 0.4 V applied potential.

the sensor may cause oxygen deficiency, which leads to false reading. If GLM layer is too thick, it reduces the amount of oxygen and glucose diffusing in, which leads to lower current density.

The polarization curve with GLM layer thickness as a parameter was simulated using the mathematical model with Bicarbonate Buffer Saline, in Figure 7-19. The limiting current density decreases as GLM layer thickness increases. The detailed study of the influence on oxygen curve, steady-state profiles and impedance response are shown at both 0.4 V applied potential at the mass-transfer limited plateau and 0.2 V applied potential at the kinetic controlled region.

At 0.4 V applied potential, the oxygen curve is shown in Figure 7-20. Steady-state profiles

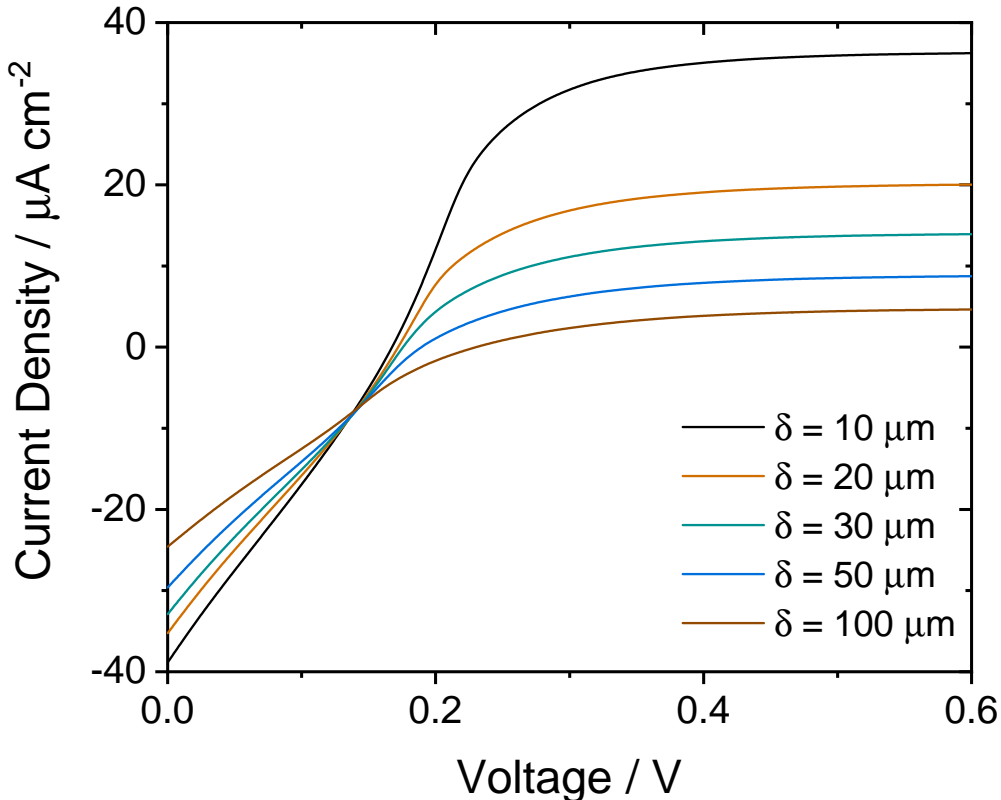


Figure 7-19. Polarization curve with GLM thickness as a parameter, 400 mg/dL of glucose and 5% of oxygen partial pressure.

7.4 Summary of Influence on Steady-State Profiles and Impedance

To match the experimental results, the values of parameters need to be optimized.

The polarization curve, oxygen curve and overall impedance can be measured experimentally. This section summarized the parameters that influence the polarization curve, oxygen curve and overall impedance.

The parameters that influence the polarization curve is summarized in Table 7.4. For the polarization curve, the anodic current slope were determined by the heterogeneous rate constants associated with hydrogen peroxide oxidation $K_{\text{H}_2\text{O}_2}$ and Tafel slope coefficient associated with hydrogen peroxide oxidation $b_{\text{H}_2\text{O}_2}$. The anodic current approached to a mass-transfer limited plateau at more positive applied potentials. The anodic mass-transfer limiting current density was influenced by the concentration, partition coefficient and diffusion coefficient of glucose. The slope and value of cathodic current

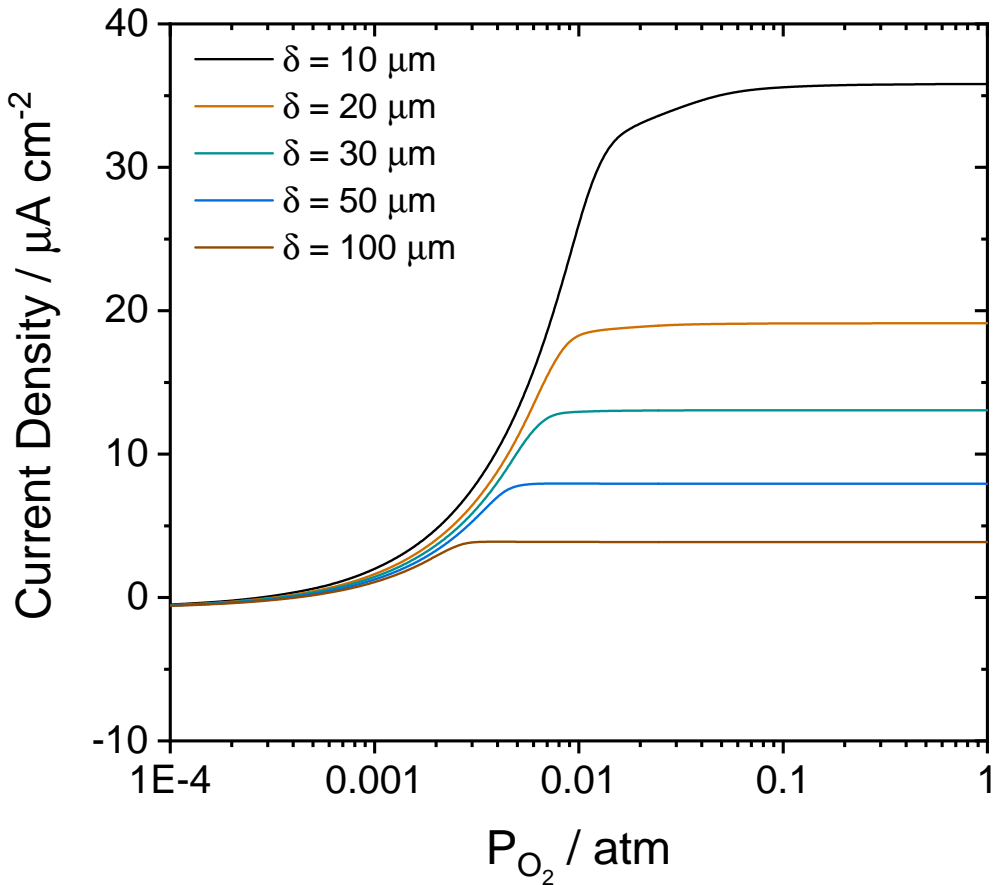


Figure 7-20. Oxygen curve with GLM thickness as a parameter at 0.4 V applied potential, 400 mg/dL of glucose and 5% of oxygen partial pressure.

Table 7-9. Parameters that Influence the Polarization Curve

| Parameters that Influence the Polarization Curve |
|-------------------------------------------------------------------|
| Heterogeneous rate constant $K_{\text{H}_2\text{O}_2}$ |
| Tafel b coefficient $b_{\text{H}_2\text{O}_2}$ |
| Glucose concentration |
| Glucose partition coefficient |
| Glucose diffusion coefficient |
| Layer thickness |
| Heterogeneous rate constant K_{red} and b_{red} |
| Heterogeneous rate constant K_{H} and b_{H} |

density was influenced by the heterogenous rate constants associated with hydrogen reduction reaction and hydrogen evolution reaction.

The parameters that influence the oxygen curve is summarized in Table 7.4. The oxygen curve determines how sensitive to oxygen deficiency the sensor is. The parameters

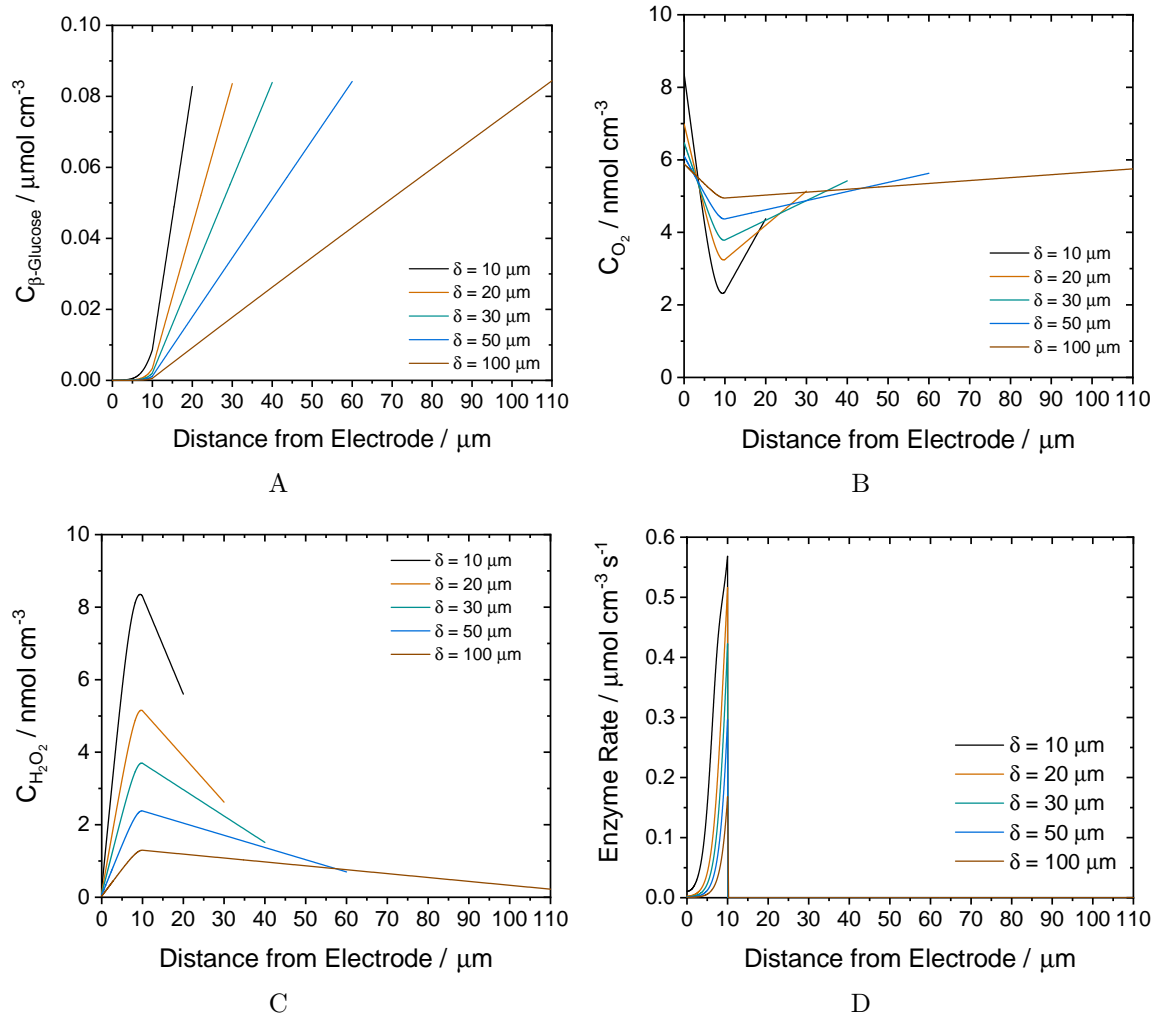


Figure 7-21. Calculated steady-state concentration profiles and reaction rate distribution as a function of distance to the electrode with GLM thickness as a parameter at 0.4 V applied potential: (a) Beta-glucose concentration profile (b) Oxygen concentration profile (c) Hydrogen peroxide concentration profile (d) Enzymatic reaction rate distribution.

associated with oxygen was directly relevant in shifting the oxygen curve, including oxygen partial pressure, partition coefficient, solubility, and diffusion coefficient. The homogeneous rate constants, heterogeneous rate constants, and applied potential that influence on the generation and consumption of oxygen also affected the oxygen curve. In addition, the diffusion coefficients of hydrogen peroxide and film thickness influenced the oxygen curve indirectly.

Table 7-10. Parameters that Influence the Oxygen Curve

| Parameters that Influence the Oxygen Curve |
|-------------------------------------------------------------------------------|
| Oxygen partial pressure |
| Oxygen partition coefficient |
| Oxygen solubility in water |
| Oxygen diffusion coefficient in GOx and GLM |
| Diffusion coefficients of hydrogen peroxide in GOx and GLM |
| Homogeneous rate constant associated with oxygen |
| Heterogeneous rate constants associated with oxygen consumption or generation |
| Applied Potential |
| Film thickness |

Table 7-11. Parameters that Influence the Impedance Response

| Parameters that Influence the Overall Impedance |
|----------------------------------------------------------------------------------|
| Ion partition coefficient |
| Diffusion coefficient of buffer species in GOx layer |
| Diffusion coefficient of H ₂ O ₂ in both GOx and GLM layer |
| Diffusion coefficient of H ⁺ in both GOx and GLM layer |

Impedance response was shown more sensitive than the polarization curve. The overall impedance appeared as part of a depressed semicircle. The magnitude of the overall impedance was a key information to match with experimental data. Besides the influence of CPE coefficients α and Q on the shape of the impedance, the parameters that influence the overall impedance are summarized in Table 7.4.

7.5 The Influence of Hydrogen Peroxide-Oxygen Redox Couple

The hydrogen peroxide-oxygen redox couple play an important role in the homogeneous enzymatic reactions and the heterogenous electrochemical reactions. The parameters associated with this redox couple influenced the steady state reaction rate profile, which determined if the sensor reaction was under kinetic control or mass-transfer control. Thus, the diffusion impedance and the overall impedance response were different.

Three parameters were chosen to explore as an example, the heterogeneous rate constant of hydrogen peroxide oxidation reaction, the applied potential and the partition coefficient of oxygen. These parameters were directly relevant to the amount of oxygen entering the sensor, the consumption and generation of the hydrogen peroxide and oxygen.

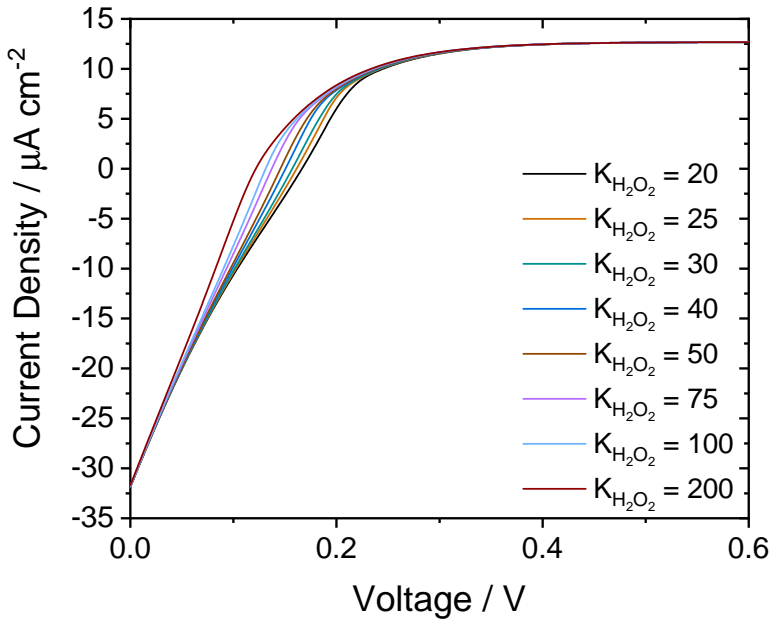


Figure 7-22. Polarization curve with $K_{H_2O_2}$ as a parameter, 400 mg/dL of glucose and 100% of enzyme concentration.

7.5.1 The Influence of $K_{H_2O_2}$ at 0.4 V

The polarization curve with $K_{H_2O_2}$ as a parameter is shown in Figure 7-22. The polarization curve presents the current density as function of applied potential from 0-0.6 V (Ag/AgCl). $K_{H_2O_2}$ affected the slope of the polarization curve. At 0.4 V applied potential, the current density reached to the mass-transfer limited plateau on polarization curve. The kinetics of the electrochemical oxidation of hydrogen peroxide was the major reaction and fast enough. Therefore, changing the heterogeneous rate constant $K_{H_2O_2}$ within the range of 20-200 Acm mol^{-1} , changed the steady-state profiles slightly, as shown in Figure 7-23. The calculated diffusion impedance with $K_{H_2O_2}$ as a parameter is presented in Figure 7-24. As shown in Figure 7-24A, the dimensionless diffusion impedance of hydrogen peroxide were almost the same in size, shape, and characteristic frequencies with $K_{H_2O_2}$ as a parameter. The overlap in dimensionless diffusion impedance of hydrogen peroxide indicated the same reaction mechanism. The heterogeneous reaction kinetics became faster as $K_{H_2O_2}$ increased. Thus, as shown in Figure 7-24B, the diffusion

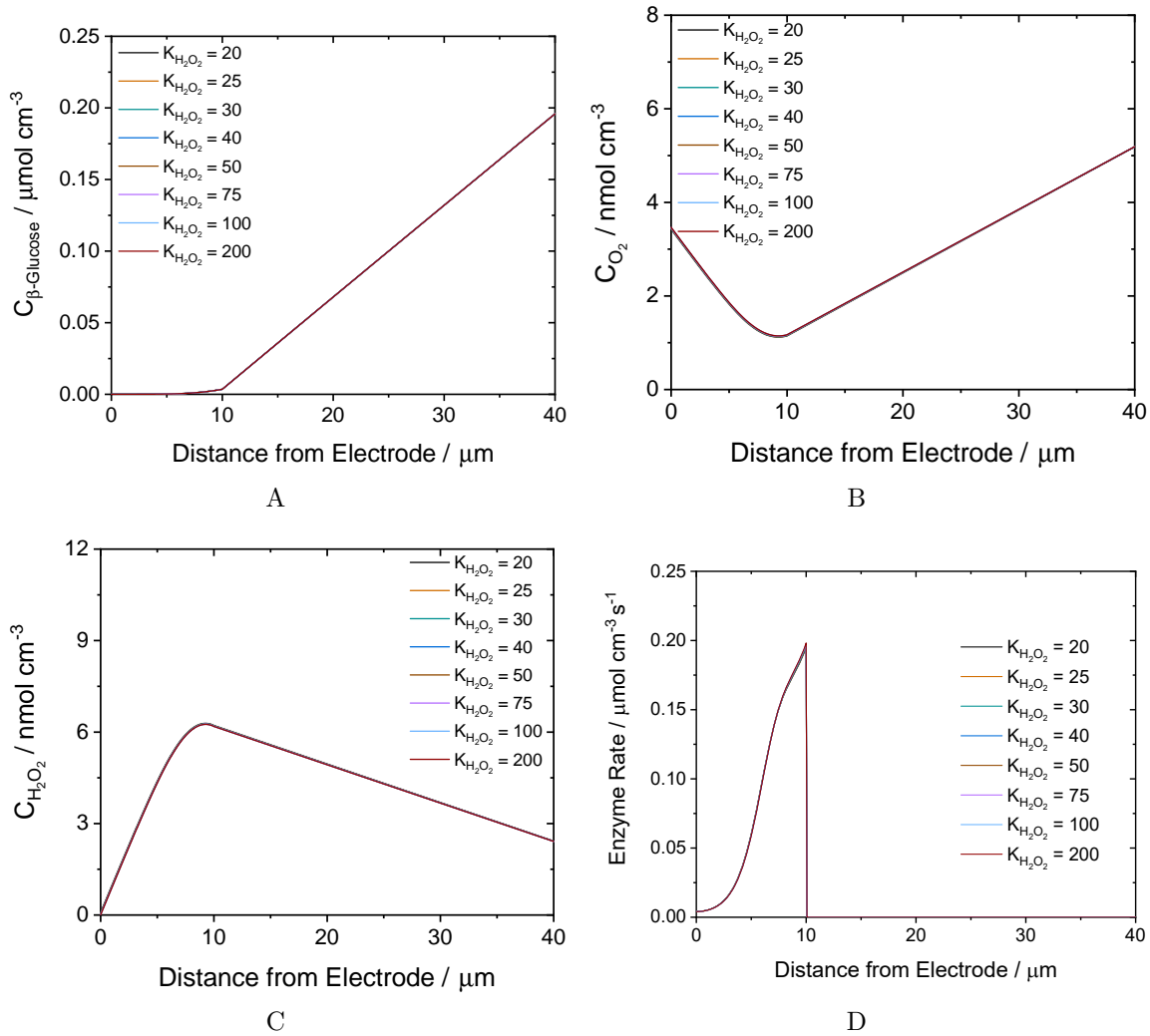
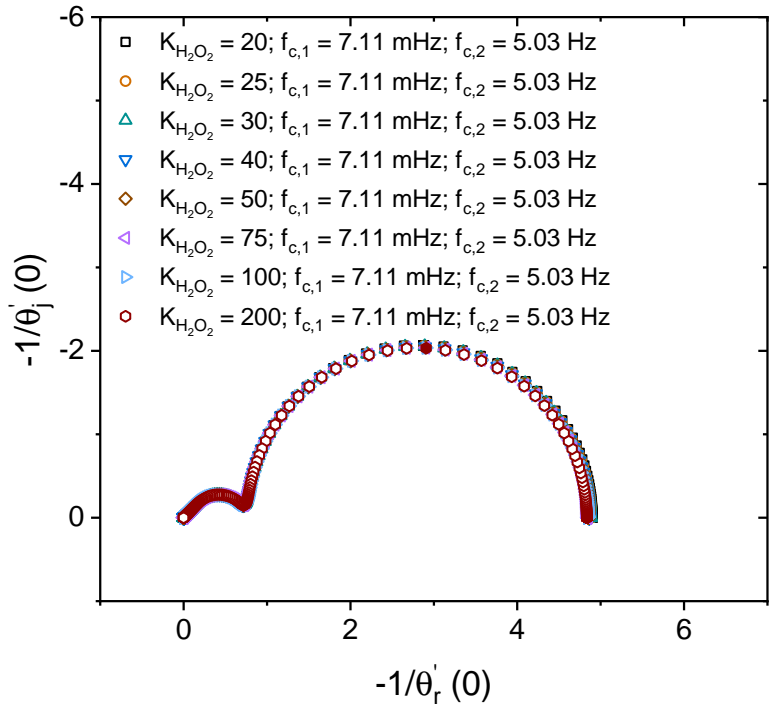


Figure 7-23. Calculated steady-state concentration profiles and reaction rate distribution as a function of distance to the electrode with $K_{\text{H}_2\text{O}_2}$ as a parameter at 0.4 V applied potential: (a) Beta-glucose concentration profile (b) Oxygen concentration profile (c) Hydrogen peroxide concentration profile (d) Enzymatic reaction rate distribution.

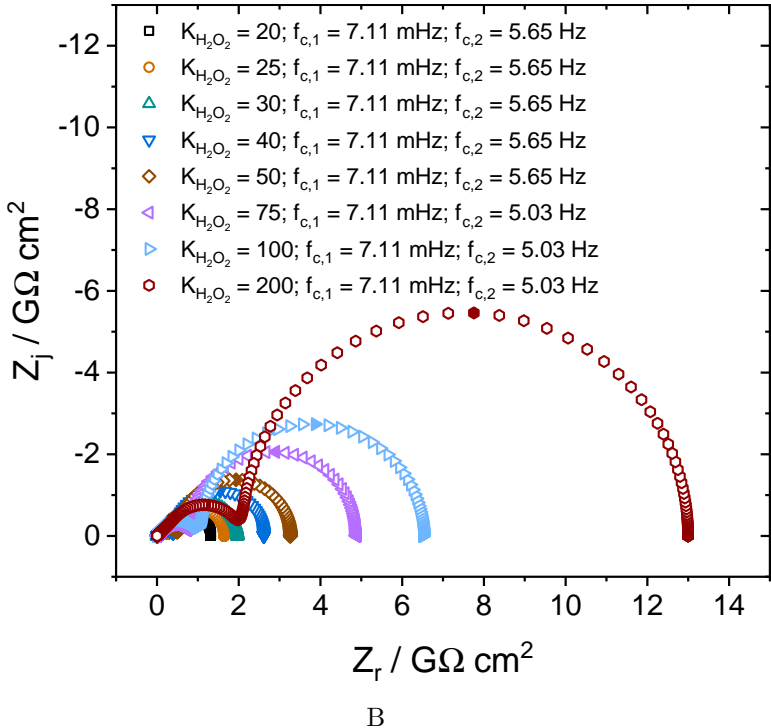
impedance increased in magnitude as $K_{\text{H}_2\text{O}_2}$ increased. Therefore, as shown in Figure 7-25, the overall impedance increased in magnitude as $K_{\text{H}_2\text{O}_2}$ increased.

7.5.2 The Influence of $K_{\text{H}_2\text{O}_2}$ at 0.2 V

At lower applied potential 0.2 V, the sensor was under kinetic control. When the heterogeneous rate constant $K_{\text{H}_2\text{O}_2}$ was small, the heterogenous oxidation of hydrogen peroxide producing oxygen was slow. The glucose can not be completely



A



B

Figure 7-24. Calculated diffusion impedance with $K_{H_2O_2}$ as a parameter at 0.4 V applied potential: (a) Dimensionless diffusion impedance of hydrogen peroxide (b) Diffusion impedance.

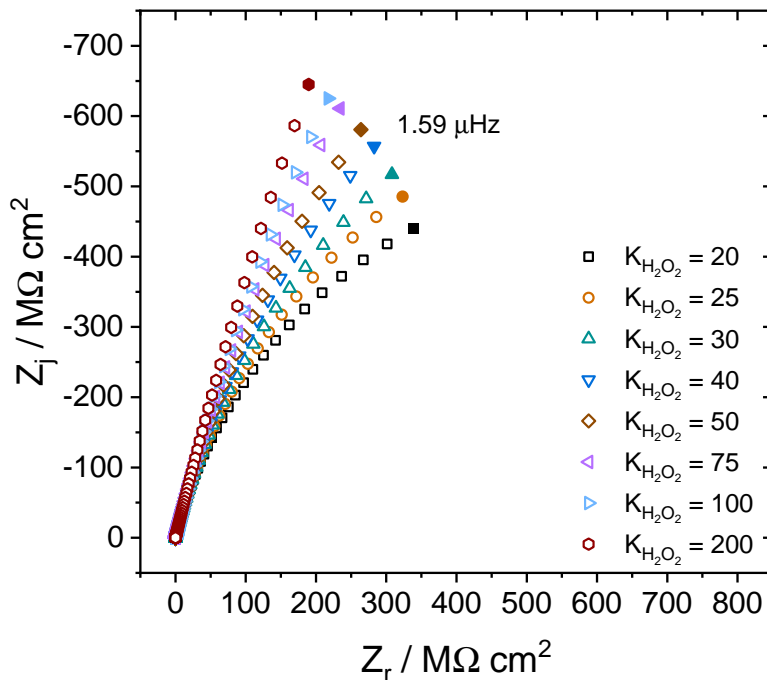


Figure 7-25. Overall impedance with $K_{H_2O_2}$ as a parameter, 400 mg/dL of glucose and 100% of enzyme concentration at 0.4 V applied potential.

consumed, in Figure 7-26A due to the low concentration of enzyme, shown in Figure 7-26. The homogeneous reaction rate profiles shifted towards the electrode surface as the concentration distribution of GOx enzyme shifts, as shown in Figure 7-26D.

The calculated diffusion impedance with $K_{H_2O_2}$ as a parameter at 0.2 V applied potential is presented in Figure 7-27. The dimensionless diffusion impedance of hydrogen peroxide appeared as two loops. The high-frequency loop increased in size as $K_{H_2O_2}$ decreased. The low-frequency loop increased in size then shrank as $K_{H_2O_2}$ decreased. The diffusion impedance is shown in Figure 7-27B. The magnitude of the diffusion impedance was on the order of $100 M\Omega \text{ cm}^2$. Based on the calculation, the diffusion impedance was dominated by the diffusion impedance associated with hydrogen peroxide at 0.2 V. Both the high-frequency and low-frequency loops decreased in size as $K_{H_2O_2}$ decreased. This was due to at 0.2 V, decreasing $K_{H_2O_2}$ shifted the location of enzymatic reactions towards electrode surface, as explained with the steady-state profiles. As shown in Figure 7-28, the overall impedance at 0.2 V appeared as depressed semicircle with magnitude

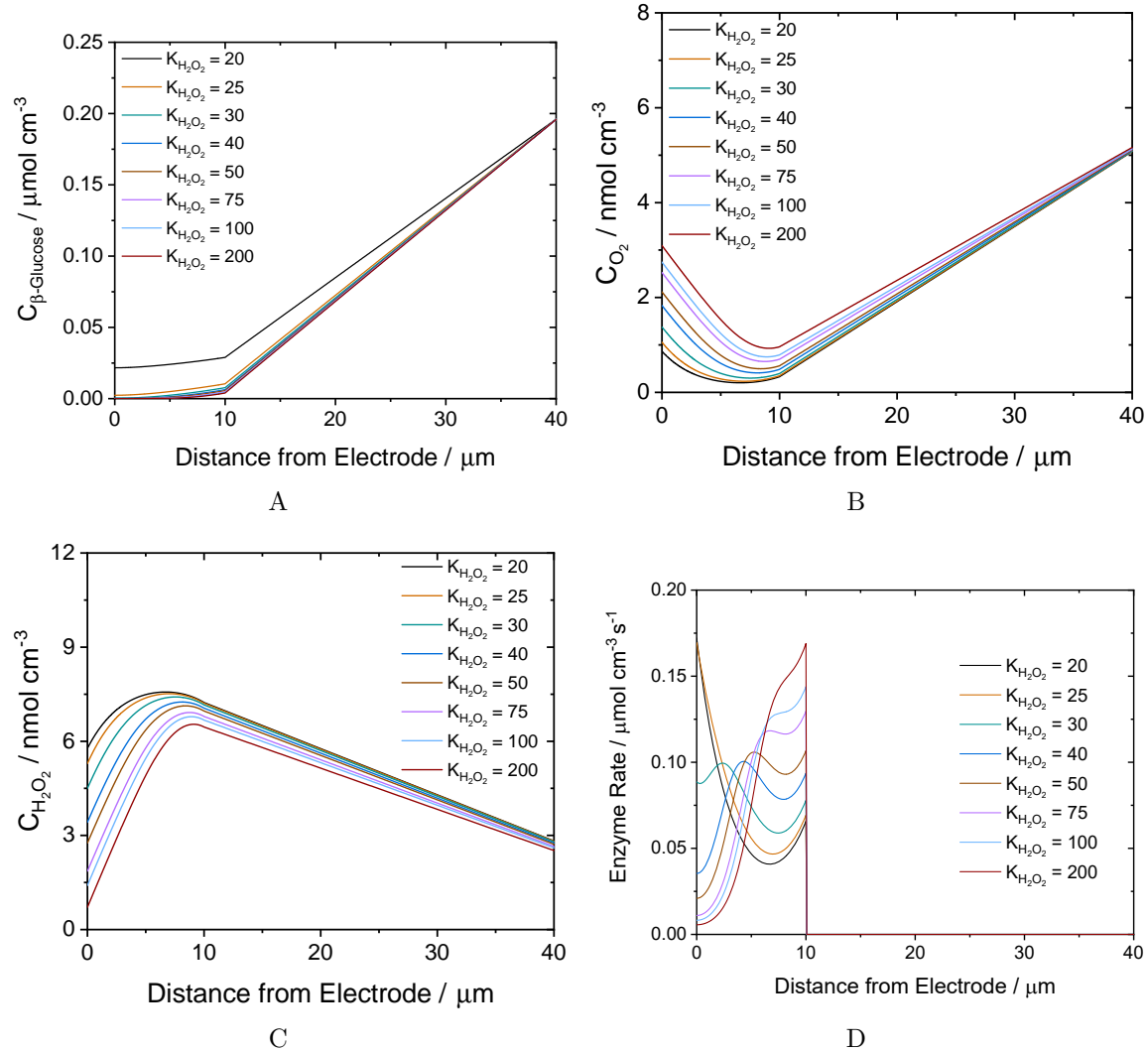
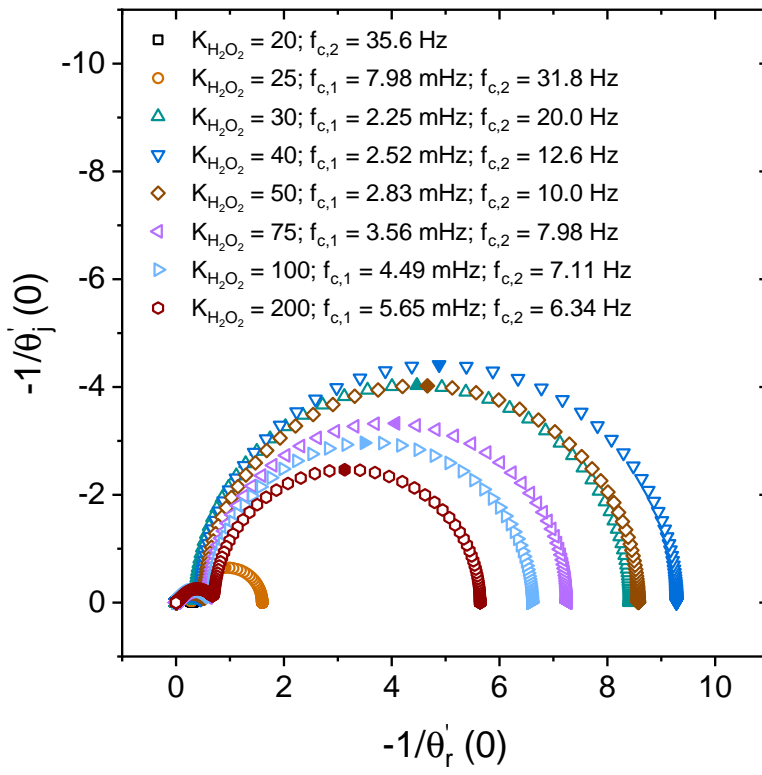
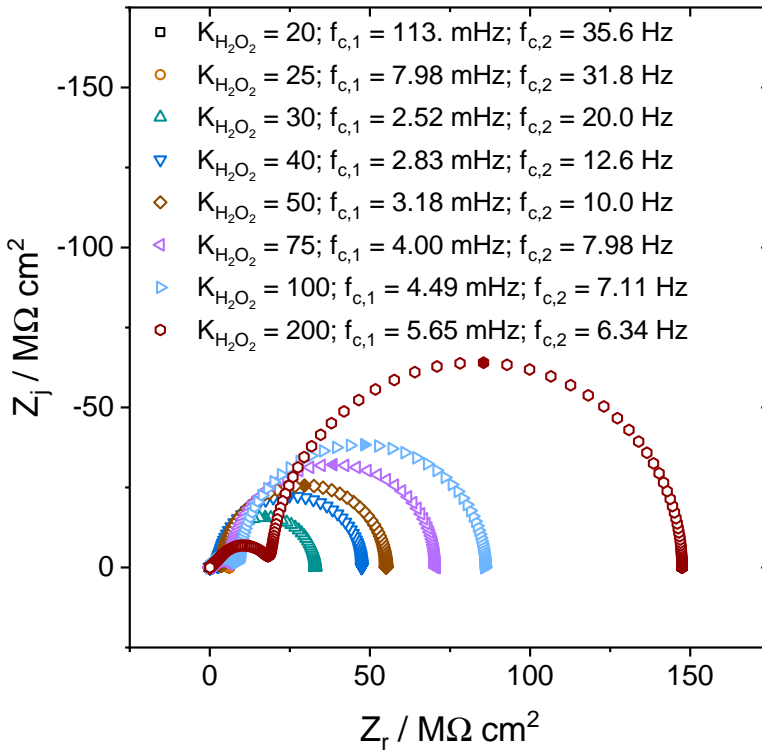


Figure 7-26. Calculated steady-state concentration profiles and reaction rate distribution as a function of distance to the electrode with oxygen partition coefficient as a parameter: (a) Beta-glucose concentration profile (b) Oxygen concentration profile (c) Hydrogen peroxide concentration profile (d) Enzymatic reaction rate distribution.



A



B

Figure 7-27. Calculated diffusion impedance with $K_{H_2O_2}$ as a parameter at 0.2 V applied potential: (a) Dimensionless diffusion impedance of hydrogen peroxide (b) Diffusion impedance.

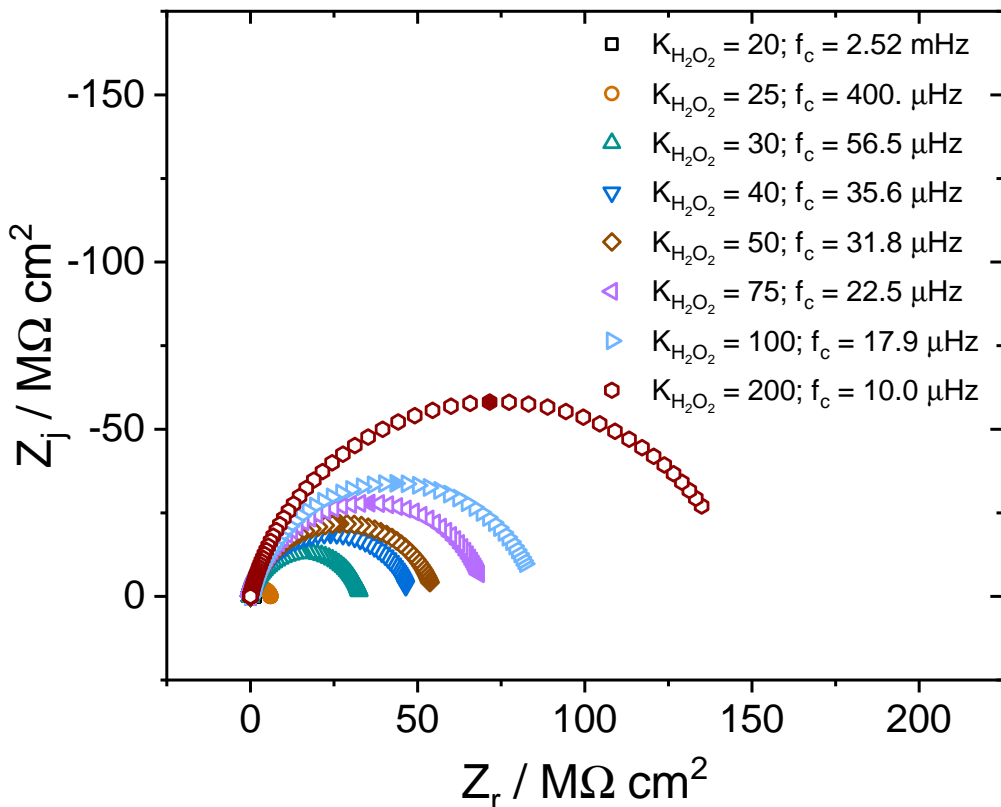


Figure 7-28. Overall impedance with $K_{H_2O_2}$ as a parameter, 400 mg/dL of glucose and 100% of enzyme concentration at 0.2 V applied potential.

much smaller than the overall impedance at 0.4 V, which was due to decreasing in diffusion impedance as enzymatic reactions shifted towards electrode surface. The overall impedance at 0.2 V decreased in size as $K_{H_2O_2}$ decreased. The characteristic frequency increased as diffusion time constant decreased. The difference of the characteristic frequency with $K_{H_2O_2} = 20 \text{ A cm mol}^{-1}$ to $K_{H_2O_2} = 30 \text{ A cm mol}^{-1}$ was much larger than the characteristic frequencies with larger the characteristic frequency with $K_{H_2O_2}$. This was due to the impedance was dominated by the Gerischer impedance with low the characteristic frequency with $K_{H_2O_2}$.

7.5.3 The Influence of Oxygen Partition Coefficient at 0.4 V

The other parameter presented had influence on the hydrogen peroxide and oxygen redox couple was oxygen partition coefficient. This parameter is related to the physical property of the GLM layer of the sensor. The oxygen partition coefficient measures the

equilibrium concentration of oxygen in the membrane divided by that in the adjacent tissue or solution. The oxygen partition coefficient is directly proportional to the oxygen concentration diffuses into the sensor.

The steady-state profiles with the oxygen partition coefficient as a parameter are shown in Figure 7-29. The oxygen partition coefficient had direct influence on oxygen concentration distribution, as shown in Figure 7-29B. With smaller oxygen partition coefficient, lower oxygen concentration was distributed across the sensor. The oxygen was shown also generated electrochemically at the electrode. For γ_{O_2} smaller than 0.05, the oxygen diffusing from the tissue was insufficient. The oxygen profiles appeared parallel with difference in oxygen concentration levels. As a result, the concentration profiles of hydrogen peroxide were different, as shown in Figure 7-29C. As the oxygen partition coefficient decreased, the concentration of hydrogen peroxide was lower and shifted towards electrode surface. This could be explained by the enzymatic reaction rate distribution, as shown in Figure fig:ParO2SSReactionRate. Because of the oxygen deficiency with γ_{O_2} smaller than 0.05, the enzymatic reactions were dependent on the oxygen generated electrochemically. Thus, the location of enzyme reactions shifted towards electrode surface as γ_{O_2} decreased. The diffusion impedance with oxygen partition coefficient as a parameter is presented in Figure 7-30. The diffusion impedance appeared as two loops. For $\gamma_{O_2} = 0.05$, the high-frequency Gerischer impedance was small and the low-frequency semicircle was large. It was due to the enzymatic reactions shifted near electrode while the oxygen concentration diffused into the sensor was too low. As the oxygen partition coefficient decreased, the high-frequency loop decreased in size and low-frequency loop increase in size.

The overall impedance with oxygen partition coefficient as a parameter is presented in Figure 7-31. The overall impedance appeared as part of depressed semicircle. Due to the impedance was dominated by the low-frequency diffusion impedance, the overall impedance decreased in size as the oxygen partition coefficient increased. With γ_{O_2} larger

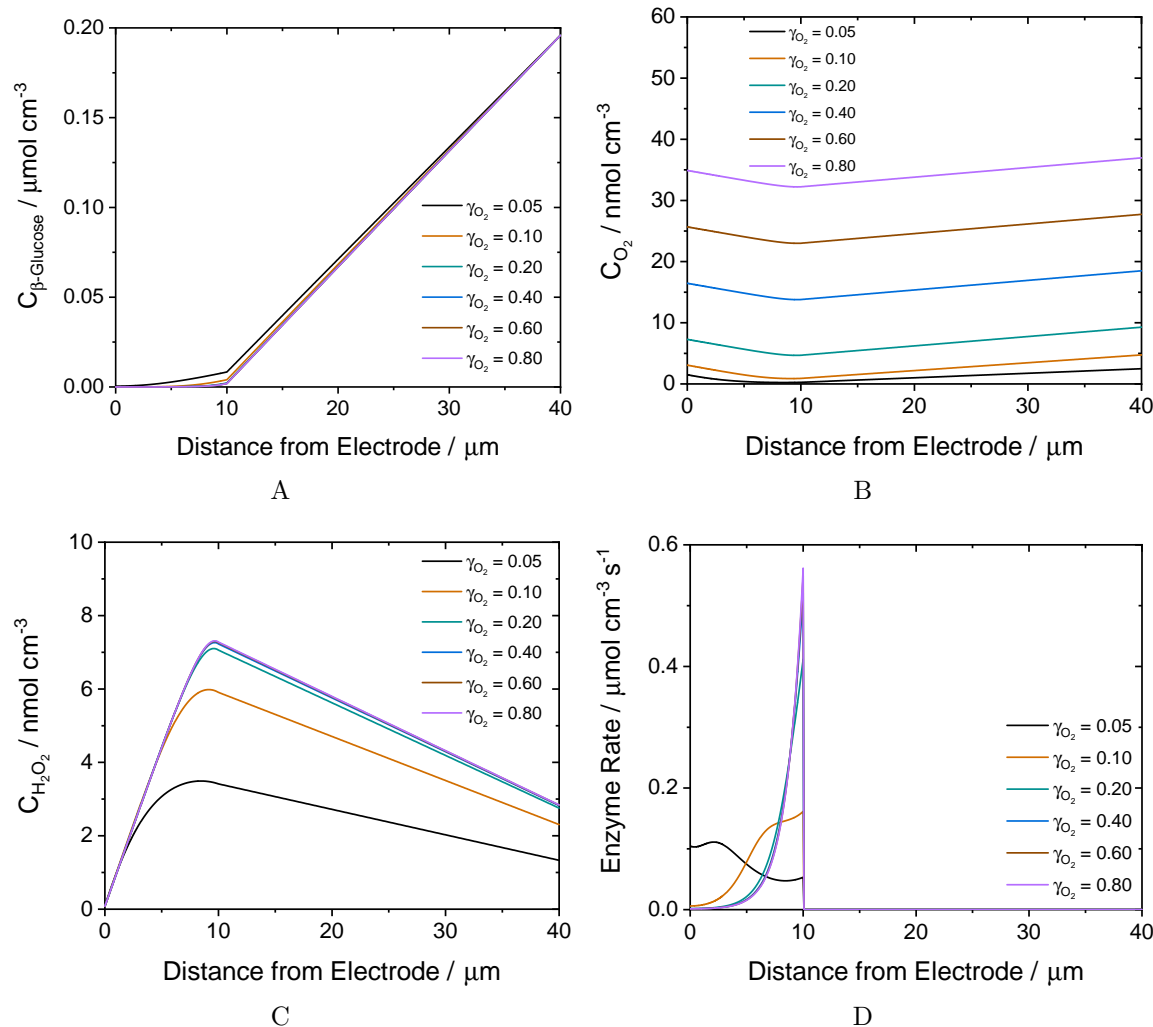


Figure 7-29. Calculated steady-state concentration profiles and reaction rate distribution as a function of distance to the electrode with oxygen partition coefficient as a parameter: (a) Beta-glucose concentration profile (b) Oxygen concentration profile (c) Hydrogen peroxide concentration profile (d) Enzymatic reaction rate distribution.

than 0.6, the sensor was limited by the oxygen partial pressure in tissue instead of the oxygen partition coefficient. Therefore, the overall impedance were almost the same as the oxygen partition coefficient further increased.

The steady-state reaction rate profile can be used to predict the reaction mechanism (kinetic controlled or mass-transport controlled) and reaction-transport time constants.

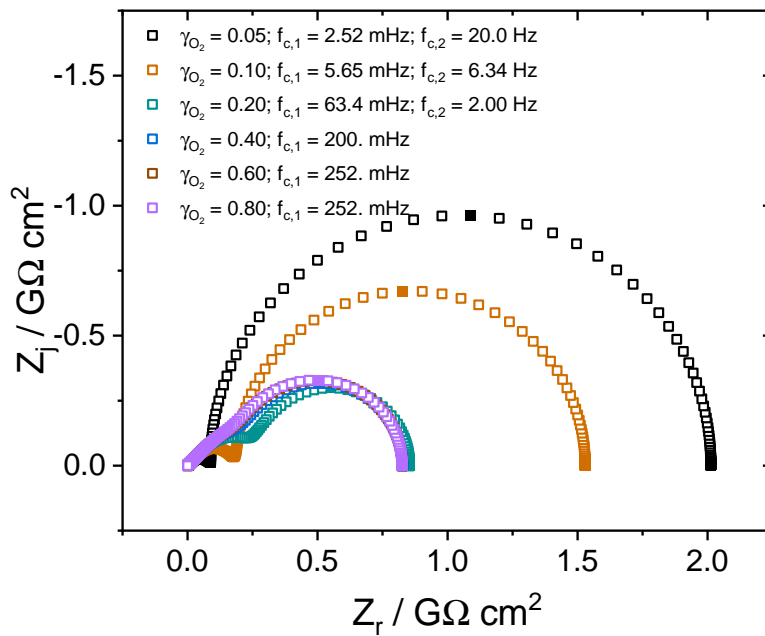


Figure 7-30. Diffusion impedance with oxygen partition coefficient as a parameter, 400 mg/dL of glucose and 100% of enzyme concentration at 0.4 V applied potential.

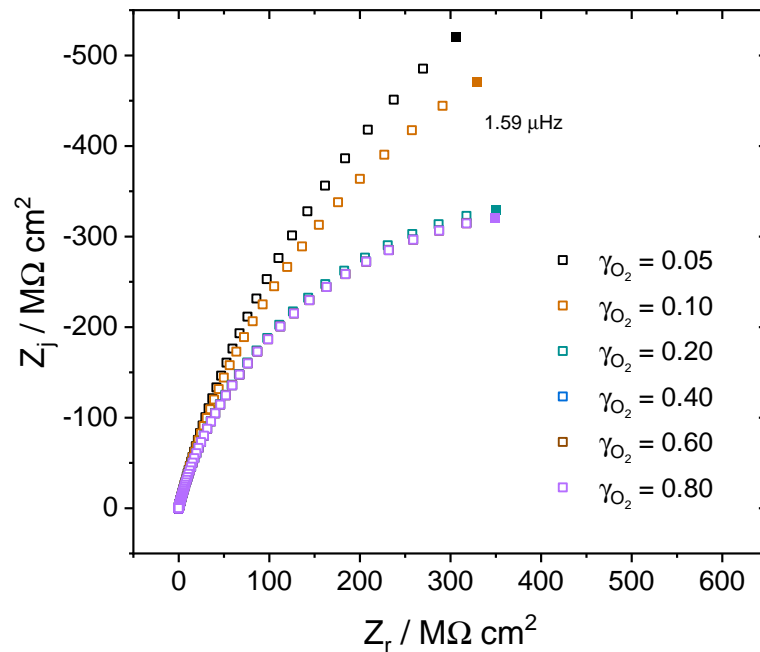


Figure 7-31. Overall impedance with oxygen partition coefficient as a parameter, 400 mg/dL of glucose and 100% of enzyme concentration at 0.4 V applied potential.

Hydrogen peroxide and oxygen redox couple determines the steady-state reaction rate profile.

CHAPTER 8 CONCLUSIONS

A series of mathematical models were developed to describe both the steady-state behavior and the electrochemical impedance response of the continuous glucose monitors (CGM). The models are advanced in following aspects: 1) The models use the ping-pong kinetics and law of mass action to account for the enzyme kinetics of the continuous glucose sensor, while the commonly used Michaelis-Menten kinetics does not apply here. 2) The models are the most realistic mechanistic models to date. The chemistry of the CGMs was considered, including the enzymatic reactions, the anomeration equilibrium of the glucose, the pH-dependent enzyme activities and the biological buffers. The physical properties of the sensor and the transport process are also considered, including the effective diffusion coefficients of the species within different films and the partition coefficients at the interface. 3) The electrochemical impedance response can be simulated based on the physics of the CGM. 4) The models help visualize the reaction mechanism and concentration distributions. The coupling between the homogeneous reactions and heterogeneous reactions was described specifically. The models can be applied in predicting sensor design and diagnosing sensor failure mechanisms.

Based on the understanding of the physics and chemistry of continuous glucose sensors, process models were proposed. By using the measurement model, the error structure of the experimental results was obtained. The fitting parameters were extrapolated from the impedance measurements, including the effective capacitance, ohmic resistance and diffusion impedance. The characteristic frequency for the geometry-induced frequency dispersion was estimated. The surface roughness factor of the working electrodes in the sensor was calculated to be around 200-300.

The extensive and systematic study on model parameters is also a major contribution of this work. The choice of the default values of the parameters are based on thorough literature research, matching with experimental results and ration of physical meanings.

The influence of the system parameters on the steady-state profiles and impedance response was explored associated with sensor failure mechanism and sensor design.

The simulated results of comparison between the normal working sensor and the sensor with failure in oxygen deficiency and enzyme deactivation are shown. Oxygen deficiency and enzyme deactivation may cause the current density measured for high glucose levels to be the same as for lower glucose levels. The steady-state profiles illustrate that the transport-reaction phenomena are different for the three cases. The high-frequency impedance, indicating kinetic information, is not useful for differentiating the three cases. Lower frequencies are needed because the three cases are distinguished by mass transfer.

CHAPTER 9 FUTURE WORK

The one-dimensional steady-state and impedance response model was fully developed. A systematic parametric study was done to understand the influence of parameters on the steady-state profiles and impedance response. The sensor failure mechanism and various sensor design were explored with respect to the system parameters. Further development of models for continuous glucose monitors should focus more on studying the transient behavior of the glucose sensor and the geometric influence of the sensor on impedance spectroscopy.

9.1 2-D or 3-D Models for Continuous Glucose Monitors

Previous analysis of the impedance data of the continuous glucose monitors suggested that the geometry induced frequency dispersion expected above 2 Hz. The measurable frequency range of the built-in potentiostat of CGM devices is usually very narrow, within 0.01 Hz to 1 MHz. That means most of the impedance data points are influenced by frequency dispersion at high frequencies. If a two-dimensional or three-dimensional model could be built, considering the time-constant dispersion caused by the geometry of the electrodes, the number of usable experimental data points can increase a lot. More information could be extrapolated from the impedance measurements.

9.2 Experimental Measurement and Regression Analysis of EIS for Continuous Glucose Monitors

The mathematical modeling of continuous glucose monitors suggests that the electrochemical impedance measurement should be taken at lower frequencies and with smaller sensors, such that more regression parameters could be extracted from fitting the experimental results. The understanding of the physical meaning of the fitting parameters associated with sensor failure mechanism need to be further studied. A more extensive experimental study needs to be performed for the sensor. Further experimental measurement could be explored include

- Different sensor design, including shiny or roughened electrodes, different sizes or shape of the electrodes
- Oxygen partial pressure
- Enzyme deactivation
- Thickness of GOx and GLM layer
- Presence of the buffer or pH of the solution
- Temperature
- Interfering species

9.3 The Influence of Coupled Faradaic and Charging Currents on Electrochemical Impedance Spectroscopy

There has been a controversy over the way of treating the current density as a priori separation of faradaic and double layer charging currents, since 1960s. For the deterministic model for impedance, people keep using the convention proposed by Sluyters [66], which the two processes are considered separately into the faradaic impedance and the capacitance. The controversy raised by Delahay et al. [67–69] that the flux of reacting species should contribute both to the faradaic reaction and to the charging of double-layer capacitance. In 2012, Nisancioglu and Newman [70] readdressed the issue and investigated the basic assumptions and concepts of the transient electrode process from the basic principles of electrochemistry. The rigorous derivation showed that the treatment of a priori separation of the double-layer charging and faradic current is valid only if the time-dependent variations in the concentration of the species are neglected. However, for the frequency-dependent electrochemical impedance, the oscillating concentration contributes to the diffusion impedance and is a function of position and time.

Wu et al. [71] investigated the influence of coupled faradaic and charging currents on impedance spectroscopy for a rotating disk electrode. The simulation results showed the coupling of faradaic and charging current resulted in high-frequency dispersion. The simulation matched with experimental results for the electrochemical system

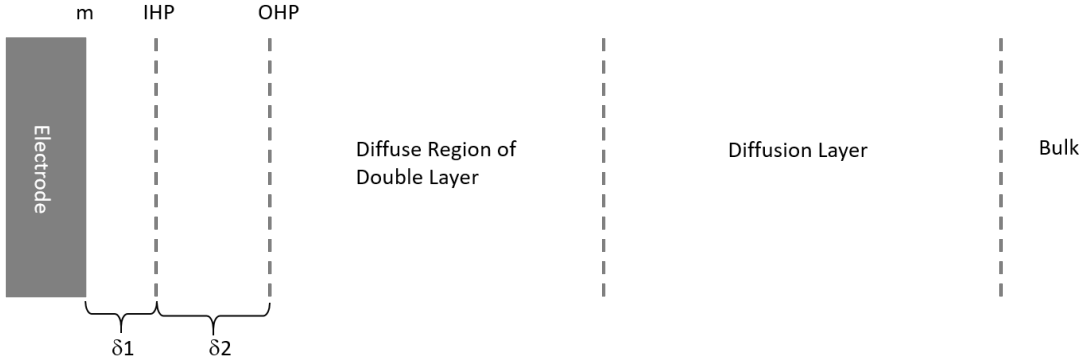


Figure 9-1. Schematic representation of the electrode-electrolyte interface following Stern-Gouy-Chapman model.

of AgNO_3 in KNO_3 electrolyte very well but not for the electrochemical system of $\text{Fe}(\text{CN})_6(\text{III})/(\text{IV})$ in KCl electrolyte. The hypotheses is that the simulations of the coupled faradaic and charging currents performed by Wu et al. did not consider the thermodynamic properties of the interface specifically. The simulation is assumed in the absence of ion-specific adsorption and only considered the diffuse part of double layer in the Stern-Gouy-Chapman model.

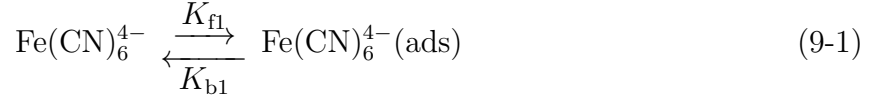
To match with preliminary experimental result carried by Harding [72], further simulation for electrochemical impedance response under the influence of coupled faradaic and charging current need to be study in consideration of implicit surface thermodynamics and the ion-specific surface adsorption. A finite-element one-dimensional mathematical model need to be developed to further characterize and understand the phenomenon. Some preliminary results are presented below.

9.3.1 Physical Model

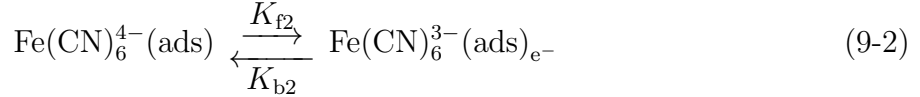
A one-dimensional schematic representation of the electrode-electrolyte interface is shown in Figure 9-1 following Stern-Gouy-Chapman model.

A one-dimensional finite-difference model was built on the electrochemical system of the redox of ferrocyanide and ferricyanide in KCl supporting electrolyte. Considering the ion-specific adsorption, the heterogeneous reactions at the electrode surface are the surface

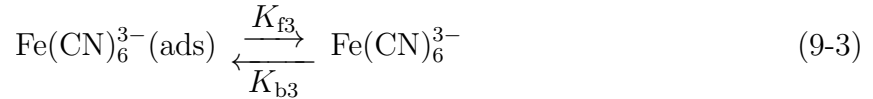
adsorption of $\text{Fe}(\text{CN})_6^{4-}$,



the electrochemical oxidation of $\text{Fe}(\text{CN})_6^{4-}$ into $\text{Fe}(\text{CN})_6^{3-}$,



the surface desorption of $\text{Fe}(\text{CN})_6^{3-}$,



the surface desorption of K^+ ,



and the surface desorption of Cl^- , which is expressed as



Equations (9-1)–(9-5) are the conservation equations at the electrode surface serving as boundary conditions.

9.3.2 Governing Equations

The material-balance equation

$$\frac{\partial c_i}{\partial t} = z_i F \nabla \cdot (u_i c_c \nabla \Phi) + \nabla \cdot (D_i \nabla c_i) + R_i - \underline{v} \cdot \nabla c_i \quad (9-6)$$

The Nernst-Einstein equation

$$D_i = RT u_i \quad (9-7)$$

Combine equation 9-6 and equation 9-7 and get

$$\frac{\partial c_i}{\partial t} = \frac{z_i F D_i}{RT} (\nabla c_i \nabla \Phi + c_i \nabla^2 \Phi h_i) \quad (9-8)$$

$$+ D_i \nabla^2 c_i - \underline{v} \cdot \nabla c_i + R_i \quad (9-9)$$

The reaction rates corresponding to the heterogeneous reactions are expressed as

$$\begin{aligned} r_1 &= k_{f1} c_{\text{Fe}(\text{CN})_6^{4-}} \left(\gamma_{\text{total}} - \sum_k \gamma_k \right) \exp \left(\frac{z_{\text{Fe}(\text{CN})_6^{4-}} F}{RT} (\Phi_{\text{IHP}} - \Phi_{\text{OHP}}) \right) \\ &\quad - k_{b1} \gamma_{\text{Fe}(\text{CN})_6^{4-}} \exp \left(- \frac{z_{\text{Fe}(\text{CN})_6^{4-}} F}{RT} (\Phi_{\text{IHP}} - \Phi_{\text{OHP}}) \right) \end{aligned} \quad (9-10)$$

which is the reaction rate of surface adsorption of $\text{Fe}(\text{CN})_6^{4-}$,

$$\begin{aligned} r_2 &= k_{f2} \gamma_{\text{Fe}(\text{CN})_6^{4-}} \exp \left(b_{\text{Fe}(\text{CN})_6^{4-}} (\Phi_m - \Phi_{\text{IHP}}) \right) \\ &\quad - k_{b2} \gamma_{\text{Fe}(\text{CN})_6^{3-}} \exp \left(- b_{\text{Fe}(\text{CN})_6^{3-}} (\Phi_m - \Phi_{\text{IHP}}) \right) \end{aligned} \quad (9-11)$$

which is the reaction rate of the electrochemical oxidation of $\text{Fe}(\text{CN})_6^{4-}$ into $\text{Fe}(\text{CN})_6^{3-}$,

$$\begin{aligned} r_3 &= k_{f3} \gamma_{\text{Fe}(\text{CN})_6^{3-}} \exp \left(\frac{z_{\text{Fe}(\text{CN})_6^{3-}} F}{RT} (\Phi_{\text{IHP}} - \Phi_{\text{OHP}}) \right) \\ &\quad - k_{b3} c_{\text{Fe}(\text{CN})_6^{3-}} \left(\gamma_{\text{total}} - \sum_k \gamma_k \right) \exp \left(- \frac{z_{\text{Fe}(\text{CN})_6^{3-}} F}{RT} (\Phi_{\text{IHP}} - \Phi_{\text{OHP}}) \right) \end{aligned} \quad (9-12)$$

which is the reaction rate of surface desorption of $\text{Fe}(\text{CN})_6^{3-}$,

$$\begin{aligned} r_4 &= k_{f4} \gamma_{\text{K}^+} \exp \left(\frac{z_{\text{K}^+} F}{RT} (\Phi_{\text{IHP}} - \Phi_{\text{OHP}}) \right) \\ &\quad - k_{b4} c_{\text{K}^+} \left(\gamma_{\text{total}} - \sum_k \gamma_k \right) \exp \left(- \frac{z_{\text{K}^+} F}{RT} (\Phi_{\text{IHP}} - \Phi_{\text{OHP}}) \right) \end{aligned} \quad (9-13)$$

which is the reaction rate of surface desorption of K^+ ,

$$\begin{aligned} r_5 &= k_{f5} \gamma_{\text{Cl}^-} \exp \left(\frac{z_{\text{Cl}^-} F}{RT} (\Phi_{\text{IHP}} - \Phi_{\text{OHP}}) \right) \\ &\quad - k_{b5} c_{\text{Cl}^-} \left(\gamma_{\text{total}} - \sum_k \gamma_k \right) \exp \left(- \frac{z_{\text{Cl}^-} F}{RT} (\Phi_{\text{IHP}} - \Phi_{\text{OHP}}) \right) \end{aligned} \quad (9-14)$$

which is the reaction rate of surface desorption of Cl^- .

9.3.3 Ionic Adsorption at Equilibrium

A mathematical model for the specific ionic adsorption on the electrode surface at equilibrium was built in Matlab®. The condition of equilibrium is assumed such that 1) the ionic specific adsorption is considered to happen from OHP to IHP; 2) the distribution of ionic species in the diffuse part of double layer obeys Boltzmann distribution, which can be expressed as

$$c_i = c_\infty \exp(-z_i F \Phi / RT) \quad (9-15)$$

. In the model, the bulk solution consists of 0.01 mol cm^{-3} of NaCl and 0.01 mol cm^{-3} of ZnCl. As shown in Figure 9-2, for the surface adsorption, when the potential at the electrode surface is negative, positive ions are adsorbed; when the potential at the electrode surface is positive, the negative ions are adsorbed. As the applied potential goes more negative, Zn^{2+} is the predominant species adsorbed at the electrode surface because of its stronger covalence binding to the surface.

At equilibrium, the charge in the diffuse part of the double layer should balance the charge on the surface. The charge of species in the diffuse part of double layer as function of applied potential is calculated in Figure 9-3. The total charge in the diffuse part of double layer (purple curve) is negative when the potential is negative and positive when the potential at the electrode is positive.

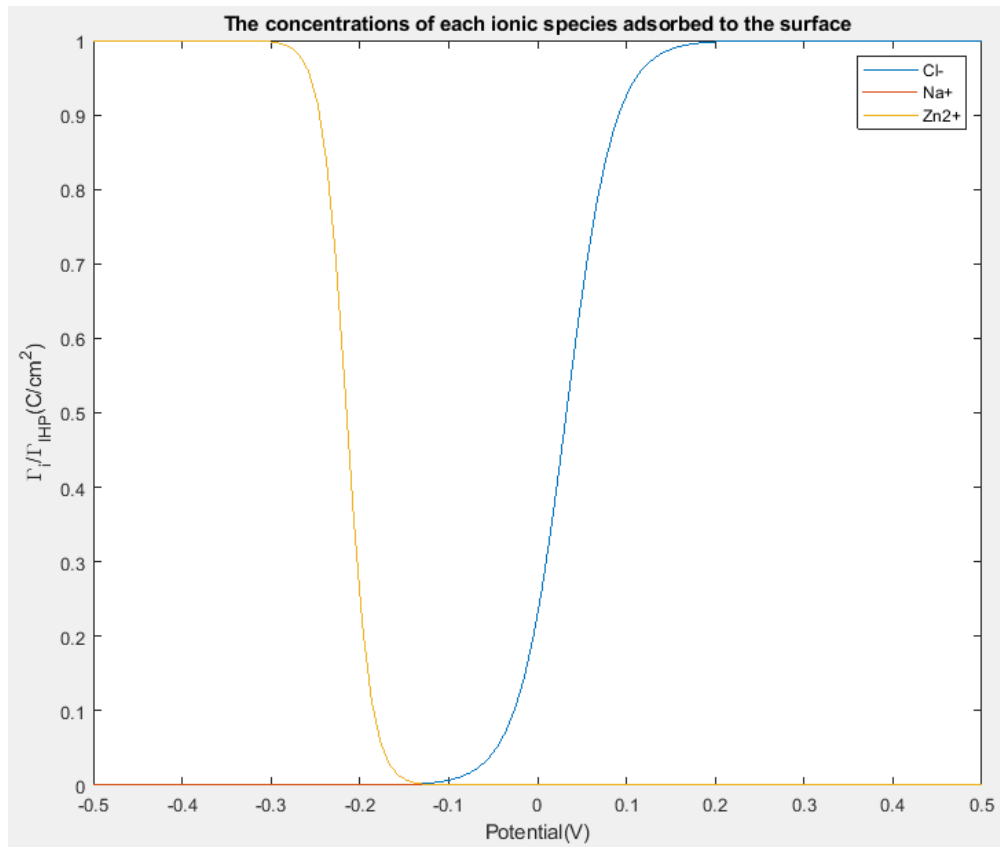


Figure 9-2. The concentration of ionic species adsorbed on electrode as a function of applied potential. The surface concentration is normalized by the total active sites on the IHP.

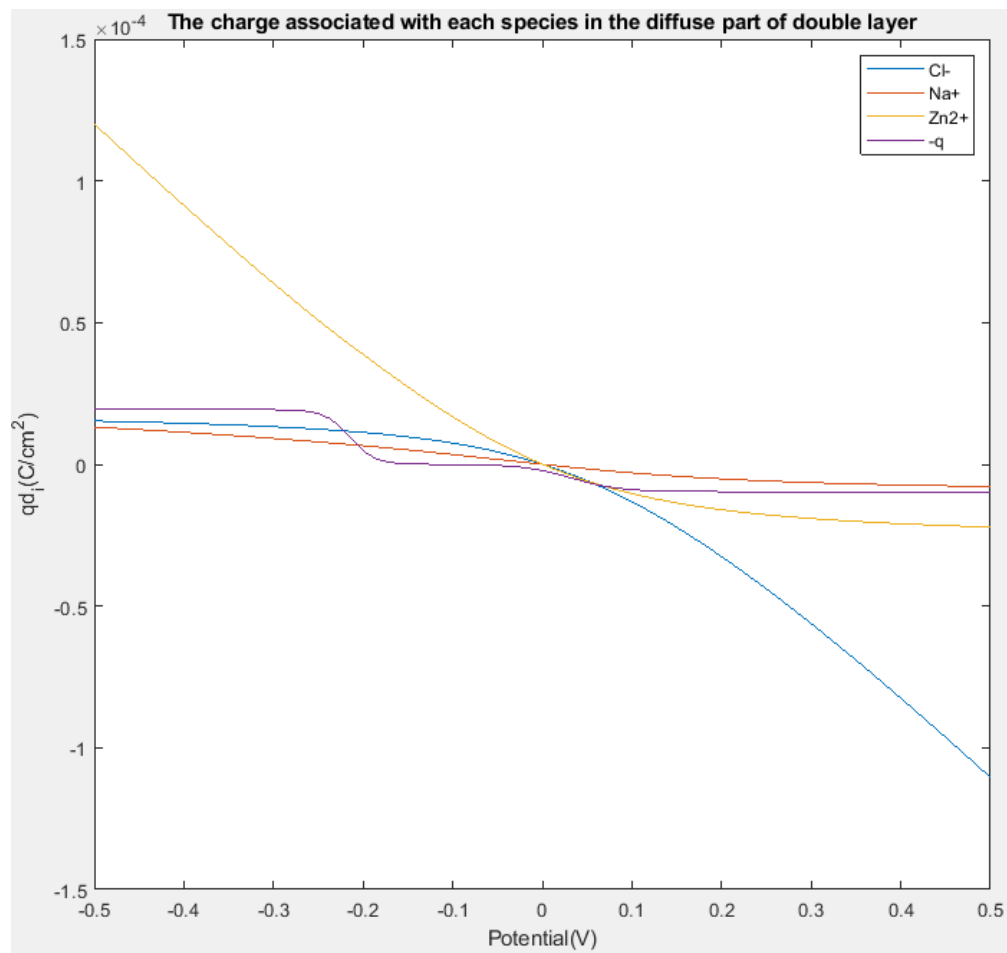


Figure 9-3. The Charge of Species in the Diffuse Part of Double Layer as a Function of Applied Potential.

APPENDIX A

CODES FOR UNBUFFERED CONTINUOUS GLUCOSE SENSOR

This appendix contains the different FORTRAN codes and Matlab® codes for the model of unbuffered continuous glucose sensor, which is described in detail in Chapter 3.

A.1 Input File

The input parameters for the model of unbuffered continuous glucose sensor are read into the FORTRAN and Matlab® codes from the text files. The main input text file [A.1](#) has the parameters related to the geometry of the one-dimensional model, such as number of species being solved, the total number of points, the number of points until the coupler, the distance of the reaction region in cm, the distance of the inner layer in cm. The input file [A.1](#) includes the physical properties of the biological films of the sensor, such as the partition coefficients (or so called solubility coefficients) for the corresponding species in from the tissue electrolyte to the glucose limiting membrane (GLM). The input file [A.1](#) includes the parameters related to the kinetics of the model, such as the forward rate constants, equilibrium rate constants of the homogeneous reactions, the heterogeneous reaction rate constants and values related to the Tafel slope. The input file [A.1](#) includes the error allowed for the BIG values. It also includes the initial input concentration of the species involved in the model.

There are other input files corresponding to the diffusion coefficients of each individual species within GOx layer, GLM and Bulk respectively, the total amount of enzyme, the oxygen partial pressure, the pH in the bulk, the potential and the temperature. The values are summarized in the table of input parameters.

```

1 19
2 1201
3 801
4 401
5 0.0002
6 0.0005
7 0.0015
8 0.32
9 0.11
10 0.025
11 0.2
12 1.056E-6
13 1.E9
14 1.E7
15 1.E3
16 1.E9
17 1.E7
18 1.E9
19 6.E-3
20 1.7397
21 3.32E-6
22 2.37E-20
23 2.0E-4
24 2.0E-6
25 3.95E-11
26 20.
27 5.E15
28 5.E21
29 1.38E10
30 22.4
31 38.4
32 32.
33 20.
34 1.E-14
35 2.2203E-05
36 8.9E-8
37 1.E-20
38 8.9E-8
39 0.05
40 1.E-20
41 8.9E-8
42 8.9E-8
43 5.4954E-11
44 4.3126E-10
45 3.6394E-14
46 1.E-20
47 1.E-20
48
49
50
51
52
53
54
55 C      line 1 is the number of species
56 C      line 2 is the number of points , NJ
57 C      line 3 is the point where the domains split , value of IJ
58 C      line 4 is the point where the reaction layer is , value of KJ

```

```

59 C line 5 is the distance of the inner reaction later in cm (2um)
60 C line 6 is the distance of the inner GOx layer in cm (5 um)
61 C line 7 is the distance of the outer GLM layer in cm (15 um)
62 C line 8 is the solubility coefficient of H2O2
63 C line 9 is the solubility coefficient of O2
64 c line 10 is the solubility coefficient of Glucose
65 C line 11 is the solubility coefficient of H+, OH- and buffer ions
66 C line 12 is the solubility of O2 in water. mol/cm^3/percentage partial
pressure
67 C line 13 is the ratef1 of rxn1, cm^3/(mol*s)
68 C line 14 is the equilib1 of rxn1, cm^3/mol
69 C line 15 is the ratef2 of rxn2, s^-1
70 C line 16 is the ratef3 of rxn3, cm^3/(mol*s)
71 C line 17 is the equilib3 of rxn3, cm^3/mol
72 C line 18 is the ratef4 of rxn4, s^-1
73 C line 19 is the ratef5 of rxn5, s^-1
74 C line 20 is the equilib5 of rxn5, cm^3/mol
75 C line 21 is the ratef6 of rxn6 water dissociation, s^-1
76 C line 22 is the equilib6 of rxn6 water dissociation, (mol/cm^3)^2
77 C line 23 is the equilib7 of rxn7 gluconic acid dissociation, mol/cm^3
78 C line 24 is the equilib8 of rxn8 H+Eo dissociates into H+ and oxidized
form of GOx(Eo), mol/cm^3
79 C line 25 is the equilib9 of rxn9 reduced GOx2(Er) dissociates into H+ and
Er-, mol/cm^3
80 C line 26 is the forward rate constant (Kf) for the flux of the reacting
species , A/cm2 cm3/mol
81 C line 27 is the backward rate constant (Kb) for the flux of the reacting
species , A/cm2 cm3/mol
82 C line 28 is the heterogeneous rate constant (K2) for hydrogen peroxide
reduction
83 C line 29 is the heterogeneous rate constant (KH) for hydrogen evolution
84 C line 30 is the tafel b_a value for the anodic flux of the reacting
species
85 C line 31 is the tafel b_c value for the cathodic flux of the reacting
species
86 C line 32 is the tafel b_2 value for hydrogen peroxide reduction
87 C line 33 is the tafel b_H value for hydrogen evolution
88 C line 34 is the error allowed for the BIGs
89 C line 35 is bulk concentration of glucose
90 C line 36 is bulk concentration of oxidized glucose oxidase(GOx(ox.))
91 C line 37 is bulk concentration of gluconic acid
92 C line 38 is bulk concentration of reduced glucose oxidase(GOx(red.))
93 C line 39 is bulk concentration of oxygen (O2)
94 C line 40 is bulk concentration of hydrogen peroxide (H2O2)
95 C line 41 is bulk concentration of enzyme complex (GOx(red.)-GA)
96 C line 42 is bulk concentration of enzyme complex(GOx(ox.)-H2O2)
97 C line 43 is bulk concentration of hydrogen ion (H+)
98 C line 44 is bulk concentration of hydroxide ion (OH-)
99 C line 45 is bulk concentration of gluconate ion
100 C line 46 is bulk concentration of enzyme complex(HEo+)
101 C line 47 is bulk concentration of enzyme complex(HER-)

```

Code A.1. Input files for the Model of Unbuffered Continuous Glucose Sensor

A.2 Code for Steady-State Calculation

This section contains the steady-state FORTRAN code used to solve 19 coupled differential equations. The mathematical development of the model including the governing equation and the boundary conditions are described in Chapter 3. The distributions of concentration of the species and reaction rates at steady- state are calculated for the FORTRAN code. The Matlab® code visualizes and organizes the output results from the steady-state FORTRAN code. The second Matlab® code calculates the polarization curve, which is the current density at a specific steady-state as a function of various potential. The third Matlab® code calculates the oxygen curve, which is the current density as function of oxygen partial pressure.

The main program in the FORTRAN code, called CONVDIFF, which outlines the global variables, reads the values of parameters from input files, calls the subroutines and writes the output results to the files. There are 7 subroutines called by the main program. The subroutine BC1 solves the boundary condition at the electrode surface. The subroutines REACTION and INNER solve the nonlinear coupled differential equations in GOx layer and the subroutine OUTER solves the governing equations in GLM layer, respectively. There are two subroutines named COUPLER1 and COUPLER2, uniform the fluxes at the interfaces where the mesh size changes. The subroutine BCNJ solves the boundary condition in the bulk. The BAND algorithm are used to solve the coupled non-linear differential equations, in subroutine BAND and MATINV.

Code A.2. FORTRAN Code for Steady-State Calculations of Unbuffered Continuous Glucose Sensor

```

1 C      Convective Diffusion Equation with Homogeneous Reaction
2 C      Enzyme kinetics added
3 C      14 species system
4 C      SPECIES 1 = beta-glucose , SPECIES 2 = GOx-FAD, SPECIES 3 = Gluconic acid
5 C      SPECIES 4 = GOx-FADH2, SPECIES 5 = O2, SPECIES 6 = H2O2
6 C      SPECIES 7 = GOx-FADH2-GA, SPECIES 8 = GOx-FAD-H2O2, SPECIES 9 = Alpha-
Glucose
7 C      SPECIES 10 = hydrogen ion , SPECIES 11= hydroxide ion , SPECIES 12=
gluconate ion
8 C      SPECIES 13 = H+Eo, SPECIES 14 = Er-
9 C      Species 5 and 6 are the electrochemical reacting species
10 C     This is the steady state solution only
11 C     It should be ran prior to cdhgox_ss.for
12 C     The input file is the same for both
13 C     This version of the code is reversible normal kinetics for reactions
1,3,5,6 and 7
14 C     Reactions 2, 4 are irreversible
15 C     Assume water dissociation and GA dissociation are fast and equilibrated
16 C     Assume the complex between H+ and enzymes are equilibrated.
17 C
*****  

18 C      THIS CODE SEPARATES THE EFFECTIVE DIFFUSION COEFFICIENTS FOR EACH
SPECIES IN DIFFERENT LAYERS
19 C      There are 4 electrochemical reaction in this code: H2O2 oxidation and
reduction , O2 reduction
20 C      and H2 evolution at low applied potential
21 C
*****  

22 C      MODIFICATION: Adding partition coefficients at BCNJ for H+, OH-
23 C
*****  

24 C      THIS CODE SEPARATES THE EFFECTIVE DIFFUSION COEFFICIENTS FOR EACH
SPECIES IN DIFFERENT LAYERS
25 C
*****  

26 C      Copy and paste the appropriate lines to create the executable
27 C      cd C:\Ming\FORTRAN2019\CGM Basic no buffer H2Evolution_Par
28 C      gfortran -static cdhgox_ss.for -o cdhgox_ss.exe
29
30      PROGRAM CONVDIFF
31      IMPLICIT DOUBLE PRECISION (A-H, O-Z)
32      COMMON/BAB/ A(19,19),B(19,19),C(19,80001),D(19,39),G(19),X(19,19)
33      1,Y(19,19)
34      COMMON/NSN/ N, NJ
35      COMMON/VAR/ CONC(14,80001),RXN(7,80001),H,EBIG,HH,IJ
36      COMMON/VARR/ COEFFMT(13), HHH, KJ
37      COMMON/POR/ DGOX(13),DGIM(13),DBULK(13)
38      COMMON/BCI/ FLUXF,FLUXB,FLUXR,FLUXH,Current3
39      COMMON/RTE/ ratef1, equilib1, ratef2, ratef3, equilib3, ratef4, ratef5,
40      1 equilib5, ratef6, equilib6, equilib7, equilib8, equilib9

```

```

41 COMMON/BUL/ CBULK(13),PARH2O2,PARO2,PARGLUCOSE,SOLO2,PARION,JCOUNT
42 COMMON/VARIN/ V,PO2,pH,GOx
43 COMMON/TEMP/ T
44 COMMON/DLT/ DELTA
45 COMMON/EXTRA/ REF(13)
46 CHARACTER REF*13
47
48
49 102 FORMAT (/30H THE NEXT RUN DID NOT CONVERGE)
50 103 FORMAT ('Error=',E16.6/(1X,'Species=',A6,2X,'C at Electrode=',
51      1 E12.5E3,2X,'C at Bulk=',E12.5E3))
52 104 FORMAT (('Species=',A6,2X,'mass-transfer coefficient=',E12.5E3))
53 300 FORMAT (18x,'b-Glucose',13x,'GOx',17x,'GA',16x,'GOx2',14x,'O2',
54      1     14x,'H2O2',14x,'CX-GOx2',14x,'CX-GOx',14x,'a-glucose',14x,
55      2     'H ion',12x,'OH ion',12x,'Gluconate ion',13x,'H+EO',13x,'Er-',
56      3     12x,'RXN1',13x,'RXN2',13x,'RXN3',13x,'RXN4',13x,'RXN5')
57 301 FORMAT (5x,'J=' 15, 19E19.9E3)
58 334 FORMAT (21(E25.15E3,5X))
59 302 FORMAT ('Iteration='I4)
60 303 FORMAT ('Limitting current density=',E12.5)
61
62 OPEN(UNIT=13, FILE='cdhgcox_out.txt')
63 CLOSE(UNIT=13, STATUS='DELETE')
64 OPEN(UNIT=13, FILE='cdhgcox_out.txt')
65
66 OPEN(12,FILE='cdhgcox_G_out.txt')
67 CLOSE(12, STATUS='DELETE')
68 OPEN(12, FILE='cdhgcox_G_out.txt')
69 WRITE(12,300)
70
71 open(14,file='cdhgcox_in.txt',status='old')
72 106 FORMAT (I2/I7/I7/E15.4/E15.4/E15.4/E15.4/E15.4/E15.4/E15.4/
73      1 /E15.4/E15.4/E15.4/E15.4/E15.4/E15.4/E15.4/E15.4/E15.4/
74      2 E15.4/E15.4/E15.4/E15.4/E15.4/E15.4/E15.4/E15.4)
75 read(14,*) N,NJ,IJ,KJ,Y1,Y2,Y3,PARH2O2,PARO2,PARGLUCOSE,PARION,
76      1 SOLO2,ratef1,equilib1,ratef2,ratef3,equilib3,
77      2 ratef4,ratef5,equilib5,ratef6,equilib6,equilib7,equilib8,
78      3 equilib9,AKF,AKB,AK2,AKH,BBA,BBC,BB2,BBH,EBIG
79 read(14,*)(CBULK(I),I=1,(N-6))
80
81 open(16,file='pot_in.txt',status='old')
82 read(16,*) V
83
84 open(17,file='O2_in.txt',status='old')
85 read(17,*) PO2
86
87 open(18,file='pH_in.txt',status='old')
88 read(18,*) pH
89
90 open(19,file='enzyme_in.txt',status='old')
91 305 FORMAT (E15.5)
92 read(19,305) GOx
93 C PRINT *, 'GOx=',GOx
94 C PRINT *, 'pH=',pH
95
96 open(20,file='temperature_in.txt',status='old')
97 read(20,*) T
98

```

```

99      open(21,file='Diff_in.txt',status='old')
100     read(21,*) DELTA
101   c   PRINT *, 'DELTA=',DELTA
102   C   IMPORT EFFECTIVE DIFFUSION COEFFICIENTS
103   open(22,file='DGOx_in.txt',status='old')
104   read(22,*)(DGOX(I),I=1,(N-6))
105
106   open(23,file='DGLM_in.txt',status='old')
107   read(23,*)(DGLM(I),I=1,(N-6))
108   PRINT *, 'DGLM(2)=', DGLM(2)
109
110   open(24,file='DBULK_in.txt',status='old')
111   read(24,*)(DBULK(I),I=1,(N-6))
112   C   Convert T in degree Celsius to degree Fahrenheit
113   T=T+273.15
114   C   ESTIMATE THE MASS TRANSFER COEFFICIENTS OUTSIDE THE SENSOR
115   COEFFMT = DBULK/DELTA
116   C   PRINT 104, (REF(I),COEFFMT(I),I=1,(N-6))
117   C   Calculate bulk concentration of O2
118   CBULK(5)=PO2*SOLO2
119   PRINT *, 'CBULK_O2=', CBULK(5)
120   C   Calculate bulk concentration of H+
121   CBULK(9)=10.**(-pH)*1.E-3
122   PRINT *, 'H+ BULK=', CBULK(9)
123   C   Calculate bulk concentration of OH-
124   CBULK(10)=equilib6/CBULK(9)
125   C   Calculate bulk concentration of enzyme
126   CBULK(2)=GOx/4.
127   CBULK(4)=GOx/4.
128   CBULK(7)=GOx/4.
129   CBULK(8)=GOx/4.
130   CBULK(12)=1.E-20
131   CBULK(13)=1.E-20
132   C   Constants
133   F=96487.
134
135   c   THIS IS SPACING FOR OUTER LAYER, BCNJ
136   H=Y3/(NJ-IJ)
137   PRINT *, 'H=', H
138   PRINT *, 'Y3=', Y3
139   PRINT *, 'NJ-IJ=', NJ-IJ
140
141   c   THIS IS SPACING FOR INNER LAYER
142   HH=(Y2)/(IJ-KJ)
143   PRINT *, 'HH=', HH
144   PRINT *, 'Y2=', Y2
145   PRINT *, 'IJ-KJ=', IJ-KJ
146
147   c   THIS IS SPACING FOR REACTION LAYER
148   HHH=(Y1)/(KJ-1)
149   PRINT *, 'Y1=', Y1
150   PRINT *, 'KJ-1=', KJ-1
151   PRINT *, 'HHH=', HHH
152
153
154   OPEN(15,FILE='cdhgox_ssvalues_out.txt')
155   CLOSE(15, STATUS='DELETE')
156   OPEN(15, FILE='cdhgox_ssvalues_out.txt')

```

```

157 337 FORMAT (I2/I7/I7/I7/E25.15/E25.15/E25.15/E15.8/E15.8/E15.8
158   1      /E15.8/E15.4/E15.4/E15.4/E15.4/E15.4/E15.4)
159   WRITE (15,337) N,NJ,IJ,KJ,H,HH,HHH,DGOX(6),DGOX(5),DGOX(9),
160   1      AKF,AKB,AK2,AKH,BBA,BBC,BB2,BBH,V
161
162 C Create flux of the reacting species constants
163 FLUXF=AKF*exp(BBA*V)/F/2.
164 FLUXB=AKB*exp(-BBC*V)/F/2.
165 FLUXR=AK2*exp(-BB2*V)/F/2.
166 FLUXH=AKH*exp(-BBH*V)/F/2.
167 C   PRINT *, 'FLUXF=' , FLUXF
168 C   PRINT *, 'FLUXB=' , FLUXB
169 C   PRINT *, 'FLUXR=' , FLUXR
170 C   PRINT *, 'FLUXH=' , FLUXH
171 c THIS IS THE MAIN PART OF THE PROGRAM
172 DO 21 J=1,NJ
173 RXN(1,J)=0.00001
174 RXN(2,J)=0.00001
175 RXN(3,J)=0.00001
176 RXN(4,J)=0.00001
177 RXN(5,J)=0.00001
178 RXN(6,J)=0.00001
179 RXN(7,J)=0.00001
180 CONC(1,J)=PARGLUCOSE*CBULK(1)*equilib5/(1+equilib5)
181 CONC(2,J)=CBULK(2)
182 CONC(3,J)=PARGLUCOSE*CBULK(3)/(equilib7/CBULK(9)+1.)
183 CONC(4,J)=CBULK(4)
184 CONC(5,J)=PARO2*CBULK(5)
185 CONC(6,J)=PARH2O2*CBULK(6)
186 CONC(7,J)=CBULK(7)
187 CONC(8,J)=CBULK(8)
188 CONC(9,J)=PARGLUCOSE*CBULK(1)/(1+equilib5)
189 CONC(10,J)=CBULK(9)
190 CONC(11,J)=CBULK(10)
191 CONC(12,J)=PARGLUCOSE*CBULK(3)/(CBULK(9)/equilib7+1.)
192 CONC(13,J)=CBULK(12)
193 CONC(14,J)=CBULK(13)
194 DO 21 I=1,N
195 21 C(I,J)=0.0
196 JCOUNT=0
197 TOL=1.E-10*N*NJ/1.E12
198 PRINT *, 'TOL=' , TOL
199 22 JCOUNT=JCOUNT+1
200 AMP=0.0
201 J=0
202 DO 23 I=1,N
203 DO 23 K=1,N
204 Y(I,K)=0.0
205 23 X(I,K)=0.0
206 24 J=J+1
207 DO 25 I=1,N
208 G(I)=0.0
209 DO 25 K=1,N
210 A(I,K)=0.0
211 B(I,K)=0.0
212 25 D(I,K)=0.0
213
214 IF (J.EQ.1) CALL BC1(J)

```

```

215 IF ( J .GT. 1 .AND. J .LT .KJ) CALL REACTION(J)
216 IF ( J .EQ .KJ) CALL COUPLER1(J)
217 IF ( J .GT .KJ .AND. J .LT .IJ ) CALL INNER(J)
218 IF ( J .EQ .IJ ) CALL COUPLER2(J)
219 IF ( J .GT .IJ .AND. J .LT .NJ) CALL OUTER(J)
220 IF ( J .EQ .NJ) CALL BCNJ(J)
221 CALL BAND(J)
222
223 AMP=AMP+DABS(G( 1 ))+DABS(G( 2 ))+DABS(G( 3 ))+DABS(G( 4 ))+DABS(G( 5 ))
224 1 +DABS(G( 6 ))+DABS(G( 7 ))+DABS(G( 8 ))+DABS(G( 9 ))+DABS(G( 10 ))
225 2 +DABS(G( 11 ))+DABS(G( 12 ))+DABS(G( 13 ))+DABS(G( 14 ))
226 3 +DABS(G( 15 ))+DABS(G( 16 ))+DABS(G( 17 ))+DABS(G( 18 ))+DABS(G( 19 ))
227
228 IF ( J .LT .NJ) GO TO 24
229
230 PRINT *, 'ERROR=' , AMP
231
232 DO 16 K=1,NJ
233 RXN(1 ,K)=RXN(1 ,K)+C(15 ,K)
234 RXN(2 ,K)=RXN(2 ,K)+C(16 ,K)
235 RXN(3 ,K)=RXN(3 ,K)+C(17 ,K)
236 RXN(4 ,K)=RXN(4 ,K)+C(18 ,K)
237 RXN(5 ,K)=RXN(5 ,K)+C(19 ,K)
238 DO 16 I=1,N-5
239 IF ( C(I ,K) .LT. -0.999*CONC(I ,K) ) C(I ,K)=-0.999*CONC(I ,K)
240 IF ( C(I ,K) .GT. 999.*CONC(I ,K) ) C(I ,K)= 999.*CONC(I ,K)
241 CONC(I ,K)=CONC(I ,K)+C(I ,K)
242 16 CONTINUE
243 C PRINT *, 'B-GLUCOSE AT J=1' , CONC(1 ,1)
244 C PRINT *, 'B-GLUCOSE AT J=2' , CONC(1 ,2)
245 WRITE(12 ,302) (JCOUNT)
246
247 c If the error is less then the tolerance , finish program
248 IF (DABS(AMP) .LT .DABS(TOL)) GO TO 15
249
250 c If the error is greater then tolerance , do another iteration
251 33 IF (JCOUNT.LE.80) GO TO 22
252 print 102
253
254 15 PRINT 103 , AMP,(REF(I) ,CONC(I ,1) ,CONC(I ,NJ) ,I=1,N-6)
255 c Calculate the current density
256 CURRENT3=AKF*CONC(6 ,1)*EXP(BBA*V)
257 1 -AKB*CONC(5 ,1)*(CONC(10 ,1)**2)*EXP(-BBC*V)
258 2 -AK2*CONC(6 ,1)*(CONC(10 ,1)**2)*EXP(-BB2*V)
259 3 -AKH*(CONC(10 ,1)**2)*EXP(-BBH*V)
260 PRINT *, 'CURRENT=' ,CURRENT3
261 PRINT *, 'JCOUNT=' ,JCOUNT
262
263 C Calculate currents for each reaction
264 CURRENTHO=AKF*CONC(6 ,1)*EXP(BBA*V)
265 CURRENTOR=-AKB*CONC(5 ,1)*(CONC(10 ,1)**2)*EXP(-BBC*V)
266 CURRENTHR=-AK2*CONC(6 ,1)*(CONC(10 ,1)**2)*EXP(-BB2*V)
267 CURRENTH2=-AKH*(CONC(10 ,1)**2)*EXP(-BBH*V)
268 PRINT *, 'H2O2 OXIDATION CURRENT=' ,CURRENTHO
269 PRINT *, 'O2 REDUCTION CURRENT=' ,CURRENTOR
270 PRINT *, 'H2O2 REDUCTION CURRENT=' ,CURRENTHR
271 C Calculate Reaction6 and Reaction7
272

```

```

273 DO 26 J=1,NJ
274 IF ( J.EQ.1) RXN(6,J)==DGOX(10)*
275 1 (CONC(11,J+2)-2*CONC(11,J+1)+CONC(11,J)) )
276 2 /(HHH**2.)
277 IF ( J.GT.1 .AND. J.LT.KJ) RXN(6,J)==DGOX(10)*(CONC(11,J+1)
278 2 -2.*CONC(11,J)+CONC(11,J-1))/HHH**2.
279 IF ( J.GT.KJ .AND. J.LT.IJ) RXN(6,J)==DGOX(10)*(CONC(11,J+1)
280 2 -2.*CONC(11,J)+CONC(11,J-1))/HH**2.
281 IF ( J.GT.IJ .AND. J.LT.NJ) RXN(6,J)==DGLM(10)*(CONC(11,J+1)
282 2 -2.*CONC(11,J)+CONC(11,J-1))/H**2.
283 26 IF ( J.EQ.NJ) RXN(6,J)==DGLM(10)*(CONC(11,J)-2.*CONC(11,J-1)
284 1 +CONC(11,J-2))/(H**2.)
285 RXN(6,KJ)==-(DGOX(10)/(HH)*
286 1 (CONC(11,KJ+1)-CONC(11,KJ))-DGOX(10)/(HHH)*(CONC(11,KJ)
287 2 -CONC(11,KJ-1)))/((HHH+HHH)/2.)*4./3.-1./3.*RXN(6,KJ-1)*
288 3 HHH/(HHH+HH)-1./3.*RXN(6,KJ+1)*HH/(HHH+HH)
289 RXN(6,IJ)==-(DGLM(10)/(H)*
290 1 (CONC(11,IJ+1)-CONC(11,IJ))-DGOX(10)/(HH)*(CONC(11,IJ)
291 2 -CONC(11,IJ-1)))/((H+HH)/2.)*4./3.-1./3.*RXN(6,IJ-1)*HH/(HH+H)
292 3 -1./3.*RXN(6,IJ+1)*H/(HH+H)
293
294 DO 27 J=1,NJ
295 IF ( J.EQ.1) RXN(7,J)==DGOX(11)*(CONC(12,J+2)-2*CONC(12,J+1)
296 1 +CONC(12,J))/(HHH**2.)
297 IF ( J.GT.1 .AND. J.LT.KJ) RXN(7,J)==DGOX(11)*(CONC(12,J+1)
298 1 -2.*CONC(12,J)+CONC(12,J-1))/HHH**2.
299 IF ( J.GT.KJ .AND. J.LT.IJ) RXN(7,J)==DGOX(11)*(CONC(12,J+1)
300 1 -2.*CONC(12,J)+CONC(12,J-1))/HH**2.
301 IF ( J.GT.IJ .AND. J.LT.NJ) RXN(7,J)==DGLM(11)*(CONC(12,J+1)
302 1 -2.*CONC(12,J)+CONC(12,J-1))/H**2.
303 27 IF ( J.EQ.NJ) RXN(7,J)==DGLM(11)*
304 1 (CONC(12,J)-2.*CONC(12,J-1)+CONC(12,J-2))/(H**2.)
305 RXN(7,KJ)==-(DGOX(11)/(HH)*
306 1 (CONC(12,KJ+1)-CONC(12,KJ))-DGOX(11)/(HHH)*(CONC(12,KJ)
307 2 -CONC(12,KJ-1)))/((HHH+HHH)/2.)*4./3.-1./3.*RXN(7,KJ-1)*
308 3 HHH/(HHH+HH)-1./3.*RXN(7,KJ+1)*HH/(HHH+HH)
309 RXN(7,IJ)==-(DGLM(11)/(H)*
310 1 (CONC(12,IJ+1)-CONC(12,IJ))-DGOX(11)/(HH)*(CONC(12,IJ)
311 2 -CONC(12,IJ-1)))/((H+HH)/2.)*4./3.-1./3.*RXN(7,IJ-1)*HH/(HH+H)
312 3 -1./3.*RXN(7,IJ+1)*H/(HH+H)
313
314 C DO 26 J=1,NJ
315 C 26 RXN(6,J)=ratef6-ratef6/EQUILIB6*CONC(10,J)*CONC(11,J)
316
317 WRITE(13,334) (CONC(1,J),CONC(2,J),CONC(3,J),CONC(4,J),CONC(5,J),
318 1 CONC(6,J),CONC(7,J),CONC(8,J),CONC(9,J),CONC(10,J),CONC(11,J),
319 2 CONC(12,J),CONC(13,J),CONC(14,J),RXN(1,J),RXN(2,J),RXN(3,J),
320 3 RXN(4,J),RXN(5,J),RXN(6,J),RXN(7,J),J=1,NJ)
321
322 C WRITE(13,334) (CONC(1,J),CONC(2,J),CONC(3,J),CONC(4,J),CONC(5,J),
323 C 1 CONC(6,J),CONC(7,J),CONC(8,J),J=1,NJ)
324
325 END PROGRAM CONVDIFF
326
327 SUBROUTINE BC1(J)
328 IMPLICIT DOUBLE PRECISION (A-H, O-Z)
329 COMMON/BAB/ A(19,19),B(19,19),C(19,80001),D(19,39),G(19),X(19,19)
330 1 ,Y(19,19)

```

```

331 COMMON/NSN/ N, NJ
332 COMMON/VAR/ CONC(14,80001),RXN(7,80001),H,EBIG,HH,IJ
333 COMMON/VARR/ COEFFMT(13), HHH, KJ
334 COMMON/POR/ DGOX(13),DGLM(13),DBULK(13)
335 COMMON/BCI/ FLUXF,FLUXB,FLUXR,FLUXH, Current3
336 COMMON/RTE/ ratef1, equilib1, ratef2, ratef3, equilib3, ratef4, ratef5,
337 1 equilib5, ratef6, equilib6, equilib7, equilib8, equilib9
338 COMMON/BUL/ CBULK(13),PARH2O2,PARO2,PARGLUCOSE,SOLO2,PARION,JCOUNT
339 COMMON/VARIN/ V,PO2,pH,GOx
340 COMMON/TEMP/ T
341 COMMON/DLT/ DELTA
342
343
344 301 FORMAT (5x, 'J=' I5 , 19E19.9E3)
345
346 C For beta-Glucose, being consumed only
347 G(1)=2.*DGOX(1)*(CONC(1,J+1)-CONC(1,J))/HHH**2.
348 2 -(3.*RXN(1,J)+RXN(1,J+1))/4.+(3.*RXN(5,J)+RXN(5,J+1))/4.
349 B(1,1)=2.*DGOX(1)/HHH**2.
350 D(1,1)=-2.*DGOX(1)/HHH**2.
351 B(1,15)=+0.75
352 D(1,15)=+0.25
353 B(1,19)=-0.75
354 D(1,19)=-0.25
355
356 BIG=ABS(2.*DGOX(1)*(CONC(1,J+1))/HHH**2.)
357 C PRINT *, "BIG=", BIG
358 BIG2=ABS(2.*DGOX(1)*(-CONC(1,J))/HHH**2.)
359 C PRINT *, "BIG2=", BIG2
360 IF (BIG2.GT.BIG) BIG=BIG2
361 IF (ABS(-3.*RXN(1,J)/4.).GT.BIG) BIG=ABS(-3.*RXN(1,J)/4.)
362 IF (ABS(-RXN(1,J+1)/4.).GT.BIG) BIG=ABS(-RXN(1,J+1)/4.)
363 IF (ABS(3.*RXN(5,J)/4.).GT.BIG) BIG=ABS(3.*RXN(5,J)/4.)
364 IF (ABS(RXN(5,J+1)/4.).GT.BIG) BIG=ABS(RXN(5,J+1)/4.)
365 IF (ABS(G(1)).LT.BIG*EBIG) G(1)=0
366
367 C For GOx, enzyme
368 G(2)=-RXN(1,J)+RXN(4,J)
369 B(2,15)=+1.
370 B(2,18)=-1.
371
372 IF (ABS(RXN(1,J)).GT.BIG) BIG=ABS(RXN(1,J))
373 IF (ABS(RXN(4,J)).GT.BIG) BIG=ABS(RXN(4,J))
374 IF (ABS(G(2)).LT.BIG*EBIG) G(2)=0
375
376 C For flux of Gluconic Acid and Gluconate ion,
377 G(3)=2.*DGOX(3)*(CONC(3,J+1)-CONC(3,J))/HHH**2.
378 2 +(3.*RXN(2,J)+RXN(2,J+1))/4.
379 3 +2.*DGOX(11)*(CONC(12,J+1)-CONC(12,J))/HHH**2.
380 B(3,3)=2.*DGOX(3)/HHH**2.
381 D(3,3)=-2.*DGOX(3)/HHH**2.
382 B(3,16)=-0.75
383 D(3,16)=-0.25
384 B(3,12)=2.*DGOX(11)/HHH**2.
385 D(3,12)=-2.*DGOX(11)/HHH**2.
386
387 BIG=ABS(2.*DGOX(3)*(CONC(3,J+1))/HHH**2.)
388 BIG2=ABS(2.*DGOX(3)*(-CONC(3,J))/HHH**2.)

```

```

389 IF (BIG2.GT.BIG) BIG=BIG2
390 IF (ABS(3.*RXN(2,J)/4.).GT.BIG) BIG=ABS(3.*RXN(2,J)/4.)
391 IF (ABS(RXN(2,J+1)/4.).GT.BIG) BIG=ABS(RXN(2,J+1)/4.)
392 BIG3=ABS(2.*DGOX(11)*CONC(12,J+1)/(HHH**2.))
393 IF (BIG3.GT.BIG) BIG=BIG3
394 BIG4=ABS(2.*DGOX(11)*CONC(12,J)/(HHH**2.))
395 IF (BIG4.GT.BIG) BIG=BIG4
396 IF (ABS(G(3)).LT.BIG*EBIG) G(3)=0
397
398 C For GOx2, enzyme
399 G(4)=GOx
400 1 -CONC(2,J)-CONC(4,J)-CONC(7,J)-CONC(8,J)-CONC(13,J)-CONC(14,J)
401 B(4,2)=+1.
402 B(4,4)=+1.
403 B(4,7)=+1.
404 B(4,8)=+1.
405 B(4,13)=+1.
406 B(4,14)=+1.
407
408 BIG=ABS(GOx)
409 IF (ABS(CONC(2,J)).GT.BIG) BIG=ABS(CONC(2,J))
410 IF (ABS(CONC(4,J)).GT.BIG) BIG=ABS(CONC(4,J))
411 IF (ABS(CONC(7,J)).GT.BIG) BIG=ABS(CONC(7,J))
412 IF (ABS(CONC(8,J)).GT.BIG) BIG=ABS(CONC(8,J))
413 IF (ABS(CONC(13,J)).GT.BIG) BIG=ABS(CONC(13,J))
414 IF (ABS(CONC(14,J)).GT.BIG) BIG=ABS(CONC(14,J))
415 IF (ABS(G(4)).LT.BIG*EBIG) G(4)=0
416
417 C For O2, being consumed only
418 G(5)=2.*DGOX(5)*(CONC(5,J+1)-CONC(5,J))/HHH**2.
419 1 +FLUXF*CONC(6,J)/(HHH/2.)
420 2 -FLUXB/(HHH/2.)*CONC(5,J)*(CONC(10,J)**2)
421 3 -(3.*RXN(3,J)+RXN(3,J+1))/4.
422 B(5,5)=2.*DGOX(5)/HHH**2.+FLUXB*(CONC(10,J)**2)/(HHH/2.)
423 D(5,5)=-2.*DGOX(5)/HHH**2.
424 B(5,17)=+0.75
425 D(5,17)=+0.25
426 B(5,6)=-FLUXF/(HHH/2.)
427 B(5,10)=2.*FLUXB/(HHH/2.)*CONC(5,J)*CONC(10,J)
428
429 BIG=ABS(2.*DGOX(5)*(CONC(5,J+1))/HHH**2.)
430 BIG2=ABS(2.*DGOX(5)*(-CONC(5,J))/HHH**2.)
431 IF (BIG2.GT.BIG) BIG=BIG2
432 IF (ABS(FLUXF*CONC(6,J)/(HHH/2.)).GT.BIG)
433 1 BIG=ABS(FLUXF*CONC(6,J)/(HHH/2.))
434 1 IF (ABS(-FLUXB/(HHH/2.)*CONC(5,J)*(CONC(10,J)**2)).GT.BIG)
435 1 BIG=ABS(-FLUXB/(HHH/2.)*CONC(5,J)*(CONC(10,J)**2))
436 1 IF (ABS(-3.*RXN(3,J)/4.).GT.BIG) BIG=ABS(-3.*RXN(3,J)/4.)
437 1 IF (ABS(-RXN(3,J+1)/4.).GT.BIG) BIG=ABS(-RXN(3,J+1)/4.)
438 1 IF (ABS(G(5)).LT.BIG*EBIG) G(5)=0
439
440 C For H2O2, reacting species
441 G(6)=2.*DGOX(6)*(CONC(6,J+1)-CONC(6,J))/HHH**2.
442 2 -FLUXF*CONC(6,J)/(HHH/2.)
443 3 +FLUXB/(HHH/2.)*CONC(5,J)*(CONC(10,J)**2.)
444 4 -FLUXR*CONC(6,J)*(CONC(10,J)**2)/(HHH/2.)
445 5 +(3.*RXN(4,J)+RXN(4,J+1))/4.
446 B(6,6)=2.*DGOX(6)/HHH**2.+FLUXF/(HHH/2.)

```

```

447   1      +FLUXR*(CONC(10,J)**2.) / (HHH/2.)
448   D(6,6)=-2.*DGOX(6)/HHH**2.
449   B(6,18)=-0.75
450   D(6,18)=-0.25
451   B(6,5)=-FLUXB*(CONC(10,J)**2) / (HHH/2.)
452   B(6,10)=-2.*FLUXB/(HHH/2.)*CONC(5,J)*CONC(10,J)
453   1      +2.*FLUXR*CONC(6,J)*CONC(10,J)/(HHH/2.)
454
455   BIG=ABS(2.*DGOX(6)*(CONC(6,J+1))/HHH**2.)
456   BIG2=ABS(2.*DGOX(6)*(-CONC(6,J))/HHH**2.)
457   IF (BIG2.GT.BIG) BIG=BIG2
458   IF (ABS(-FLUXF*CONC(6,J)/(HHH/2.)).GT.BIG)
459   1      BIG=ABS(-FLUXF*CONC(6,J)/(HHH/2.))
460   IF (ABS(+FLUXB/(HHH/2.)*CONC(5,J)*(CONC(10,J)**2)).GT.BIG)
461   1      BIG=ABS(+FLUXB/(HHH/2.)*CONC(5,J)*(CONC(10,J)**2))
462   IF (ABS(-FLUXR*CONC(6,J)/(HHH/2.)*(CONC(10,J)**2)).GT.BIG)
463   1      BIG=ABS(-FLUXR*CONC(6,J)/(HHH/2.)*(CONC(10,J)**2))
464   IF (ABS(3.*RXN(4,J)/4.).GT.BIG) BIG=ABS(3.*RXN(4,J)/4.)
465   IF (ABS(RXN(4,J+1)/4.).GT.BIG) BIG=ABS(RXN(4,J+1)/4.)
466   IF (ABS(G(6))).LT.BIG*EBIG) G(6)=0
467
468 C   For CX-GOx2, enzyme
469   G(7)=RXN(1,J)-RXN(2,J)
470   B(7,15)=-1.
471   B(7,16)=1.
472
473   IF (ABS(RXN(1,J)).GT.BIG) BIG=ABS(RXN(1,J))
474   IF (ABS(RXN(2,J)).GT.BIG) BIG=ABS(RXN(2,J))
475   IF (ABS(G(7))).LT.BIG*EBIG) G(7)=0
476
477 C   For CX-GOx, enzyme
478   G(8)=RXN(3,J)-RXN(4,J)
479   B(8,17)=-1.
480   B(8,18)=1.
481
482   IF (ABS(RXN(3,J)).GT.BIG) BIG=ABS(RXN(3,J))
483   IF (ABS(RXN(4,J)).GT.BIG) BIG=ABS(RXN(4,J))
484   IF (ABS(G(8))).LT.BIG*EBIG) G(8)=0
485
486 C   For Alpha-Glucose ,
487   G(9)=2.*DGOX(1)*(CONC(9,J+1)-CONC(9,J))/HHH**2.
488   2      -(3.*RXN(5,J)+RXN(5,J+1))/4.
489   B(9,9)=2.*DGOX(1)/HHH**2.
490   D(9,9)=-2.*DGOX(1)/HHH**2.
491   B(9,19)=+0.75
492   D(9,19)=+0.25
493
494   BIG=ABS(2.*DGOX(1)*(CONC(9,J+1))/HHH**2.)
495   BIG2=ABS(2.*DGOX(1)*(-CONC(9,J))/HHH**2.)
496   IF (BIG2.GT.BIG) BIG=BIG2
497   IF (ABS(-3.*RXN(5,J)/4.).GT.BIG) BIG=ABS(-3.*RXN(5,J)/4.)
498   IF (ABS(-RXN(5,J+1)/4.).GT.BIG) BIG=ABS(-RXN(5,J+1)/4.)
499 C   PRINT *, "G(9)=", ABS(G(9))
500   IF (ABS(G(9))).LT.BIG*EBIG) G(9)=0
501
502 C   For flux of H+, OH- ions and gluconate ions ,
503   G(10)=2.*DGOX(9)*(CONC(10,J+1)-CONC(10,J))/HHH**2.
504   2      +2.*FLUXF*CONC(6,J)/(HHH/2.)

```

```

505      3      -2.*FLUXB/(HHH/2.) *CONC(5,J)*(CONC(10,J)**2.)
506      4      -FLUXR*2.*CONC(6,J)*(CONC(10,J)**2)/(HHH/2.)
507      5      -2.*DGOX(10)*(CONC(11,J+1)-CONC(11,J))/HHH**2.
508      6      -2.*DGOX(11)*(CONC(12,J+1)-CONC(12,J))/HHH**2.
509
510      B(10,10)=2.*DGOX(9)/HHH**2.
511      1      +4.*FLUXB/(HHH/2.) *CONC(5,J)*CONC(10,J)
512      2      +FLUXR*4.*CONC(6,J)*CONC(10,J)/(HHH/2.)
513      3      -FLUXH*2.*((CONC(10,J)**2)/(HHH/2.))
514      B(10,6)=-2.*FLUXF/(HHH/2.) +2.*FLUXR*(CONC(10,J)**2.)/(HHH/2.)
515      D(10,10)=-2.*DGOX(9)/HHH**2.
516      B(10,5)=2.*FLUXB*(CONC(10,J)**2.)/(HHH/2.)
517      B(10,11)=-2.*DGOX(10)/HHH**2.
518      D(10,11)=2.*DGOX(10)/HHH**2.
519      B(10,12)=-2.*DGOX(11)/HHH**2.
520      D(10,12)=2.*DGOX(11)/HHH**2.
521
522      BIG=ABS(2.*DGOX(9)*(CONC(10,J+1))/HHH**2.)
523      BIG2=ABS(2.*DGOX(9)*(-CONC(10,J))/HHH**2.)
524      IF (BIG2.GT.BIG) BIG=BIG2
525      IF (ABS(2*FLUXF*CONC(6,J)/(HHH/2.)).GT.BIG)
526      1      BIG=ABS(2*FLUXF*CONC(6,J)/(HHH/2.))
527      IF (ABS(-2*FLUXB/(HHH/2.)*CONC(5,J)*(CONC(10,J)**2)).GT.BIG)
528      1      BIG=ABS(-2*FLUXB/(HHH/2.)*CONC(5,J)*(CONC(10,J)**2))
529      IF (ABS(-FLUXR*2.*CONC(6,J)*(CONC(10,J)**2)/(HHH/2.)).GT.BIG)
530      1      BIG=ABS(-FLUXR*2.*CONC(6,J)*(CONC(10,J)**2)/(HHH/2.))
531      IF (ABS(-FLUXH*2.*((CONC(10,J)**2)/(HHH/2.))).GT.BIG)
532      1      BIG=ABS(-FLUXH*2.*((CONC(10,J)**2)/(HHH/2.)))
533      IF (ABS(2.*DGOX(10)*(CONC(11,J+1))/HHH**2.).GT.BIG)
534      1      BIG=ABS(2.*DGOX(10)*(CONC(11,J+1))/HHH**2.)
535      IF (ABS(2.*DGOX(10)*(-CONC(11,J))/HHH**2.).GT.BIG)
536      1      BIG=ABS(2.*DGOX(10)*(-CONC(11,J))/HHH**2.)
537      IF (ABS(2.*DGOX(11)*(CONC(12,J+1))/HHH**2.).GT.BIG)
538      1      BIG=ABS(2.*DGOX(11)*(CONC(12,J+1))/HHH**2.)
539      IF (ABS(2.*DGOX(11)*(-CONC(12,J))/HHH**2.).GT.BIG)
540      1      BIG=ABS(2.*DGOX(11)*(-CONC(12,J))/HHH**2.)
541      IF (ABS(G(10)).LT.BIG*EBIG) G(10)=0
542
543 C   FOR water dissociation equilibrium ,
544     G(11)=equilib6-CONC(10,J)*CONC(11,J)
545     B(11,10)=CONC(11,J)
546     B(11,11)=CONC(10,J)
547
548
549     BIG=ABS(equilib6)
550     BIG2=ABS(CONC(10,J)*CONC(11,J))
551     IF (BIG2.GT.BIG) BIG=BIG2
552     IF (ABS(G(11)).LT.BIG*EBIG) G(11)=0
553
554 C   For gluconic acid dissociation equilibrium ,
555     G(12)=equilib7*CONC(3,J)-CONC(10,J)*CONC(12,J)
556     B(12,3)=-equilib7
557     B(12,10)=CONC(12,J)
558     B(12,12)=CONC(10,J)
559
560     BIG=ABS(equilib7*CONC(3,J))
561     BIG2=ABS(-CONC(10,J)*CONC(12,J))
562     IF (BIG2.GT.BIG) BIG=BIG2

```

```

563 IF (ABS(G(12)) .LT. BIG*EBIG) G(12)=0
564
565 C For oxidized enzyme equilibrium ,
566 G(13)=equilib8*CONC(13,J)-CONC(10,J)*CONC(2,J)
567 B(13,13)==equilib8
568 B(13,10)=CONC(2,J)
569 B(13,2)=CONC(10,J)
570
571 BIG=ABS(equilib8*CONC(13,J))
572 BIG2=ABS(-CONC(10,J)*CONC(2,J))
573 IF (BIG2.GT.BIG) BIG=BIG2
574 IF (ABS(G(13)) .LT. BIG*EBIG) G(13)=0
575
576 C For reduced enzyme equilibrium ,
577 G(14)=equilib9*CONC(4,J)-CONC(10,J)*CONC(14,J)
578 B(14,4)==equilib9
579 B(14,10)=CONC(14,J)
580 B(14,14)=CONC(10,J)
581
582 BIG=ABS(equilib9*CONC(4,J))
583 BIG2=ABS(-CONC(10,J)*CONC(14,J))
584 IF (BIG2.GT.BIG) BIG=BIG2
585 IF (ABS(G(14)) .LT. BIG*EBIG) G(14)=0
586
587 C REACTION1
588 214 G(15)=-RXN(1,J)+ratef1*(CONC(1,J)*CONC(2,J)-(CONC(7,J)/equilib1))
589 B(15,1)=-ratef1*CONC(2,J)
590 B(15,2)=-ratef1*CONC(1,J)
591 B(15,7)=ratef1/equilib1
592 B(15,15)=+1.
593
594 BIG=ABS(RXN(1,J))
595 BIG2=ABS(ratef1*CONC(1,J)*CONC(2,J))
596 IF (BIG2.GT.BIG) BIG=BIG2
597 BIG3=ABS(ratef1*(CONC(7,J)/equilib1))
598 IF (BIG3.GT.BIG) BIG=BIG3
599 IF (ABS(G(15)) .LT. BIG*EBIG) G(15)=0
600
601 C REACTION2
602 215 G(16)=-RXN(2,J)+ratef2*CONC(7,J)
603 B(16,7)=-ratef2
604 B(16,16)=+1.
605
606 BIG=ABS(RXN(2,J))
607 BIG2=ABS(ratef2*CONC(7,J))
608 IF (BIG2.GT.BIG) BIG=BIG2
609 IF (ABS(G(16)) .LT. BIG*EBIG) G(16)=0
610
611 C REACTION3
612 216 G(17)=-RXN(3,J)+ratef3*(CONC(4,J)*CONC(5,J)-(CONC(8,J)/equilib3))
613 B(17,4)=-ratef3*CONC(5,J)
614 B(17,5)=-ratef3*CONC(4,J)
615 B(17,8)=ratef3/equilib3
616 B(17,17)=+1.
617
618 BIG=ABS(RXN(3,J))
619 BIG2=ABS(ratef3*CONC(4,J)*CONC(5,J))
620 IF (BIG2.GT.BIG) BIG=BIG2

```

```

621     BIG3=ABS( ratef3 *(CONC(8 ,J) / equilib3 ))
622     IF (BIG3.GT.BIG) BIG=BIG3
623     IF (ABS(G(17 )) .LT .BIG*EBIG) G(17)=0
624
625 C   REACTION4
626 217 G(18)=-RXN(4 ,J)+ratef4 *CONC(8 ,J)
627     B(18 ,8)=-ratef4
628     B(18 ,18)=+1.
629
630     BIG=ABS(RXN(4 ,J))
631     BIG2=ABS( ratef4 *CONC(8 ,J))
632     IF (BIG2.GT.BIG) BIG=BIG2
633     IF (ABS(G(18 )) .LT .BIG*EBIG) G(18)=0
634
635 C   REACTION5
636 218 G(19)=-RXN(5 ,J)+ratef5 *CONC(9 ,J)-ratef5 /equilib5 *CONC(1 ,J)
637     B(19 ,1)=ratef5 /equilib5
638     B(19 ,9)=-ratef5
639     B(19 ,19)=+1.
640
641     BIG=ABS(RXN(5 ,J))
642     BIG2=ABS( ratef5 *CONC(9 ,J))
643     IF (BIG2.GT.BIG) BIG=BIG2
644     BIG3=ABS( ratef5 /equilib5 *CONC(1 ,J))
645     IF (BIG3.GT.BIG) BIG=BIG3
646     IF (ABS(G(19 )) .LT .BIG*EBIG) G(19)=0
647
648 212 WRITE(12 ,301) J , (G(K) ,K=1,N)
649
650
651      RETURN
652
653
654      SUBROUTINE REACTION(J)
655      IMPLICIT DOUBLE PRECISION (A-H, O-Z)
656      COMMON/BAB/ A(19 ,19) ,B(19 ,19) ,C(19 ,80001) ,D(19 ,39) ,G(19) ,X(19 ,19)
657      1 ,Y(19 ,19)
658      COMMON/NSN/ N, NJ
659      COMMON/VAR/ CONC(14 ,80001) ,RXN(7 ,80001) ,H, EBIG, HH, IJ
660      COMMON/VARR/ COEFFMT(13) , HHH, KJ
661      COMMON/POR/ DGOX(13) ,DGIM(13) ,DBULK(13)
662      COMMON/BCI/ FLUXF,FLUXB,FLUXR,FLUXH, Current3
663      COMMON/RTE/ ratef1 , equilib1 , ratef2 , ratef3 , equilib3 , ratef4 , ratef5 ,
664      1 equilib5 , ratef6 , equilib6 , equilib7 , equilib8 , equilib9
665      COMMON/BUL/ CBULK(13) ,PARH2O2,PARO2,PARGLUCOSE,SOLO2,PARION,JCOUNT
666      COMMON/VARIN/ V,PO2,pH,GOx
667      COMMON/TEMP/ T
668      COMMON/DLT/ DELTA
669
670 301 FORMAT (5x, 'J=' I5 , 19E19.9E3)
671
672 C   For Beta-Glucose , being consumed only
673     G(1)=DGOX(1)*(CONC(1 ,J+1)-2.*CONC(1 ,J)+CONC(1 ,J-1))/HHH**2.
674     2 -RXN(1 ,J)+RXN(5 ,J)
675     B(1 ,1)=2.*DGOX(1 )/HHH**2.
676     D(1 ,1)=-DGOX(1 )/HHH**2.
677     A(1 ,1)=-DGOX(1 )/HHH**2.
678     B(1 ,15)=+1.

```

```

679 B(1,19)=-1.
680
681 BIG=ABS(DGOX(1)*(CONC(1,J+1))/HHH**2.)
682 BIG2=ABS(DGOX(1)*(-2.*CONC(1,J))/HHH**2.)
683 IF (BIG2.GT.BIG) BIG=BIG2
684 BIG3=ABS(DGOX(1)*(CONC(1,J-1))/HHH**2.)
685 IF (BIG3.GT.BIG) BIG=BIG3
686 IF (ABS(-RXN(1,J)).GT.BIG) BIG=ABS(-RXN(1,J))
687 IF (ABS(RXN(5,J)).GT.BIG) BIG=ABS(RXN(5,J))
688 IF (ABS(G(1)).LT.BIG*EBIG) G(1)=0
689
690 C For GOx, enzyme
691 G(2)=-RXN(1,J)+RXN(4,J)
692 B(2,15)=+1.
693 B(2,18)=-1.
694
695 IF (ABS(RXN(1,J)).GT.BIG) BIG=ABS(RXN(1,J))
696 IF (ABS(RXN(4,J)).GT.BIG) BIG=ABS(RXN(4,J))
697 IF (ABS(G(2)).LT.BIG*EBIG) G(2)=0
698
699 C For Flux of Gluconic Acid and Gluconate Ions,
700 G(3)=DGOX(3)*(CONC(3,J+1)-2.*CONC(3,J)+CONC(3,J-1))/HHH**2.
701 2 -RXN(2,J)
702 3 -DGOX(11)*(CONC(12,J+1)-2.*CONC(12,J)+CONC(12,J-1))/HHH**2.
703 B(3,3)=2.*DGOX(3)/HHH**2.
704 D(3,3)=-DGOX(3)/HHH**2.
705 A(3,3)=-DGOX(3)/HHH**2.
706 B(3,16)=-1.
707 B(3,12)=2.*DGOX(11)/HHH**2.
708 D(3,12)=-DGOX(11)/HHH**2.
709 A(3,12)=-DGOX(11)/HHH**2.
710
711 BIG=ABS(DGOX(3)*(CONC(3,J+1))/HHH**2.)
712 BIG2=ABS(DGOX(3)*(-2.*CONC(3,J))/HHH**2.)
713 IF (BIG2.GT.BIG) BIG=BIG2
714 BIG3=ABS(DGOX(3)*(CONC(3,J-1))/HHH**2.)
715 IF (BIG3.GT.BIG) BIG=BIG3
716 IF (ABS(RXN(2,J)).GT.BIG) BIG=ABS(RXN(2,J))
717 BIG4=ABS(DGOX(11)*CONC(12,J+1)/(HHH**2.))
718 IF (BIG4.GT.BIG) BIG=BIG4
719 BIG5=ABS(DGOX(11)*(-2.*CONC(12,J))/HHH**2.)
720 IF (BIG5.GT.BIG) BIG=BIG5
721 BIG6=ABS(DGOX(11)*(CONC(12,J-1))/HHH**2.)
722 IF (BIG6.GT.BIG) BIG=BIG6
723 IF (ABS(G(3)).LT.BIG*EBIG) G(3)=0
724
725 C For GOx2, enzyme
726 G(4)=GOx
727 1 -CONC(2,J)-CONC(4,J)-CONC(7,J)-CONC(8,J)-CONC(13,J)-CONC(14,J)
728 B(4,2)=+1.
729 B(4,4)=+1.
730 B(4,7)=+1.
731 B(4,8)=+1.
732 B(4,13)=+1.
733 B(4,14)=+1.
734
735 BIG=ABS(GOx)
736 IF (ABS(CONC(2,J)).GT.BIG) BIG=ABS(CONC(2,J))

```

```

737 IF (ABS(CONC(4,J)).GT.BIG) BIG=ABS(CONC(4,J))
738 IF (ABS(CONC(7,J)).GT.BIG) BIG=ABS(CONC(7,J))
739 IF (ABS(CONC(8,J)).GT.BIG) BIG=ABS(CONC(8,J))
740 IF (ABS(CONC(13,J)).GT.BIG) BIG=ABS(CONC(13,J))
741 IF (ABS(CONC(14,J)).GT.BIG) BIG=ABS(CONC(14,J))
742 IF (ABS(G(4)).LT.BIG*EBIG) G(4)=0
743
744 C For O2, being consumed only
745 G(5)=DGOX(5)*(CONC(5,J+1)-2.*CONC(5,J)+CONC(5,J-1))/HHH**2.
746 2 -RXN(3,J)
747 B(5,5)=2.*DGOX(5)/HHH**2.
748 D(5,5)=-DGOX(5)/HHH**2.
749 A(5,5)=-DGOX(5)/HHH**2.
750 B(5,17)=+1.
751
752 BIG=ABS(DGOX(5)*(CONC(5,J+1))/HHH**2.)
753 BIG2=ABS(DGOX(5)*(-2.*CONC(5,J))/HHH**2.)
754 IF (BIG2.GT.BIG) BIG=BIG2
755 BIG3=ABS(DGOX(5)*(CONC(5,J-1))/HHH**2.)
756 IF (BIG3.GT.BIG) BIG=BIG3
757 IF (ABS(-RXN(3,J)).GT.BIG) BIG=ABS(-RXN(3,J))
758 IF (ABS(G(5)).LT.BIG*EBIG) G(5)=0
759
760 C For H2O2, reacting species
761 G(6)=DGOX(6)*(CONC(6,J+1)-2.*CONC(6,J)+CONC(6,J-1))/HHH**2.
762 2 +RXN(4,J)
763 B(6,6)=2.*DGOX(6)/HHH**2.
764 D(6,6)=-DGOX(6)/HHH**2.
765 A(6,6)=-DGOX(6)/HHH**2.
766 B(6,18)=-1.
767
768 BIG=ABS(DGOX(6)*(CONC(6,J+1))/HHH**2.)
769 BIG2=ABS(DGOX(6)*(-2.*CONC(6,J))/HHH**2.)
770 IF (BIG2.GT.BIG) BIG=BIG2
771 BIG3=ABS(DGOX(6)*(CONC(6,J-1))/HHH**2.)
772 IF (BIG3.GT.BIG) BIG=BIG3
773 IF (ABS(RXN(4,J)).GT.BIG) BIG=ABS(RXN(4,J))
774 IF (ABS(G(6)).LT.BIG*EBIG) G(6)=0
775
776 C For CX-GOx2, enzyme
777 G(7)=RXN(1,J)-RXN(2,J)
778 B(7,15)=-1.
779 B(7,16)=1.
780
781 IF (ABS(RXN(1,J)).GT.BIG) BIG=ABS(RXN(1,J))
782 IF (ABS(RXN(2,J)).GT.BIG) BIG=ABS(RXN(2,J))
783 IF (ABS(G(7)).LT.BIG*EBIG) G(7)=0
784
785 C For CX-GOx, enzyme
786 G(8)=RXN(3,J)-RXN(4,J)
787 B(8,17)=-1.
788 B(8,18)=1.
789
790 IF (ABS(RXN(3,J)).GT.BIG) BIG=ABS(RXN(3,J))
791 IF (ABS(RXN(4,J)).GT.BIG) BIG=ABS(RXN(4,J))
792 IF (ABS(G(8)).LT.BIG*EBIG) G(8)=0
793
794 C For Alpha-Glucose ,

```

```

795 G(9)=DGOX(1)*(CONC(9,J+1)-2.*CONC(9,J)+CONC(9,J-1))/HHH**2.
796 2 -RXN(5,J)
797 B(9,9)=2.*DGOX(1)/HHH**2.
798 D(9,9)=-DGOX(1)/HHH**2.
799 A(9,9)=-DGOX(1)/HHH**2.
800 B(9,19)=+1.
801
802 BIG=ABS(DGOX(1)*(CONC(9,J+1))/HHH**2.)
803 BIG2=ABS(DGOX(1)*(-2.*CONC(9,J))/HHH**2.)
804 IF (BIG2.GT.BIG) BIG=BIG2
805 BIG3=ABS(DGOX(1)*(CONC(9,J-1))/HHH**2.)
806 IF (BIG3.GT.BIG) BIG=BIG3
807 IF (ABS(-RXN(5,J)).GT.BIG) BIG=ABS(-RXN(5,J))
808 IF (ABS(G(9))).LT.BIG*EBIG) G(9)=0
809
810 C For flux of H+, OH- ions and gluconate ions,
811 G(10)=DGOX(9)*(CONC(10,J+1)-2.*CONC(10,J)+CONC(10,J-1))
812 2 /HHH**2.
813 3 -DGOX(10)*(CONC(11,J+1)-2.*CONC(11,J)+CONC(11,J-1))
814 4 /HHH**2.
815 5 -DGOX(11)*(CONC(12,J+1)-2.*CONC(12,J)+CONC(12,J-1))
816 6 /HHH**2.
817 B(10,10)=2.*DGOX(9)/HHH**2.
818 D(10,10)=-DGOX(9)/HHH**2.
819 A(10,10)=-DGOX(9)/HHH**2.
820 B(10,11)=-2.*DGOX(10)/HHH**2.
821 D(10,11)=DGOX(10)/HHH**2.
822 A(10,11)=DGOX(10)/HHH**2.
823 B(10,12)=-2.*DGOX(11)/HHH**2.
824 D(10,12)=DGOX(11)/HHH**2.
825 A(10,12)=DGOX(11)/HHH**2.
826
827 BIG=ABS(DGOX(9)*(CONC(10,J+1))/HHH**2.)
828 BIG2=ABS(DGOX(9)*(-2.*CONC(10,J))/HHH**2.)
829 IF (BIG2.GT.BIG) BIG=BIG2
830 BIG3=ABS(DGOX(9)*(CONC(10,J-1))/HHH**2.)
831 IF (BIG3.GT.BIG) BIG=BIG3
832 BIG4=ABS(DGOX(10)*(CONC(11,J+1))/HHH**2.)
833 IF (BIG4.GT.BIG) BIG=BIG4
834 BIG5=ABS(DGOX(10)*(-2.*CONC(11,J))/HHH**2.)
835 IF (BIG5.GT.BIG) BIG=BIG5
836 BIG6=ABS(DGOX(10)*(CONC(11,J-1))/HHH**2.)
837 IF (BIG6.GT.BIG) BIG=BIG6
838 BIG7=ABS(DGOX(11)*(CONC(12,J+1))/HHH**2.)
839 IF (BIG7.GT.BIG) BIG=BIG7
840 BIG8=ABS(DGOX(11)*(-2.*CONC(12,J))/HHH**2.)
841 IF (BIG8.GT.BIG) BIG=BIG8
842 BIG9=ABS(DGOX(11)*(CONC(12,J-1))/HHH**2.)
843 IF (BIG9.GT.BIG) BIG=BIG9
844 IF (ABS(G(10)).LT.BIG*EBIG) G(10)=0
845
846 C FOR water dissociation equilibrium ,
847 G(11)=equilib6-CONC(10,J)*CONC(11,J)
848 B(11,10)=CONC(11,J)
849 B(11,11)=CONC(10,J)
850
851 BIG=ABS(equilib6)
852 BIG2=ABS(CONC(10,J)*CONC(11,J))

```

```

853 IF (BIG2.GT.BIG) BIG=BIG2
854 IF (ABS(G(11)).LT.BIG*EBIG) G(11)=0
855
856 C FOR gluconic acid dissociation equilibrium ,
857 G(12)=equilib7*CONC(3,J)-CONC(10,J)*CONC(12,J)
858 B(12,3)=-equilib7
859 B(12,10)=CONC(12,J)
860 B(12,12)=CONC(10,J)
861
862
863 BIG=ABS(equilib7*CONC(3,J))
864 BIG2=ABS(-CONC(10,J)*CONC(12,J))
865 IF (BIG2.GT.BIG) BIG=BIG2
866 IF (ABS(G(12)).LT.BIG*EBIG) G(12)=0
867
868 C For oxidized enzyme equilibrium ,
869 G(13)=equilib8*CONC(13,J)-CONC(10,J)*CONC(2,J)
870 B(13,13)=-equilib8
871 B(13,10)=CONC(2,J)
872 B(13,2)=CONC(10,J)
873
874 BIG=ABS(equilib8*CONC(13,J))
875 BIG2=ABS(-CONC(10,J)*CONC(2,J))
876 IF (BIG2.GT.BIG) BIG=BIG2
877 IF (ABS(G(13)).LT.BIG*EBIG) G(13)=0
878
879 C For reduced enzyme equilibrium ,
880 G(14)=equilib9*CONC(4,J)-CONC(10,J)*CONC(14,J)
881 B(14,4)=-equilib9
882 B(14,10)=CONC(14,J)
883 B(14,14)=CONC(10,J)
884
885 BIG=ABS(equilib9*CONC(4,J))
886 BIG2=ABS(-CONC(10,J)*CONC(14,J))
887 IF (BIG2.GT.BIG) BIG=BIG2
888 IF (ABS(G(14)).LT.BIG*EBIG) G(14)=0
889
890 C REACTION1
891 214 G(15)=-RXN(1,J)+ratef1*(CONC(1,J)*CONC(2,J)-(CONC(7,J)/equilib1))
892 B(15,1)=-ratef1*CONC(2,J)
893 B(15,2)=-ratef1*CONC(1,J)
894 B(15,7)=ratef1/equilib1
895 B(15,15)=+1.
896
897 BIG=ABS(RXN(1,J))
898 BIG2=ABS(ratef1*CONC(1,J)*CONC(2,J))
899 IF (BIG2.GT.BIG) BIG=BIG2
900 BIG3=ABS(ratef1*(CONC(7,J)/equilib1))
901 IF (BIG3.GT.BIG) BIG=BIG3
902 IF (ABS(G(15)).LT.BIG*EBIG) G(15)=0
903
904 C REACTION2
905 215 G(16)=-RXN(2,J)+ratef2*CONC(7,J)
906 B(16,7)=-ratef2
907 B(16,16)=+1.
908
909 BIG=ABS(RXN(2,J))
910 BIG2=ABS(ratef2*CONC(7,J))

```

```

911 IF (BIG2.GT.BIG) BIG=BIG2
912 IF (ABS(G(16)).LT.BIG*EBIG) G(16)=0
913
914 C REACTION3
915 216 G(17)=-RXN(3,J)+ratef3*(CONC(4,J)*CONC(5,J)-(CONC(8,J)/equilib3))
916 B(17,4)=-ratef3*CONC(5,J)
917 B(17,5)=-ratef3*CONC(4,J)
918 B(17,8)=ratef3/equilib3
919 B(17,17)=+1.
920
921 BIG=ABS(RXN(3,J))
922 BIG2=ABS(ratef3*CONC(4,J)*CONC(5,J))
923 IF (BIG2.GT.BIG) BIG=BIG2
924 BIG3=ABS(ratef3*(CONC(8,J)/equilib3))
925 IF (BIG3.GT.BIG) BIG=BIG3
926 IF (ABS(G(17)).LT.BIG*EBIG) G(17)=0
927
928 C REACTION4
929 217 G(18)=-RXN(4,J)+ratef4*CONC(8,J)
930 B(18,8)=-ratef4
931 B(18,18)=+1.
932
933 BIG=ABS(RXN(4,J))
934 BIG2=ABS(ratef4*CONC(8,J))
935 IF (BIG2.GT.BIG) BIG=BIG2
936 IF (ABS(G(18)).LT.BIG*EBIG) G(18)=0
937
938 C REACTION5
939 218 G(19)=-RXN(5,J)+ratef5*CONC(9,J)-ratef5/equilib5*CONC(1,J)
940 B(19,1)=ratef5/equilib5
941 B(19,9)=-ratef5
942 B(19,19)=+1.
943
944 BIG=ABS(RXN(5,J))
945 BIG2=ABS(ratef5*CONC(9,J))
946 IF (BIG2.GT.BIG) BIG=BIG2
947 BIG3=ABS(ratef5/equilib5*CONC(1,J))
948 IF (BIG3.GT.BIG) BIG=BIG3
949 IF (ABS(G(19)).LT.BIG*EBIG) G(19)=0
950
951
952 c SAVE G OUT DATA
953 212 DO 11 I=2,20
954 11 If (I.EQ.J) WRITE(12,301) J, (G(K),K=1,N)
955 IF (J.EQ.KJ/2) THEN
956 WRITE(12,301) J, (G(K),K=1,N)
957 ELSE IF (J.EQ.(KJ-1)) THEN
958 WRITE(12,301) J, (G(K),K=1,N)
959 ELSE IF (J.EQ.(KJ-2)) THEN
960 WRITE(12,301) J, (G(K),K=1,N)
961 ELSE IF (J.EQ.(KJ-3)) THEN
962 WRITE(12,301) J, (G(K),K=1,N)
963 END IF
964
965 RETURN
966
967
968 SUBROUTINE COUPLER1(J)

```

```

969 IMPLICIT DOUBLE PRECISION (A–H, O–Z)
970 COMMON/BAB/ A(19,19),B(19,19),C(19,80001),D(19,39),G(19),X(19,19)
971 1, Y(19,19)
972 COMMON/NSN/ N, NJ
973 COMMON/VAR/ CONC(14,80001),RXN(7,80001),H,EBIG,HH,IJ
974 COMMON/VARR/ COEFFMT(13),HHH,KJ
975 COMMON/POR/ DGOX(13),DGML(13),DBULK(13)
976 COMMON/BCI/ FLUXF,FLUXB,FLUXR,FLUXH,Current3
977 COMMON/RTE/ ratef1,equilib1,ratef2,ratef3,equilib3,ratef4,ratef5,
978 1 equilib5,ratef6,equilib6,equilib7,equilib8,equilib9
979 COMMON/BUL/ CBULK(13),PARH2O2,PARO2,PARGLUCOSE,SOLO2,PARION,JCOUNT
980 COMMON/VARIN/ V,PO2,pH,GOx
981 COMMON/TEMP/ T
982 COMMON/DLT/ DELTA
983
984 301 FORMAT (5x,'J=' I5, 19E19.9E3)
985
986 C      DIMENSION COEFF1, COEFF3, COEFF5, COEFF6, COEFF9, COEFF10, COEFF11
987
988 COEFF1HH=DGOX(1)/(HH)
989 COEFF1HHH=DGOX(1)/(HHH)
990 COEFF3HH=DGOX(3)/(HH)
991 COEFF3HHH=DGOX(3)/(HHH)
992 COEFF5HH=DGOX(5)/(HH)
993 COEFF5HHH=DGOX(5)/(HHH)
994 COEFF6HH=DGOX(6)/(HH)
995 COEFF6HHH=DGOX(6)/(HHH)
996 COEFF9HH=DGOX(9)/(HH)
997 COEFF9HHH=DGOX(9)/(HHH)
998 COEFF10HH=DGOX(10)/(HH)
999 COEFF10HHH=DGOX(10)/(HHH)
1000 COEFF11HH=DGOX(11)/(HH)
1001 COEFF11HHH=DGOX(11)/(HHH)
1002
1003 C      For BETA–Glucose, being consumed only
1004 G(1)=COEFF1HH*(CONC(1,J+1)-CONC(1,J))
1005 1 -COEFF1HHH*(CONC(1,J)-CONC(1,J-1))
1006 2 -(HH/2.)*(RXN(1,J+1)+3.*RXN(1,J))/4.
1007 3 -(HHH/2.)*(RXN(1,J-1)+3.*RXN(1,J))/4.
1008 4 +(HH/2.)*(RXN(5,J+1)+3.*RXN(5,J))/4.
1009 5 +(HHH/2.)*(RXN(5,J-1)+3.*RXN(5,J))/4.
1010 B(1,1)=COEFF1HH+COEFF1HHH
1011 D(1,1)=-COEFF1HH
1012 A(1,1)=-COEFF1HHH
1013 B(1,15)=+(HH/2.)*(3./4.)+(HHH/2.)*(3./4.)
1014 D(1,15)=+(HH/2.)*(1./4.)
1015 A(1,15)=+(HHH/2.)*(1./4.)
1016 B(1,19)=-(HH/2.)*(3./4.)-(HHH/2.)*(3./4.)
1017 D(1,19)=-(HH/2.)*(1./4.)
1018 A(1,19)=-(HHH/2.)*(1./4.)
1019
1020 BIG=ABS(COEFF1HH*CONC(1,J+1))
1021 BIG2=ABS(COEFF1HH*CONC(1,J))
1022 IF (BIG2.GT.BIG) BIG=BIG2
1023 BIG3=ABS(-COEFF1HHH*CONC(1,J))
1024 IF (BIG3.GT.BIG) BIG=BIG3
1025 BIG4=ABS(-COEFF1HHH*CONC(1,J-1))
1026 IF (BIG4.GT.BIG) BIG=BIG4

```

```

1027 BIG5=ABS((HH/2.)*(RXN(1,J+1)/4.))
1028 IF (BIG5.GT.BIG) BIG=BIG5
1029 BIG6=ABS((HH/2.)*(3.*RXN(1,J))/4.)
1030 IF (BIG6.GT.BIG) BIG=BIG6
1031 BIG7=ABS((HHH/2.)*(RXN(1,J-1)/4.))
1032 IF (BIG7.GT.BIG) BIG=BIG7
1033 BIG8=ABS((HHH/2.)*(3.*RXN(1,J))/4.)
1034 IF (BIG8.GT.BIG) BIG=BIG8
1035 BIG9=ABS((HH/2.)*(RXN(5,J+1)/4.))
1036 IF (BIG9.GT.BIG) BIG=BIG9
1037 BIG10=ABS((HH/2.)*(3.*RXN(5,J))/4.)
1038 IF (BIG10.GT.BIG) BIG=BIG10
1039 BIG11=ABS((HHH/2.)*(RXN(5,J-1)/4.))
1040 IF (BIG11.GT.BIG) BIG=BIG11
1041 BIG12=ABS((HHH/2.)*(3.*RXN(5,J))/4.)
1042 IF (BIG12.GT.BIG) BIG=BIG12
1043 IF (ABS(G(1)).LT.BIG*EBIG) G(1)=0
1044
1045 C For GOx, enzyme
1046 G(2)=-RXN(1,J)+RXN(4,J)
1047 B(2,15)=+1.
1048 B(2,18)=-1.
1049
1050 BIG=ABS(RXN(1,J))
1051 BIG2=ABS(RXN(4,J))
1052 IF (BIG2.GT.BIG) BIG=BIG2
1053 IF (ABS(G(2)).LT.BIG*EBIG) G(2)=0
1054
1055 C For flux of Gluconic Acid and Gluconate ions ,
1056 G(3)=COEFF3HH*(CONC(3,J+1)-CONC(3,J))
1057 1 -COEFF3HHH*(CONC(3,J)-CONC(3,J-1))
1058 2 +(HH/2.)*(RXN(2,J+1)+3.*RXN(2,J))/4.
1059 3 +(HHH/2.)*(RXN(2,J-1)+3.*RXN(2,J))/4.
1060 4 +COEFF11HH*(CONC(12,J+1)-CONC(12,J))
1061 5 -COEFF11HHH*(CONC(12,J)-CONC(12,J-1))
1062 B(3,3)=COEFF3HH+COEFF3HHH
1063 D(3,3)=-COEFF3HH
1064 A(3,3)=-COEFF3HHH
1065 B(3,16)=-(HH/2.)*(3./4.)-(HHH/2.)*(3./4.)
1066 D(3,16)=-(HH/2.)*(1./4.)
1067 A(3,16)=-(HHH/2.)*(1./4.)
1068 B(3,12)=COEFF11HH+COEFF11HHH
1069 D(3,12)=-COEFF11HH
1070 A(3,12)=-COEFF11HHH
1071
1072 BIG=ABS(COEFF3HH*CONC(3,J+1))
1073 BIG2=ABS(COEFF3HH*CONC(3,J))
1074 IF (BIG2.GT.BIG) BIG=BIG2
1075 BIG3=ABS(-COEFF3HHH*CONC(3,J))
1076 IF (BIG3.GT.BIG) BIG=BIG3
1077 BIG4=ABS(-COEFF3HHH*CONC(3,J-1))
1078 IF (BIG4.GT.BIG) BIG=BIG4
1079 BIG5=ABS((HH/2.)*(RXN(2,J+1)/4.))
1080 IF (BIG5.GT.BIG) BIG=BIG5
1081 BIG6=ABS((HH/2.)*(3.*RXN(2,J))/4.)
1082 IF (BIG6.GT.BIG) BIG=BIG6
1083 BIG7=ABS((HHH/2.)*(RXN(2,J-1)/4.))
1084 IF (BIG7.GT.BIG) BIG=BIG7

```

```

1085 BIG8=ABS((HHH/2.)*(3.*RXN(2,J))/4.)
1086 IF (BIG8.GT.BIG) BIG=BIG8
1087 BIG9=ABS(COEFF11HH*CONC(12,J+1))
1088 IF (BIG9.GT.BIG) BIG=BIG9
1089 BIG10=ABS(COEFF11HH*CONC(12,J))
1090 IF (BIG10.GT.BIG) BIG=BIG10
1091 BIG11=ABS(-COEFF11HHH*CONC(12,J))
1092 IF (BIG11.GT.BIG) BIG=BIG11
1093 BIG12=ABS(-COEFF11HHH*CONC(12,J-1))
1094 IF (BIG12.GT.BIG) BIG=BIG12
1095 IF (ABS(G(3)).LT.BIG*EBIG) G(3)=0
1096

1097 C For GOx2, enzyme
1098 G(4)=GOx
1099 1 -CONC(2,J)-CONC(4,J)-CONC(7,J)-CONC(8,J)-CONC(13,J)-CONC(14,J)
1100 B(4,2)=+1.
1101 B(4,4)=+1.
1102 B(4,7)=+1.
1103 B(4,8)=+1.
1104 B(4,13)=+1.
1105 B(4,14)=+1.
1106
1107 BIG=ABS(GOx)
1108 IF (ABS(CONC(2,J)).GT.BIG) BIG=ABS(CONC(2,J))
1109 IF (ABS(CONC(4,J)).GT.BIG) BIG=ABS(CONC(4,J))
1110 IF (ABS(CONC(7,J)).GT.BIG) BIG=ABS(CONC(7,J))
1111 IF (ABS(CONC(8,J)).GT.BIG) BIG=ABS(CONC(8,J))
1112 IF (ABS(CONC(13,J)).GT.BIG) BIG=ABS(CONC(13,J))
1113 IF (ABS(CONC(14,J)).GT.BIG) BIG=ABS(CONC(14,J))
1114 IF (ABS(G(4)).LT.BIG*EBIG) G(4)=0
1115

1116 C For O2, being consumed only
1117 G(5)=COEFF5HH*(CONC(5,J+1)-CONC(5,J))
1118 1 -COEFF5HHH*(CONC(5,J)-CONC(5,J-1))
1119 2 -(HH/2.)*(RXN(3,J+1)+3.*RXN(3,J))/4.
1120 3 -(HHH/2.)*(RXN(3,J-1)+3.*RXN(3,J))/4.
1121 B(5,5)=COEFF5HH+COEFF5HHH
1122 D(5,5)=-COEFF5HH
1123 A(5,5)=-COEFF5HHH
1124 B(5,17)=+(HH/2.)*(3./4.)+(HHH/2.)*(3./4.)
1125 D(5,17)=+(HH/2.)*(1./4.)
1126 A(5,17)=+(HHH/2.)*(1./4.)
1127
1128 BIG=ABS(COEFF5HH*CONC(5,J+1))
1129 BIG2=ABS(COEFF5HH*CONC(5,J))
1130 IF (BIG2.GT.BIG) BIG=BIG2
1131 BIG3=ABS(-COEFF5HHH*CONC(5,J))
1132 IF (BIG3.GT.BIG) BIG=BIG3
1133 BIG4=ABS(-COEFF5HHH*CONC(5,J-1))
1134 IF (BIG4.GT.BIG) BIG=BIG4
1135 BIG5=ABS((HH/2.)*(RXN(3,J+1)/4.))
1136 IF (BIG5.GT.BIG) BIG=BIG5
1137 BIG6=ABS((HH/2.)*(3.*RXN(3,J))/4.)
1138 IF (BIG6.GT.BIG) BIG=BIG6
1139 BIG7=ABS((HHH/2.)*(RXN(3,J-1)/4.))
1140 IF (BIG7.GT.BIG) BIG=BIG7
1141 BIG8=ABS((HHH/2.)*(3.*RXN(3,J))/4.)
1142 IF (BIG8.GT.BIG) BIG=BIG8

```

```

1143 IF (ABS(G(5)) .LT. BIG*EBIG) G(5)=0
1144
1145 C For H2O2, reacting species
1146 G(6)=COEFF6HH*(CONC(6,J+1)-CONC(6,J))
1147 1 -COEFF6HHH*(CONC(6,J)-CONC(6,J-1))
1148 2 +(HH/2.)*(RXN(4,J+1)+3.*RXN(4,J))/4.
1149 3 +(HHH/2.)*(RXN(4,J-1)+3.*RXN(4,J))/4.
1150 B(6,6)=COEFF6HH+COEFF6HHH
1151 D(6,6)=-COEFF6HH
1152 A(6,6)=-COEFF6HHH
1153 B(6,18)=-(HH/2.)*(3./4.)-(HHH/2.)*(3./4.)
1154 D(6,18)=-(HH/2.)*(1./4.)
1155 A(6,18)=-(HHH/2.)*(1./4.)
1156
1157 BIG=ABS(COEFF6HH*CONC(6,J+1))
1158 BIG2=ABS(COEFF6HH*CONC(6,J))
1159 IF (BIG2.GT.BIG) BIG=BIG2
1160 BIG3=ABS(-COEFF6HHH*CONC(6,J))
1161 IF (BIG3.GT.BIG) BIG=BIG3
1162 BIG4=ABS(-COEFF6HHH*CONC(6,J-1))
1163 IF (BIG4.GT.BIG) BIG=BIG4
1164 BIG5=ABS((HH/2.)*(RXN(4,J+1)/4.))
1165 IF (BIG5.GT.BIG) BIG=BIG5
1166 BIG6=ABS((HH/2.)*(3.*RXN(4,J))/4.)
1167 IF (BIG6.GT.BIG) BIG=BIG6
1168 BIG7=ABS((HHH/2.)*(RXN(4,J-1)/4.))
1169 IF (BIG7.GT.BIG) BIG=BIG7
1170 BIG8=ABS((HHH/2.)*(3.*RXN(4,J))/4.)
1171 IF (BIG8.GT.BIG) BIG=BIG8
1172 IF (ABS(G(6)) .LT. BIG*EBIG) G(6)=0
1173
1174 C For CX-GOx2, enzyme
1175 G(7)=RXN(1,J)-RXN(2,J)
1176 B(7,15)=-1.
1177 B(7,16)=1.
1178
1179 IF (ABS(RXN(1,J)).GT.BIG) BIG=ABS(RXN(1,J))
1180 IF (ABS(RXN(2,J)).GT.BIG) BIG=ABS(RXN(2,J))
1181 IF (ABS(G(7)) .LT. BIG*EBIG) G(7)=0
1182
1183 C For CX-GOx, enzyme
1184 G(8)=RXN(3,J)-RXN(4,J)
1185 B(8,17)=-1.
1186 B(8,18)=1.
1187
1188 IF (ABS(RXN(3,J)).GT.BIG) BIG=ABS(RXN(3,J))
1189 IF (ABS(RXN(4,J)).GT.BIG) BIG=ABS(RXN(4,J))
1190 IF (ABS(G(8)) .LT. BIG*EBIG) G(8)=0
1191
1192 C For Alpha-Glucose ,
1193 G(9)=COEFF1HH*(CONC(9,J+1)-CONC(9,J))
1194 1 -COEFF1HHH*(CONC(9,J)-CONC(9,J-1))
1195 2 -(HH/2.)*(RXN(5,J+1)+3.*RXN(5,J))/4.
1196 3 -(HHH/2.)*(RXN(5,J-1)+3.*RXN(5,J))/4.
1197
1198 B(9,9)=COEFF1HH+COEFF1HHH
1199 D(9,9)=-COEFF1HH
1200 A(9,9)=-COEFF1HHH

```

```

1201 B(9,19)=+(HH/2.)*(3./4.)+(HHH/2.)*(3./4.)
1202 D(9,19)=+(HH/2.)*(1./4.)
1203 A(9,19)=+(HHH/2.)*(1./4.)
1204
1205 BIG=ABS(COEFF1HH*CONC(1,J+1))
1206 BIG2=ABS(COEFF1HH*CONC(1,J))
1207 IF (BIG2.GT.BIG) BIG=BIG2
1208 BIG3=ABS(-COEFF1HHH*CONC(1,J))
1209 IF (BIG3.GT.BIG) BIG=BIG3
1210 BIG4=ABS(-COEFF1HHH*CONC(1,J-1))
1211 IF (BIG4.GT.BIG) BIG=BIG4
1212 BIG5=ABS((HH/2.)*(RXN(5,J+1)/4.))
1213 IF (BIG5.GT.BIG) BIG=BIG5
1214 BIG6=ABS((HH/2.)*(3.*RXN(5,J))/4.)
1215 IF (BIG6.GT.BIG) BIG=BIG6
1216 BIG7=ABS((HHH/2.)*(RXN(5,J-1)/4.))
1217 IF (BIG7.GT.BIG) BIG=BIG7
1218 BIG8=ABS((HHH/2.)*(3.*RXN(5,J))/4.)
1219 IF (BIG8.GT.BIG) BIG=BIG8
1220 IF (ABS(G(9)).LT.BIG*EBIG) G(9)=0
1221
1222 C For Flux of H+, OH- ions and gluconate ions ,
1223 G(10)=COEFF9HH*(CONC(10,J+1)-CONC(10,J))
1224 1 -COEFF9HHH*(CONC(10,J)-CONC(10,J-1))
1225 2 -COEFF10HH*(CONC(11,J+1)-CONC(11,J))
1226 3 +COEFF10HHH*(CONC(11,J)-CONC(11,J-1))
1227 4 -COEFF11HH*(CONC(12,J+1)-CONC(12,J))
1228 5 +COEFF11HHH*(CONC(12,J)-CONC(12,J-1))
1229 B(10,10)=COEFF9HH+COEFF9HHH
1230 D(10,10)=-COEFF9HH
1231 A(10,10)=-COEFF9HHH
1232 B(10,11)=-COEFF10HH-COEFF10HHH
1233 D(10,11)=COEFF10HH
1234 A(10,11)=COEFF10HHH
1235 B(10,12)=-COEFF11HH-COEFF11HHH
1236 D(10,12)=COEFF11HH
1237 A(10,12)=COEFF11HHH
1238
1239 BIG=ABS(COEFF9HH*CONC(10,J+1))
1240 BIG2=ABS(COEFF9HH*CONC(10,J))
1241 IF (BIG2.GT.BIG) BIG=BIG2
1242 BIG3=ABS(COEFF9HHH*CONC(10,J))
1243 IF (BIG3.GT.BIG) BIG=BIG3
1244 BIG4=ABS(COEFF9HHH*CONC(10,J-1))
1245 IF (BIG4.GT.BIG) BIG=BIG4
1246 BIG5=ABS(COEFF10HH*CONC(11,J+1))
1247 IF (BIG5.GT.BIG) BIG=BIG5
1248 BIG6=ABS(COEFF10HH*CONC(11,J))
1249 IF (BIG6.GT.BIG) BIG=BIG6
1250 BIG7=ABS(COEFF10HHH*CONC(11,J))
1251 IF (BIG7.GT.BIG) BIG=BIG7
1252 BIG8=ABS(COEFF10HHH*CONC(11,J-1))
1253 IF (BIG8.GT.BIG) BIG=BIG8
1254 BIG9=ABS(COEFF11HH*CONC(12,J+1))
1255 IF (BIG9.GT.BIG) BIG=BIG9
1256 BIG10=ABS(COEFF11HH*CONC(12,J))
1257 IF (BIG10.GT.BIG) BIG=BIG10
1258 BIG11=ABS(COEFF11HHH*CONC(12,J))

```

```

1259 IF (BIG11.GT.BIG) BIG=BIG11
1260 BIG12=ABS(COEFF11HHH*CONC(12,J-1))
1261 IF (BIG12.GT.BIG) BIG=BIG12
1262 IF (ABS(G(10)).LT.BIG*EBIG) G(10)=0
1263
1264 C FOR H+ and OH- ions equilibrium,
1265 G(11)=equilib6-CONC(10,J)*CONC(11,J)
1266 B(11,10)=CONC(11,J)
1267 B(11,11)=CONC(10,J)
1268
1269
1270 BIG=ABS(CBULK(9)*CBULK(10))
1271 BIG2=ABS(CONC(10,J)*CONC(11,J))
1272 IF (BIG2.GT.BIG) BIG=BIG2
1273 IF (ABS(G(11)).LT.BIG*EBIG) G(11)=0
1274
1275 C FOR gluconic acid dissociation equilibrium,
1276 G(12)=equilib7*CONC(3,J)-CONC(10,J)*CONC(12,J)
1277 B(12,3)=-equilib7
1278 B(12,10)=CONC(12,J)
1279 B(12,12)=CONC(10,J)
1280
1281 BIG=ABS(equilib7*CONC(3,J))
1282 BIG2=ABS(-CONC(10,J)*CONC(12,J))
1283 IF (BIG2.GT.BIG) BIG=BIG2
1284 IF (ABS(G(12)).LT.BIG*EBIG) G(12)=0
1285
1286 C For oxidized enzyme equilibrium,
1287 G(13)=equilib8*CONC(13,J)-CONC(10,J)*CONC(2,J)
1288 B(13,13)=-equilib8
1289 B(13,10)=CONC(2,J)
1290 B(13,2)=CONC(10,J)
1291
1292 BIG=ABS(equilib8*CONC(13,J))
1293 BIG2=ABS(-CONC(10,J)*CONC(2,J))
1294 IF (BIG2.GT.BIG) BIG=BIG2
1295 IF (ABS(G(13)).LT.BIG*EBIG) G(13)=0
1296
1297 C For reduced enzyme equilibrium,
1298 G(14)=equilib9*CONC(4,J)-CONC(10,J)*CONC(14,J)
1299 B(14,4)=-equilib9
1300 B(14,10)=CONC(14,J)
1301 B(14,14)=CONC(10,J)
1302
1303 BIG=ABS(equilib9*CONC(4,J))
1304 BIG2=ABS(-CONC(10,J)*CONC(14,J))
1305 IF (BIG2.GT.BIG) BIG=BIG2
1306 IF (ABS(G(14)).LT.BIG*EBIG) G(14)=0
1307
1308 C REACTION1
1309 214 G(15)=-RXN(1,J)+ratef1*(CONC(1,J)*CONC(2,J)-(CONC(7,J)/equilib1))
1310 B(15,1)=-ratef1*CONC(2,J)
1311 B(15,2)=-ratef1*CONC(1,J)
1312 B(15,7)=ratef1/equilib1
1313 B(15,15)=+1.
1314
1315 BIG=ABS(RXN(1,J))
1316 BIG2=ABS(ratef1*CONC(1,J)*CONC(2,J))

```

```

1317 IF (BIG2.GT.BIG) BIG=BIG2
1318 BIG3=ABS( ratef1*(CONC(7,J)/equilib1))
1319 IF (BIG3.GT.BIG) BIG=BIG3
1320 IF (ABS(G(15)).LT.BIG*EBIG) G(15)=0
1321
1322 C REACTION2
1323 215 G(16)=-RXN(2,J)+ratef2*CONC(7,J)
1324 B(16,7)=-ratef2
1325 B(16,16)=+1.
1326
1327 BIG=ABS(RXN(2,J))
1328 BIG2=ABS( ratef2*CONC(7,J))
1329 IF (BIG2.GT.BIG) BIG=BIG2
1330 IF (ABS(G(16)).LT.BIG*EBIG) G(16)=0
1331
1332 C REACTION3
1333 216 G(17)=-RXN(3,J)+ratef3*(CONC(4,J)*CONC(5,J)-(CONC(8,J)/equilib3))
1334 B(17,4)=-ratef3*CONC(5,J)
1335 B(17,5)=-ratef3*CONC(4,J)
1336 B(17,8)=ratef3/equilib3
1337 B(17,17)=+1.
1338
1339 BIG=ABS(RXN(3,J))
1340 BIG2=ABS( ratef3*CONC(4,J)*CONC(5,J))
1341 IF (BIG2.GT.BIG) BIG=BIG2
1342 BIG3=ABS( ratef3*(CONC(8,J)/equilib3))
1343 IF (BIG3.GT.BIG) BIG=BIG3
1344 IF (ABS(G(17)).LT.BIG*EBIG) G(17)=0
1345
1346 C REACTION4
1347 217 G(18)=-RXN(4,J)+ratef4*CONC(8,J)
1348 B(18,8)=-ratef4
1349 B(18,18)=+1.
1350
1351 BIG=ABS(RXN(4,J))
1352 BIG2=ABS( ratef4*CONC(8,J))
1353 IF (BIG2.GT.BIG) BIG=BIG2
1354 IF (ABS(G(18)).LT.BIG*EBIG) G(18)=0
1355
1356 C REACTION5
1357 218 G(19)=-RXN(5,J)+ratef5*CONC(9,J)-ratef5/equilib5*CONC(1,J)
1358 B(19,1)=ratef5/equilib5
1359 B(19,9)=-ratef5
1360 B(19,19)=+1.
1361
1362 BIG=ABS(RXN(5,J))
1363 BIG2=ABS( ratef5*CONC(9,J))
1364 IF (BIG2.GT.BIG) BIG=BIG2
1365 BIG3=ABS( ratef5/equilib5*CONC(1,J))
1366 IF (BIG3.GT.BIG) BIG=BIG3
1367 IF (ABS(G(19)).LT.BIG*EBIG) G(19)=0
1368
1369 212 WRITE(12,301) J, (G(K),K=1,N)
1370 RETURN
1371 END
1372
1373 SUBROUTINE INNER(J)
1374 IMPLICIT DOUBLE PRECISION (A-H, O-Z)

```

```

1375 COMMON/BAB/ A(19,19),B(19,19),C(19,80001),D(19,39),G(19),X(19,19)
1376 1,Y(19,19)
1377 COMMON/NSN/ N, NJ
1378 COMMON/VAR/ CONC(14,80001),RXN(7,80001),H,EBIG,HH,IJ
1379 COMMON/VARR/ COEFFMT(13),HHH,KJ
1380 COMMON/POR/ DGOX(13),DGIM(13),DBULK(13)
1381 COMMON/BCI/ FLUXF,FLUXB,FLUXR,FLUXH,Current3
1382 COMMON/RTE/ ratef1, equilib1, ratef2, ratef3, equilib3, ratef4, ratef5,
1383 1 equilib5, ratef6, equilib6, equilib7, equilib8, equilib9
1384 COMMON/BUL/ CBULK(13),PARH2O2,PARO2,PARGLUCOSE,SOLO2,PARION,JCOUNT
1385 COMMON/VARIN/ V,PO2,pH,GOx
1386 COMMON/TEMP/ T
1387 COMMON/DLT/ DELTA
1388
1389 301 FORMAT (5x,'J=' I5, 19E19.9E3)
1390
1391 C For Glucose, being consumed only
1392 G(1)=DGOX(1)*(CONC(1,J+1)-2.*CONC(1,J)+CONC(1,J-1))/HH**2.
1393 2 -RXN(1,J)+RXN(5,J)
1394 B(1,1)=2.*DGOX(1)/HH**2.
1395 D(1,1)=-DGOX(1)/HH**2.
1396 A(1,1)=-DGOX(1)/HH**2.
1397 B(1,15)=+1.
1398 B(1,19)=-1.
1399
1400 BIG=ABS(DGOX(1)*(CONC(1,J+1))/HH**2.)
1401 BIG2=ABS(DGOX(1)*(-2.*CONC(1,J))/HH**2.)
1402 IF (BIG2.GT.BIG) BIG=BIG2
1403 BIG3=ABS(DGOX(1)*(CONC(1,J-1))/HH**2.)
1404 IF (BIG3.GT.BIG) BIG=BIG3
1405 IF (ABS(-RXN(1,J)).GT.BIG) BIG=ABS(-RXN(1,J))
1406 IF (ABS(RXN(5,J)).GT.BIG) BIG=ABS(RXN(5,J))
1407 IF (ABS(G(1)).LT.BIG*EBIG) G(1)=0
1408
1409 C For GOx, enzyme
1410 G(2)=-RXN(1,J)+RXN(4,J)
1411 B(2,15)=+1.
1412 B(2,18)=-1.
1413
1414 BIG=ABS(RXN(1,J))
1415 BIG2=ABS(RXN(4,J))
1416 IF (BIG2.GT.BIG) BIG=BIG2
1417 IF (ABS(G(2)).LT.BIG*EBIG) G(2)=0
1418
1419 C For Flux of Gluconic Acid and Gluconate Ions,
1420 G(3)=DGOX(3)*(CONC(3,J+1)-2.*CONC(3,J)+CONC(3,J-1))/HH**2.
1421 2 -RXN(2,J)
1422 3 -DGOX(11)*(CONC(12,J+1)-2.*CONC(12,J)+CONC(12,J-1))/HH**2.
1423 B(3,3)=2.*DGOX(3)/HH**2.
1424 D(3,3)=-DGOX(3)/HH**2.
1425 A(3,3)=-DGOX(3)/HH**2.
1426 B(3,16)=-1.
1427 B(3,12)=2.*DGOX(11)/HH**2.
1428 D(3,12)=-DGOX(11)/HH**2.
1429 A(3,12)=-DGOX(11)/HH**2.
1430
1431 BIG=ABS(DGOX(3)*(CONC(3,J+1))/HH**2.)
1432 BIG2=ABS(DGOX(3)*(-2.*CONC(3,J))/HH**2.)

```

```

1433 IF (BIG2.GT.BIG) BIG=BIG2
1434 BIG3=ABS(DGOX(3)*(CONC(3,J-1))/HH**2.)
1435 IF (BIG3.GT.BIG) BIG=BIG3
1436 IF (ABS(RXN(2,J)).GT.BIG) BIG=ABS(RXN(2,J))
1437 IF (ABS(DGOX(11)*CONC(12,J+1)/(HH**2.)).GT.BIG)
1438 1 BIG=ABS(DGOX(11)*(CONC(12,J+1))/HH**2.)
1439 BIG4=ABS(DGOX(11)*(-2.*CONC(12,J))/HH**2.)
1440 IF (BIG4.GT.BIG) BIG=BIG4
1441 BIG5=ABS(DGOX(11)*(CONC(12,J-1))/HH**2.)
1442 IF (BIG5.GT.BIG) BIG=BIG5
1443 IF (ABS(G(3)).LT.BIG*EBIG) G(3)=0
1444

1445 C For GOx2, enzyme
1446 G(4)=GOx
1447 1 -CONC(2,J)-CONC(4,J)-CONC(7,J)-CONC(8,J)-CONC(13,J)-CONC(14,J)
1448 B(4,2)=+1.
1449 B(4,4)=+1.
1450 B(4,7)=+1.
1451 B(4,8)=+1.
1452 B(4,13)=+1.
1453 B(4,14)=+1.
1454
1455 BIG=ABS(GOx)
1456 IF (ABS(CONC(2,J)).GT.BIG) BIG=ABS(CONC(2,J))
1457 IF (ABS(CONC(4,J)).GT.BIG) BIG=ABS(CONC(4,J))
1458 IF (ABS(CONC(7,J)).GT.BIG) BIG=ABS(CONC(7,J))
1459 IF (ABS(CONC(8,J)).GT.BIG) BIG=ABS(CONC(8,J))
1460 IF (ABS(CONC(13,J)).GT.BIG) BIG=ABS(CONC(13,J))
1461 IF (ABS(CONC(14,J)).GT.BIG) BIG=ABS(CONC(14,J))
1462 IF (ABS(G(4)).LT.BIG*EBIG) G(4)=0
1463

1464 C For O2, being consumed only
1465 G(5)=DGOX(5)*(CONC(5,J+1)-2.*CONC(5,J)+CONC(5,J-1))/HH**2.
1466 2 -RXN(3,J)
1467 B(5,5)=2.*DGOX(5)/HH**2.
1468 D(5,5)=-DGOX(5)/HH**2.
1469 A(5,5)=-DGOX(5)/HH**2.
1470 B(5,17)=+1.
1471
1472 BIG=ABS(DGOX(5)*(CONC(5,J+1))/HH**2.)
1473 BIG2=ABS(DGOX(5)*(-2.*CONC(5,J))/HH**2.)
1474 IF (BIG2.GT.BIG) BIG=BIG2
1475 BIG3=ABS(DGOX(5)*(CONC(5,J-1))/HH**2.)
1476 IF (BIG3.GT.BIG) BIG=BIG3
1477 IF (ABS(-RXN(3,J)).GT.BIG) BIG=ABS(-RXN(3,J))
1478 IF (ABS(G(5)).LT.BIG*EBIG) G(5)=0
1479

1480 C For H2O2, reacting species
1481 G(6)=DGOX(6)*(CONC(6,J+1)-2.*CONC(6,J)+CONC(6,J-1))/HH**2.
1482 2 +RXN(4,J)
1483 B(6,6)=2.*DGOX(6)/HH**2.
1484 D(6,6)=-DGOX(6)/HH**2.
1485 A(6,6)=-DGOX(6)/HH**2.
1486 B(6,18)=-1.
1487
1488 BIG=ABS(DGOX(6)*(CONC(6,J+1))/HH**2.)
1489 BIG2=ABS(DGOX(6)*(-2.*CONC(6,J))/HH**2.)
1490 IF (BIG2.GT.BIG) BIG=BIG2

```

```

1491 BIG3=ABS(DGOX(6)*(CONC(6,J-1))/HH**2.)
1492 IF (BIG3.GT.BIG) BIG=BIG3
1493 IF (ABS(RXN(4,J)).GT.BIG) BIG=ABS(RXN(4,J))
1494 IF (ABS(G(6)).LT.BIG*EBIG) G(6)=0
1495
1496 C For CX-GOx2, enzyme
1497 G(7)=RXN(1,J)-RXN(2,J)
1498 B(7,15)=-1.
1499 B(7,16)=1.
1500
1501 IF (ABS(RXN(1,J)).GT.BIG) BIG=ABS(RXN(1,J))
1502 IF (ABS(RXN(2,J)).GT.BIG) BIG=ABS(RXN(2,J))
1503 IF (ABS(G(7)).LT.BIG*EBIG) G(7)=0
1504
1505 C For CX-GOx, enzyme
1506 G(8)=RXN(3,J)-RXN(4,J)
1507 B(8,17)=-1.
1508 B(8,18)=1.
1509
1510 IF (ABS(RXN(3,J)).GT.BIG) BIG=ABS(RXN(3,J))
1511 IF (ABS(RXN(4,J)).GT.BIG) BIG=ABS(RXN(4,J))
1512 IF (ABS(G(8)).LT.BIG*EBIG) G(8)=0
1513
1514 C For Alpha-Glucose,
1515 G(9)=DGOX(1)*(CONC(9,J+1)-2.*CONC(9,J)+CONC(9,J-1))/HH**2.
1516 2 -RXN(5,J)
1517 B(9,9)=2.*DGOX(1)/HH**2.
1518 D(9,9)=-DGOX(1)/HH**2.
1519 A(9,9)=-DGOX(1)/HH**2.
1520 B(9,19)=+1.
1521
1522 BIG=ABS(DGOX(1)*(CONC(9,J+1))/HH**2.)
1523 BIG2=ABS(DGOX(1)*(-2.*CONC(9,J))/HH**2.)
1524 IF (BIG2.GT.BIG) BIG=BIG2
1525 BIG3=ABS(DGOX(1)*(CONC(9,J-1))/HH**2.)
1526 IF (BIG3.GT.BIG) BIG=BIG3
1527 IF (ABS(-RXN(5,J)).GT.BIG) BIG=ABS(-RXN(5,J))
1528 IF (ABS(G(9)).LT.BIG*EBIG) G(9)=0
1529
1530 C For FLUX OF H+, OH- ions and gluconate ions,
1531 G(10)=DGOX(9)*(CONC(10,J+1)-2.*CONC(10,J)+CONC(10,J-1))
1532 2 /HH**2.
1533 3 -DGOX(10)*(CONC(11,J+1)-2.*CONC(11,J)+CONC(11,J-1))
1534 4 /HH**2.
1535 5 -DGOX(11)*(CONC(12,J+1)-2.*CONC(12,J)+CONC(12,J-1))
1536 6 /HH**2.
1537 B(10,10)=2.*DGOX(9)/HH**2.
1538 D(10,10)=-DGOX(9)/HH**2.
1539 A(10,10)=-DGOX(9)/HH**2.
1540 B(10,11)=-2.*DGOX(10)/HH**2.
1541 D(10,11)=DGOX(10)/HH**2.
1542 A(10,11)=DGOX(10)/HH**2.
1543 B(10,12)=-2.*DGOX(11)/HH**2.
1544 D(10,12)=DGOX(11)/HH**2.
1545 A(10,12)=DGOX(11)/HH**2.
1546
1547 BIG=ABS(DGOX(9)*(CONC(10,J+1))/HH**2.)
1548 BIG2=ABS(DGOX(9)*(-2.*CONC(10,J))/HH**2.)

```

```

1549 IF (BIG2.GT.BIG) BIG=BIG2
1550 BIG3=ABS(DGOX(9)*(CONC(10,J-1))/HH**2.)
1551 IF (BIG3.GT.BIG) BIG=BIG3
1552 BIG4=ABS(DGOX(10)*(CONC(11,J+1))/HH**2.)
1553 IF (BIG4.GT.BIG) BIG=BIG4
1554 BIG5=ABS(DGOX(10)*(-2.*CONC(11,J))/HH**2.)
1555 IF (BIG5.GT.BIG) BIG=BIG5
1556 BIG6=ABS(DGOX(10)*(CONC(11,J-1))/HH**2.)
1557 IF (BIG6.GT.BIG) BIG=BIG6
1558 BIG7=ABS(DGOX(11)*(CONC(12,J+1))/HH**2.)
1559 IF (BIG7.GT.BIG) BIG=BIG7
1560 BIG8=ABS(DGOX(11)*(-2.*CONC(12,J))/HH**2.)
1561 IF (BIG8.GT.BIG) BIG=BIG8
1562 BIG9=ABS(DGOX(11)*(CONC(12,J-1))/HH**2.)
1563 IF (BIG9.GT.BIG) BIG=BIG9
1564 IF (ABS(G(10)).LT.BIG*EBIG) G(10)=0
1565
1566 C FOR H+ and OH- ions equilibrium,
1567 G(11)=equilib6-CONC(10,J)*CONC(11,J)
1568 B(11,10)=CONC(11,J)
1569 B(11,11)=CONC(10,J)
1570
1571
1572 BIG=ABS(equilib6)
1573 BIG2=ABS( CONC(10,J)*CONC(11,J))
1574 IF (BIG2.GT.BIG) BIG=BIG2
1575 IF (ABS(G(11)).LT.BIG*EBIG) G(11)=0
1576
1577 C FOR gluconic acid dissociation equilibrium,
1578 G(12)=equilib7*CONC(3,J)-CONC(10,J)*CONC(12,J)
1579 B(12,3)=-equilib7
1580 B(12,10)=CONC(12,J)
1581 B(12,12)=CONC(10,J)
1582
1583 BIG=ABS(equilib7*CONC(3,J))
1584 BIG2=ABS(-CONC(10,J)*CONC(12,J))
1585 IF (BIG2.GT.BIG) BIG=BIG2
1586 IF (ABS(G(12)).LT.BIG*EBIG) G(12)=0
1587
1588 C For oxidized enzyme equilibrium,
1589 G(13)=equilib8*CONC(13,J)-CONC(10,J)*CONC(2,J)
1590 B(13,13)=-equilib8
1591 B(13,10)=CONC(2,J)
1592 B(13,2)=CONC(10,J)
1593
1594 BIG=ABS(equilib8*CONC(13,J))
1595 BIG2=ABS(-CONC(10,J)*CONC(2,J))
1596 IF (BIG2.GT.BIG) BIG=BIG2
1597 IF (ABS(G(13)).LT.BIG*EBIG) G(13)=0
1598
1599 C For reduced enzyme equilibrium,
1600 G(14)=equilib9*CONC(4,J)-CONC(10,J)*CONC(14,J)
1601 B(14,4)=-equilib9
1602 B(14,10)=CONC(14,J)
1603 B(14,14)=CONC(10,J)
1604
1605 BIG=ABS(equilib9*CONC(4,J))
1606 BIG2=ABS(-CONC(10,J)*CONC(14,J))

```

```

1607 IF (BIG2.GT.BIG) BIG=BIG2
1608 IF (ABS(G(14)).LT.BIG*EBIG) G(14)=0
1609
1610 C REACTION1
1611 214 G(15)=-RXN(1,J)+ratef1*(CONC(1,J)*CONC(2,J)-(CONC(7,J)/equilib1))
1612 B(15,1)=-ratef1*CONC(2,J)
1613 B(15,2)=-ratef1*CONC(1,J)
1614 B(15,7)=ratef1/equilib1
1615 B(15,15)=+1.
1616
1617 BIG=ABS(RXN(1,J))
1618 BIG2=ABS(ratef1*CONC(1,J)*CONC(2,J))
1619 IF (BIG2.GT.BIG) BIG=BIG2
1620 BIG3=ABS(ratef1*(CONC(7,J)/equilib1))
1621 IF (BIG3.GT.BIG) BIG=BIG3
1622 IF (ABS(G(15)).LT.BIG*EBIG) G(15)=0
1623
1624 C REACTION2
1625 215 G(16)=-RXN(2,J)+ratef2*CONC(7,J)
1626 B(16,7)=-ratef2
1627 B(16,16)=+1.
1628
1629 BIG=ABS(RXN(2,J))
1630 BIG2=ABS(ratef2*CONC(7,J))
1631 IF (BIG2.GT.BIG) BIG=BIG2
1632 IF (ABS(G(16)).LT.BIG*EBIG) G(16)=0
1633
1634 C REACTION3
1635 216 G(17)=-RXN(3,J)+ratef3*(CONC(4,J)*CONC(5,J)-(CONC(8,J)/equilib3))
1636 B(17,4)=-ratef3*CONC(5,J)
1637 B(17,5)=-ratef3*CONC(4,J)
1638 B(17,8)=ratef3/equilib3
1639 B(17,17)=+1.
1640
1641 BIG=ABS(RXN(3,J))
1642 BIG2=ABS(ratef3*CONC(4,J)*CONC(5,J))
1643 IF (BIG2.GT.BIG) BIG=BIG2
1644 BIG3=ABS(ratef3*(CONC(8,J)/equilib3))
1645 IF (BIG3.GT.BIG) BIG=BIG3
1646 IF (ABS(G(17)).LT.BIG*EBIG) G(17)=0
1647
1648 C REACTION4
1649 217 G(18)=-RXN(4,J)+ratef4*CONC(8,J)
1650 B(18,8)=-ratef4
1651 B(18,18)=+1.
1652
1653 BIG=ABS(RXN(4,J))
1654 BIG2=ABS(ratef4*CONC(8,J))
1655 IF (BIG2.GT.BIG) BIG=BIG2
1656 IF (ABS(G(18)).LT.BIG*EBIG) G(18)=0
1657
1658 C REACTION5
1659 218 G(19)=-RXN(5,J)+ratef5*CONC(9,J)-ratef5/equilib5*CONC(1,J)
1660 B(19,1)=ratef5/equilib5
1661 B(19,9)=-ratef5
1662 B(19,19)=+1.
1663
1664 BIG=ABS(RXN(5,J))

```

```

1665 BIG2=ABS( ratef5 *CONC(9 ,J) )
1666 IF (BIG2.GT.BIG) BIG=BIG2
1667 BIG3=ABS( ratef5 /equilib5 *CONC(1 ,J) )
1668 IF (BIG3.GT.BIG) BIG=BIG3
1669 IF (ABS(G(19)) .LT. BIG*EBIG) G(19)=0
1670
1671
1672 c   SAVE G OUT DATA
1673 212 DO 11 I=2,20
1674 11 If (I.EQ.J) WRITE(12,301) J, (G(K),K=1,N)
1675 IF (J.EQ.IJ/2) THEN
1676 WRITE(12,301) J, (G(K),K=1,N)
1677 ELSE IF (J.EQ.(KJ+1)) THEN
1678 WRITE(12,301) J, (G(K),K=1,N)
1679 ELSE IF (J.EQ.(KJ+2)) THEN
1680 WRITE(12,301) J, (G(K),K=1,N)
1681 ELSE IF (J.EQ.(KJ+3)) THEN
1682 WRITE(12,301) J, (G(K),K=1,N)
1683 ELSE IF (J.EQ.(KJ+4)) THEN
1684 WRITE(12,301) J, (G(K),K=1,N)
1685 ELSE IF (J.EQ.(IJ-1)) THEN
1686 WRITE(12,301) J, (G(K),K=1,N)
1687 ELSE IF (J.EQ.(IJ-2)) THEN
1688 WRITE(12,301) J, (G(K),K=1,N)
1689 ELSE IF (J.EQ.(IJ-3)) THEN
1690 WRITE(12,301) J, (G(K),K=1,N)
1691 END IF
1692
1693 RETURN
1694 END
1695
1696 SUBROUTINE COUPLER2(J)
1697 IMPLICIT DOUBLE PRECISION (A-H, O-Z)
1698 COMMON/BAB/ A(19,19),B(19,19),C(19,80001),D(19,39),G(19),X(19,19)
1699 1, Y(19,19)
1700 COMMON/NSN/ N, NJ
1701 COMMON/VAR/ CONC(14,80001),RXN(7,80001),H,EBIG,HH,IJ
1702 COMMON/VARR/ COEFFMT(13), HHH, KJ
1703 COMMON/POR/ DGOX(13),DGIM(13),DBULK(13)
1704 COMMON/BCI/ FLUXF,FLUXB,FLUXR,FLUXH,Current3
1705 COMMON/RTE/ ratef1, equilib1, ratef2, ratef3, equilib3, ratef4, ratef5,
1706 1 equilib5, ratef6, equilib6, equilib7, equilib8, equilib9
1707 COMMON/BUL/ CBULK(13),PARH2O2,PARO2,PARGLUCOSE,SOLO2,PARION,JCOUNT
1708 COMMON/VARIN/ V,PO2,pH,GOx
1709 COMMON/TEMP/ T
1710 COMMON/DLT/ DELTA
1711
1712 301 FORMAT (5x, 'J=' I5, 19E19.9E3)
1713
1714 COEFF1H=DGIM(1)/H
1715 COEFF1HH=DGOX(1)/HH
1716 COEFF3H=DGIM(3)/H
1717 COEFF3HH=DGOX(3)/HH
1718 COEFF5H=DGIM(5)/H
1719 COEFF5HH=DGOX(5)/HH
1720 COEFF6H=DGIM(6)/H
1721 COEFF6HH=DGOX(6)/HH
1722 COEFF9H=DGIM(9)/H

```

```

1723 COEFF9HH=DGOX( 9 )/HH
1724 COEFF10H=DGLM( 10 )/H
1725 COEFF10HH=DGOX( 10 )/HH
1726 COEFF11H=DGLM( 11 )/H
1727 COEFF11HH=DGOX( 11 )/HH
1728
1729 C For beta-Glucose , being consumed only
1730 G(1)=COEFF1H*(CONC( 1 , J+1)-CONC( 1 , J ))
1731 1 -COEFF1HH*(CONC( 1 , J)-CONC( 1 , J-1 ))
1732 2 -(HH/ 2 .)*(RXN( 1 , J-1)+3.*RXN( 1 , J ))/ 4 .
1733 3 +(H/ 2 .)*(RXN( 5 , J+1)+3.*RXN( 5 , J ))/ 4 .
1734 4 +(HH/ 2 .)*(RXN( 5 , J-1)+3.*RXN( 5 , J ))/ 4 .
1735 B( 1 , 1 )=COEFF1H+COEFF1HH
1736 D( 1 , 1 )=-COEFF1H
1737 A( 1 , 1 )=-COEFF1HH
1738 B( 1 , 15 )=+(HH/ 2 .)*( 3 ./ 4 .)
1739 A( 1 , 15 )=+(HH/ 2 .)*( 1 ./ 4 .)
1740 B( 1 , 19 )=-(HH/ 2 .)*( 3 ./ 4 .)-(H/ 2 .)*( 3 ./ 4 .)
1741 A( 1 , 19 )=-(HH/ 2 .)*( 1 ./ 4 .)
1742 D( 1 , 19 )=-(H/ 2 .)*( 1 ./ 4 .)
1743
1744 BIG=ABS(COEFF1H*CONC( 1 , IJ+1 ))
1745 BIG2=ABS(COEFF1H*CONC( 1 , IJ ))
1746 IF (BIG2.GT.BIG) BIG=BIG2
1747 BIG5=ABS(COEFF1HH*CONC( 1 , IJ ))
1748 IF (BIG5.GT.BIG) BIG=BIG5
1749 BIG6=ABS(COEFF1HH*CONC( 1 , IJ-1 ))
1750 IF (BIG6.GT.BIG) BIG=BIG6
1751 BIG7=ABS( 3 *(HH/ 2 .)*RXN( 1 , J )/ 4 )
1752 IF (BIG7.GT.BIG) BIG=BIG7
1753 BIG8=ABS((HH/ 2 .)*RXN( 1 , J-1 )/ 4 )
1754 IF (BIG8.GT.BIG) BIG=BIG8
1755 BIG9=ABS( 3 *(HH/ 2 .)*RXN( 5 , J )/ 4 )
1756 IF (BIG9.GT.BIG) BIG=BIG9
1757 BIG10=ABS((HH/ 2 .)*RXN( 5 , J-1 )/ 4 )
1758 IF (BIG10.GT.BIG) BIG=BIG10
1759 BIG11=ABS((H/ 2 .)*RXN( 5 , J+1 )/ 4 .)
1760 IF (BIG11.GT.BIG) BIG=BIG11
1761 BIG12=ABS((H/ 2 .)* 3 .*RXN( 5 , J )/ 4 .)
1762 IF (BIG12.GT.BIG) BIG=BIG12
1763 IF (ABS(G( 1 )).LT.BIG*EBIG) G( 1 )=0
1764
1765 C For GOx, enzyme
1766 G( 2 )=-RXN( 1 , J )+RXN( 4 , J )
1767 B( 2 , 15 )=+1.
1768 B( 2 , 18 )=-1.
1769
1770 BIG=ABS(RXN( 1 , J ))
1771 BIG2=ABS(RXN( 4 , J ))
1772 IF (BIG2.GT.BIG) BIG=BIG2
1773 IF (ABS(G( 2 )).LT.BIG*EBIG) G( 2 )=0
1774
1775 C For Gluconic Acid , being produced only
1776 G( 3 )=COEFF3H*(CONC( 3 , J+1)-CONC( 3 , J ))
1777 1 -COEFF3HH*(CONC( 3 , J)-CONC( 3 , J-1 ))
1778 2 +(HH/ 2 .)*(RXN( 2 , J-1)+3.*RXN( 2 , J ))/ 4 .
1779 3 +COEFF11H*(CONC( 12 , J+1)-CONC( 12 , J ))
1780 4 -COEFF11HH*(CONC( 12 , J)-CONC( 12 , J-1 ))

```

```

1781      B(3,3)=COEFF3H+COEFF3HH
1782      D(3,3)=-COEFF3H
1783      A(3,3)=-COEFF3HH
1784      B(3,16)=-HH/2.* (3./4.)
1785      A(3,16)=-HH/2.* (1./4.)
1786      B(3,12)=COEFF11H+COEFF11HH
1787      D(3,12)=-COEFF11H
1788      A(3,12)=-COEFF11HH
1789
1790      BIG=ABS(COEFF3H*CONC(3,J+1))
1791      BIG2=ABS(COEFF3H*CONC(3,J))
1792      IF (BIG2.GT.BIG) BIG=BIG2
1793      BIG3=ABS(COEFF3HH*CONC(3,J))
1794      IF (BIG3.GT.BIG) BIG=BIG3
1795      BIG4=ABS(COEFF3HH*CONC(3,J-1))
1796      IF (BIG4.GT.BIG) BIG=BIG4
1797      BIG5=ABS(3.* (HH/2.)*RXN(2,J)/4.)
1798      IF (BIG5.GT.BIG) BIG=BIG5
1799      BIG6=ABS((HH/2.)*RXN(2,J-1)/4.)
1800      IF (BIG6.GT.BIG) BIG=BIG6
1801      BIG7=ABS(COEFF11H*CONC(12,J+1))
1802      IF (BIG7.GT.BIG) BIG=BIG7
1803      BIG8=ABS(COEFF11H*CONC(12,J))
1804      IF (BIG8.GT.BIG) BIG=BIG8
1805      BIG9=ABS(COEFF11HH*CONC(12,J))
1806      IF (BIG9.GT.BIG) BIG=BIG9
1807      BIG10=ABS(COEFF11HH*CONC(12,J-1))
1808      IF (BIG10.GT.BIG) BIG=BIG10
1809      IF (ABS(G(3)).LT.BIG*EBIG) G(3)=0
1810
1811 C   For GOx2, enzyme
1812      G(4)=GOx
1813      1 -CONC(2,J)-CONC(4,J)-CONC(7,J)-CONC(8,J)-CONC(13,J)-CONC(14,J)
1814      B(4,2)=+1.
1815      B(4,4)=+1.
1816      B(4,7)=+1.
1817      B(4,8)=+1.
1818      B(4,13)=+1.
1819      B(4,14)=+1.
1820
1821      BIG=ABS(GOx)
1822      IF (ABS(CONC(2,J)).GT.BIG) BIG=ABS(CONC(2,J))
1823      IF (ABS(CONC(4,J)).GT.BIG) BIG=ABS(CONC(4,J))
1824      IF (ABS(CONC(7,J)).GT.BIG) BIG=ABS(CONC(7,J))
1825      IF (ABS(CONC(8,J)).GT.BIG) BIG=ABS(CONC(8,J))
1826      IF (ABS(CONC(13,J)).GT.BIG) BIG=ABS(CONC(13,J))
1827      IF (ABS(CONC(14,J)).GT.BIG) BIG=ABS(CONC(14,J))
1828      IF (ABS(G(4)).LT.BIG*EBIG) G(4)=0
1829
1830 C   For O2, being consumed only
1831      G(5)=COEFF5H*(CONC(5,J+1)-CONC(5,J))
1832      1 -COEFF5HH*(CONC(5,J)-CONC(5,J-1))
1833      2 -(HH/2.)*(RXN(3,J-1)+3.*RXN(3,J))/4.
1834      B(5,5)=COEFF5H+COEFF5HH
1835      D(5,5)=-COEFF5H
1836      A(5,5)=-COEFF5HH
1837      B(5,17)=(HH/2.)*(3./4.)
1838      A(5,17)=(HH/2.)*(1./4.)

```

```

1839
1840 BIG=ABS(COEFF5H*CONC(5,IJ+1))
1841 BIG2=ABS(COEFF5H*CONC(5,IJ))
1842 IF (BIG2.GT.BIG) BIG=BIG2
1843 BIG5=ABS(COEFF5HH*CONC(5,IJ))
1844 IF (BIG5.GT.BIG) BIG=BIG5
1845 BIG6=ABS(COEFF5HH*CONC(5,IJ-1))
1846 IF (BIG6.GT.BIG) BIG=BIG6
1847 BIG7=ABS(3.* (HH/2.) *RXN(3,J)/4.)
1848 IF (BIG7.GT.BIG) BIG=BIG7
1849 BIG8=ABS((HH/2.) *RXN(3,J-1)/4.)
1850 IF (BIG8.GT.BIG) BIG=BIG8
1851 IF (ABS(G(5)).LT.BIG*EBIG) G(5)=0
1852

1853 C For H2O2, reacting species
1854 G(6)=COEFF6H*(CONC(6,J+1)-CONC(6,J))
1855 1 -COEFF6HH*(CONC(6,J)-CONC(6,J-1))
1856 2 +(HH/2.) *(RXN(4,J-1)+3.*RXN(4,J))/4.
1857 B(6,6)=COEFF6H+COEFF6HH
1858 D(6,6)=-COEFF6H
1859 A(6,6)=-COEFF6HH
1860 B(6,18)=-(HH/2.) *(3./4.)
1861 A(6,18)=-(HH/2.) *(1./4.)
1862
1863 BIG=ABS(COEFF6H*CONC(6,IJ+1))
1864 BIG2=ABS(COEFF6H*CONC(6,IJ))
1865 IF (BIG2.GT.BIG) BIG=BIG2
1866 BIG5=ABS(COEFF6HH*CONC(6,IJ))
1867 IF (BIG5.GT.BIG) BIG=BIG5
1868 BIG6=ABS(COEFF6HH*CONC(6,IJ-1))
1869 IF (BIG6.GT.BIG) BIG=BIG6
1870 BIG7=ABS(3.* (HH/2.) *RXN(4,J)/4.)
1871 IF (BIG7.GT.BIG) BIG=BIG7
1872 BIG8=ABS((HH/2.) *RXN(4,J-1)/4.)
1873 IF (BIG8.GT.BIG) BIG=BIG8
1874 IF (ABS(G(6)).LT.BIG*EBIG) G(6)=0
1875

1876 C For CX-GOx2, enzyme
1877 G(7)=RXN(1,J)-RXN(2,J)
1878 B(7,15)=-1.
1879 B(7,16)=1.
1880
1881 IF (ABS(RXN(1,J)).GT.BIG) BIG=ABS(RXN(1,J))
1882 IF (ABS(RXN(2,J)).GT.BIG) BIG=ABS(RXN(2,J))
1883 IF (ABS(G(7)).LT.BIG*EBIG) G(7)=0
1884

1885 C For CX-GOx, enzyme
1886 G(8)=RXN(3,J)-RXN(4,J)
1887 B(8,17)=-1.
1888 B(8,18)=1.
1889
1890 IF (ABS(RXN(3,J)).GT.BIG) BIG=ABS(RXN(3,J))
1891 IF (ABS(RXN(4,J)).GT.BIG) BIG=ABS(RXN(4,J))
1892 IF (ABS(G(8)).LT.BIG*EBIG) G(8)=0
1893

1894 C For Alpha-Glucose,
1895 G(9)=COEFF1H*(CONC(9,J+1)-CONC(9,J))
1896 1 -COEFF1HH*(CONC(9,J)-CONC(9,J-1))

```

```

1897      2      -(H / 2.) *(RXN(5 ,J+1)+3.*RXN(5 ,J)) / 4.
1898      3      -(HH / 2.) *(RXN(5 ,J-1)+3.*RXN(5 ,J)) / 4.
1899      B(9 ,9)=COEFF1H+COEFF1HH
1900      D(9 ,9)=-COEFF1H
1901      A(9 ,9)=-COEFF1HH
1902      B(9 ,19)=+(HH/2.) *(3 ./ 4.) +(H / 2.) *(3 ./ 4.)
1903      A(9 ,19)=+(HH/2.) *(1 ./ 4.)
1904      D(9 ,19)=+(H / 2.) *(1 ./ 4.)
1905
1906      BIG=ABS(COEFF1H*CONC(9 ,IJ+1))
1907      BIG2=ABS(COEFF1H*CONC(9 ,IJ))
1908      IF (BIG2.GT.BIG) BIG=BIG2
1909      BIG3=ABS(COEFF1HH*CONC(9 ,IJ))
1910      IF (BIG3.GT.BIG) BIG=BIG3
1911      BIG4=ABS(COEFF1HH*CONC(9 ,IJ-1))
1912      IF (BIG4.GT.BIG) BIG=BIG4
1913      BIG5=ABS(3*(HH/2.) *RXN(5 ,J) / 4)
1914      IF (BIG5.GT.BIG) BIG=BIG5
1915      BIG6=ABS((HH/2.) *RXN(5 ,J-1) / 4)
1916      IF (BIG6.GT.BIG) BIG=BIG6
1917      BIG7=ABS((H / 2.) *RXN(5 ,J+1) / 4)
1918      IF (BIG7.GT.BIG) BIG=BIG7
1919      BIG8=ABS((H / 2.) *3 .*RXN(5 ,J) / 4.)
1920      IF (BIG8.GT.BIG) BIG=BIG8
1921      IF (ABS(G(9)) .LT. BIG*EBIG) G(9)=0
1922
1923 C   For Flux of H+, OH- ions and gluconate ions ,
1924      G(10)=COEFF9H*(CONC(10 ,J+1)-CONC(10 ,J))
1925      1      -COEFF9HH*(CONC(10 ,J)-CONC(10 ,J-1))
1926      2      -COEFF10H*(CONC(11 ,J+1)-CONC(11 ,J))
1927      3      +COEFF10HH*(CONC(11 ,J)-CONC(11 ,J-1))
1928      4      -COEFF11H*(CONC(12 ,J+1)-CONC(12 ,J))
1929      5      +COEFF11HH*(CONC(12 ,J)-CONC(12 ,J-1))
1930      B(10 ,10)=COEFF9H+COEFF9HH
1931      D(10 ,10)=-COEFF9H
1932      A(10 ,10)=-COEFF9HH
1933      B(10 ,11)=-COEFF10H-COEFF10HH
1934      D(10 ,11)=COEFF10H
1935      A(10 ,11)=COEFF10HH
1936      B(10 ,12)=-COEFF11H-COEFF11HH
1937      D(10 ,12)=COEFF11H
1938      A(10 ,12)=COEFF11HH
1939
1940      BIG=ABS(COEFF9H*CONC(10 ,J+1))
1941      BIG2=ABS(COEFF9H*CONC(10 ,J))
1942      IF (BIG2.GT.BIG) BIG=BIG2
1943      BIG3=ABS(COEFF9HH*CONC(10 ,J))
1944      IF (BIG3.GT.BIG) BIG=BIG3
1945      BIG4=ABS(COEFF9HH*CONC(10 ,J-1))
1946      IF (BIG4.GT.BIG) BIG=BIG4
1947      BIG5=ABS(COEFF10H*CONC(11 ,J+1))
1948      IF (BIG5.GT.BIG) BIG=BIG5
1949      BIG6=ABS(COEFF10H*CONC(11 ,J))
1950      IF (BIG6.GT.BIG) BIG=BIG6
1951      BIG7=ABS(COEFF10HH*CONC(11 ,J-1))
1952      IF (BIG7.GT.BIG) BIG=BIG7
1953      BIG8=ABS(COEFF10HH*CONC(11 ,J))
1954      IF (BIG8.GT.BIG) BIG=BIG8

```

```

1955 BIG9=ABS(COEFF11H*CONC(12,J+1))
1956 IF (BIG9.GT.BIG) BIG=BIG9
1957 BIG10=ABS(COEFF11H*CONC(12,J))
1958 IF (BIG10.GT.BIG) BIG=BIG10
1959 BIG11=ABS(COEFF11HH*CONC(12,J-1))
1960 IF (BIG11.GT.BIG) BIG=BIG11
1961 BIG12=ABS(COEFF11HH*CONC(12,J))
1962 IF (BIG12.GT.BIG) BIG=BIG12
1963 IF (ABS(G(10)).LT.BIG*EBIG) G(10)=0
1964

1965 C FOR H+ and OH- ions equilibrium,
1966 G(11)=equilib6-CONC(10,J)*CONC(11,J)
1967 B(11,10)=CONC(11,J)
1968 B(11,11)=CONC(10,J)
1969
1970
1971 BIG=ABS(equilib6)
1972 BIG2=ABS(CONC(10,J)*CONC(11,J))
1973 IF (BIG2.GT.BIG) BIG=BIG2
1974 IF (ABS(G(11)).LT.BIG*EBIG) G(11)=0
1975

1976 C FOR gluconic acid dissociation equilibrium,
1977 G(12)=equilib7*CONC(3,J)-CONC(10,J)*CONC(12,J)
1978 B(12,3)=-equilib7
1979 B(12,10)=CONC(12,J)
1980 B(12,12)=CONC(10,J)
1981
1982 BIG=ABS(equilib7*CONC(3,J))
1983 BIG2=ABS(-CONC(10,J)*CONC(12,J))
1984 IF (BIG2.GT.BIG) BIG=BIG2
1985 IF (ABS(G(12)).LT.BIG*EBIG) G(12)=0
1986

1987 C For oxidized enzyme equilibrium,
1988 G(13)=equilib8*CONC(13,J)-CONC(10,J)*CONC(2,J)
1989 B(13,13)=-equilib8
1990 B(13,10)=CONC(2,J)
1991 B(13,2)=CONC(10,J)
1992
1993 BIG=ABS(equilib8*CONC(13,J))
1994 BIG2=ABS(-CONC(10,J)*CONC(2,J))
1995 IF (BIG2.GT.BIG) BIG=BIG2
1996 IF (ABS(G(13)).LT.BIG*EBIG) G(13)=0
1997

1998 C For reduced enzyme equilibrium,
1999 G(14)=equilib9*CONC(4,J)-CONC(10,J)*CONC(14,J)
2000 B(14,4)=-equilib9
2001 B(14,10)=CONC(14,J)
2002 B(14,14)=CONC(10,J)
2003
2004 BIG=ABS(equilib9*CONC(4,J))
2005 BIG2=ABS(-CONC(10,J)*CONC(14,J))
2006 IF (BIG2.GT.BIG) BIG=BIG2
2007 IF (ABS(G(14)).LT.BIG*EBIG) G(14)=0
2008

2009 C REACTION1
2010 214 G(15)=-RXN(1,J)+ratef1*(CONC(1,J)*CONC(2,J)-(CONC(7,J)/equilib1))
2011 B(15,1)=-ratef1*CONC(2,J)
2012 B(15,2)=-ratef1*CONC(1,J)

```

```

2013 B(15,7)=ratef1 / equilib1
2014 B(15,15)=+1.
2015
2016 BIG=ABS(RXN(1,J))
2017 BIG2=ABS( ratef1*CONC(1,J)*CONC(2,J) )
2018 IF (BIG2.GT.BIG) BIG=BIG2
2019 BIG3=ABS( ratef1*(CONC(7,J) / equilib1) )
2020 IF (BIG3.GT.BIG) BIG=BIG3
2021 IF (ABS(G(15)).LT.BIG*EBIG) G(15)=0
2022
2023 C REACTION2
2024 215 G(16)=-RXN(2,J)+ratef2 *CONC(7,J)
2025 B(16,7)=-ratef2
2026 B(16,16)=+1.
2027
2028 BIG=ABS(RXN(2,J))
2029 BIG2=ABS( ratef2*CONC(7,J) )
2030 IF (BIG2.GT.BIG) BIG=BIG2
2031 IF (ABS(G(16)).LT.BIG*EBIG) G(16)=0
2032
2033 C REACTION3
2034 216 G(17)=-RXN(3,J)+ratef3 *(CONC(4,J)*CONC(5,J)-(CONC(8,J) / equilib3) )
2035 B(17,4)=-ratef3 *CONC(5,J)
2036 B(17,5)=-ratef3 *CONC(4,J)
2037 B(17,8)=ratef3 / equilib3
2038 B(17,17)=+1.
2039
2040 BIG=ABS(RXN(3,J))
2041 BIG2=ABS( ratef3*CONC(4,J)*CONC(5,J) )
2042 IF (BIG2.GT.BIG) BIG=BIG2
2043 BIG3=ABS( ratef3*(CONC(8,J) / equilib3) )
2044 IF (BIG3.GT.BIG) BIG=BIG3
2045 IF (ABS(G(17)).LT.BIG*EBIG) G(17)=0
2046
2047 C REACTION4
2048 217 G(18)=-RXN(4,J)+ratef4 *CONC(8,J)
2049 B(18,8)=-ratef4
2050 B(18,18)=+1.
2051
2052 BIG=ABS(RXN(4,J))
2053 BIG2=ABS( ratef4*CONC(8,J) )
2054 IF (BIG2.GT.BIG) BIG=BIG2
2055 IF (ABS(G(18)).LT.BIG*EBIG) G(18)=0
2056
2057 C REACTION5
2058 218 G(19)=-RXN(5,J)+ratef5 *CONC(9,J)-ratef5 / equilib5 *CONC(1,J)
2059 B(19,1)=ratef5 / equilib5
2060 B(19,9)=-ratef5
2061 B(19,19)=+1.
2062
2063 BIG=ABS(RXN(5,J))
2064 BIG2=ABS( ratef5*CONC(9,J) )
2065 IF (BIG2.GT.BIG) BIG=BIG2
2066 BIG3=ABS( ratef5 / equilib5 *CONC(1,J) )
2067 IF (BIG3.GT.BIG) BIG=BIG3
2068 IF (ABS(G(19)).LT.BIG*EBIG) G(19)=0
2069
2070

```

```

2071 212 WRITE(12,301) J, (G(K),K=1,N)
2072 RETURN
2073 END
2074
2075 SUBROUTINE OUTER(J)
2076 IMPLICIT DOUBLE PRECISION (A-H, O-Z)
2077 COMMON/BAB/ A(19,19),B(19,19),C(19,80001),D(19,39),G(19),X(19,19)
2078 1 ,Y(19,19)
2079 COMMON/NSN/ N, NJ
2080 COMMON/VAR/ CONC(14,80001),RXN(7,80001),H,EBIG,HH,IJ
2081 COMMON/VARR/ COEFFMT(13), HHH, KJ
2082 COMMON/POR/ DGOX(13),DGLM(13),DBULK(13)
2083 COMMON/BCI/ FLUXF,FLUXB,FLUXR,FLUXH,Current3
2084 COMMON/RTE/ ratef1, equilib1, ratef2, ratef3, equilib3, ratef4, ratef5,
2085 1 equilib5, ratef6, equilib6, equilib7, equilib8, equilib9
2086 COMMON/BUL/ CBULK(13),PARH2O2,PARO2,PARGLUCOSE,SOLO2,PARION,JCOUNT
2087 COMMON/VARIN/ V,PO2,pH,GOx
2088 COMMON/TEMP/ T
2089 COMMON/DLT/ DELTA
2090
2091 301 FORMAT (5x, 'J=' 15, 19E19.9E3)
2092
2093 C For Beta-Glucose, being consumed only
2094 G(1)=DGLM(1)*(CONC(1,J+1)-2.*CONC(1,J)+CONC(1,J-1))/H**2.
2095 1 +RXN(5,J)
2096 B(1,1)=2.*DGLM(1)/H**2.
2097 D(1,1)=-DGLM(1)/H**2.
2098 A(1,1)=-DGLM(1)/H**2.
2099 B(1,19)=-1.
2100
2101 BIG=ABS(DGLM(1)*(CONC(1,J+1))/H**2.)
2102 BIG2=ABS(DGLM(1)*(-2.*CONC(1,J))/H**2.)
2103 IF (BIG2.GT.BIG) BIG=BIG2
2104 BIG3=ABS(DGLM(1)*(CONC(1,J-1))/H**2.)
2105 IF (BIG3.GT.BIG) BIG=BIG3
2106 BIG4=ABS(RXN(5,J))
2107 IF (BIG4.GT.BIG) BIG=BIG4
2108 IF (ABS(G(1)).LT.BIG*EBIG) G(1)=0
2109
2110 C For GOx, enzyme
2111 G(2)=CONC(2,J)
2112 B(2,2)=-1.
2113
2114 BIG=ABS(CONC(2,J))
2115 IF (ABS(G(2)).LT.BIG*EBIG) G(2)=0
2116
2117 C For FLUX OF Gluconic Acid AND GLUCONATE IONS
2118 G(3)=DGLM(3)*(CONC(3,J+1)-2.*CONC(3,J)+CONC(3,J-1))/H**2.
2119 1 +DGLM(11)*(CONC(12,J+1)-2.*CONC(12,J)+CONC(12,J-1))/H**2.
2120 B(3,3)=2.*DGLM(3)/H**2.
2121 D(3,3)=-DGLM(3)/H**2.
2122 A(3,3)=-DGLM(3)/H**2.
2123 B(3,12)=2.*DGLM(11)/H**2.
2124 D(3,12)=-DGLM(11)/H**2.
2125 A(3,12)=-DGLM(11)/H**2.
2126
2127 BIG=ABS(DGLM(3)*(CONC(3,J+1))/H**2.)
2128 BIG2=ABS(DGLM(3)*(-2.*CONC(3,J))/H**2.)

```

```

2129 IF (BIG2.GT.BIG) BIG=BIG2
2130 BIG3=ABS(DGLM(3)*(CONC(3,J-1))/H**2.)
2131 IF (BIG3.GT.BIG) BIG=BIG3
2132 BIG4=ABS(DGLM(11)*(CONC(12,J+1))/H**2.)
2133 IF (BIG4.GT.BIG) BIG=BIG4
2134 BIG5=ABS(DGLM(11)*(-2.*CONC(12,J))/H**2.)
2135 IF (BIG5.GT.BIG) BIG=BIG5
2136 BIG6=ABS(DGLM(11)*(CONC(12,J-1))/H**2.)
2137 IF (BIG6.GT.BIG) BIG=BIG6
2138 IF (ABS(G(3)).LT.BIG*EBIG) G(3)=0
2139
2140 C For GOx2, enzyme
2141 G(4)=CONC(4,J)
2142 B(4,4)=-1.
2143
2144 BIG=ABS(CONC(4,J))
2145 IF (ABS(G(4)).LT.BIG*EBIG) G(4)=0
2146
2147 C For O2, being consumed only
2148 G(5)=DGLM(5)*(CONC(5,J+1)-2.*CONC(5,J)+CONC(5,J-1))/H**2.
2149 B(5,5)=2.*DGLM(5)/H**2.
2150 D(5,5)=-DGLM(5)/H**2.
2151 A(5,5)=-DGLM(5)/H**2.
2152
2153 BIG=ABS(DGLM(5)*(CONC(5,J+1))/H**2.)
2154 BIG2=ABS(DGLM(5)*(-2.*CONC(5,J))/H**2.)
2155 IF (BIG2.GT.BIG) BIG=BIG2
2156 BIG3=ABS(DGLM(5)*(CONC(5,J-1))/H**2.)
2157 IF (BIG3.GT.BIG) BIG=BIG3
2158 IF (ABS(G(5)).LT.BIG*EBIG) G(5)=0
2159
2160 C For H2O2, reacting species
2161 G(6)=DGLM(6)*(CONC(6,J+1)-2.*CONC(6,J)+CONC(6,J-1))/H**2.
2162 B(6,6)=2.*DGLM(6)/H**2.
2163 D(6,6)=-DGLM(6)/H**2.
2164 A(6,6)=-DGLM(6)/H**2.
2165
2166 BIG=ABS(DGLM(6)*(CONC(6,J+1))/H**2.)
2167 BIG2=ABS(DGLM(6)*(-2.*CONC(6,J))/H**2.)
2168 IF (BIG2.GT.BIG) BIG=BIG2
2169 BIG3=ABS(DGLM(6)*(CONC(6,J-1))/H**2.)
2170 IF (BIG3.GT.BIG) BIG=BIG3
2171 IF (ABS(G(6)).LT.BIG*EBIG) G(6)=0
2172
2173 C For CX-GOx2, enzyme complex
2174 G(7)=CONC(7,J)
2175 B(7,7)=-1.
2176
2177 BIG=ABS(CONC(7,J))
2178 IF (ABS(G(7)).LT.BIG*EBIG) G(7)=0
2179
2180 C For CX-GOx, enzyme complex
2181 G(8)=CONC(8,J)
2182 B(8,8)=-1.
2183
2184 BIG=ABS(CONC(8,J))
2185 IF (ABS(G(8)).LT.BIG*EBIG) G(8)=0
2186

```

```

2187 C For Alpha-Glucose ,
2188 G(9)=DGLM(1)*(CONC(9,J+1)-2.*CONC(9,J)+CONC(9,J-1))/H**2.
2189 1 -RXN(5,J)
2190 B(9,9)=2.*DGLM(1)/H**2.
2191 D(9,9)=-DGLM(1)/H**2.
2192 A(9,9)=-DGLM(1)/H**2.
2193 B(9,19)=+1.
2194
2195 BIG=ABS(DGLM(1)*(CONC(9,J+1))/H**2.)
2196 BIG2=ABS(DGLM(1)*(-2.*CONC(9,J))/H**2.)
2197 IF (BIG2.GT.BIG) BIG=BIG2
2198 BIG3=ABS(DGLM(1)*(CONC(9,J-1))/H**2.)
2199 IF (BIG3.GT.BIG) BIG=BIG3
2200 BIG4=ABS(-RXN(5,J))
2201 IF (BIG4.GT.BIG) BIG=BIG4
2202 IF (ABS(G(9)).LT.BIG*EBIG) G(9)=0
2203
2204 C For Flux of H+, OH- ions and gluconate ions ,
2205 G(10)=DGLM(9)*(CONC(10,J+1)-2.*CONC(10,J)+CONC(10,J-1))
2206 2 /H**2.
2207 3 -DGLM(10)*(CONC(11,J+1)-2.*CONC(11,J)+CONC(11,J-1))/H**2.
2208 4 -DGLM(11)*(CONC(12,J+1)-2.*CONC(12,J)+CONC(12,J-1))
2209 5 /H**2.
2210 B(10,10)=2.*DGLM(9)/H**2.
2211 D(10,10)=-DGLM(9)/H**2.
2212 A(10,10)=-DGLM(9)/H**2.
2213 B(10,11)=-2.*DGLM(10)/H**2.
2214 D(10,11)=DGLM(10)/H**2.
2215 A(10,11)=DGLM(10)/H**2.
2216 B(10,12)=-2.*DGLM(11)/H**2.
2217 D(10,12)=DGLM(11)/H**2.
2218 A(10,12)=DGLM(11)/H**2.
2219
2220 BIG=ABS(DGLM(9)*(CONC(10,J+1))/H**2.)
2221 BIG2=ABS(DGLM(9)*(-2.*CONC(10,J))/H**2.)
2222 IF (BIG2.GT.BIG) BIG=BIG2
2223 BIG3=ABS(DGLM(9)*(CONC(10,J-1))/H**2.)
2224 IF (BIG3.GT.BIG) BIG=BIG3
2225 BIG4=ABS(DGLM(10)*(CONC(11,J+1))/H**2.)
2226 IF (BIG4.GT.BIG) BIG=BIG4
2227 BIG5=ABS(DGLM(10)*(-2.*CONC(11,J))/H**2.)
2228 IF (BIG5.GT.BIG) BIG=BIG5
2229 BIG6=ABS(DGLM(10)*(CONC(11,J-1))/H**2.)
2230 IF (BIG6.GT.BIG) BIG=BIG6
2231 BIG7=ABS(DGLM(11)*(CONC(12,J+1))/H**2.)
2232 IF (BIG7.GT.BIG) BIG=BIG7
2233 BIG8=ABS(DGLM(11)*(-2.*CONC(12,J))/H**2.)
2234 IF (BIG8.GT.BIG) BIG=BIG8
2235 BIG9=ABS(DGLM(11)*(CONC(12,J-1))/H**2.)
2236 IF (BIG9.GT.BIG) BIG=BIG9
2237 IF (ABS(G(10)).LT.BIG*EBIG) G(10)=0
2238
2239 C FOR H+ and OH- ions equilibrium ,
2240 G(11)=equilib6-CONC(10,J)*CONC(11,J)
2241 B(11,10)=CONC(11,J)
2242 B(11,11)=CONC(10,J)
2243
2244

```

```

2245 BIG=ABS(equilib6)
2246 BIG2=ABS(CONC(10,J)*CONC(11,J))
2247 IF (BIG2.GT.BIG) BIG=BIG2
2248 IF (ABS(G(11)).LT.BIG*EBIG) G(11)=0
2249
2250 C FOR gluconic acid dissociation equilibrium ,
2251 G(12)=equilib7*CONC(3,J)-CONC(10,J)*CONC(12,J)
2252 B(12,3)=-equilib7
2253 B(12,10)=CONC(12,J)
2254 B(12,12)=CONC(10,J)
2255
2256 BIG=ABS(equilib7*CONC(3,J))
2257 BIG2=ABS(-CONC(10,J)*CONC(12,J))
2258 IF (BIG2.GT.BIG) BIG=BIG2
2259 IF (ABS(G(12)).LT.BIG*EBIG) G(12)=0
2260
2261 C For oxidized enzyme equilibrium ,
2262 G(13)=CONC(13,J)
2263 B(13,13)=-1.
2264
2265 BIG=ABS(CONC(13,J))
2266 IF (ABS(G(13)).LT.BIG*EBIG) G(13)=0
2267
2268 C For reduced enzyme equilibrium ,
2269 G(14)=CONC(14,J)
2270 B(14,14)=-1.
2271
2272 BIG=ABS(CONC(14,J))
2273 IF (ABS(G(14)).LT.BIG*EBIG) G(14)=0
2274
2275 C For Reaction 1 Enzymatic Catalysis
2276 G(15)=RXN(1,J)
2277 B(15,15)=-1.
2278
2279 BIG=ABS(RXN(1,J))
2280 IF (ABS(G(15)).LT.BIG*EBIG) G(15)=0
2281
2282 C For Reaction 2
2283 G(16)=RXN(2,J)
2284 B(16,16)=-1.
2285
2286 BIG=ABS(RXN(2,J))
2287 IF (ABS(G(16)).LT.BIG*EBIG) G(16)=0
2288
2289 C For Reaction 3 Meditation/regeneration
2290 G(17)=RXN(3,J)
2291 B(17,17)=-1.
2292
2293 BIG=ABS(RXN(3,J))
2294 IF (ABS(G(17)).LT.BIG*EBIG) G(17)=0
2295
2296 C For Reaction 4
2297 G(18)=RXN(4,J)
2298 B(18,18)=-1.
2299
2300 BIG=ABS(RXN(4,J))
2301 IF (ABS(G(18)).LT.BIG*EBIG) G(18)=0
2302

```

```

2303 C REACTION5
2304 G(19)=-RXN(5,J)+ratef5*CONC(9,J)-ratef5/equilib5*CONC(1,J)
2305 B(19,1)=ratef5/equilib5
2306 B(19,9)=-ratef5
2307 B(19,19)=+1.
2308
2309 BIG=ABS(RXN(5,J))
2310 BIG2=ABS(ratef5*CONC(9,J))
2311 IF (BIG2.GT.BIG) BIG=BIG2
2312 BIG3=ABS(ratef5/equilib5*CONC(1,J))
2313 IF (BIG3.GT.BIG) BIG=BIG3
2314 IF (ABS(G(19)).LT.BIG*EBIG) G(19)=0
2315
2316
2317 C SAVE G OUT DATA
2318 IF (J.EQ.(IJ+(NJ-IJ)/2)) THEN
2319 WRITE(12,301) J, (G(K),K=1,N)
2320 ELSE IF (J.EQ.(NJ-1)) THEN
2321 WRITE(12,301) J, (G(K),K=1,N)
2322 ELSE IF (J.EQ.(IJ+1)) THEN
2323 WRITE(12,301) J, (G(K),K=1,N)
2324 END IF
2325
2326 RETURN
2327 END
2328
2329 SUBROUTINE BCNJ(J)
2330 IMPLICIT DOUBLE PRECISION (A-H, O-Z)
2331 COMMON/BAB/ A(19,19),B(19,19),C(19,80001),D(19,39),G(19),X(19,19)
2332 1 ,Y(19,19)
2333 COMMON/NSN/ N, NJ
2334 COMMON/VAR/ CONC(14,80001),RXN(7,80001),H,EBIG,HH,IJ
2335 COMMON/VARR/ COEFFMT(13), HHH, KJ
2336 COMMON/POR/ DGOX(13),DGLM(13),DBULK(13)
2337 COMMON/BCI/ FLUXF,FLUXB,FLUXR,FLUXH,Current3
2338 COMMON/RTE/ ratef1,equilib1,ratef2,ratef3,equilib3,ratef4,ratef5,
2339 1 equilib5,ratef6,equilib6,equilib7,equilib8,equilib9
2340 COMMON/BUL/ CBULK(13),PARH2O2,PARO2,PARGLUCOSE,SOLO2,PARION,JCOUNT
2341 COMMON/VARIN/ V,PO2,pH,GOx
2342 COMMON/TEMP/ T
2343 COMMON/DLT/ DELTA
2344
2345 301 FORMAT (5x,'J=' I5, 19E19.9E3)
2346
2347 C For Beta-Glucose, being consumed only
2348 G(1)=COEFFMT(1)*
2349 1 (CONC(1,J)/PARGLUCOSE-CBULK(1)*equilib5/(1+equilib5))/(H/2.)
2350 2 -DGLM(1)*(CONC(1,J)-CONC(1,J-1))/(H**2./2.)
2351 3 +(3.*RXN(5,J)+RXN(5,J-1))/4.
2352 B(1,1)=COEFFMT(1)/PARGLUCOSE/(H/2.)+DGLM(1)/(H**2./2.)
2353 A(1,1)=-DGLM(1)/(H**2./2.)
2354 B(1,19)=-0.75
2355 A(1,19)=-0.25
2356
2357 BIG=ABS(COEFFMT(1)*CONC(1,J)/PARGLUCOSE/(H/2.))
2358 BIG2=ABS(COEFFMT(1)*CBULK(1)*equilib5/(1+equilib5)/(H/2.))
2359 IF (BIG2.GT.BIG) BIG=BIG2
2360 BIG3=ABS(DGLM(1)*(CONC(1,J))/(H**2./2.))

```

```

2361 IF (BIG3.GT.BIG) BIG=BIG3
2362 BIG4=ABS(DGLM(1)*(CONC(1,J-1))/(H**2./2.))
2363 IF (BIG4.GT.BIG) BIG=BIG4
2364 BIG5=ABS(3.*RXN(5,J)/4.)
2365 IF (BIG5.GT.BIG) BIG=BIG5
2366 BIG6=ABS(RXN(5,J-1)/4.)
2367 IF (BIG6.GT.BIG) BIG=BIG6
2368 IF (ABS(G(1)).LT.BIG*EBIG) G(1)=0
2369
2370 C For GOx, enzyme
2371 G(2)=CONC(2,J)
2372 B(2,2)=-1.
2373
2374 BIG=ABS(CONC(2,J))
2375 IF (ABS(G(2)).LT.BIG*EBIG) G(2)=0
2376
2377 C For Gluconic Acid and Gluconic Ion boundary condition is ,
2378 G(3)=-COEFFMT(3)*CONC(3,J)/PARGLUCOSE/(H/2.)
2379 1 -DGLM(3)/(H**2./2.)*(CONC(3,J)-CONC(3,J-1))
2380 2 -COEFFMT(11)*CONC(12,J)/PARGLUCOSE/(H/2.)
2381 3 -DGLM(11)*(CONC(12,J)-CONC(12,J-1))/(H**2./2.)
2382 B(3,3)=COEFFMT(3)/PARGLUCOSE/(H/2.)+DGLM(3)/(H**2./2.)
2383 A(3,3)=-DGLM(3)/(H**2./2.)
2384 B(3,12)=COEFFMT(11)/PARGLUCOSE/(H/2.)+DGLM(11)/(H**2./2.)
2385 A(3,12)=-DGLM(11)/(H**2./2.)
2386
2387 BIG=ABS(COEFFMT(3)*CONC(3,J)/PARGLUCOSE/(H/2.))
2388 BIG2=ABS(DGLM(3)*(CONC(3,J))/(H**2./2.))
2389 IF (BIG2.GT.BIG) BIG=BIG2
2390 BIG3=ABS(DGLM(3)*(CONC(3,J-1))/(H**2./2.))
2391 IF (BIG3.GT.BIG) BIG=BIG3
2392 BIG4=ABS(COEFFMT(11)*CONC(12,J)/PARGLUCOSE/(H/2.))
2393 IF (BIG4.GT.BIG) BIG=BIG4
2394 BIG5=ABS(DGLM(11)*(CONC(12,J))/(H**2./2.))
2395 IF (BIG5.GT.BIG) BIG=BIG5
2396 BIG6=ABS(DGLM(11)*(CONC(12,J-1))/(H**2./2.))
2397 IF (BIG6.GT.BIG) BIG=BIG6
2398 IF (ABS(G(3)).LT.BIG*EBIG) G(3)=0
2399
2400 C For GOx2, enzyme
2401 G(4)=CONC(4,J)
2402 B(4,4)=-1.
2403
2404 BIG=ABS(CONC(4,J))
2405 IF (ABS(G(4)).LT.BIG*EBIG) G(4)=0
2406
2407 C For O2, being consumed only
2408 G(5)=-COEFFMT(5)*(CONC(5,J)/PARO2-CBULK(5))/(H/2.)
2409 1 -DGLM(5)*(CONC(5,J)-CONC(5,J-1))/(H**2./2.)
2410 B(5,5)=COEFFMT(5)/PARO2/(H/2.)+DGLM(5)/(H**2./2.)
2411 A(5,5)=-DGLM(5)/(H**2./2.)
2412
2413 BIG=ABS(COEFFMT(5)*CONC(5,J)/PARO2/(H/2.))
2414 BIG2=ABS(COEFFMT(5)*CBULK(5)/(H/2.))
2415 IF (BIG2.GT.BIG) BIG=BIG2
2416 BIG3=ABS(DGLM(5)*(CONC(5,J))/(H**2./2.))
2417 IF (BIG3.GT.BIG) BIG=BIG3
2418 BIG4=ABS(DGLM(5)*(CONC(5,J-1))/(H**2./2.))

```

```

2419 IF (BIG4.GT.BIG) BIG=BIG4
2420 IF (ABS(G(5)).LT.BIG*EBIG) G(5)=0
2421
2422 C For H2O2, reacting species
2423 G(6)=COEFFMT(6)*CONC(6,J)/PARH2O2/(H/2.)-DGLM(6)*
2424 1 (CONC(6,J)-CONC(6,J-1))/(H**2./2.)
2425 B(6,6)=COEFFMT(6)/PARH2O2/(H/2.)+DGLM(6)/(H**2./2.)
2426 A(6,6)=-DGLM(6)/(H**2./2.)
2427
2428 BIG=ABS(COEFFMT(6)*CONC(6,J)/PARH2O2/(H/2.))
2429 BIG2=ABS(DGLM(6)*(CONC(6,J))/(H**2./2.))
2430 IF (BIG2.GT.BIG) BIG=BIG2
2431 BIG3=ABS(DGLM(6)*(CONC(6,J-1))/(H**2./2.))
2432 IF (BIG3.GT.BIG) BIG=BIG3
2433 IF (ABS(G(6)).LT.BIG*EBIG) G(6)=0
2434
2435 C For CX-GOx2, enzyme complex
2436 G(7)=CONC(7,J)
2437 B(7,7)=-1.
2438
2439 BIG=ABS(CONC(7,J))
2440 IF (ABS(G(7)).LT.BIG*EBIG) G(7)=0
2441
2442 C For CX-GOx, enzyme complex
2443 G(8)=CONC(8,J)
2444 B(8,8)=-1.
2445
2446 BIG=ABS(CONC(8,J))
2447 IF (ABS(G(8)).LT.BIG*EBIG) G(8)=0
2448
2449 C For Alpha-Glucose, being consumed only
2450 G(9)=COEFFMT(1)*
2451 1 (CONC(9,J)/PARGLUCOSE-CBULK(1)/(1+equilib5))/(H/2.)
2452 2 -DGLM(1)*(CONC(9,J)-CONC(9,J-1))/(H**2./2.)
2453 3 -(3.*RXN(5,J)+RXN(5,J-1))/4.
2454 B(9,9)=COEFFMT(1)/PARGLUCOSE/(H/2.)+DGLM(1)/(H**2./2.)
2455 A(9,9)=-DGLM(1)/(H**2./2.)
2456 B(9,19)=0.75
2457 A(9,19)=0.25
2458
2459 BIG=ABS(COEFFMT(1)*CONC(9,J)/PARGLUCOSE/(H/2.))
2460 BIG2=ABS(COEFFMT(1)*CBULK(1)/(1+equilib5)/(H/2.))
2461 IF (BIG2.GT.BIG) BIG=BIG2
2462 BIG3=ABS(DGLM(1)*(CONC(9,J))/(H**2./2.))
2463 IF (BIG3.GT.BIG) BIG=BIG3
2464 BIG4=ABS(DGLM(1)*(CONC(9,J-1))/(H**2./2.))
2465 IF (BIG4.GT.BIG) BIG=BIG4
2466 BIG5=ABS(3.*RXN(5,J)/4.)
2467 IF (BIG5.GT.BIG) BIG=BIG5
2468 BIG6=ABS(RXN(5,J-1)/4.)
2469 IF (BIG6.GT.BIG) BIG=BIG6
2470 IF (ABS(G(9)).LT.BIG*EBIG) G(9)=0
2471
2472 C For Flux of H+, OH- ions and gluconate ions,
2473 G(10)=-COEFFMT(9)*(CONC(10,J)/PARION-CBULK(9))/(H/2.)
2474 1 -DGLM(9)/(H**2./2.)*(CONC(10,J)-CONC(10,J-1))
2475 2 +COEFFMT(10)*(CONC(11,J)/PARION-CBULK(10))/(H/2.)
2476 3 +DGLM(10)/(H**2./2.)*(CONC(11,J)-CONC(11,J-1))

```

```

2477   4      +COEFFMT(11)*CONC(12,J)/PARGLUCOSE/(H/2.)
2478   5      +DGLM(11)*(CONC(12,J)-CONC(12,J-1))/(H**2./2.)
2479   B(10,10)=COEFFMT(9)/PARION/(H/2.)+DGLM(9)/(H**2./2.)
2480   A(10,10)=-DGLM(9)/(H**2./2.)
2481   B(10,11)=-COEFFMT(10)/PARION/(H/2.)-DGLM(10)/(H**2./2.)
2482   A(10,11)=DGLM(10)/(H**2./2.)
2483   B(10,12)=-COEFFMT(11)/PARGLUCOSE/(H/2.)-DGLM(11)/(H**2./2.)
2484   A(10,12)=DGLM(11)/(H**2./2.)
2485
2486   BIG=ABS(COEFFMT(9)*CONC(10,J)/PARION/(H/2.))
2487   BIG2=ABS(COEFFMT(9)*CBULK(9)/(H/2.))
2488   IF (BIG2.GT.BIG) BIG=BIG2
2489   BIG3=ABS(DGLM(9)*(CONC(10,J))/(H**2./2.))
2490   IF (BIG3.GT.BIG) BIG=BIG3
2491   BIG4=ABS(DGLM(9)*(CONC(10,J-1))/(H**2./2.))
2492   IF (BIG4.GT.BIG) BIG=BIG4
2493   BIG5=ABS(COEFFMT(10)*CONC(11,J)/PARION/(H/2.))
2494   IF (BIG5.GT.BIG) BIG=BIG5
2495   BIG6=ABS(COEFFMT(10)*CBULK(10)/(H/2.))
2496   IF (BIG6.GT.BIG) BIG=BIG6
2497   BIG7=ABS(DGLM(10)*(CONC(11,J))/(H**2./2.))
2498   IF (BIG7.GT.BIG) BIG=BIG7
2499   BIG8=ABS(DGLM(10)*(CONC(11,J-1))/(H**2./2.))
2500   IF (BIG8.GT.BIG) BIG=BIG8
2501   BIG9=ABS(COEFFMT(11)*CONC(12,J)/PARGLUCOSE/(H/2.))
2502   IF (BIG9.GT.BIG) BIG=BIG9
2503   BIG10=ABS(DGLM(11)*(CONC(12,J))/(H**2./2.))
2504   IF (BIG10.GT.BIG) BIG=BIG10
2505   BIG11=ABS(DGLM(11)*(CONC(12,J-1))/(H**2./2.))
2506   IF (BIG11.GT.BIG) BIG=BIG11
2507   IF (ABS(G(10)).LT.BIG*EBIG) G(10)=0
2508
2509 C FOR H+ and OH- ions equilibrium,
2510 G(11)=equilib6-CONC(10,J)*CONC(11,J)
2511 B(11,10)=CONC(11,J)
2512 B(11,11)=CONC(10,J)
2513
2514
2515 BIG=ABS(equilib6)
2516 BIG2=ABS(CONC(10,J)*CONC(11,J))
2517 IF (BIG2.GT.BIG) BIG=BIG2
2518 IF (ABS(G(11)).LT.BIG*EBIG) G(11)=0
2519
2520 C FOR gluconic acid dissociation equilibrium,
2521 G(12)=equilib7*CONC(3,J)-CONC(10,J)*CONC(12,J)
2522 B(12,3)=-equilib7
2523 B(12,10)=CONC(12,J)
2524 B(12,12)=CONC(10,J)
2525
2526 BIG=ABS(equilib7*CONC(3,J))
2527 BIG2=ABS(-CONC(10,J)*CONC(12,J))
2528 IF (BIG2.GT.BIG) BIG=BIG2
2529 IF (ABS(G(12)).LT.BIG*EBIG) G(12)=0
2530
2531 C For oxidized enzyme equilibrium,
2532 G(13)=CONC(13,J)
2533 B(13,13)=-1.
2534

```

```

2535     BIG=ABS(CONC(13,J))
2536     IF (ABS(G(13)).LT.BIG*EBIG) G(13)=0
2537
2538 C   For reduced enzyme equilibrium ,
2539     G(14)=CONC(14,J)
2540     B(14,14)=-1.
2541
2542     BIG=ABS(CONC(14,J))
2543     IF (ABS(G(14)).LT.BIG*EBIG) G(14)=0
2544
2545 C   For Reaction 1 Enzymatic Catalysis
2546     G(15)=RXN(1,J)
2547     B(15,15)=-1.
2548
2549     BIG=ABS(RXN(1,J))
2550     IF (ABS(G(15)).LT.BIG*EBIG) G(15)=0
2551
2552 C   For Reaction 2
2553     G(16)=RXN(2,J)
2554     B(16,16)=-1.
2555
2556     BIG=ABS(RXN(2,J))
2557     IF (ABS(G(16)).LT.BIG*EBIG) G(16)=0
2558
2559 C   For Reaction 3 Meditation/regeneration
2560     G(17)=RXN(3,J)
2561     B(17,17)=-1.
2562
2563     BIG=ABS(RXN(3,J))
2564     IF (ABS(G(17)).LT.BIG*EBIG) G(17)=0
2565
2566 C   For Reaction 4
2567     G(18)=RXN(4,J)
2568     B(18,18)=-1.
2569
2570     BIG=ABS(RXN(4,J))
2571     IF (ABS(G(18)).LT.BIG*EBIG) G(18)=0
2572
2573 C   REACTION5
2574     G(19)=-RXN(5,J)+ratef5*CONC(9,J)-ratef5/equilib5*CONC(1,J)
2575     B(19,1)=ratef5/equilib5
2576     B(19,9)=-ratef5
2577     B(19,19)=+1.
2578
2579     BIG=ABS(RXN(5,J))
2580     BIG2=ABS(ratef5*CONC(9,J))
2581     IF (BIG2.GT.BIG) BIG=BIG2
2582     BIG3=ABS(ratef5/equilib5*CONC(1,J))
2583     IF (BIG3.GT.BIG) BIG=BIG3
2584     IF (ABS(G(19)).LT.BIG*EBIG) G(19)=0
2585
2586
2587 C   SAVE G OUT DATA
2588 206   WRITE(12,301) J, (G(K),K=1,N)
2589   PRINT *, 'ITERATION=' , JCOUNT
2590   RETURN
2591 END
2592

```

```

2593
2594 C Subroutine MATINV
2595 SUBROUTINE MATINV(N,M,DETERM)
2596 IMPLICIT DOUBLE PRECISION (A-H,O-Z)
2597 COMMON/BAB/ A(19,19),B(19,19),C(19,80001),D(19,39),G(19),X(19,19)
2598 1 ,Y(19,19)
2599 COMMON/NSN/ NTEMP, NJ
2600 DIMENSION ID(19)
2601 DETERM=1.01
2602 DO 1 I=1,N
2603 1 ID(I)=0
2604 DO 18 NN=1,N
2605 BMAX=1.1
2606 DO 6 I=1,N
2607 IF (ID(I).NE.0) GO TO 6
2608 BNEXT=0.0
2609 BTRY=0.0
2610 DO 5 J=1,N
2611 IF (ID(J).NE.0) GO TO 5
2612 IF (DABS(B(I,J)).LE.BNEXT) GO TO 5
2613 BNEXT=DABS(B(I,J))
2614 IF (BNEXT.LE.BTRY) GO TO 5
2615 BNEXT=BTRY
2616 BTRY=DABS(B(I,J))
2617 JC=J
2618 5 CONTINUE
2619 IF (BNEXT.GE.BMAX*BTRY) GO TO 6
2620 BMAX=BNEXT/BTRY
2621 IROW=I
2622 JCOL=JC
2623 6 CONTINUE
2624 IF (ID(JC).EQ.0) GO TO 8
2625 DETERM=0.0
2626 RETURN
2627 8 ID(JCOL)=1
2628 IF (JCOL.EQ.IROW) GO TO 12
2629 DO 10 J=1,N
2630 SAVE=B(IROW,J)
2631 B(IROW,J)=B(JCOL,J)
2632 10 B(JCOL,J)=SAVE
2633 DO 11 K=1,M
2634 SAVE=D(IROW,K)
2635 D(IROW,K)=D(JCOL,K)
2636 11 D(JCOL,K)=SAVE
2637 12 F=1.0/B(JCOL,JCOL)
2638 DO 13 J=1,N
2639 13 B(JCOL,J)=B(JCOL,J)*F
2640 DO 14 K=1,M
2641 14 D(JCOL,K)=D(JCOL,K)*F
2642 DO 18 I=1,N
2643 IF (I.EQ.JCOL) GO TO 18
2644 F=B(I,JCOL)
2645 DO 16 J=1,N
2646 16 B(I,J)=B(I,J)-F*B(JCOL,J)
2647 DO 17 K=1,M
2648 17 D(I,K)=D(I,K)-F*D(JCOL,K)
2649 18 CONTINUE
2650 RETURN

```

```

2651      END
2652
2653 C   SUBROUTINE BAND(J)
2654     SUBROUTINE BAND(J)
2655     IMPLICIT DOUBLE PRECISION (A-H,O-Z)
2656     DIMENSION E(19,20,80001)
2657     COMMON/BAB/ A(19,19),B(19,19),C(19,80001),D(19,39),G(19),X(19,19)
2658     1 ,Y(19,19)
2659     COMMON/NSN/ N,NJ
2660     SAVE E, NP1
2661 101  FORMAT(15H DETERM=0 AT J=,I4)
2662     IF (J-2) 1,6,8
2663     1 NP1=N+1
2664     DO 2 I=1,N
2665     D(I,2*N+1)=G(I)
2666     DO 2 L=1,N
2667     LPN=L+N
2668     2 D(I,LPN)=X(I,L)
2669     CALL MATINV(N, 2*N+1,DETERM)
2670     IF (DETERM) 4,3,4
2671     3 PRINT 101,J
2672     4 DO 5 K=1,N
2673     E(K,NP1,1)=D(K,2*N+1)
2674     DO 5 L=1,N
2675     E(K,L,1)=-D(K,L)
2676     LPN=L+N
2677     5 X(K,L)=-D(K,LPN)
2678     RETURN
2679     6 DO 7 I=1,N
2680     DO 7 K=1,N
2681     DO 7 L=1,N
2682     7 D(I,K)=D(I,K)+A(I,L)*X(L,K)
2683     8 IF (J-NJ) 11,9,9
2684     9 DO 10 I=1,N
2685     DO 10 L=1,N
2686     G(I)=G(I)-Y(I,L)*E(L,NP1,J-2)
2687     DO 10 M=1,N
2688     10 A(I,L)=A(I,L)+Y(I,M)*E(M,L,J-2)
2689     11 DO 12 I=1,N
2690     D(I,NP1)=-G(I)
2691     DO 12 L=1,N
2692     D(I,NP1)=D(I,NP1)+A(I,L)*E(L,NP1,J-1)
2693     DO 12 K=1,N
2694     12 B(I,K)=B(I,K)+A(I,L)*E(L,K,J-1)
2695     CALL MATINV(N,NP1,DETERM)
2696     IF (DETERM) 14, 13, 14
2697     13 PRINT 101,J
2698     14 DO 15 K=1,N
2699     DO 15 M=1,NP1
2700     15 E(K,M,J)=-D(K,M)
2701     IF (J-NJ) 20,16,16
2702     16 DO 17 K=1,N
2703     17 C(K,J)=E(K,NP1,J)
2704     DO 18 JJ=2,NJ
2705     M=NJ-JJ+1
2706     DO 18 K=1,N
2707     C(K,M)=E(K,NP1,M)
2708     DO 18 L=1,N

```

```
2709 18 C(K,M)=C(K,M)+E(K,L,M)*C(L,M+1)
2710 DO 19 L=1,N
2711 DO 19 K=1,N
2712 19 C(K,1)=C(K,1)+X(K,L)*C(L,3)
2713 20 RETURN
2714 END
```

Code A.3. Matlab code to create and plot polarization curve

```

1 clc; close all; clear all;
2 format longE;
3
4 h=0.02; %Step-size
5 V=-0.:h:0.6; %Potential range
6
7 % h=0.005; %Step-size
8 % V=0.14:h:0.24; %Potential range
9
10 % h=0.001; %Step-size
11 % V=0.20:h:0.22; %Potential range
12 Current=length(V); %Current to be saved
13 C_H2O2=length(V); %Hydrogenperoxide concentration to be saved
14 C_O2=length(V); %oxygen concentration to be saved
15 for k=1:length(V);
16
17 potential = fopen('pot_in.txt','w');
18 fprintf(potential,'%8.3f',V(k));
19 fclose(potential);
20 %Run the executable
21 system('cdhgox_ss_newBC6.exe')
22 pause(1);
23 %Read constant values used in the Fortran code
24 M = dlmread('cdhgox_ssvalues_out.txt');
25
26 NM(1);
27 NJ=M(2);
28 IJ=M(3);
29 KJ=M(4);
30 H=M(5);
31 HH=M(6);
32 HHH=M(7);
33 DGOX_H2O2=M(8);
34 DGOX_O2=M(9);
35 DGOX_H=M(10);
36 AKF=M(11);
37 AKB=M(12);
38 AK2=M(13);
39 AKH=M(14);
40 BBA=M(15);
41 BBC=M(16);
42 BB2=M(17);
43 BBH=M(18);
44 POT=M(19);
45
46 %Read the steady state values for CB
47 Bss1 = dlmread('cdhgox_out.txt');
48 Bss(:,1)=Bss1(:,6);
49 Bss(:,2)=Bss1(:,5);
50
51
52 %Other constants
53 F=96487;
54
55 %Create rates
56 eea=BBA*POT;

```

```

57 eec=BBC*POT;
58 ee2=BB2*POT;
59 i3=AKF*Bss1(1,6)*exp(eea)-AKB*Bss1(1,5)*(Bss1(1,10)^2)*exp(-eec)...
60 -AK2*Bss1(1,6)*(Bss1(1,10)^2)*exp(-ee2);
61
62
63
64 %Save current
65 Current(k)=i3;
66 C_H2O2(k)=Bss1(1,6);
67 C_O2(k)=Bss1(1,5);
68 end
69
70
71 figure(1)
72 plot(V,Current,'-. b'); hold on;
73 title('Polarization Curve');
74
75 Current=Current';
76 V=V';
77 C_O2=C_O2';
78 C_H2O2=C_H2O2';

```

Code A.4. Matlab code to plot results from steady-state solutions

```

1 %Steady State
2 clc; close all; clear all;
3 format longE;
4
5
6 %Read constant values used in the Fortran code
7 M = dlmread('cdhgox_ssvalues_out.txt');
8
9 N=M(1);
10 NJ=M(2);
11 IJ=M(3);
12 KJ=M(4);
13 H=M(5);
14 HH=M(6);
15 HHH=M(7);
16 DGOX_H2O2=M(8);
17 DGOX_O2=M(9);
18 DGOX_H=M(10);
19 AKF=M(11);
20 AKB=M(12);
21 AK2=M(13);
22 AKH=M(14);
23 BBA=M(15);
24 BBC=M(16);
25 BB2=M(17);
26 BBH=M(18);
27 POT=M(19);
28
29 %Read the steady state values for CB
30 Bss1 = dlmread('cdhgox_out.txt');
31 Bss (:,1)=Bss1 (:,6);
32 Bss (:,2)=Bss1 (:,5);
33
34
35 %Other constants
36 F=96487;
37
38 %Create rates
39 eea=BBA*POT;
40 eec=BBC*POT;
41 ee2=BB2*POT;
42 i3=AKF*Bss1(1,6)*exp(eea)-AKB*Bss1(1,5)*(Bss1(1,10)^2)*exp(-eec)-AK2*Bss1(1,6)
    *(Bss1(1,10)^2)*exp(-ee2);
43
44 % Deffh2o2=AKF*Bss1(1,6)*exp(eea)/(2*F*((-Bss(3,1)+4*Bss(2,1)-3*Bss(1,1))/(2*
    HHH)));
45 % DeffO2=AKB*Bss1(1,5)*exp(-eec)/(2*F*((-Bss(3,2)+4*Bss(2,2)-3*Bss(1,2))/(2*
    HHH)));
46 % N_H2O2=DiffF*POR1*((-Bss(3,1)+4*Bss(2,1)-3*Bss(1,1))/(2*HHH));
47 % N_O2=DiffB*POR1*((-Bss(3,2)+4*Bss(2,2)-3*Bss(1,2))/(2*HHH));
48 % i2=-2.*F*N_H2O2;
49
50 %Create y values for plotting
51 y=zeros(NJ,1);
52
53 far=HHH*(KJ-1);

```

```

54 y1=0:HHH:far ;
55
56 far1=HH*(IJ-KJ) ;
57 y2=y1(KJ):HH:y1(KJ)+far1 ;
58
59 far2=H*(NJ-IJ) ;
60 y3=y2(IJ-KJ+1):H:y2(IJ-KJ+1)+far2 ;
61
62 for i=1:KJ-1
63 y(i)=y1(i) ;
64 end
65 for i=KJ:IJ-1
66 y(i)=y2(i-KJ+1) ;
67 end
68 for i=IJ:NJ;
69 y(i)=y3(i-IJ+1) ;
70 end
71
72
73 figure(1)
74 plot(y,Bss1(:,2),'-b'); hold on;
75 plot(y,Bss1(:,4),'-k'); hold on;
76 title('GOx and GOx2') ;
77
78
79 figure(2)
80 semilogy(y,Bss1(:,2),'-b'); hold on;
81 semilogy(y,Bss1(:,4),'-k'); hold on;
82 title('GOx and GOx2') ;
83
84 figure(3)
85 plot(y,Bss1(:,7),'-b'); hold on;
86 plot(y,Bss1(:,8),'-k'); hold on;
87 title('CX-GOx2 and CX-GOx') ;
88
89 figure(4)
90 semilogy(y,Bss1(:,7),'-b'); hold on;
91 semilogy(y,Bss1(:,8),'-k'); hold on;
92 title('CX-GOx2 and CX-GOx') ;
93
94 figure(5)
95 plot(y,Bss1(:,1),'-b'); hold on;
96 title('beta-Glucose') ;
97
98 figure(6)
99 plot(y,Bss1(:,9),'-b'); hold on;
100 title('alpha-Glucose') ;
101
102 figure(7)
103 plot(y,Bss1(:,5),'-m'); hold on;
104 title('Oxygen') ;
105
106 figure(8)
107 plot(y,Bss1(:,6),'-r'); hold on;
108 %plot(y,Bss1(:,3),'-k'); hold on;
109 title('H2O2') ;
110 figure(9)
111 plot(y,Bss1(:,3),'-r'); hold on;

```

```

112 %plot(y,Bss1(:,3),'-k'); hold on;
113 title('Gluconic Acid')
114 figure(10)
115 plot(y,Bss1(:,12),'-r'); hold on;
116 %plot(y,Bss1(:,3),'-k'); hold on;
117 title('Gluconic Ion')
118
119 figure(11)
120 plot(y,Bss1(:,10),'-b'); hold on;
121 title('H+ ion');
122
123 figure(12)
124 plot(y,Bss1(:,11),'-b'); hold on;
125 title('OH- ion');
126
127 figure(13)
128 plot(y,Bss1(:,13),'-b'); hold on;
129 title('H+Eo');
130
131 figure(14)
132 plot(y,Bss1(:,14),'-b'); hold on;
133 title('Er-');
134 %
135 % figure(5)
136 % plot(y,Bss1(:,6),'-r'); hold on;
137 % title('Hydrogen Peroxide');
138 % %plot(y,Bss1(:,1),'-b')
139 % %plot(y,Bss1(:,2),'-g')
140 % %axis([0 H*4000 0 10.05e-5]);
141 % % title('Steady State Concentration away from Electrode Surface');
142 % % xlabel('Length, cm');
143 % % ylabel('Concentration, moles/cm3');
144
145 figure(15)
146 plot(y,Bss1(:,15),'-r'); hold on;
147 plot(y,Bss1(:,16),'-k'); hold on;
148 plot(y,Bss1(:,17),'-b'); hold on;
149 plot(y,Bss1(:,18),'-g'); hold on;
150 plot(y,Bss1(:,19),'-.b'); hold on;
151 figure(16)
152 semilogy(y,Bss1(:,15),'-r'); hold on;
153 semilogy(y,Bss1(:,16),'-k'); hold on;
154 semilogy(y,Bss1(:,17),'-b'); hold on;
155 semilogy(y,Bss1(:,18),'-g'); hold on;
156 semilogy(y,Bss1(:,19),'-.b'); hold on;
157 title('Reaction');
158
159 figure(17)
160 semilogy(y(1:1200),abs(Bss1(1:1200,20)),'-.o'); hold on;
161 title('Water dissociation Rate');
162 figure(18)
163 plot(y(1:1200),Bss1(1:1200,21),'-.r'); hold on;
164 title('Gluconic acid dissociation Rate');
165
166
167 % figure (6)
168 % plot(y,V(:,2),'-k'); hold on;
169 % plot(y,V(:,1),'-r'); hold on;

```

```

170 % plot(y,V(:,4),'- b') ;
171
172 y1=y1';
173 RTB = 1./(AKF*Bss1(1,6)*exp(eea)*BBA+AKB*Bss1(1,5)*(Bss1(1,10)^2)*exp(-eec)*
    BBC+AK2*Bss1(1,6)*(Bss1(1,10)^2)*exp(-ee2)*BB2);
174 Zd_H2O2 = RTB*(AKF*exp(BBA*POT)-AK2*Bss1(1,10)^2*exp(-BB2*POT));
175 Zd_H = RTB*(2*AKB*Bss1(1,10)*Bss1(1,5)*exp(-BBC*POT)+2*AK2*Bss1(1,10)*Bss1
    (1,6)*exp(-BB2*POT));

```

Code A.5. Matlab code for Oxygen Curve Calculation

```

1 clc; close all; clear all;
2 format longE;
3
4 O2=logspace(-4,0,40);
5
6 col=1;
7 CurrentDensity=zeros(length(O2),length(col));
8
9 for l=1:length(O2)
10     ConcO2 = fopen('O2_in.txt','w');
11     fprintf(ConcO2,'%e',O2(l));
12     fclose(ConcO2);
13
14     %Run the executable
15 system('cdhgox_ss.exe')
16 pause(0.1);
17
18 %Read constant values used in the Fortran code
19 M = dlmread('cdhgox_ssvalues_out.txt');
20
21 N=M(1);
22 NJ=M(2);
23 IJ=M(3);
24 KJ=M(4);
25 H=M(5);
26 HH=M(6);
27 HHH=M(7);
28 DGOX_H2O2=M(8);
29 DGOX_O2=M(9);
30 DGOX_H=M(10);
31 AKF=M(11);
32 AKB=M(12);
33 AK2=M(13);
34 AKH=M(14);
35 BBA=M(15);
36 BBC=M(16);
37 BB2=M(17);
38 BBH=M(18);
39 POT=M(19);
40
41 %Read the steady state values for CB
42 Bss1 = dlmread('cdhgox_out.txt');
43 Bss(:,1)=Bss1(:,6);
44 Bss(:,2)=Bss1(:,5);
45
46
47 %Other constants
48 F=96487;
49
50 %Create rates
51 eea=BBA*POT;
52 eec=BBC*POT;
53 ee2=BB2*POT;
54 eeH=BBH*POT;
55 i3=AKF*Bss1(1,6)*exp(eea)-AKB*Bss1(1,5)*(Bss1(1,10)^2)*exp(-eec) -...
56     AK2*Bss1(1,6)*(Bss1(1,10)^2)*exp(-ee2)-AKH*(Bss1(1,10)^2)*exp(-eeH);

```

```
57 CurrentDensity(1) = i3;
58 end
59
60
61 figure(1)
62 semilogx(O2, CurrentDensity(:,1), '-. b'); hold on;
63 title('Oxygen-Current Density Curve');
64 xlabel('Oxygen Concentration, mol/cm^3');
65 ylabel('Current Density, A/cm^2');
66 set(gcf, 'Tag', 'plt')
67
68 O2=O2';
```

A.3 Code for Impedance Calculation

This section contains the FORTRAN code for impedance calculation solving 38 coupled differential equations. The mathematical development of the model including the governing equation and the boundary conditions are described in Chapter 3. The distributions of concentration of the species and reaction rates at steady-state calculated are input for this program. The Matlab® code visualizes and organizes the output results from the FORTRAN code. After solving phasor of concentrations in FORTRAN executables, the impedance is calculated based on proposed equivalent circuit framework in the Matlab® program with output variables and parameters. The calculation results are visualized for dimensionless diffusion impedance response, diffusion impedance response, faradaic impedance response and overall impedance response.

Code A.6. FORTRAN Code for Impedance Calculations

```

1 C      Convective Diffusion Equation with Homogeneous Reaction
2 C      Enzyme kinetics added
3 C      14 species system
4 C      SPECIES 1 = beta-glucose , SPECIES 2 = GOx-FAD, SPECIES 3 = Gluconic acid
5 C      SPECIES 4 = GOx-FADH2, SPECIES 5 = O2, SPECIES 6 = H2O2
6 C      SPECIES 7 = GOx-FADH2-GA, SPECIES 8 = GOx-FAD-H2O2, SPECIES 9 = Alpha-
Glucose
7 C      SPECIES 10 = hydrogen ion , SPECIES 11= hydroxide ion , SPECIES 12=
gluconate ion
8 C      SPECIES 13 = H+Eo, SPECIES 14 = Er-
9 C      Species 5 , 6 and 10 are the reacting species
10 C     This is the unsteady state solution that will eventually lead to
11 c     the impedance!
12
13 C     This should be ran after cdhgox_ss.for
14 C     The input file is the same for both of these
15 C
*****THIS CODE SEPERATES THE EFFECTIVE DIFFUSION COEFFICIENTS FOR EACH
SPECIES IN DIFFERENT LAYERS
17 C     There are 4 electrochemical reaction in this code: H2O2 oxidation and
reduction , O2 reduction
18 C     and H2 evolution at low applied potential
19 C
*****MODIFICATION: Adding partiction coefficients at BCNJ for H+, OH-
*****THIS CODE SEPERATES THE EFFECTIVE DIFFUSION COEFFICIENTS FOR EACH
SPECIES IN DIFFERENT LAYERS
24 C      cd C:\Ming\FORTRAN2019\CGM Basic no buffer H2Evolution_Par
25 C      gfortran -static cdhgox_os.for -o cdhgox_os.exe
26
27      PROGRAM CONVDIFFOSCILLATING
28      IMPLICIT DOUBLE PRECISION (A-H, O-Z)
29      COMMON/BAT/ A(38,38),B(38,38),C(38,10001),D(38,77),G(38),
1      X(38,38),Y(38,38)
31      COMMON/NST/ N, NJ
32      COMMON/VAR/ CONCSS(14,10001),RXNSS(7,10001)
33      COMMON/VARR/ COEFFMT(13),HHH, KJ
34      COMMON/CON/ C1(2,10001),C2(2,10001),C3(2,10001),C4(2,10001),
1      C5(2,10001),C6(2,10001),C7(2,10001),C8(2,10001),C9(2,10001),
2      C10(2,10001),C11(2,10001),C12(2,10001),C13(2,10001),
2      C14(2,10001),RXN1(2,10001),RXN2(2,10001),RXN3(2,10001),
3      RXN4(2,10001),RXN5(2,10001)
39      COMMON/RTE/ ratef1, equilib1, ratef2, ratef3, equilib3, ratef4, ratef5,
40      1 equilib5, ratef6, equilib6, equilib7, equilib8, equilib9
41      COMMON/OTH/ H,EBIG,HH,IJ
42      COMMON/POR/ DGOX(17),DGLM(17),DBULK(17)
43      COMMON/BCI/ FLUXF,FLUXB,FLUXR,FLUXH,omega

```

```

44 COMMON/BUL/ CBULK(13),PARH2O2,PAR02,PARGLUCOSE,PARION,SOLO2,JCOUNT
45 COMMON/DELT/ DELTA1, DELTA2, FREQ(400),CH2O2(1000,10001),
46 1 CO2(1000,10001),CH(1000,10001)
47 COMMON/POT/ VTILDE
48 COMMON/EXTRA/ Z(13),REF(13)
49 CHARACTER REF*13
50
51 102 FORMAT (/30H THE NEXT RUN DID NOT CONVERGE)
52 103 FORMAT ('Error=' ,E16.6/(1X,'Species=' ,A6,2X,'Conc at Electrode=' ,
53 1 E12.5 ,2X,'Conc at Bulk=' ,E12.5E3))
54 334 FORMAT (21(E25.15E3,5X))
55 335 FORMAT (38(E25.15E3,5X))
56 336 FORMAT (1000(E25.15E3,1X))
57 339 FORMAT (1000(E16.9 ,1X))
58 301 FORMAT (5x,'J=' I5 , 38E15.6E3)
59 302 FORMAT ('Iteration=' I4)
60 C   Read input values used in steady state
61 open(10,file='cdhgox_in.txt',status='old')
62 read(10,*) N,NJ,IJ,KJ,Y1,Y2,Y3,PARH2O2,PARO2,PARGLUCOSE,PARION,
63 1 SOLO2,ratef1,equilib1,ratef2,ratef3,equilib3,
64 2 ratef4,ratef5,equilib5,ratef6,equilib6,equilib7,equilib8,
65 3 equilib9,AKF,AKB,AK2,AKH,BBA,BBC,BB2,BBH,EBIG
66 read(10,*)(CBULK(I),I=1,(N-6))
67
68
69 open(21,file='pot_in.txt',status='old')
70 read(21,*) V
71
72 open(22,file='O2_in.txt',status='old')
73 read(22,*) PO2
74
75 open(23,file='pH_in.txt',status='old')
76 read(23,*) pH
77
78 open(24,file='enzyme_in.txt',status='old')
79 305 FORMAT (E15.5)
80 read(24,305) GOx
81 C   PRINT *, 'GOx=' ,GOx
82 C   PRINT *, 'pH=' ,pH
83
84 C   IMPORT EFFECTIVE DIFFUSION COEFFICIENTS
85 open(25,file='DGox_in.txt',status='old')
86 read(25,*)(DGOX(I),I=1,(N-6))
87
88 open(26,file='DGLM_in.txt',status='old')
89 read(26,*)(DGLM(I),I=1,(N-6))
90 PRINT *, 'DGLM(2)= ', DGLM(2)
91
92 open(27,file='DBULK_in.txt',status='old')
93 read(27,*)(DBULK(I),I=1,(N-6))
94
95 C   Calculate bulk concentration of O2
96 CBULK(5)=PO2*SOLO2
97 C   PRINT *, 'CBULK_O2=' ,CBULK(5)
98 C   Calculate bulk concentration of H+
99 CBULK(9)=10.**(-pH)*1.E-3
100 C   PRINT *, 'H+ BULK=' ,CBULK(9)
101 C   Calculate bulk concentration of OH-

```

```

102 CBULK(10)=equilib6 /CBULK(9)
103 C Calculate bulk concentration of enzyme
104 CBULK(2)=GOx/6.
105 CBULK(4)=GOx/6.
106 CBULK(7)=GOx/6.
107 CBULK(8)=GOx/6.
108 CBULK(12)=GOx/6.
109 CBULK(13)=GOx/6.
110
111 C Read steady state values from previous file
112 OPEN(UNIT=11, FILE='cdhgox_out.txt')
113 READ(11,334) (CONCSS(1,I),CONCSS(2,I),CONCSS(3,I),CONCSS(4,I),
114 1 CONCSS(5,I),CONCSS(6,I),CONCSS(7,I),CONCSS(8,I),CONCSS(9,I),
115 2 CONCSS(10,I),CONCSS(11,I),CONCSS(12,I),CONCSS(13,I),
116 3 CONCSS(14,I),RXNSS(1,I),RXNSS(2,I),RXNSS(3,I),
117 3 RXNSS(4,I),RXNSS(5,I),RXNSS(6,I),RXNSS(7,I),I=1,NJ)
118
119 OPEN(UNIT=13, FILE='cdhgox_os_out.txt')
120 CLOSE(UNIT=13, STATUS='DELETE')
121 OPEN(UNIT=13, FILE='cdhgox_os_out.txt')
122
123 OPEN(14,FILE='cdhgox_G_out.txt')
124 CLOSE(14, STATUS='DELETE')
125 OPEN(14, FILE='cdhgox_G_out.txt')
126
127 OPEN(15,FILE='cdhgox_H2O2_out.txt')
128 CLOSE(15, STATUS='DELETE')
129 OPEN(15, FILE='cdhgox_H2O2_out.txt')
130
131 OPEN(16,FILE='cdhgox_values_out.txt')
132 CLOSE(16, STATUS='DELETE')
133 OPEN(16, FILE='cdhgox_values_out.txt')
134
135 OPEN(17,FILE='kgox_values_out.txt')
136 CLOSE(17, STATUS='DELETE')
137 OPEN(17, FILE='kgox_values_out.txt')
138
139 OPEN(19,FILE='cdhgox_O2_out.txt')
140 CLOSE(19, STATUS='DELETE')
141 OPEN(19, FILE='cdhgox_O2_out.txt')
142
143 OPEN(20,FILE='cdhgox_H_ion_out.txt')
144 CLOSE(20, STATUS='DELETE')
145 OPEN(20, FILE='cdhgox_H_ion_out.txt')
146
147 C Constants
148 F=96487.
149 C Applied oscillating potential
150 VTILDE=0.01
151 c THIS IS SPACING FOR OUTER LAYER, BCNJ
152 H=Y3/(NJ-IJ)
153
154 c THIS IS SPACING FOR INNER LAYER, BC1
155 HH=Y2/(IJ-KJ)
156
157 c THIS IS SPACING FOR REACTION LAYER
158 HHH=Y1/(KJ-1)
159

```

```

160 C      Create flux of the reacting species constants
161 FLUXF=AKF*exp(BBA*V)/F/2.
162 FLUXB=AKB*exp(-BBC*V)/F/2.
163 FLUXR=AK2*exp(-BB2*V)/F/2.
164 FLUXH=AKH*exp(-BBH*V)/F/2.
165
166
167 C      Create charge transfer resistance
168 RTB=1./(AKF*BBA*CONCSS(6,1)*EXP(BBA*V)
169     +AKB*BBC*CONCSS(5,1)*(CONCSS(10,1)**2.)*EXP(-BBC*V)
170     +AK2*BB2*CONCSS(6,1)*(CONCSS(10,1)**2.)*EXP(-BB2*V)
171     +AKH*BBH*(CONCSS(10,1)**2.)*EXP(-BBH*V))
172 PRINT *, 'Charge Transfer Resistance', RTB
173
174 N=2*N
175 PRINT *, 'N=' , N
176
177 337 FORMAT (I2/I7/I7/I7/15(E15.8/)E15.8)
178   write (16,337) N,NJ,IJ,KJ,H,HH,HHH,V,AKF,AKB,AK2,AKH,BBA,BBC,BB2,
179   1 BBH,DGOX(6),DGOX(5),DGOX(9),RTB
180
181 C      The number of points for frequency
182 NPTS=241
183 C      PRINT *, 'NPTS=' , NPTS
184 c      Create range for the frequency
185 DO 261 I=1,NPTS
186 FREQ(I)=10.**(-5.+0.05*(I-1.))
187 261 WRITE (17,339) FREQ(I)
188
189
190 C C      The number of points for frequency
191 C      NPTS=13
192 C C      PRINT *, 'NPTS=' , NPTS
193 C C      Create range for the dimensionless frequency
194 C      DO 261 I=1,NPTS
195 C      FREQ(I)=10.**(-3.+0.5*(I-1.))
196 C      261 WRITE (17,339) FREQ(I)
197
198      DO 19 nf=1,NPTS
199 C      DO 19 nf=1,3
200
201
202 C      PRINT *, 'FREQ(NF)=' , FREQ(NF)
203 omega=FREQ(NF)
204
205 IF (ratef1.LT.1E-10) omega=FREQ(NF)
206
207      PRINT *, 'omega=' , omega
208 C      340 FORMAT (E12.6)
209 C      write (17,340) omega
210 C      Start actual code
211      DO 20 J=1,NJ
212      DO 20 I=1,N
213 20 C(I,J)=0.0
214      DO 21 J=1,NJ
215      DO 21 K=1,2
216      C1(K,J)=0.0
217      C2(K,J)=0.0

```

```

218      C3(K,J)=0.0
219      C4(K,J)=0.0
220      C5(K,J)=0.0
221      C6(K,J)=0.0
222      C7(K,J)=0.0
223      C8(K,J)=0.0
224      C9(K,J)=0.0
225      C10(K,J)=0.0
226      C11(K,J)=0.0
227      C12(K,J)=0.0
228      C13(K,J)=0.0
229      C14(K,J)=0.0
230      RXN1(K,J)=0.0
231      RXN2(K,J)=0.0
232      RXN3(K,J)=0.0
233      RXN4(K,J)=0.0
234      21 RXN5(K,J)=0.0
235      JCOUNT=0
236      TOL=1.E-10*N*NJ/100000000
237      22 JCOUNT=JCOUNT+1
238      AMP=0.0
239      J=0
240      DO 23 I=1,N
241      DO 23 K=1,N
242      Y(I,K)=0.0
243      23 X(I,K)=0.0
244      24 J=J+1
245      DO 25 I=1,N
246      G(I)=0.0
247      DO 25 K=1,N
248      A(I,K)=0.0
249      B(I,K)=0.0
250      25 D(I,K)=0.0
251
252      IF (J.EQ.1) CALL BC1(J)
253      IF (J.GT.1 .AND. J.LT.KJ) CALL REACTION(J)
254      IF (J.EQ.KJ) CALL COUPLER1(J)
255      IF (J.GT.KJ .AND. J.LT.IJ) CALL INNER(J)
256      IF (J.EQ.IJ) CALL COUPLER2(J)
257      IF (J.GT.IJ .AND. J.LT.NJ) CALL OUTER(J)
258      IF (J.EQ.NJ) CALL BCNJ(J)
259      CALL BAND(J)
260
261      AMP=DABS(G(1))+DABS(G(2))+DABS(G(3))+DABS(G(4))+DABS(G(5))
262      1 +DABS(G(6))+DABS(G(7))+DABS(G(8))+DABS(G(9))+DABS(G(10))
263      2 +DABS(G(11))+DABS(G(12))+DABS(G(13))+DABS(G(14))
264      3 +DABS(G(15))+DABS(G(16))+DABS(G(17))+DABS(G(18))
265      4 +DABS(G(19))+DABS(G(20))+DABS(G(21))+DABS(G(22))
266      5 +DABS(G(23))+DABS(G(24))+DABS(G(25))+DABS(G(26))
267      6 +DABS(G(27))+DABS(G(28))+DABS(G(29))+DABS(G(30))
268      2 +DABS(G(31))+DABS(G(32))+DABS(G(33))+DABS(G(34))
269      3 +DABS(G(35))+DABS(G(36))+DABS(G(37))+DABS(G(38))
270
271      IF (J.LT.NJ) GO TO 24
272 C      PRINT *, 'ERROR=' , AMP
273
274      DO 16 K=1,NJ
275      DO 16 I=1,2

```

```

276 C1(I ,K)=C1(I ,K)+C(I ,K)
277 C2(I ,K)=C2(I ,K)+C(I+2,K)
278 C3(I ,K)=C3(I ,K)+C(I+4,K)
279 C4(I ,K)=C4(I ,K)+C(I+6,K)
280 C5(I ,K)=C5(I ,K)+C(I+8,K)
281 C6(I ,K)=C6(I ,K)+C(I+10,K)
282 C7(I ,K)=C7(I ,K)+C(I+12,K)
283 C8(I ,K)=C8(I ,K)+C(I+14,K)
284 C9(I ,K)=C9(I ,K)+C(I+16,K)
285 C10(I ,K)=C10(I ,K)+C(I+18,K)
286 C11(I ,K)=C11(I ,K)+C(I+20,K)
287 C12(I ,K)=C12(I ,K)+C(I+22,K)
288 C13(I ,K)=C13(I ,K)+C(I+24,K)
289 C14(I ,K)=C14(I ,K)+C(I+26,K)
290 RXN1(I ,K)=RXN1(I ,K)+C(I+28,K)
291 RXN2(I ,K)=RXN2(I ,K)+C(I+30,K)
292 RXN3(I ,K)=RXN3(I ,K)+C(I+32,K)
293 RXN4(I ,K)=RXN4(I ,K)+C(I+34,K)
294 RXN5(I ,K)=RXN5(I ,K)+C(I+36,K)
295 16 CONTINUE
296
297 WRITE(14 ,302) (JCOUNT)
298
299 IF (DABS(AMP) .LT .DABS(TOL)) GO TO 15
300
301 IF (JCOUNT.LE.40) GO TO 22
302 print 102
303
304 15 CONTINUE
305 C PRINT *, 'JCOUNT=' ,JCOUNT
306
307 PRINT *, 'nf1=' , nf
308
309 DO 18 I=1,2
310 DO 18 J=1,NJ
311 BIG=C6(I ,J)
312 BIG2=1.0E-40
313 18 IF (ABS(BIG) .LE. BIG2) C6(I ,J)=0.0
314 C DO 26 I=1,2
315 C DO 26 J=1,NJ
316 C BIG2=1.0E-40
317 C IF (ABS(C5(I ,J)) .LE. BIG2) C5(I ,J)=0.0
318 C 26 IF (ABS(C10(I ,J)) .LE. BIG2) C10(I ,J)=0.0
319 WRITE(13 ,335) (C1(1 ,J) ,C1(2 ,J) ,C2(1 ,J) ,C2(2 ,J) ,C3(1 ,J) ,C3(2 ,J) ,
320 1 C4(1 ,J) ,C4(2 ,J) ,C5(1 ,J) ,C5(2 ,J) ,C6(1 ,J) ,C6(2 ,J) ,C7(1 ,J) ,
321 2 C7(2 ,J) ,C8(1 ,J) ,C8(2 ,J) ,
322 3 C9(1 ,J) ,C9(2 ,J) ,C10(1 ,J) ,C10(2 ,J) ,C11(1 ,J) ,C11(2 ,J) ,
323 4 C12(1 ,J) ,C12(2 ,J) ,C13(1 ,J) ,C13(2 ,J) ,C14(1 ,J) ,C14(2 ,J) ,
324 5 RXN1(1 ,J) ,RXN1(2 ,J) ,RXN2(1 ,J) ,RXN2(2 ,J) ,
325 6 RXN3(1 ,J) ,RXN3(2 ,J) ,RXN4(1 ,J) ,RXN4(2 ,J) ,
326 7 RXN5(1 ,J) ,RXN5(2 ,J) ,J=1,NJ)
327
328 DO 19 J=1,NJ
329 CH2O2(2*nf-1,J)=C6(1 ,J)
330 CH2O2(2*nf ,J)=C6(2 ,J)
331 CO2(2*nf-1,J)=C5(1 ,J)
332 CO2(2*nf ,J)=C5(2 ,J)
333 CH(2*nf-1,J)=C10(1 ,J)

```

```

334      19 CH(2*nf,J)=C10(2,J)
335
336 C      for some reason nf is one greater then necessary
337      PRINT *, 'nf2=' , nf
338
339 C      DO 17 I=1,2*nf-2
340      nf=nf-1
341      DO 17 J=1,NJ
342      WRITE(19,336) (CO2(I,J), I=1,2*nf)
343      WRITE(15,336) (CH2O2(I,J), I=1,2*nf)
344      17 WRITE(20,336) (CH(I,J), I=1,2*nf)
345
346      338 FORMAT (I5)
347      write (16,338) nf
348
349 C      PRINT *, 'DIFF(6)=' , DIFF(6)
350
351      END PROGRAM CONVDIFFOSCILLATING
352
353      SUBROUTINE BC1(J)
354      IMPLICIT DOUBLE PRECISION (A-H, O-Z)
355      COMMON/BAT/ A(38,38),B(38,38),C(38,10001),D(38,77),G(38),
356      1 X(38,38),Y(38,38)
357      COMMON/NST/ N, NJ
358      COMMON/VAR/ CONCSS(14,10001),RXNSS(7,10001)
359      COMMON/VARR/ COEFFMT(13),HHH, KJ
360      COMMON/CON/ C1(2,10001),C2(2,10001),C3(2,10001),C4(2,10001),
361      1 C5(2,10001),C6(2,10001),C7(2,10001),C8(2,10001),C9(2,10001),
362      2 C10(2,10001),C11(2,10001),C12(2,10001),C13(2,10001),
363      2 C14(2,10001),RXN1(2,10001),RXN2(2,10001),RXN3(2,10001),
364      3 RXN4(2,10001),RXN5(2,10001)
365      COMMON/RTE/ ratef1, equilib1, ratef2, ratef3, equilib3, ratef4, ratef5,
366      1 equilib5, ratef6, equilib6, equilib7, equilib8, equilib9
367      COMMON/OTH/ H,EBIG,HH,IJ
368      COMMON/POR/ DGOX(17),DGLM(17),DBULK(17)
369      COMMON/BCI/ FLUXF,FLUXB,FLUXR,FLUXH,omega
370      COMMON/BUL/ CBULK(13),PARH2O2,PAR02,PARGLUCOSE,PARION,SOLO2,JCOUNT
371      COMMON/DELT/ DELTA1, DELTA2, FREQ(400),CH2O2(1000,10001),
372      1 CO2(1000,10001),CH(1000,10001)
373      COMMON/POT/ VTILDE
374
375
376      301 FORMAT (5x,'J=' I5, 38E15.6E3)
377
378 C      BOUNDARY CONDITION AT THE ELECTRODE, J=1
379 C      For beta-Glucose, being consumed only
380      G(1)=omega*(3.*C1(2,J)+C1(2,J+1))/4.
381      1 +2.*DGOX(1)*(C1(1,J+1)-C1(1,J))/HHH**2.
382      2 -(3.*RXN1(1,J)+RXN1(1,J+1))/4.+(3.*RXN5(1,J)+RXN5(1,J+1))/4.
383      B(1,1)=+2.*DGOX(1)/HHH**2.
384      D(1,1)=-2.*DGOX(1)/HHH**2.
385      B(1,2)=-omega*(3./4.)
386      D(1,2)=-omega*(1./4.)
387      B(1,29)=+3./4.
388      D(1,29)=+1./4.
389      B(1,37)=-3./4.
390      D(1,37)=-1./4.
391

```

```

392 G(2)==-omega*(3.*C1(1,J)+C1(1,J+1))/4.
393 1 +2.*DGOX(1)*(C1(2,J+1)-C1(2,J))/HHH**2.
394 2 -(3.*RXN1(2,J)+RXN1(2,J+1))/4.+ (3.*RXN5(2,J)+RXN5(2,J+1))/4.
395 B(2,2)=+2.*DGOX(1)/HHH**2.
396 D(2,2)=-2.*DGOX(1)/HHH**2.
397 B(2,1)=omega*(3./4.)
398 D(2,1)=omega*(1./4.)
399 B(2,30)=+3./4.
400 D(2,30)=+1./4.
401 B(2,38)=-3./4.
402 D(2,38)=-1./4.
403
404 C For GOx and H+GOx enzyme,
405 G(3)=omega*(3.*C2(2,J)+C2(2,J+1))/4.
406 1 +omega*(3.*C13(2,J)+C13(2,J+1))/4.
407 2 -(3.*RXN1(1,J)+RXN1(1,J+1))/4.
408 3 +(3.*RXN4(1,J)+RXN4(1,J+1))/4.
409 B(3,4)==-omega*(3./4.)
410 D(3,4)==-omega*(1./4.)
411 B(3,26)==-omega*(3./4.)
412 D(3,26)==-omega*(1./4.)
413 B(3,29)=+3./4.
414 D(3,29)=+1./4.
415 B(3,35)=-3./4.
416 D(3,35)=-1./4.
417
418 G(4)==-omega*(3.*C2(1,J)+C2(1,J+1))/4.
419 1 -omega*(3.*C13(1,J)+C13(1,J+1))/4.
420 2 -(3.*RXN1(2,J)+RXN1(2,J+1))/4.
421 3 +(3.*RXN4(2,J)+RXN4(2,J+1))/4.
422 B(4,3)=omega*(3./4.)
423 D(4,3)=omega*(1./4.)
424 B(4,25)=omega*(3./4.)
425 D(4,25)=omega*(1./4.)
426 B(4,30)=+3./4.
427 D(4,30)=+1./4.
428 B(4,36)=-3./4.
429 D(4,36)=-1./4.
430
431 C For flux of Gluconic Acid and Gluconate ion ,
432 G(5)=omega*(3.*C3(2,J)+C3(2,J+1))/4.
433 1 +2.*DGOX(3)*(C3(1,J+1)-C3(1,J))/HHH**2.
434 2 +omega*(3.*C12(2,J)+C12(2,J+1))/4.
435 3 +2.*DGOX(11)*(C12(1,J+1)-C12(1,J))/HHH**2.
436 4 +(3.*RXN2(1,J)+RXN2(1,J+1))/4.
437 B(5,5)=+2.*DGOX(3)/HHH**2.
438 D(5,5)=-2.*DGOX(3)/HHH**2.
439 B(5,6)==-omega*(3./4.)
440 D(5,6)==-omega*(1./4.)
441 B(5,23)=+2.*DGOX(11)/HHH**2.
442 D(5,23)=-2.*DGOX(11)/HHH**2.
443 B(5,24)==-omega*(3./4.)
444 D(5,24)==-omega*(1./4.)
445 B(5,31)=-3./4.
446 D(5,31)=-1./4.
447
448 G(6)==-omega*(3.*C3(1,J)+C3(1,J+1))/4.
449 1 +2.*DGOX(3)*(C3(2,J+1)-C3(2,J))/HHH**2.

```

```

450      2 -omega *(3.*C12(1,J)+C12(1,J+1))/4.
451      3 +2.*DGOX(11)*(C12(2,J+1)-C12(2,J))/HHH**2.
452      4 +(3.*RXN2(2,J)+RXN2(2,J+1))/4.
453      B(6,6)=+2.*DGOX(3)/HHH**2.
454      D(6,6)=-2.*DGOX(3)/HHH**2.
455      B(6,5)=omega *(3./4.)
456      D(6,5)=omega *(1./4.)
457      B(6,24)=+2.*DGOX(11)/HHH**2.
458      D(6,24)=-2.*DGOX(11)/HHH**2.
459      B(6,23)=omega *(3./4.)
460      D(6,23)=omega *(1./4.)
461      B(6,32)=-3./4.
462      D(6,32)=-1./4.
463
464 C   For GOx2 and GOx-(red.) enzyme complex ,
465      G(7)=omega *(3.*C4(2,J)+C4(2,J+1))/4.
466      1 +omega *(3.*C14(2,J)+C14(2,J+1))/4.
467      2 +(3.*RXN2(1,J)+RXN2(1,J+1))/4.
468      3 -(3.*RXN3(1,J)+RXN3(1,J+1))/4.
469      B(7,8)=-omega *(3./4.)
470      D(7,8)=-omega *(1./4.)
471      B(7,28)=-omega *(3./4.)
472      D(7,28)=-omega *(1./4.)
473      B(7,31)=-3./4.
474      D(7,31)=-1./4.
475      B(7,33)=+3./4.
476      D(7,33)=+1./4.
477
478      G(8)=-omega *(3.*C4(1,J)+C4(1,J+1))/4.
479      1 -omega *(3.*C14(1,J)+C14(1,J+1))/4.
480      2 +(3.*RXN2(2,J)+RXN2(2,J+1))/4.
481      3 -(3.*RXN3(2,J)+RXN3(2,J+1))/4.
482      B(8,7)=omega *(3./4.)
483      D(8,7)=omega *(1./4.)
484      B(8,27)=omega *(3./4.)
485      D(8,27)=omega *(1./4.)
486      B(8,32)=-3./4.
487      D(8,32)=-1./4.
488      B(8,34)=+3./4.
489      D(8,34)=+1./4.
490
491 C   For O2 and H2O2,
492      G(9)=+(HHH/2.)*omega *(3.*C5(2,J)+C5(2,J+1))*(1./4.)
493      1 +(DGOX(5)/HHH)*(C5(1,J+1)-C5(1,J))
494      2 -(HHH/2.)*(3.*RXN3(1,J)+RXN3(1,J+1))*(1./4.)
495      3 +(HHH/2.)*omega *(3.*C6(2,J)+C6(2,J+1))*(1./4.)
496      4 +(DGOX(6)/HHH)*(C6(1,J+1)-C6(1,J))
497      5 +FLUXR*(CONCSS(10,J)**2.)*CONCSS(6,J)*BB2*VTILDE
498      6 -FLUXR*(CONCSS(10,J)**2.)*C6(1,J)
499      7 -2.*FLUXR*CONCSS(10,J)*CONCSS(6,J)*C10(1,J)
500      8 +(HHH/2.)*(3.*RXN4(1,J)+RXN4(1,J+1))*(1./4.)
501      B(9,9)=DGOX(5)/HHH
502      D(9,9)=-DGOX(5)/HHH
503      B(9,10)=-(HHH/2.)*omega *(3./4.)
504      D(9,10)=-(HHH/2.)*omega *(1./4.)
505      B(9,33)=(HHH/2.)*(3./4.)
506      D(9,33)=(HHH/2.)*(1./4.)
507      B(9,11)=DGOX(6)/HHH+FLUXR*(CONCSS(10,J)**2.)

```

```

508 D(9,11)=-DGOX(6)/HHH
509 B(9,12)=-(HHH/2.)*omega*(3./4.)
510 D(9,12)=-(HHH/2.)*omega*(1./4.)
511 B(9,19)=2.*FLUXR*CONCSS(10,J)*CONCSS(6,J)
512 B(9,35)=-(HHH/2.)*(3./4.)
513 D(9,35)=-(HHH/2.)*(1./4.)
514
515 G(10)=-(HHH/2.)*omega*(3.*C5(1,J)+C5(1,J+1))*(1./4.)
516 1 +(DGOX(5)/HHH)*(C5(2,J+1)-C5(2,J))
517 2 -(HHH/2.)*(3.*RXN3(2,J)+RXN3(2,J+1))*(1./4.)
518 3 -(HHH/2.)*omega*(3.*C6(1,J)+C6(1,J+1))*(1./4.)
519 4 +(DGOX(6)/HHH)*(C6(2,J+1)-C6(2,J))
520 5 -FLUXR*(CONCSS(10,J)**2.)*C6(2,J)
521 6 -2.*FLUXR*CONCSS(10,J)*CONCSS(6,J)*C10(2,J)
522 7 +(HHH/2.)*(3.*RXN4(2,J)+RXN4(2,J+1))*(1./4.)
523 B(10,9)=(HHH/2.)*omega*(3./4.)
524 D(10,9)=(HHH/2.)*omega*(1./4.)
525 B(10,10)=DGOX(5)/HHH
526 D(10,10)=-DGOX(5)/HHH
527 B(10,34)=(HHH/2.)*(3./4.)
528 D(10,34)=(HHH/2.)*(1./4.)
529 B(10,12)=DGOX(6)/HHH+FLUXR*(CONCSS(10,J)**2.)
530 D(10,12)=-DGOX(6)/HHH
531 B(10,11)=(HHH/2.)*omega*(3./4.)
532 D(10,11)=(HHH/2.)*omega*(1./4.)
533 B(10,20)=2.*FLUXR*CONCSS(10,J)*CONCSS(6,J)
534 B(10,36)=-(HHH/2.)*(3./4.)
535 D(10,36)=-(HHH/2.)*(1./4.)
536
537 C For H2O2, reacting species
538 G(11)=1.-C6(1,J)
539 B(11,11)=1.
540
541 G(12)=C6(2,J)
542 B(12,12)=-1.
543
544 C For CX-GOx2, enzyme
545 G(13)=omega*(3.*C7(2,J)+C7(2,J+1))/4.
546 1 +(3.*RXN1(1,J)+RXN1(1,J+1))/4.
547 2 -(3.*RXN2(1,J)+RXN2(1,J+1))/4.
548 B(13,14)=-omega*(3./4.)
549 D(13,14)=-omega*(1./4.)
550 B(13,29)=-3./4.
551 D(13,29)=-1./4.
552 B(13,31)=+3./4.
553 D(13,31)=+1./4.
554
555 G(14)=-omega*(3.*C7(1,J)+C7(1,J+1))/4.
556 1 +(3.*RXN1(2,J)+RXN1(2,J+1))/4.
557 2 -(3.*RXN2(2,J)+RXN2(2,J+1))/4.
558 B(14,13)=omega*(3./4.)
559 D(14,13)=omega*(1./4.)
560 B(14,30)=-3./4.
561 D(14,30)=-1./4.
562 B(14,32)=+3./4.
563 D(14,32)=+1./4.
564
565 C For CX-GOx, enzyme

```

```

566 G(15)=omega*(3.*C8(2,J)+C8(2,J+1))/4.
567 1 +(3.*RXN3(1,J)+RXN3(1,J+1))/4.
568 2 -(3.*RXN4(1,J)+RXN4(1,J+1))/4.
569 B(15,16)=-omega*(3./4.)
570 D(15,16)=-omega*(1./4.)
571 B(15,33)=-3./4.
572 D(15,33)=-1./4.
573 B(15,35)=+3./4.
574 D(15,35)=+1./4.
575
576 G(16)=-omega*(3.*C8(1,J)+C8(1,J+1))/4.
577 1 +(3.*RXN3(2,J)+RXN3(2,J+1))/4.
578 2 -(3.*RXN4(2,J)+RXN4(2,J+1))/4.
579 B(16,15)=omega*(3./4.)
580 D(16,15)=omega*(1./4.)
581 B(16,34)=-3./4.
582 D(16,34)=-1./4.
583 B(16,36)=+3./4.
584 D(16,36)=+1./4.
585
586 C For alpha-glucose,
587 G(17)=omega*(3.*C9(2,J)+C9(2,J+1))/4.
588 1 +2.*DGOX(1)*(C9(1,J+1)-C9(1,J))/HHH**2.
589 2 -(3.*RXN5(1,J)+RXN5(1,J+1))/4.
590 B(17,17)=+2.*DGOX(1)/HHH**2.
591 D(17,17)=-2.*DGOX(1)/HHH**2.
592 B(17,18)=-omega*(3./4.)
593 D(17,18)=-omega*(1./4.)
594 B(17,37)=+3./4.
595 D(17,37)=+1./4.
596
597
598 G(18)=-omega*(3.*C9(1,J)+C9(1,J+1))/4.
599 1 +2.*DGOX(1)*(C9(2,J+1)-C9(2,J))/HHH**2.
600 2 -(3.*RXN5(2,J)+RXN5(2,J+1))/4.
601 B(18,18)=+2.*DGOX(1)/HHH**2.
602 D(18,18)=-2.*DGOX(1)/HHH**2.
603 B(18,17)=omega*(3./4.)
604 D(18,17)=omega*(1./4.)
605 B(18,38)=+3./4.
606 D(18,38)=+1./4.
607
608 C For H+ ions , H2O2, OH- ions , gluconate ions and complex enzyme
609 G(19)=-(HHH/2.)*omega*(3.*C11(2,J)+C11(2,J+1))*(1./4.)
610 1 +(HHH/2.)*omega*(3.*C10(2,J)+C10(2,J+1))*(1./4.)
611 2 +(DGOX(9)/HHH)*(C10(1,J+1)-C10(1,J))
612 3 -(DGOX(10)/HHH)*(C11(1,J+1)-C11(1,J))
613 4 +2.*(HHH/2.)*omega*(3.*C6(2,J)+C6(2,J+1))*(1./4.)
614 5 +2.*(DGOX(6)/HHH)*(C6(1,J+1)-C6(1,J))
615 6 +4.*FLUXR*(CONCSS(10,J)**2.)*CONCSS(6,J)*BB2*VTILDE
616 7 -4.*FLUXR*(CONCSS(10,J)**2.)*C6(1,J)
617 8 -4.*2.*FLUXR*CONCSS(10,J)*CONCSS(6,J)*C10(1,J)
618 1 +2.*FLUXH*(CONCSS(10,J)**2.)*BBH*VTILDE
619 2 -4.*FLUXH*CONCSS(10,J)*C10(1,J)
620 3 +2.*(HHH/2.)*(3.*RXN4(1,J)+RXN4(1,J+1))*(1./4.)
621 4 -(HHH/2.)*omega*(3.*C12(2,J)+C12(2,J+1))*(1./4.)
622 5 -(DGOX(11)/HHH)*(C12(1,J+1)-C12(1,J))
623 6 +(HHH/2.)*omega*(3.*C13(2,J)+C13(2,J+1))*(1./4.)

```

```

624      7      -(HHH/2.)*omega*(3.*C14(2,J)+C14(2,J+1))*(1./4.)
625
626      B(19,11)=2.*DGOX(6)/HHH+4.*FLUXR*(CONCSS(10,J)**2.)
627      D(19,11)=-2.*DGOX(6)/HHH
628      B(19,12)=-2.*HHH/2.*omega*(3./4.)
629      D(19,12)=-2.*HHH/2.*omega*(1./4.)
630      B(19,19)=DGOX(9)/HHH+4.*2.*FLUXR*CONCSS(10,J)*CONCSS(6,J)
631          +4.*FLUXH*CONCSS(10,J)
632      D(19,19)=-DGOX(9)/HHH
633      B(19,20)=-(HHH/2.)*omega*(3./4.)
634      D(19,20)=-(HHH/2.)*omega*(1./4.)
635      B(19,21)=-DGOX(10)/HHH
636      D(19,21)=DGOX(10)/HHH
637      B(19,22)=(HHH/2.)*omega*(3./4.)
638      D(19,22)=(HHH/2.)*omega*(1./4.)
639      B(19,23)=-DGOX(11)/HHH
640      D(19,23)=DGOX(11)/HHH
641      B(19,24)=(HHH/2.)*omega*(3./4.)
642      D(19,24)=(HHH/2.)*omega*(1./4.)
643      B(19,26)=-(HHH/2.)*omega*(3./4.)
644      D(19,26)=-(HHH/2.)*omega*(1./4.)
645      B(19,28)=(HHH/2.)*omega*(3./4.)
646      D(19,28)=(HHH/2.)*omega*(1./4.)
647      B(19,35)=-2.*HHH/2.*omega*(3./4.)
648      D(19,35)=-2.*HHH/2.*omega*(1./4.)
649
650
651      G(20)=(HHH/2.)*omega*(3.*C11(1,J)+C11(1,J+1))*(1./4.)
652          -(HHH/2.)*omega*(3.*C10(1,J)+C10(1,J+1))*(1./4.)
653          +(DGOX(9)/HHH)*(C10(2,J+1)-C10(2,J))
654          -(DGOX(10)/HHH)*(C11(2,J+1)-C11(2,J))
655          -2.*HHH/2.*omega*(3.*C6(1,J)+C6(1,J+1))*(1./4.)
656          +2.*DGOX(6)/HHH*(C6(2,J+1)-C6(2,J))
657          -4.*FLUXR*(CONCSS(10,J)**2.)*C6(2,J)
658          -4.*2.*FLUXR*CONCSS(10,J)*CONCSS(6,J)*C10(2,J)
659          -4.*FLUXH*CONCSS(10,J)*C10(2,J)
660          +2.*HHH/2.*omega*(3.*RXN4(2,J)+RXN4(2,J+1))*(1./4.)
661          +(HHH/2.)*omega*(3.*C12(1,J)+C12(1,J+1))*(1./4.)
662          -(DGOX(11)/HHH)*(C12(2,J+1)-C12(2,J))
663          -(HHH/2.)*omega*(3.*C13(1,J)+C13(1,J+1))*(1./4.)
664          +(HHH/2.)*omega*(3.*C14(1,J)+C14(1,J+1))*(1./4.)
665
666      B(20,12)=2.*DGOX(6)/HHH+4.*FLUXR*(CONCSS(10,J)**2.)
667      D(20,12)=-2.*DGOX(6)/HHH
668      B(20,11)=2.*HHH/2.*omega*(3./4.)
669      D(20,11)=2.*HHH/2.*omega*(1./4.)
670      B(20,20)=DGOX(9)/HHH+4.*2.*FLUXR*CONCSS(10,J)*CONCSS(6,J)
671          +4.*FLUXH*CONCSS(10,J)
672      D(20,20)=-DGOX(9)/HHH
673      B(20,19)=(HHH/2.)*omega*(3./4.)
674      D(20,19)=(HHH/2.)*omega*(1./4.)
675      B(20,22)=-DGOX(10)/HHH
676      D(20,22)=DGOX(10)/HHH
677      B(20,21)=-(HHH/2.)*omega*(3./4.)
678      D(20,21)=-(HHH/2.)*omega*(1./4.)
679      B(20,24)=-DGOX(11)/HHH
680      D(20,24)=DGOX(11)/HHH
681      B(20,23)=-(HHH/2.)*omega*(3./4.)

```

```

682 D(20,23)=-(HHH/2.)*omega*(1./4.)
683 B(20,25)=(HHH/2.)*omega*(3./4.)
684 D(20,25)=(HHH/2.)*omega*(1./4.)
685 B(20,27)=-(HHH/2.)*omega*(3./4.)
686 D(20,27)=-(HHH/2.)*omega*(1./4.)
687 B(20,36)=-2.*(HHH/2.)*(3./4.)
688 D(20,36)=-2.*(HHH/2.)*(1./4.)
689 C For H+ and OH- ions equilibrium ,
690
691 G(21)=CONCSS(10,J)*C11(1,J)-CONCSS(11,J)*C10(1,J)
692
693 B(21,19)=CONCSS(11,J)
694 B(21,21)=CONCSS(10,J)
695
696 G(22)=CONCSS(10,J)*C11(2,J)-CONCSS(11,J)*C10(2,J)
697 B(22,20)=CONCSS(11,J)
698 B(22,22)=CONCSS(10,J)
699
700 C For gluconic acid dissociation ,
701 G(23)=equilib7*C3(1,J)-CONCSS(10,J)*C12(1,J)-CONCSS(12,J)*C10(1,J)
702
703 B(23,5)=-equilib7
704 B(23,23)=CONCSS(10,J)
705 B(23,19)=CONCSS(12,J)
706
707 G(24)=equilib7*C3(2,J)-CONCSS(10,J)*C12(2,J)-CONCSS(12,J)*C10(2,J)
708 B(24,6)=-equilib7
709 B(24,24)=CONCSS(10,J)
710 B(24,20)=CONCSS(12,J)
711
712 C For H+GOx dissociation into H+ and GOx(ox.) ,
713 G(25)=equilib8*C13(1,J)-CONCSS(10,J)*C2(1,J)-CONCSS(2,J)*C10(1,J)
714 B(25,25)=-equilib8
715 B(25,3)=CONCSS(10,J)
716 B(25,19)=CONCSS(2,J)
717
718 G(26)=equilib8*C13(2,J)-CONCSS(10,J)*C2(2,J)-CONCSS(2,J)*C10(2,J)
719 B(26,26)=-equilib8
720 B(26,4)=CONCSS(10,J)
721 B(26,20)=CONCSS(2,J)
722
723 C For GOx(red.) dissociation into H+ and GOx-(red.) ,
724 G(27)=equilib9*C4(1,J)-CONCSS(10,J)*C14(1,J)-CONCSS(14,J)*C10(1,J)
725 B(27,7)=-equilib9
726 B(27,27)=CONCSS(10,J)
727 B(27,19)=CONCSS(14,J)
728
729 G(28)=equilib9*C4(2,J)-CONCSS(10,J)*C14(2,J)-CONCSS(14,J)*C10(2,J)
730 B(28,8)=-equilib9
731 B(28,28)=CONCSS(10,J)
732 B(28,20)=CONCSS(14,J)
733
734 C REACTION1
735 G(29)=-RXN1(1,J)+ratef1*CONCSS(2,J)*C1(1,J)
736 1 +ratef1*CONCSS(1,J)*C2(1,J)
737 2 -C7(1,J)*ratef1/equilib1
738 B(29,1)=-ratef1*CONCSS(2,J)
739 B(29,3)=-ratef1*CONCSS(1,J)

```

```

740 B(29,13)=+ratef1/equilib1
741 B(29,29)=+1.
742
743 G(30)=-RXN1(2,J)+ratef1*CONCSS(2,J)*C1(2,J)
744 1 +ratef1*CONCSS(1,J)*C2(2,J)
745 2 -C7(2,J)*ratef1/equilib1
746 B(30,2)=-ratef1*CONCSS(2,J)
747 B(30,4)=-ratef1*CONCSS(1,J)
748 B(30,14)=+ratef1/equilib1
749 B(30,30)=+1.
750
751 C REACTION2
752 G(31)=-RXN2(1,J)+ratef2*C7(1,J)
753 B(31,13)=-ratef2
754 B(31,31)=+1.
755
756 G(32)=-RXN2(2,J)+ratef2*C7(2,J)
757 B(32,14)=-ratef2
758 B(32,32)=+1.
759
760 C REACTION3
761 G(33)=-RXN3(1,J)+ratef3*CONCSS(4,J)*C5(1,J)
762 1 +ratef3*CONCSS(5,J)*C4(1,J)
763 2 -C8(1,J)*ratef3/equilib3
764 B(33,7)=-ratef3*CONCSS(5,J)
765 B(33,9)=-ratef3*CONCSS(4,J)
766 B(33,15)=+ratef3/equilib3
767 B(33,33)=+1.
768
769 G(34)=-RXN3(2,J)+ratef3*CONCSS(4,J)*C5(2,J)
770 1 +ratef3*CONCSS(5,J)*C4(2,J)
771 2 -C8(2,J)*ratef3/equilib3
772 B(34,8)=-ratef3*CONCSS(5,J)
773 B(34,10)=-ratef3*CONCSS(4,J)
774 B(34,16)=+ratef3/equilib3
775 B(34,34)=+1.
776
777 C REACTION4
778 G(35)=-RXN4(1,J)+ratef4*C8(1,J)
779 B(35,15)=-ratef4
780 B(35,35)=+1.
781
782 G(36)=-RXN4(2,J)+ratef4*C8(2,J)
783 B(36,16)=-ratef4
784 B(36,36)=+1.
785
786 C REACTION5
787 G(37)=-RXN5(1,J)+ratef5*C9(1,J)-ratef5/equilib5*C1(1,J)
788 B(37,17)=-ratef5
789 B(37,1)=ratef5/equilib5
790 B(37,37)=+1.
791
792 G(38)=-RXN5(2,J)+ratef5*C9(2,J)-ratef5/equilib5*C1(2,J)
793 B(38,18)=-ratef5
794 B(38,2)=ratef5/equilib5
795 B(38,38)=+1.
796
797 WRITE(14,301) J, (G(K),K=1,N)

```

```

798
799      RETURN
800      END
801      SUBROUTINE REACTION(J)
802      IMPLICIT DOUBLE PRECISION (A-H, O-Z)
803      COMMON/BAT/ A(38,38),B(38,38),C(38,10001),D(38,77),G(38),
804      1      X(38,38),Y(38,38)
805      COMMON/NST/ N, NJ
806      COMMON/VAR/ CONCSS(14,10001),RXNSS(7,10001)
807      COMMON/VARR/ COEFFMT(13),HHH, KJ
808      COMMON/CON/ C1(2,10001),C2(2,10001),C3(2,10001),C4(2,10001),
809      1      C5(2,10001),C6(2,10001),C7(2,10001),C8(2,10001),C9(2,10001),
810      2      C10(2,10001),C11(2,10001),C12(2,10001),C13(2,10001),
811      2      C14(2,10001),RXN1(2,10001),RXN2(2,10001),RXN3(2,10001),
812      3      RXN4(2,10001),RXN5(2,10001)
813      COMMON/RTE/ ratef1, equilib1, ratef2, ratef3, equilib3, ratef4, ratef5,
814      1      equilib5, ratef6, equilib6, equilib7, equilib8, equilib9
815      COMMON/OTH/ H, EBIG, HH, IJ
816      COMMON/POR/ DGOX(17),DGIM(17),DBULK(17)
817      COMMON/BCI/ FLUXF,FLUXB,FLUXR,FLUXH,omega
818      COMMON/BUL/ CBULK(13),PARH2O2,PAR02,PARGLUCOSE,PARION,SOLO2,JCOUNT
819      COMMON/DELT/ DELTA1, DELTA2, FREQ(400),CH2O2(1000,10001),
820      1      CO2(1000,10001),CH(1000,10001)
821      COMMON/POT/ VTILDE
822
823 301 FORMAT (5x, 'J=' I5, 38E15.6E3)
824
825 C   For BETA-Glucose, being consumed only
826 G(1)=omega*C1(2,J)
827 1      +DGOX(1)*(C1(1,J+1)-2.*C1(1,J)+C1(1,J-1))/HHH**2.
828 3      -RXN1(1,J)+RXN5(1,J)
829 B(1,1)=2.*DGOX(1)/HHH**2.
830 A(1,1)=-DGOX(1)/HHH**2.
831 D(1,1)=-DGOX(1)/HHH**2.
832 B(1,2)=-omega
833 B(1,29)=+1.
834 B(1,37)=-1.
835
836 G(2)=-omega*C1(1,J)
837 1      +DGOX(1)*(C1(2,J+1)-2.*C1(2,J)+C1(2,J-1))/HHH**2.
838 3      -RXN1(2,J)+RXN5(2,J)
839 B(2,2)=2.*DGOX(1)/HHH**2.
840 A(2,2)=-DGOX(1)/HHH**2.
841 D(2,2)=-DGOX(1)/HHH**2.
842 B(2,1)=omega
843 B(2,30)=+1.
844 B(2,38)=-1.
845
846 C   For GOx and H+GOx enzyme,
847 G(3)=omega*C2(2,J)+omega*C13(2,J)
848 1      -RXN1(1,J)
849 2      +RXN4(1,J)
850 B(3,4)=-omega
851 B(3,26)=-omega
852 B(3,29)=+1.
853 B(3,35)=-1.
854
855 G(4)=-omega*C2(1,J)-omega*C13(1,J)

```

```

856      1      -RXN1(2 ,J)
857      2      +RXN4(2 ,J)
858      B(4 ,3)=omega
859      B(4 ,25)=omega
860      B(4 ,30)=+1.
861      B(4 ,36)=-1.
862
863 C   For flux of Gluconic Acid and Gluconate ion ,
864      G(5)=omega*C3(2 ,J)
865      1      +DGOX(3)*(C3(1 ,J+1)-2.*C3(1 ,J)+C3(1 ,J-1))/HHH**2.
866      2      +omega*C12(2 ,J)
867      3      +DGOX(11)*(C12(1 ,J+1)-2.*C12(1 ,J)+C12(1 ,J-1))/HHH**2.
868      4      +RXN2(1 ,J)
869      B(5 ,5)=2.*DGOX(3)/HHH**2.
870      A(5 ,5)=-DGOX(3)/HHH**2.
871      D(5 ,5)=-DGOX(3)/HHH**2.
872      B(5 ,6)=-omega
873      B(5 ,23)=2.*DGOX(11)/HHH**2.
874      A(5 ,23)=-DGOX(11)/HHH**2.
875      D(5 ,23)=-DGOX(11)/HHH**2.
876      B(5 ,24)=-omega
877      B(5 ,31)=-1.
878
879      G(6)=-omega*C3(1 ,J)
880      1      +DGOX(3)*(C3(2 ,J+1)-2.*C3(2 ,J)+C3(2 ,J-1))/HHH**2.
881      2      -omega*C12(1 ,J)
882      3      +DGOX(11)*(C12(2 ,J+1)-2.*C12(2 ,J)+C12(2 ,J-1))/HHH**2.
883      4      +RXN2(2 ,J)
884      B(6 ,6)=2.*DGOX(3)/HHH**2.
885      A(6 ,6)=-DGOX(3)/HHH**2.
886      D(6 ,6)=-DGOX(3)/HHH**2.
887      B(6 ,5)=omega
888      B(6 ,24)=2.*DGOX(11)/HHH**2.
889      A(6 ,24)=-DGOX(11)/HHH**2.
890      D(6 ,24)=-DGOX(11)/HHH**2.
891      B(6 ,23)=omega
892      B(6 ,32)=-1.
893
894 C   For GOx2 and GOx-(red.) enzyme complex ,
895      G(7)=omega*C4(2 ,J)+omega*C14(2 ,J)
896      1      +RXN2(1 ,J)
897      2      -RXN3(1 ,J)
898      B(7 ,8)=-omega
899      B(7 ,28)=-omega
900      B(7 ,31)=-1.
901      B(7 ,33)=+1.
902
903      G(8)=-omega*C4(1 ,J)-omega*C14(1 ,J)
904      1      +RXN2(2 ,J)
905      2      -RXN3(2 ,J)
906      B(8 ,7)=omega
907      B(8 ,27)=omega
908      B(8 ,32)=-1.
909      B(8 ,34)=+1.
910
911 C   For O2, being consumed only
912      G(9)=omega*C5(2 ,J)
913      1      +DGOX(5)*(C5(1 ,J+1)-2.*C5(1 ,J)+C5(1 ,J-1))/HHH**2.

```

```

914      2      -RXN3(1,J)
915      B(9,9)=2.*DGOX(5)/HHH**2.
916      A(9,9)=-DGOX(5)/HHH**2.
917      D(9,9)=-DGOX(5)/HHH**2.
918      B(9,10)=-omega
919      B(9,33)=+1.
920
921      G(10)=-omega*C5(1,J)
922      +DGOX(5)*(C5(2,J+1)-2.*C5(2,J)+C5(2,J-1))/HHH**2.
923      2      -RXN3(2,J)
924      B(10,10)=2.*DGOX(5)/HHH**2.
925      A(10,10)=-DGOX(5)/HHH**2.
926      D(10,10)=-DGOX(5)/HHH**2.
927      B(10,9)=omega
928      B(10,34)=+1.
929
930 C   For H2O2, reacting species
931      G(11)=omega*C6(2,J)
932      1      +DGOX(6)*(C6(1,J+1)-2.*C6(1,J)+C6(1,J-1))/HHH**2.
933      3      +RXN4(1,J)
934      B(11,11)=2.*DGOX(6)/HHH**2.
935      A(11,11)=-DGOX(6)/HHH**2.
936      D(11,11)=-DGOX(6)/HHH**2.
937      B(11,12)=-omega
938      B(11,35)=-1.
939
940      G(12)=-omega*C6(1,J)
941      1      +DGOX(6)*(C6(2,J+1)-2.*C6(2,J)+C6(2,J-1))/HHH**2.
942      3      +RXN4(2,J)
943      B(12,12)=2.*DGOX(6)/HHH**2.
944      A(12,12)=-DGOX(6)/HHH**2.
945      D(12,12)=-DGOX(6)/HHH**2.
946      B(12,11)=omega
947      B(12,36)=-1.
948
949 C   For CX-GOx2, enzyme
950      G(13)=omega*C7(2,J)
951      1      +RXN1(1,J)
952      2      -RXN2(1,J)
953      B(13,14)=-omega
954      B(13,29)=-1.
955      B(13,31)=+1.
956
957      G(14)=-omega*C7(1,J)
958      1      +RXN1(2,J)
959      2      -RXN2(2,J)
960      B(14,13)=omega
961      B(14,30)=-1.
962      B(14,32)=+1.
963
964 C   For CX-GOx2, enzyme
965      G(15)=omega*C8(2,J)
966      1      +RXN3(1,J)
967      2      -RXN4(1,J)
968      B(15,16)=-omega
969      B(15,33)=-1.
970      B(15,35)=+1.
971

```

```

972 G(16)=-omega*C8(1,J)
973 1 +RXN3(2,J)
974 2 -RXN4(2,J)
975 B(16,15)=omega
976 B(16,34)=-1.
977 B(16,36)=+1.
978
979 C FOR ALPHA-GLUCOSE BEING CONSUMMED ONLY,
980 G(17)=omega*C9(2,J)
981 1 +DGOX(1)*(C9(1,J+1)-2.*C9(1,J)+C9(1,J-1))/HHH**2.
982 3 -RXN5(1,J)
983 B(17,17)=2.*DGOX(1)/HHH**2.
984 A(17,17)=-DGOX(1)/HHH**2.
985 D(17,17)=-DGOX(1)/HHH**2.
986 B(17,18)=-omega
987 B(17,37)=+1.
988
989 G(18)=-omega*C9(1,J)
990 1 +DGOX(1)*(C9(2,J+1)-2.*C9(2,J)+C9(2,J-1))/HHH**2.
991 3 -RXN5(2,J)
992 B(18,18)=2.*DGOX(1)/HHH**2.
993 A(18,18)=-DGOX(1)/HHH**2.
994 D(18,18)=-DGOX(1)/HHH**2.
995 B(18,17)=omega
996 B(18,38)=+1.
997
998 C For H+ ions , OH- ions , gluconate ions and complex enzyme
999 G(19)=omega*C10(2,J)-omega*C11(2,J)-omega*C12(2,J)+omega*C13(2,J)
1000 1 -omega*C14(2,J)
1001 2 +DGOX(9)*(C10(1,J+1)-2.*C10(1,J)+C10(1,J-1))/HHH**2.
1002 3 -DGOX(10)*(C11(1,J+1)-2.*C11(1,J)+C11(1,J-1))/HHH**2.
1003 4 -DGOX(11)*(C12(1,J+1)-2.*C12(1,J)+C12(1,J-1))/HHH**2.
1004 B(19,20)=-omega
1005 B(19,22)=omega
1006 B(19,24)=omega
1007 B(19,26)=-omega
1008 B(19,28)=omega
1009 B(19,19)=2.*DGOX(9)/HHH**2.
1010 A(19,19)=-DGOX(9)/HHH**2.
1011 D(19,19)=-DGOX(9)/HHH**2.
1012 B(19,21)=-2.*DGOX(10)/HHH**2.
1013 A(19,21)=DGOX(10)/HHH**2.
1014 D(19,21)=DGOX(10)/HHH**2.
1015 B(19,23)=-2.*DGOX(11)/HHH**2.
1016 A(19,23)=DGOX(11)/HHH**2.
1017 D(19,23)=DGOX(11)/HHH**2.
1018
1019 G(20)=-omega*C10(1,J)+omega*C11(1,J)+omega*C12(1,J)-omega*C13(1,J)
1020 1 +omega*C14(1,J)
1021 2 +DGOX(9)*(C10(2,J+1)-2.*C10(2,J)+C10(2,J-1))/HHH**2.
1022 3 -DGOX(10)*(C11(2,J+1)-2.*C11(2,J)+C11(2,J-1))/HHH**2.
1023 4 -DGOX(11)*(C12(2,J+1)-2.*C12(2,J)+C12(2,J-1))/HHH**2.
1024 B(20,19)=omega
1025 B(20,21)=-omega
1026 B(20,23)=-omega
1027 B(20,25)=omega
1028 B(20,27)=-omega
1029 B(20,20)=2.*DGOX(9)/HHH**2.

```

```

1030 A(20,20)=−DGOX(9)/HHH**2.
1031 D(20,20)=−DGOX(9)/HHH**2.
1032 B(20,22)=−2.*DGOX(10)/HHH**2.
1033 A(20,22)=DGOX(10)/HHH**2.
1034 D(20,22)=DGOX(10)/HHH**2.
1035 B(20,24)=−2.*DGOX(11)/HHH**2.
1036 A(20,24)=DGOX(11)/HHH**2.
1037 D(20,24)=DGOX(11)/HHH**2.
1038
1039 C For H+ and OH- ions equilibrium,
1040 G(21)=−CONCSS(10,J)*C11(1,J)−CONCSS(11,J)*C10(1,J)
1041
1042 B(21,19)=CONCSS(11,J)
1043 B(21,21)=CONCSS(10,J)
1044
1045 G(22)=−CONCSS(10,J)*C11(2,J)−CONCSS(11,J)*C10(2,J)
1046 B(22,20)=CONCSS(11,J)
1047 B(22,22)=CONCSS(10,J)
1048
1049 C For gluconic acid dissociation ,
1050 G(23)=equilib7*C3(1,J)−CONCSS(10,J)*C12(1,J)−CONCSS(12,J)*C10(1,J)
1051
1052 B(23,5)=−equilib7
1053 B(23,23)=CONCSS(10,J)
1054 B(23,19)=CONCSS(12,J)
1055
1056 G(24)=equilib7*C3(2,J)−CONCSS(10,J)*C12(2,J)−CONCSS(12,J)*C10(2,J)
1057 B(24,6)=−equilib7
1058 B(24,24)=CONCSS(10,J)
1059 B(24,20)=CONCSS(12,J)
1060
1061 C For H+GOx dissociation into H+ and GOx(ox.) ,
1062 G(25)=equilib8*C13(1,J)−CONCSS(10,J)*C2(1,J)−CONCSS(2,J)*C10(1,J)
1063 B(25,25)=−equilib8
1064 B(25,3)=CONCSS(10,J)
1065 B(25,19)=CONCSS(2,J)
1066
1067 G(26)=equilib8*C13(2,J)−CONCSS(10,J)*C2(2,J)−CONCSS(2,J)*C10(2,J)
1068 B(26,26)=−equilib8
1069 B(26,4)=CONCSS(10,J)
1070 B(26,20)=CONCSS(2,J)
1071
1072 C For GOx(red.) dissociation into H+ and GOx-(red.) ,
1073 G(27)=equilib9*C4(1,J)−CONCSS(10,J)*C14(1,J)−CONCSS(14,J)*C10(1,J)
1074 B(27,7)=−equilib9
1075 B(27,27)=CONCSS(10,J)
1076 B(27,19)=CONCSS(14,J)
1077
1078 G(28)=equilib9*C4(2,J)−CONCSS(10,J)*C14(2,J)−CONCSS(14,J)*C10(2,J)
1079 B(28,8)=−equilib9
1080 B(28,28)=CONCSS(10,J)
1081 B(28,20)=CONCSS(14,J)
1082
1083 C REACTION1
1084 G(29)=RXN1(1,J)+ratef1*CONCSS(2,J)*C1(1,J)
1085 1 +ratef1*CONCSS(1,J)*C2(1,J)
1086 2 −C7(1,J)*ratef1/equilib1
1087 B(29,1)=−ratef1*CONCSS(2,J)

```

```

1088 B(29,3)=-ratef1*CONCSS(1,J)
1089 B(29,13)=+ratef1/equilib1
1090 B(29,29)=+1.
1091
1092 G(30)=-RXN1(2,J)+ratef1*CONCSS(2,J)*C1(2,J)
1093 1 +ratef1*CONCSS(1,J)*C2(2,J)
1094 2 -C7(2,J)*ratef1/equilib1
1095 B(30,2)=-ratef1*CONCSS(2,J)
1096 B(30,4)=-ratef1*CONCSS(1,J)
1097 B(30,14)=+ratef1/equilib1
1098 B(30,30)=+1.
1099
1100 C REACTION2
1101 G(31)=-RXN2(1,J)+ratef2*C7(1,J)
1102 B(31,13)=-ratef2
1103 B(31,31)=+1.
1104
1105 G(32)=-RXN2(2,J)+ratef2*C7(2,J)
1106 B(32,14)=-ratef2
1107 B(32,32)=+1.
1108
1109 C REACTION3
1110 G(33)=-RXN3(1,J)+ratef3*CONCSS(4,J)*C5(1,J)
1111 1 +ratef3*CONCSS(5,J)*C4(1,J)
1112 2 -C8(1,J)*ratef3/equilib3
1113 B(33,7)=-ratef3*CONCSS(5,J)
1114 B(33,9)=-ratef3*CONCSS(4,J)
1115 B(33,15)=+ratef3/equilib3
1116 B(33,33)=+1.
1117
1118 G(34)=-RXN3(2,J)+ratef3*CONCSS(4,J)*C5(2,J)
1119 1 +ratef3*CONCSS(5,J)*C4(2,J)
1120 2 -C8(2,J)*ratef3/equilib3
1121 B(34,8)=-ratef3*CONCSS(5,J)
1122 B(34,10)=-ratef3*CONCSS(4,J)
1123 B(34,16)=+ratef3/equilib3
1124 B(34,34)=+1.
1125
1126 C REACTION4
1127 G(35)=-RXN4(1,J)+ratef4*C8(1,J)
1128 B(35,15)=-ratef4
1129 B(35,35)=+1.
1130
1131 G(36)=-RXN4(2,J)+ratef4*C8(2,J)
1132 B(36,16)=-ratef4
1133 B(36,36)=+1.
1134
1135 C REACTION5
1136 G(37)=-RXN5(1,J)+ratef5*C9(1,J)-ratef5/equilib5*C1(1,J)
1137 B(37,17)=-ratef5
1138 B(37,1)=ratef5/equilib5
1139 B(37,37)=+1.
1140
1141 G(38)=-RXN5(2,J)+ratef5*C9(2,J)-ratef5/equilib5*C1(2,J)
1142 B(38,18)=-ratef5
1143 B(38,2)=ratef5/equilib5
1144 B(38,38)=+1.
1145

```

```

1146
1147 c   SAVE G OUT DATA
1148 DO 11 I=2,13
1149 11 If (I.EQ.J) WRITE(14,301) J, (G(K),K=1,N)
1150 IF (J.EQ.IJ/2) THEN
1151 WRITE(14,301) J, (G(K),K=1,N)
1152 ELSE IF (J.EQ.(IJ-1)) THEN
1153 WRITE(14,301) J, (G(K),K=1,N)
1154 ELSE IF (J.EQ.(IJ-2)) THEN
1155 WRITE(14,301) J, (G(K),K=1,N)
1156 ELSE IF (J.EQ.(IJ-3)) THEN
1157 WRITE(14,301) J, (G(K),K=1,N)
1158 END IF
1159
1160 RETURN
1161 END
1162
1163 SUBROUTINE COUPLER1(J)
1164 IMPLICIT DOUBLE PRECISION (A-H, O-Z)
1165 COMMON/BAT/ A(38,38),B(38,38),C(38,10001),D(38,77),G(38),
1166 1 X(38,38),Y(38,38)
1167 COMMON/NST/ N, NJ
1168 COMMON/VAR/ CONCSS(14,10001),RXNSS(7,10001)
1169 COMMON/VARR/ COEFFMT(13),HHH, KJ
1170 COMMON/CON/ C1(2,10001),C2(2,10001),C3(2,10001),C4(2,10001),
1171 1 C5(2,10001),C6(2,10001),C7(2,10001),C8(2,10001),C9(2,10001),
1172 2 C10(2,10001),C11(2,10001),C12(2,10001),C13(2,10001),
1173 2 C14(2,10001),RXN1(2,10001),RXN2(2,10001),RXN3(2,10001),
1174 3 RXN4(2,10001),RXN5(2,10001)
1175 COMMON/RTE/ ratef1, equilib1, ratef2, ratef3, equilib3, ratef4, ratef5,
1176 1 equilib5, ratef6, equilib6, equilib7, equilib8, equilib9
1177 COMMON/OTH/ H,EBIG,HH,IJ
1178 COMMON/POR/ DGOX(17),DGLM(17),DBULK(17)
1179 COMMON/BCI/ FLUXF,FLUXB,FLUXR,FLUXH,omega
1180 COMMON/BUL/ CBULK(13),PARH2O2,PAR02,PARGLUCOSE,PARION,SOLO2,JCOUNT
1181 COMMON/DELT/ DELTA1, DELTA2, FREQ(400),CH2O2(1000,10001),
1182 1 CO2(1000,10001),CH(1000,10001)
1183 COMMON/POT/ VTILDE
1184
1185 301 FORMAT (5x, 'J=' 15, 38E15.6E3)
1186
1187 C   For beta-Glucose, being consumed only
1188 G(1)=HH/2.*omega*(C1(2,J+1)+3.*C1(2,J))/4.
1189 1 +HHH/2.*omega*(C1(2,J-1)+3.*C1(2,J))/4.
1190 2 +DGOX(1)*(C1(1,J+1)-C1(1,J))/HH
1191 3 -DGOX(1)*(C1(1,J)-C1(1,J-1))/HHH
1192 5 -(HH/2.)*(RXN1(1,J+1)+3.*RXN1(1,J))/4.
1193 6 -(HHH/2.)*(RXN1(1,J-1)+3.*RXN1(1,J))/4.
1194 7 +(HH/2.)*(RXN5(1,J+1)+3.*RXN5(1,J))/4.
1195 8 +(HHH/2.)*(RXN5(1,J-1)+3.*RXN5(1,J))/4.
1196 B(1,1)=DGOX(1)/HH+DGOX(1)/HHH
1197 D(1,1)=-DGOX(1)/HH
1198 A(1,1)=-DGOX(1)/HHH
1199 B(1,2)=-HHH/2.*omega*(3./4.)-HH/2.*omega*(3./4.)
1200 D(1,2)=-HH/2.*omega*(1./4.)
1201 A(1,2)=-HHH/2.*omega*(1./4.)
1202 B(1,29)=(HH/2.)*(3./4.)+(HHH/2.)*(3./4.)
1203 D(1,29)=(HH/2.)*(1./4.)

```

```

1204 A(1,29)=(HHH/2.)*(1./4.)
1205 B(1,37)=-(HH/2.)*(3./4.)-(HHH/2.)*(3./4.)
1206 D(1,37)=-(HH/2.)*(1./4.)
1207 A(1,37)=-(HHH/2.)*(1./4.)
1208
1209 G(2)=-HHH/2.*omega*(C1(1,J-1)+3.*C1(1,J))/4.
1210 1 -HH/2.*omega*(C1(1,J+1)+3.*C1(1,J))/4.
1211 2 +DGOX(1)*(C1(2,J+1)-C1(2,J))/HH
1212 3 -DGOX(1)*(C1(2,J)-C1(2,J-1))/HHH
1213 4 -(HH/2.)*(RXN1(2,J+1)+3.*RXN1(2,J))/4.
1214 5 -(HHH/2.)*(RXN1(2,J-1)+3.*RXN1(2,J))/4.
1215 6 +(HH/2.)*(RXN5(2,J+1)+3.*RXN5(2,J))/4.
1216 7 +(HHH/2.)*(RXN5(2,J-1)+3.*RXN5(2,J))/4.
1217 B(2,2)=DGOX(1)/HH+DGOX(1)/HHH
1218 D(2,2)=-DGOX(1)/HH
1219 A(2,2)=-DGOX(1)/HHH
1220 B(2,1)=+HHH/2.*omega*(3./4.)+HH/2.*omega*(3./4.)
1221 D(2,1)=+HH/2.*omega*(1./4.)
1222 A(2,1)=+HHH/2.*omega*(1./4.)
1223 B(2,30)=(HH/2.)*(3./4.)+(HHH/2.)*(3./4.)
1224 D(2,30)=(HH/2.)*(1./4.)
1225 A(2,30)=(HHH/2.)*(1./4.)
1226 B(2,38)=-(HH/2.)*(3./4.)-(HHH/2.)*(3./4.)
1227 D(2,38)=-(HH/2.)*(1./4.)
1228 A(2,38)=-(HHH/2.)*(1./4.)
1229
1230 C For GOx and H+GOx enzyme ,
1231 G(3)=omega*C2(2,J)+omega*C13(2,J)
1232 1 -RXN1(1,J)
1233 2 +RXN4(1,J)
1234 B(3,4)=-omega
1235 B(3,26)=-omega
1236 B(3,29)=+1.
1237 B(3,35)=-1.
1238
1239 G(4)=-omega*C2(1,J)-omega*C13(1,J)
1240 1 -RXN1(2,J)
1241 2 +RXN4(2,J)
1242 B(4,3)=omega
1243 B(4,25)=omega
1244 B(4,30)=+1.
1245 B(4,36)=-1.
1246
1247 C For flux of Gluconic Acid and Gluconate ion ,
1248 G(5)=HHH/2.*omega*(C3(2,J-1)+3.*C3(2,J))/4.
1249 1 +HH/2.*omega*(C3(2,J+1)+3.*C3(2,J))/4.
1250 2 +DGOX(3)*(C3(1,J+1)-C3(1,J))/HH
1251 3 -DGOX(3)*(C3(1,J)-C3(1,J-1))/HHH
1252 4 +HHH/2.*omega*(C12(2,J-1)+3.*C12(2,J))/4.
1253 5 +HH/2.*omega*(C12(2,J+1)+3.*C12(2,J))/4.
1254 6 +DGOX(11)*(C12(1,J+1)-C12(1,J))/HH
1255 7 -DGOX(11)*(C12(1,J)-C12(1,J-1))/HHH
1256 8 +(HH/2.)*(RXN2(1,J+1)+3.*RXN2(1,J))/4.
1257 9 +(HHH/2.)*(RXN2(1,J-1)+3.*RXN2(1,J))/4.
1258 B(5,5)=DGOX(3)/HH+DGOX(3)/HHH
1259 D(5,5)=-DGOX(3)/HH
1260 A(5,5)=-DGOX(3)/HHH
1261 B(5,6)=-HHH/2.*omega*(3./4.)-HH/2.*omega*(3./4.)

```

```

1262 D(5,6)=-HH/2.*omega*(1./4.)
1263 A(5,6)=-HHH/2.*omega*(1./4.)
1264 B(5,23)=DGOX(11)/HH+DGOX(11)/HHH
1265 D(5,23)=-DGOX(11)/HH
1266 A(5,23)=-DGOX(11)/HHH
1267 B(5,24)=-HHH/2.*omega*(3./4.)-HH/2.*omega*(3./4.)
1268 D(5,24)=-HH/2.*omega*(1./4.)
1269 A(5,24)=-HHH/2.*omega*(1./4.)
1270 B(5,31)=-(HH/2.)*(3./4.)-(HHH/2.)*(3./4.)
1271 D(5,31)=-(HH/2.)*(1./4.)
1272 A(5,31)=-(HHH/2.)*(1./4.)
1273
1274 G(6)=-HHH/2.*omega*(C3(1,J-1)+3.*C3(1,J))/4.
1275 1 -HH/2.*omega*(C3(1,J+1)+3.*C3(1,J))/4.
1276 2 +DGOX(3)*(C3(2,J+1)-C3(2,J))/HH
1277 3 -DGOX(3)*(C3(2,J)-C3(2,J-1))/HHH
1278 4 -HHH/2.*omega*(C12(1,J-1)+3.*C12(1,J))/4.
1279 5 -HH/2.*omega*(C12(1,J+1)+3.*C12(1,J))/4.
1280 6 +DGOX(11)*(C12(2,J+1)-C12(2,J))/HH
1281 7 -DGOX(11)*(C12(2,J)-C12(2,J-1))/HHH
1282 8 +(HH/2.)*(RXN2(2,J+1)+3.*RXN2(2,J))/4.
1283 9 +(HHH/2.)*(RXN2(2,J-1)+3.*RXN2(2,J))/4.
1284 B(6,6)=DGOX(3)/HH+DGOX(3)/HHH
1285 D(6,6)=-DGOX(3)/HH
1286 A(6,6)=-DGOX(3)/HHH
1287 B(6,5)=-HHH/2.*omega*(3./4.)+HH/2.*omega*(3./4.)
1288 D(6,5)=-HH/2.*omega*(1./4.)
1289 A(6,5)=-HHH/2.*omega*(1./4.)
1290 B(6,24)=DGOX(11)/HH+DGOX(11)/HHH
1291 D(6,24)=-DGOX(11)/HH
1292 A(6,24)=-DGOX(11)/HHH
1293 B(6,23)=-HHH/2.*omega*(3./4.)+HH/2.*omega*(3./4.)
1294 D(6,23)=-HH/2.*omega*(1./4.)
1295 A(6,23)=-HHH/2.*omega*(1./4.)
1296 B(6,32)=-(HH/2.)*(3./4.)-(HHH/2.)*(3./4.)
1297 D(6,32)=-(HH/2.)*(1./4.)
1298 A(6,32)=-(HHH/2.)*(1./4.)
1299
1300 C For GOx2 and GOx-(red.) enzyme complex ,
1301 G(7)=omega*C4(2,J)+omega*C14(2,J)
1302 1 +RXN2(1,J)
1303 2 -RXN3(1,J)
1304 B(7,8)=-omega
1305 B(7,28)=-omega
1306 B(7,31)=-1.
1307 B(7,33)=+1.
1308
1309 G(8)=-omega*C4(1,J)-omega*C14(1,J)
1310 1 +RXN2(2,J)
1311 2 -RXN3(2,J)
1312 B(8,7)=omega
1313 B(8,27)=omega
1314 B(8,32)=-1.
1315 B(8,34)=+1.
1316
1317 C For O2, being consumed only
1318 G(9)=-HHH/2.*omega*(C5(2,J-1)+3.*C5(2,J))/4.
1319 1 +HH/2.*omega*(C5(2,J+1)+3.*C5(2,J))/4.

```

```

1320      2      +DGOX(5)*(C5(1,J+1)-C5(1,J))/HH
1321      3      -DGOX(5)*(C5(1,J)-C5(1,J-1))/HHH
1322      4      -(HH/2.)*(RXN3(1,J+1)+3.*RXN3(1,J))/4.
1323      5      -(HHH/2.)*(RXN3(1,J-1)+3.*RXN3(1,J))/4.
1324      B(9,9)=DGOX(5)/HH+DGOX(5)/HHH
1325      D(9,9)=-DGOX(5)/HH
1326      A(9,9)=-DGOX(5)/HHH
1327      B(9,10)=-HHH/2.*omega*(3./4.)-HH/2.*omega*(3./4.)
1328      D(9,10)=-HH/2.*omega*(1./4.)
1329      A(9,10)=-HHH/2.*omega*(1./4.)
1330      B(9,33)=(HH/2.)*(3./4.)+(HHH/2.)*(3./4.)
1331      D(9,33)=(HH/2.)*(1./4.)
1332      A(9,33)=(HHH/2.)*(1./4.)
1333
1334      G(10)=-HHH/2.*omega*(C5(1,J-1)+3.*C5(1,J))/4.
1335      1      -HH/2.*omega*(C5(1,J+1)+3.*C5(1,J))/4.
1336      2      +DGOX(5)*(C5(2,J+1)-C5(2,J))/HH
1337      3      -DGOX(5)*(C5(2,J)-C5(2,J-1))/HHH
1338      4      -(HH/2.)*(RXN3(2,J+1)+3.*RXN3(2,J))/4.
1339      5      -(HHH/2.)*(RXN3(2,J-1)+3.*RXN3(2,J))/4.
1340      B(10,10)=DGOX(5)/HH+DGOX(5)/HHH
1341      D(10,10)=-DGOX(5)/HH
1342      A(10,10)=-DGOX(5)/HHH
1343      B(10,9)=-HHH/2.*omega*(3./4.)+HH/2.*omega*(3./4.)
1344      D(10,9)=-HH/2.*omega*(1./4.)
1345      A(10,9)=-HHH/2.*omega*(1./4.)
1346      B(10,34)=(HH/2.)*(3./4.)+(HHH/2.)*(3./4.)
1347      D(10,34)=(HH/2.)*(1./4.)
1348      A(10,34)=(HHH/2.)*(1./4.)
1349
1350 C For H2O2, reacting species
1351      G(11)=HHH/2.*omega*(C6(2,J-1)+3.*C6(2,J))/4.
1352      1      +HH/2.*omega*(C6(2,J+1)+3.*C6(2,J))/4.
1353      2      +DGOX(6)*(C6(1,J+1)-C6(1,J))/HH
1354      3      -DGOX(6)*(C6(1,J)-C6(1,J-1))/HHH
1355      4      +(HH/2.)*(RXN4(1,J+1)+3.*RXN4(1,J))/4.
1356      5      +(HHH/2.)*(RXN4(1,J-1)+3.*RXN4(1,J))/4.
1357      B(11,11)=DGOX(6)/HH+DGOX(6)/HHH
1358      D(11,11)=-DGOX(6)/HH
1359      A(11,11)=-DGOX(6)/HHH
1360      B(11,12)=-HHH/2.*omega*(3./4.)-HH/2.*omega*(3./4.)
1361      D(11,12)=-HH/2.*omega*(1./4.)
1362      A(11,12)=-HHH/2.*omega*(1./4.)
1363      B(11,35)=-(HH/2.)*(3./4.)-(HHH/2.)*(3./4.)
1364      D(11,35)=-(HH/2.)*(1./4.)
1365      A(11,35)=-(HHH/2.)*(1./4.)
1366
1367      G(12)=-HHH/2.*omega*(C6(1,J-1)+3.*C6(1,J))/4.
1368      1      -HH/2.*omega*(C6(1,J+1)+3.*C6(1,J))/4.
1369      2      +DGOX(6)*(C6(2,J+1)-C6(2,J))/HH
1370      3      -DGOX(6)*(C6(2,J)-C6(2,J-1))/HHH
1371      4      +(HH/2.)*(RXN4(2,J+1)+3.*RXN4(2,J))/4.
1372      5      +(HHH/2.)*(RXN4(2,J-1)+3.*RXN4(2,J))/4.
1373      B(12,12)=DGOX(6)/HH+DGOX(6)/HHH
1374      D(12,12)=-DGOX(6)/HH
1375      A(12,12)=-DGOX(6)/HHH
1376      B(12,11)=-HHH/2.*omega*(3./4.)+HH/2.*omega*(3./4.)
1377      D(12,11)=-HH/2.*omega*(1./4.)

```

```

1378 A(12,11)=-HHH/2.*omega*(1./4.)
1379 B(12,36)=-(HH/2.)*(3./4.)-(HHH/2.)*(3./4.)
1380 D(12,36)=-(HH/2.)*(1./4.)
1381 A(12,36)=-(HHH/2.)*(1./4.)
1382
1383 C For CX-GOx2, enzyme
1384 G(13)=omega*C7(2,J)
1385 1 +RXN1(1,J)
1386 2 -RXN2(1,J)
1387 B(13,14)=-omega
1388 B(13,29)=-1.
1389 B(13,31)=+1.
1390
1391 G(14)=-omega*C7(1,J)
1392 1 +RXN1(2,J)
1393 2 -RXN2(2,J)
1394 B(14,13)=omega
1395 B(14,30)=-1.
1396 B(14,32)=+1.
1397
1398 C For CX-GOx2, enzyme
1399 G(15)=omega*C8(2,J)
1400 1 +RXN3(1,J)
1401 2 -RXN4(1,J)
1402 B(15,16)=-omega
1403 B(15,33)=-1.
1404 B(15,35)=+1.
1405
1406 G(16)=-omega*C8(1,J)
1407 1 +RXN3(2,J)
1408 2 -RXN4(2,J)
1409 B(16,15)=omega
1410 B(16,34)=-1.
1411 B(16,36)=+1.
1412
1413 C For alpha-Glucose , being consumed only
1414 G(17)=HH/2.*omega*(C9(2,J+1)+3.*C9(2,J))/4.
1415 1 +HHH/2.*omega*(C9(2,J-1)+3.*C9(2,J))/4.
1416 2 +DGOX(1)*(C9(1,J+1)-C9(1,J))/HH
1417 3 -DGOX(1)*(C9(1,J)-C9(1,J-1))/HHH
1418 5 -(HH/2.)*(RXN5(1,J+1)+3.*RXN5(1,J))/4.
1419 6 -(HHH/2.)*(RXN5(1,J-1)+3.*RXN5(1,J))/4.
1420 B(17,17)=DGOX(1)/HH+DGOX(1)/HHH
1421 D(17,17)=-DGOX(1)/HH
1422 A(17,17)=-DGOX(1)/HHH
1423 B(17,18)=-HHH/2.*omega*(3./4.)-HH/2.*omega*(3./4.)
1424 D(17,18)=-HH/2.*omega*(1./4.)
1425 A(17,18)=-HHH/2.*omega*(1./4.)
1426 B(17,37)=(HH/2.)*(3./4.)+(HHH/2.)*(3./4.)
1427 D(17,37)=(HH/2.)*(1./4.)
1428 A(17,37)=(HHH/2.)*(1./4.)
1429
1430 G(18)=-HHH/2.*omega*(C9(1,J-1)+3.*C9(1,J))/4.
1431 1 -HH/2.*omega*(C9(1,J+1)+3.*C9(1,J))/4.
1432 2 +DGOX(1)*(C9(2,J+1)-C9(2,J))/HH
1433 3 -DGOX(1)*(C9(2,J)-C9(2,J-1))/HHH
1434 4 -(HH/2.)*(RXN5(2,J+1)+3.*RXN5(2,J))/4.
1435 5 -(HHH/2.)*(RXN5(2,J-1)+3.*RXN5(2,J))/4.

```

```

1436 B(18,18)=DGOX(1)/HH+DGOX(1)/HHH
1437 D(18,18)=-DGOX(1)/HH
1438 A(18,18)=-DGOX(1)/HHH
1439 B(18,17)=-HHH/2.*omega*(3./4.)+HH/2.*omega*(3./4.)
1440 D(18,17)=-HH/2.*omega*(1./4.)
1441 A(18,17)=-HHH/2.*omega*(1./4.)
1442 B(18,38)=(HH/2.)*(3./4.)+(HHH/2.)*(3./4.)
1443 D(18,38)=(HH/2.)*(1./4.)
1444 A(18,38)=(HHH/2.)*(1./4.)
1445

1446 C For H+ ions , OH- ions , gluconate ions and complex enzyme
1447 G(19)=HHH/2.*omega*(C10(2,J-1)+3.*C10(2,J))/4.
1448 1 +HH/2.*omega*(C10(2,J+1)+3.*C10(2,J))/4.
1449 2 +DGOX(9)*(C10(1,J+1)-C10(1,J))/HH
1450 3 -DGOX(9)*(C10(1,J)-C10(1,J-1))/HHH
1451 4 -HHH/2.*omega*(C11(2,J-1)+3.*C11(2,J))/4.
1452 5 -HH/2.*omega*(C11(2,J+1)+3.*C11(2,J))/4.
1453 6 -DGOX(10)*(C11(1,J+1)-C11(1,J))/HH
1454 7 +DGOX(10)*(C11(1,J)-C11(1,J-1))/HHH
1455 8 -HHH/2.*omega*(C12(2,J-1)+3.*C12(2,J))/4.
1456 9 -HH/2.*omega*(C12(2,J+1)+3.*C12(2,J))/4.
1457 1 -DGOX(11)*(C12(1,J+1)-C12(1,J))/HH
1458 2 +DGOX(11)*(C12(1,J)-C12(1,J-1))/HHH
1459 3 +HHH/2.*omega*(C13(2,J-1)+3.*C13(2,J))/4.
1460 4 +HH/2.*omega*(C13(2,J+1)+3.*C13(2,J))/4.
1461 5 -HHH/2.*omega*(C14(2,J-1)+3.*C14(2,J))/4.
1462 6 -HH/2.*omega*(C14(2,J+1)+3.*C14(2,J))/4.
1463 B(19,19)=DGOX(9)/HH+DGOX(9)/HHH
1464 D(19,19)=-DGOX(9)/HH
1465 A(19,19)=-DGOX(9)/HHH
1466 B(19,20)=-HHH/2.*omega*(3./4.)-HH/2.*omega*(3./4.)
1467 D(19,20)=-HH/2.*omega*(1./4.)
1468 A(19,20)=-HHH/2.*omega*(1./4.)
1469 B(19,21)=-DGOX(10)/HH-DGOX(10)/HHH
1470 D(19,21)=DGOX(10)/HH
1471 A(19,21)=DGOX(10)/HHH
1472 B(19,22)=HHH/2.*omega*(3./4.)+HH/2.*omega*(3./4.)
1473 D(19,22)=HH/2.*omega*(1./4.)
1474 A(19,22)=HHH/2.*omega*(1./4.)
1475 B(19,23)=-DGOX(11)/HH-DGOX(11)/HHH
1476 D(19,23)=DGOX(11)/HH
1477 A(19,23)=DGOX(11)/HHH
1478 B(19,24)=HHH/2.*omega*(3./4.)+HH/2.*omega*(3./4.)
1479 D(19,24)=HH/2.*omega*(1./4.)
1480 A(19,24)=HHH/2.*omega*(1./4.)
1481 B(19,26)=-HHH/2.*omega*(3./4.)-HH/2.*omega*(3./4.)
1482 D(19,26)=-HH/2.*omega*(1./4.)
1483 A(19,26)=-HHH/2.*omega*(1./4.)
1484 B(19,28)=HHH/2.*omega*(3./4.)+HH/2.*omega*(3./4.)
1485 D(19,28)=HH/2.*omega*(1./4.)
1486 A(19,28)=HHH/2.*omega*(1./4.)
1487
1488 G(20)=-HHH/2.*omega*(C10(1,J-1)+3.*C10(1,J))/4.
1489 1 -HH/2.*omega*(C10(1,J+1)+3.*C10(1,J))/4.
1490 2 +DGOX(9)*(C10(2,J+1)-C10(2,J))/HH
1491 3 -DGOX(9)*(C10(2,J)-C10(2,J-1))/HHH
1492 4 +HHH/2.*omega*(C11(1,J-1)+3.*C11(1,J))/4.
1493 5 +HH/2.*omega*(C11(1,J+1)+3.*C11(1,J))/4.

```

```

1494      6      -DGOX(10)*(C11(2,J+1)-C11(2,J))/HH
1495      7      +DGOX(10)*(C11(2,J)-C11(2,J-1))/HHH
1496      8      +HHH/2.*omega*(C12(1,J-1)+3.*C12(1,J))/4.
1497      9      +HH/2.*omega*(C12(1,J+1)+3.*C12(1,J))/4.
1498      1      -DGOX(11)*(C12(2,J+1)-C12(2,J))/HH
1499      2      +DGOX(11)*(C12(2,J)-C12(2,J-1))/HHH
1500      3      -HHH/2.*omega*(C13(1,J-1)+3.*C13(1,J))/4.
1501      4      -HH/2.*omega*(C13(1,J+1)+3.*C13(1,J))/4.
1502      5      +HHH/2.*omega*(C14(1,J-1)+3.*C14(1,J))/4.
1503      6      +HH/2.*omega*(C14(1,J+1)+3.*C14(1,J))/4.
1504      B(20,20)=DGOX(9)/HH+DGOX(9)/HHH
1505      D(20,20)=-DGOX(9)/HH
1506      A(20,20)=-DGOX(9)/HHH
1507      B(20,19)=HHH/2.*omega*(3./4.)+HH/2.*omega*(3./4.)
1508      D(20,19)=HH/2.*omega*(1./4.)
1509      A(20,19)=HHH/2.*omega*(1./4.)
1510      B(20,22)=-DGOX(10)/HH-DGOX(10)/HHH
1511      D(20,22)=DGOX(10)/HH
1512      A(20,22)=DGOX(10)/HHH
1513      B(20,21)=-HHH/2.*omega*(3./4.)-HH/2.*omega*(3./4.)
1514      D(20,21)=-HH/2.*omega*(1./4.)
1515      A(20,21)=-HHH/2.*omega*(1./4.)
1516      B(20,24)=-DGOX(11)/HH-DGOX(11)/HHH
1517      D(20,24)=DGOX(11)/HH
1518      A(20,24)=DGOX(11)/HHH
1519      B(20,23)=-HHH/2.*omega*(3./4.)-HH/2.*omega*(3./4.)
1520      D(20,23)=HH/2.*omega*(1./4.)
1521      A(20,23)=-HHH/2.*omega*(1./4.)
1522      B(20,25)=HHH/2.*omega*(3./4.)+HH/2.*omega*(3./4.)
1523      D(20,25)=HH/2.*omega*(1./4.)
1524      A(20,25)=HHH/2.*omega*(1./4.)
1525      B(20,27)=-HHH/2.*omega*(3./4.)-HH/2.*omega*(3./4.)
1526      D(20,27)=HH/2.*omega*(1./4.)
1527      A(20,27)=-HHH/2.*omega*(1./4.)
1528
1529 C FOR H+ AND OH- ION EQUILIBRIUM,
1530 G(21)=-CONCSS(10,J)*C11(1,J)-CONCSS(11,J)*C10(1,J)
1531
1532 B(21,19)=CONCSS(11,J)
1533 B(21,21)=CONCSS(10,J)
1534
1535 G(22)=-CONCSS(10,J)*C11(2,J)-CONCSS(11,J)*C10(2,J)
1536 B(22,20)=CONCSS(11,J)
1537 B(22,22)=CONCSS(10,J)
1538
1539 C For gluconic acid dissociation ,
1540 G(23)=equilib7*C3(1,J)-CONCSS(10,J)*C12(1,J)-CONCSS(12,J)*C10(1,J)
1541
1542 B(23,5)=-equilib7
1543 B(23,23)=CONCSS(10,J)
1544 B(23,19)=CONCSS(12,J)
1545
1546 G(24)=equilib7*C3(2,J)-CONCSS(10,J)*C12(2,J)-CONCSS(12,J)*C10(2,J)
1547 B(24,6)=-equilib7
1548 B(24,24)=CONCSS(10,J)
1549 B(24,20)=CONCSS(12,J)
1550
1551 C For H+GOx dissociation into H+ and GOx(ox.) ,

```

```

1552 G(25)=equilib8*C13(1,J)-CONCSS(10,J)*C2(1,J)-CONCSS(2,J)*C10(1,J)
1553 B(25,25)=-equilib8
1554 B(25,3)=CONCSS(10,J)
1555 B(25,19)=CONCSS(2,J)
1556
1557 G(26)=equilib8*C13(2,J)-CONCSS(10,J)*C2(2,J)-CONCSS(2,J)*C10(2,J)
1558 B(26,26)=-equilib8
1559 B(26,4)=CONCSS(10,J)
1560 B(26,20)=CONCSS(2,J)
1561
1562 C For GOx(red.) dissociation into H+ and GOx-(red.) ,
1563 G(27)=equilib9*C4(1,J)-CONCSS(10,J)*C14(1,J)-CONCSS(14,J)*C10(1,J)
1564 B(27,7)=-equilib9
1565 B(27,27)=CONCSS(10,J)
1566 B(27,19)=CONCSS(14,J)
1567
1568 G(28)=equilib9*C4(2,J)-CONCSS(10,J)*C14(2,J)-CONCSS(14,J)*C10(2,J)
1569 B(28,8)=-equilib9
1570 B(28,28)=CONCSS(10,J)
1571 B(28,20)=CONCSS(14,J)
1572
1573 C REACTION1
1574 G(29)=-RXN1(1,J)+ratef1*CONCSS(2,J)*C1(1,J)
1575 1 +ratef1*CONCSS(1,J)*C2(1,J)
1576 2 -C7(1,J)*ratef1/equilib1
1577 B(29,1)=-ratef1*CONCSS(2,J)
1578 B(29,3)=-ratef1*CONCSS(1,J)
1579 B(29,13)=+ratef1/equilib1
1580 B(29,29)=+1.
1581
1582 G(30)=-RXN1(2,J)+ratef1*CONCSS(2,J)*C1(2,J)
1583 1 +ratef1*CONCSS(1,J)*C2(2,J)
1584 2 -C7(2,J)*ratef1/equilib1
1585 B(30,2)=-ratef1*CONCSS(2,J)
1586 B(30,4)=-ratef1*CONCSS(1,J)
1587 B(30,14)=+ratef1/equilib1
1588 B(30,30)=+1.
1589
1590 C REACTION2
1591 G(31)=-RXN2(1,J)+ratef2*C7(1,J)
1592 B(31,13)=-ratef2
1593 B(31,31)=+1.
1594
1595 G(32)=-RXN2(2,J)+ratef2*C7(2,J)
1596 B(32,14)=-ratef2
1597 B(32,32)=+1.
1598
1599 C REACTION3
1600 G(33)=-RXN3(1,J)+ratef3*CONCSS(4,J)*C5(1,J)
1601 1 +ratef3*CONCSS(5,J)*C4(1,J)
1602 2 -C8(1,J)*ratef3/equilib3
1603 B(33,7)=-ratef3*CONCSS(5,J)
1604 B(33,9)=-ratef3*CONCSS(4,J)
1605 B(33,15)=+ratef3/equilib3
1606 B(33,33)=+1.
1607
1608 G(34)=-RXN3(2,J)+ratef3*CONCSS(4,J)*C5(2,J)
1609 1 +ratef3*CONCSS(5,J)*C4(2,J)

```

```

1610      2      -C8(2,J)*ratef3/equilib3
1611      B(34,8)=-ratef3*CONCSS(5,J)
1612      B(34,10)=-ratef3*CONCSS(4,J)
1613      B(34,16)=+ratef3/equilib3
1614      B(34,34)=+1.
1615
1616 C   REACTION4
1617      G(35)=-RXN4(1,J)+ratef4*C8(1,J)
1618      B(35,15)=-ratef4
1619      B(35,35)=+1.
1620
1621      G(36)=-RXN4(2,J)+ratef4*C8(2,J)
1622      B(36,16)=-ratef4
1623      B(36,36)=+1.
1624
1625 C   REACTION5
1626      G(37)=-RXN5(1,J)+ratef5*C9(1,J)-ratef5/equilib5*C1(1,J)
1627      B(37,17)=-ratef5
1628      B(37,1)=ratef5/equilib5
1629      B(37,37)=+1.
1630
1631      G(38)=-RXN5(2,J)+ratef5*C9(2,J)-ratef5/equilib5*C1(2,J)
1632      B(38,18)=-ratef5
1633      B(38,2)=ratef5/equilib5
1634      B(38,38)=+1.
1635
1636      WRITE(14,301) J, (G(K),K=1,N)
1637
1638      RETURN
1639      END
1640
1641      SUBROUTINE INNER(J)
1642      IMPLICIT DOUBLE PRECISION (A-H, O-Z)
1643      COMMON/BAT/ A(38,38),B(38,38),C(38,10001),D(38,77),G(38),
1644      1 X(38,38),Y(38,38)
1645      COMMON/NST/ N, NJ
1646      COMMON/VAR/ CONCSS(14,10001),RXNSS(7,10001)
1647      COMMON/VARR/ COEFFMT(13),HHH, KJ
1648      COMMON/CON/ C1(2,10001),C2(2,10001),C3(2,10001),C4(2,10001),
1649      1 C5(2,10001),C6(2,10001),C7(2,10001),C8(2,10001),C9(2,10001),
1650      2 C10(2,10001),C11(2,10001),C12(2,10001),C13(2,10001),
1651      2 C14(2,10001),RXN1(2,10001),RXN2(2,10001),RXN3(2,10001),
1652      3 RXN4(2,10001),RXN5(2,10001)
1653      COMMON/RTE/ ratef1, equilib1, ratef2, ratef3, equilib3, ratef4, ratef5,
1654      1 equilib5, ratef6, equilib6, equilib7, equilib8, equilib9
1655      COMMON/OTH/ H, EBIG, HH, IJ
1656      COMMON/POR/ DGOX(17), DGLM(17), DBULK(17)
1657      COMMON/BCI/ FLUXF, FLUXB, FLUXR, FLUXH, omega
1658      COMMON/BUL/ CBULK(13), PARH2O2, PAR02, PARGLUCOSE, PARION, SOLO2, JCOUNT
1659      COMMON/DELT/ DELTA1, DELTA2, FREQ(400), CH2O2(1000,10001),
1660      1 CO2(1000,10001), CH(1000,10001)
1661      COMMON/POT/ VTILDE
1662
1663      301 FORMAT (5x, 'J=' I5, 38E15.6 E3)
1664
1665 C   For BETA-Glucose, being consumed only
1666      G(1)=omega*C1(2,J)
1667      1 +DGOX(1)*(C1(1,J+1)-2.*C1(1,J)+C1(1,J-1))/HH**2.

```

```

1668      3      -RXN1(1,J)+RXN5(1,J)
1669      B(1,1)=2.*DGOX(1)/HH**2.
1670      A(1,1)=-DGOX(1)/HH**2.
1671      D(1,1)=-DGOX(1)/HH**2.
1672      B(1,2)=-omega
1673      B(1,29)=+1.
1674      B(1,37)=-1.
1675
1676      G(2)=-omega*C1(1,J)
1677      +DGOX(1)*(C1(2,J+1)-2.*C1(2,J)+C1(2,J-1))/HH**2.
1678      3      -RXN1(2,J)+RXN5(2,J)
1679      B(2,2)=2.*DGOX(1)/HH**2.
1680      A(2,2)=-DGOX(1)/HH**2.
1681      D(2,2)=-DGOX(1)/HH**2.
1682      B(2,1)=omega
1683      B(2,30)=+1.
1684      B(2,38)=-1.
1685
1686 C   For GOx and H+GOx enzyme ,
1687      G(3)=omega*C2(2,J)+omega*C13(2,J)
1688      1      -RXN1(1,J)
1689      2      +RXN4(1,J)
1690      B(3,4)=-omega
1691      B(3,26)=-omega
1692      B(3,29)=+1.
1693      B(3,35)=-1.
1694
1695      G(4)=-omega*C2(1,J)-omega*C13(1,J)
1696      1      -RXN1(2,J)
1697      2      +RXN4(2,J)
1698      B(4,3)=omega
1699      B(4,25)=omega
1700      B(4,30)=+1.
1701      B(4,36)=-1.
1702
1703 C   For Gluconic Acid and gluconate ion ,
1704      G(5)=omega*C3(2,J)+omega*C12(2,J)
1705      1      +DGOX(3)*(C3(1,J+1)-2.*C3(1,J)+C3(1,J-1))/HH**2.
1706      2      +DGOX(11)*(C12(1,J+1)-2.*C12(1,J)+C12(1,J-1))/HH**2.
1707      3      +RXN2(1,J)
1708      B(5,5)=2.*DGOX(3)/HH**2.
1709      A(5,5)=-DGOX(3)/HH**2.
1710      D(5,5)=-DGOX(3)/HH**2.
1711      B(5,6)=-omega
1712      B(5,23)=2.*DGOX(11)/HH**2.
1713      A(5,23)=-DGOX(11)/HH**2.
1714      D(5,23)=-DGOX(11)/HH**2.
1715      B(5,24)=omega
1716      B(5,31)=-1.
1717
1718      G(6)=-omega*C3(1,J)-omega*C12(1,J)
1719      1      +DGOX(3)*(C3(2,J+1)-2.*C3(2,J)+C3(2,J-1))/HH**2.
1720      2      +DGOX(11)*(C12(2,J+1)-2.*C12(2,J)+C12(2,J-1))/HH**2.
1721      3      +RXN2(2,J)
1722      B(6,6)=2.*DGOX(3)/HH**2.
1723      A(6,6)=-DGOX(3)/HH**2.
1724      D(6,6)=-DGOX(3)/HH**2.
1725      B(6,5)=omega

```

```

1726 B(6,24)=2.*DGOX(11)/HH**2.
1727 A(6,24)=-DGOX(11)/HH**2.
1728 D(6,24)=-DGOX(11)/HH**2.
1729 B(6,23)=omega
1730 B(6,32)=-1.
1731
1732 C For GOx2 and GOx-(red.) enzyme complex ,
1733 G(7)=omega*C4(2,J)+omega*C14(2,J)
1734 1 +RXN2(1,J)
1735 2 -RXN3(1,J)
1736 B(7,8)=-omega
1737 B(7,28)=-omega
1738 B(7,31)=-1.
1739 B(7,33)=+1.
1740
1741 G(8)=-omega*C4(1,J)-omega*C14(1,J)
1742 1 +RXN2(2,J)
1743 2 -RXN3(2,J)
1744 B(8,7)=omega
1745 B(8,27)=omega
1746 B(8,32)=-1.
1747 B(8,34)=+1.
1748
1749 C For O2, being consumed only
1750 G(9)=omega*C5(2,J)
1751 1 +DGOX(5)*(C5(1,J+1)-2.*C5(1,J)+C5(1,J-1))/HH**2.
1752 3 -RXN3(1,J)
1753 B(9,9)=2.*DGOX(5)/HH**2.
1754 A(9,9)=-DGOX(5)/HH**2.
1755 D(9,9)=-DGOX(5)/HH**2.
1756 B(9,10)=-omega
1757 B(9,33)=+1.
1758
1759 G(10)=-omega*C5(1,J)
1760 1 +DGOX(5)*(C5(2,J+1)-2.*C5(2,J)+C5(2,J-1))/HH**2.
1761 3 -RXN3(2,J)
1762 B(10,10)=2.*DGOX(5)/HH**2.
1763 A(10,10)=-DGOX(5)/HH**2.
1764 D(10,10)=-DGOX(5)/HH**2.
1765 B(10,9)=omega
1766 B(10,34)=+1.
1767
1768 C For H2O2, reacting species
1769 G(11)=omega*C6(2,J)
1770 1 +DGOX(6)*(C6(1,J+1)-2.*C6(1,J)+C6(1,J-1))/HH**2.
1771 3 +RXN4(1,J)
1772 B(11,11)=2.*DGOX(6)/HH**2.
1773 A(11,11)=-DGOX(6)/HH**2.
1774 D(11,11)=-DGOX(6)/HH**2.
1775 B(11,12)=-omega
1776 B(11,35)=-1.
1777
1778 G(12)=-omega*C6(1,J)
1779 1 +DGOX(6)*(C6(2,J+1)-2.*C6(2,J)+C6(2,J-1))/HH**2.
1780 3 +RXN4(2,J)
1781 B(12,12)=2.*DGOX(6)/HH**2.
1782 A(12,12)=-DGOX(6)/HH**2.
1783 D(12,12)=-DGOX(6)/HH**2.

```

```

1784      B(12,11)=omega
1785      B(12,36)=-1.
1786
1787 C   For CX-GOx2, enzyme
1788      G(13)=omega*C7(2,J)
1789      1    +RXN1(1,J)
1790      2    -RXN2(1,J)
1791      B(13,14)=-omega
1792      B(13,29)=-1.
1793      B(13,31)=+1.
1794
1795      G(14)=-omega*C7(1,J)
1796      1    +RXN1(2,J)
1797      2    -RXN2(2,J)
1798      B(14,13)=omega
1799      B(14,30)=-1.
1800      B(14,32)=+1.
1801
1802 C   For CX-GOx2, enzyme
1803      G(15)=omega*C8(2,J)
1804      1    +RXN3(1,J)
1805      2    -RXN4(1,J)
1806      B(15,16)=-omega
1807      B(15,33)=-1.
1808      B(15,35)=+1.
1809
1810      G(16)=-omega*C8(1,J)
1811      1    +RXN3(2,J)
1812      2    -RXN4(2,J)
1813      B(16,15)=omega
1814      B(16,34)=-1.
1815      B(16,36)=+1.
1816
1817 C   FOR ALPHA-GLUCOSE BEING CONSUMMED ONLY,
1818      G(17)=omega*C9(2,J)
1819      1    +DGOX(1)*(C9(1,J+1)-2.*C9(1,J)+C9(1,J-1))/HH**2.
1820      3    -RXN5(1,J)
1821      B(17,17)=2.*DGOX(1)/HH**2.
1822      A(17,17)=-DGOX(1)/HH**2.
1823      D(17,17)=-DGOX(1)/HH**2.
1824      B(17,18)=-omega
1825      B(17,37)=+1.
1826
1827      G(18)=-omega*C9(1,J)
1828      1    +DGOX(1)*(C9(2,J+1)-2.*C9(2,J)+C9(2,J-1))/HH**2.
1829      3    -RXN5(2,J)
1830      B(18,18)=2.*DGOX(1)/HH**2.
1831      A(18,18)=-DGOX(1)/HH**2.
1832      D(18,18)=-DGOX(1)/HH**2.
1833      B(18,17)=omega
1834      B(18,38)=+1.
1835
1836 C   For H+ ions , OH- ions , gluconate ions and complex enzyme
1837      G(19)=omega*C10(2,J)-omega*C11(2,J)-omega*C12(2,J)+omega*C13(2,J)
1838      1    -omega*C14(2,J)
1839      2    +DGOX(9)*(C10(1,J+1)-2.*C10(1,J)+C10(1,J-1))/HH**2.
1840      3    -DGOX(10)*(C11(1,J+1)-2.*C11(1,J)+C11(1,J-1))/HH**2.
1841      4    -DGOX(11)*(C12(1,J+1)-2.*C12(1,J)+C12(1,J-1))/HH**2.

```

```

1842 B(19,20)=-omega
1843 B(19,22)=omega
1844 B(19,24)=omega
1845 B(19,26)=-omega
1846 B(19,28)=omega
1847 B(19,19)=2.*DGOX(9)/HH**2.
1848 A(19,19)=-DGOX(9)/HH**2.
1849 D(19,19)=-DGOX(9)/HH**2.
1850 B(19,21)=-2.*DGOX(10)/HH**2.
1851 A(19,21)=DGOX(10)/HH**2.
1852 D(19,21)=DGOX(10)/HH**2.
1853 B(19,23)=-2.*DGOX(11)/HH**2.
1854 A(19,23)=DGOX(11)/HH**2.
1855 D(19,23)=DGOX(11)/HH**2.
1856
1857 G(20)=-omega*C10(1,J)+omega*C11(1,J)+omega*C12(1,J)-omega*C13(1,J)
1858 1 +omega*C14(1,J)
1859 2 +DGOX(9)*(C10(2,J+1)-2.*C10(2,J)+C10(2,J-1))/HH**2.
1860 3 -DGOX(10)*(C11(2,J+1)-2.*C11(2,J)+C11(2,J-1))/HH**2.
1861 4 -DGOX(11)*(C12(2,J+1)-2.*C12(2,J)+C12(2,J-1))/HH**2.
1862 B(20,19)=omega
1863 B(20,21)=-omega
1864 B(20,23)=-omega
1865 B(20,25)=omega
1866 B(20,27)=-omega
1867 B(20,20)=2.*DGOX(9)/HH**2.
1868 A(20,20)=-DGOX(9)/HH**2.
1869 D(20,20)=DGOX(9)/HH**2.
1870 B(20,22)=-2.*DGOX(10)/HH**2.
1871 A(20,22)=DGOX(10)/HH**2.
1872 D(20,22)=DGOX(10)/HH**2.
1873 B(20,24)=-2.*DGOX(11)/HH**2.
1874 A(20,24)=DGOX(11)/HH**2.
1875 D(20,24)=DGOX(11)/HH**2.
1876
1877 C For H+ and OH- ions equilibrium ,
1878 G(21)=-CONCSS(10,J)*C11(1,J)-CONCSS(11,J)*C10(1,J)
1879
1880 B(21,19)=CONCSS(11,J)
1881 B(21,21)=CONCSS(10,J)
1882
1883 G(22)=-CONCSS(10,J)*C11(2,J)-CONCSS(11,J)*C10(2,J)
1884 B(22,20)=CONCSS(11,J)
1885 B(22,22)=CONCSS(10,J)
1886
1887 C For gluconic acid dissociation ,
1888 G(23)=equilib7*C3(1,J)-CONCSS(10,J)*C12(1,J)-CONCSS(12,J)*C10(1,J)
1889
1890 B(23,5)=-equilib7
1891 B(23,23)=CONCSS(10,J)
1892 B(23,19)=CONCSS(12,J)
1893
1894 G(24)=equilib7*C3(2,J)-CONCSS(10,J)*C12(2,J)-CONCSS(12,J)*C10(2,J)
1895 B(24,6)=-equilib7
1896 B(24,24)=CONCSS(10,J)
1897 B(24,20)=CONCSS(12,J)
1898
1899 C For H+GOx dissociation into H+ and GOx(ox.) ,

```

```

1900 G(25)=equilib8*C13(1,J)-CONCSS(10,J)*C2(1,J)-CONCSS(2,J)*C10(1,J)
1901 B(25,25)=-equilib8
1902 B(25,3)=CONCSS(10,J)
1903 B(25,19)=CONCSS(2,J)
1904
1905 G(26)=equilib8*C13(2,J)-CONCSS(10,J)*C2(2,J)-CONCSS(2,J)*C10(2,J)
1906 B(26,26)=-equilib8
1907 B(26,4)=CONCSS(10,J)
1908 B(26,20)=CONCSS(2,J)
1909
1910 C For GOx(red.) dissociation into H+ and GOx-(red.) ,
1911 G(27)=equilib9*C4(1,J)-CONCSS(10,J)*C14(1,J)-CONCSS(14,J)*C10(1,J)
1912 B(27,7)=-equilib9
1913 B(27,27)=CONCSS(10,J)
1914 B(27,19)=CONCSS(14,J)
1915
1916 G(28)=equilib9*C4(2,J)-CONCSS(10,J)*C14(2,J)-CONCSS(14,J)*C10(2,J)
1917 B(28,8)=-equilib9
1918 B(28,28)=CONCSS(10,J)
1919 B(28,20)=CONCSS(14,J)
1920
1921 C REACTION1
1922 G(29)=-RXN1(1,J)+ratef1*CONCSS(2,J)*C1(1,J)
1923 1 +ratef1*CONCSS(1,J)*C2(1,J)
1924 2 -C7(1,J)*ratef1/equilib1
1925 B(29,1)=-ratef1*CONCSS(2,J)
1926 B(29,3)=-ratef1*CONCSS(1,J)
1927 B(29,13)=+ratef1/equilib1
1928 B(29,29)=+1.
1929
1930 G(30)=-RXN1(2,J)+ratef1*CONCSS(2,J)*C1(2,J)
1931 1 +ratef1*CONCSS(1,J)*C2(2,J)
1932 2 -C7(2,J)*ratef1/equilib1
1933 B(30,2)=-ratef1*CONCSS(2,J)
1934 B(30,4)=-ratef1*CONCSS(1,J)
1935 B(30,14)=+ratef1/equilib1
1936 B(30,30)=+1.
1937
1938 C REACTION2
1939 G(31)=-RXN2(1,J)+ratef2*C7(1,J)
1940 B(31,13)=-ratef2
1941 B(31,31)=+1.
1942
1943 G(32)=-RXN2(2,J)+ratef2*C7(2,J)
1944 B(32,14)=-ratef2
1945 B(32,32)=+1.
1946
1947 C REACTION3
1948 G(33)=-RXN3(1,J)+ratef3*CONCSS(4,J)*C5(1,J)
1949 1 +ratef3*CONCSS(5,J)*C4(1,J)
1950 2 -C8(1,J)*ratef3/equilib3
1951 B(33,7)=-ratef3*CONCSS(5,J)
1952 B(33,9)=-ratef3*CONCSS(4,J)
1953 B(33,15)=+ratef3/equilib3
1954 B(33,33)=+1.
1955
1956 G(34)=-RXN3(2,J)+ratef3*CONCSS(4,J)*C5(2,J)
1957 1 +ratef3*CONCSS(5,J)*C4(2,J)

```

```

1958      2      -C8(2,J)*ratef3/equilib3
1959      B(34,8)=-ratef3*CONCSS(5,J)
1960      B(34,10)=-ratef3*CONCSS(4,J)
1961      B(34,16)=+ratef3/equilib3
1962      B(34,34)=+1.
1963
1964 C   REACTION4
1965 G(35)=-RXN4(1,J)+ratef4*C8(1,J)
1966 B(35,15)=-ratef4
1967 B(35,35)=+1.
1968
1969 G(36)=-RXN4(2,J)+ratef4*C8(2,J)
1970 B(36,16)=-ratef4
1971 B(36,36)=+1.
1972
1973 C   REACTION5
1974 G(37)=-RXN5(1,J)+ratef5*C9(1,J)-ratef5/equilib5*C1(1,J)
1975 B(37,17)=-ratef5
1976 B(37,1)=ratef5/equilib5
1977 B(37,37)=+1.
1978
1979 G(38)=-RXN5(2,J)+ratef5*C9(2,J)-ratef5/equilib5*C1(2,J)
1980 B(38,18)=-ratef5
1981 B(38,2)=ratef5/equilib5
1982 B(38,38)=+1.
1983
1984 c   SAVE G OUT DATA
1985 DO 11 I=2,13
1986 11 If (I.EQ.J) WRITE(14,301) J, (G(K),K=1,N)
1987 IF (J.EQ.IJ/2) THEN
1988 WRITE(14,301) J, (G(K),K=1,N)
1989 ELSE IF (J.EQ.(IJ-1)) THEN
1990 WRITE(14,301) J, (G(K),K=1,N)
1991 ELSE IF (J.EQ.(IJ-2)) THEN
1992 WRITE(14,301) J, (G(K),K=1,N)
1993 ELSE IF (J.EQ.(IJ-3)) THEN
1994 WRITE(14,301) J, (G(K),K=1,N)
1995 END IF
1996
1997 RETURN
1998 END
1999
2000 SUBROUTINE COUPLER2(J)
2001 IMPLICIT DOUBLE PRECISION (A-H, O-Z)
2002 COMMON/BAT/ A(38,38),B(38,38),C(38,10001),D(38,77),G(38),
2003 1 X(38,38),Y(38,38)
2004 COMMON/NST/ N, NJ
2005 COMMON/VAR/ CONCSS(14,10001),RXNSS(7,10001)
2006 COMMON/VARR/ COEFFMT(13),HHH, KJ
2007 COMMON/CON/ C1(2,10001),C2(2,10001),C3(2,10001),C4(2,10001),
2008 1 C5(2,10001),C6(2,10001),C7(2,10001),C8(2,10001),C9(2,10001),
2009 2 C10(2,10001),C11(2,10001),C12(2,10001),C13(2,10001),
2010 2 C14(2,10001),RXN1(2,10001),RXN2(2,10001),RXN3(2,10001),
2011 3 RXN4(2,10001),RXN5(2,10001)
2012 COMMON/RTE/ ratef1, equilib1, ratef2, ratef3, equilib3, ratef4, ratef5,
2013 1 equilib5, ratef6, equilib6, equilib7, equilib8, equilib9
2014 COMMON/OTH/ H,EBIG,HH,IJ
2015 COMMON/POR/ DGOX(17),DGLM(17),DBULK(17)

```

```

2016 COMMON/BCI/ FLUXF,FLUXB,FLUXR,FLUXH,omega
2017 COMMON/BUL/ CBULK(13),PARH2O2,PAR02,PARGLUCOSE,PARION,SOLO2,JCOUNT
2018 COMMON/DELT/ DELTA1, DELTA2, FREQ(400),CH2O2(1000,10001),
2019 1 CO2(1000,10001),CH(1000,10001)
2020 COMMON/POT/ VTILDE
2021
2022 301 FORMAT (5x,'J=' I5 , 38E15.6E3)
2023
2024 C For beta-Glucose, being consumed only
2025 G(1)=H/2.*omega*(C1(2,J+1)+3.*C1(2,J))/4.
2026 1 +HH/2.*omega*(C1(2,J-1)+3.*C1(2,J))/4.
2027 2 +DGLM(1)*(C1(1,J+1)-C1(1,J))/H
2028 3 -DGOX(1)*(C1(1,J)-C1(1,J-1))/HH
2029 4 -(HH/2.)*(RXN1(1,J-1)+3.*RXN1(1,J))/4.
2030 5 +(H/2.)*(RXN5(1,J+1)+3.*RXN5(1,J))/4.
2031 6 +(HH/2.)*(RXN5(1,J-1)+3.*RXN5(1,J))/4.
2032 B(1,1)=DGLM(1)/HH+DGOX(1)/HH
2033 D(1,1)=-DGLM(1)/H
2034 A(1,1)=-DGOX(1)/HH
2035 B(1,2)=-HH/2.*omega*(3./4.)-H/2.*omega*(3./4.)
2036 D(1,2)=-H/2.*omega*(1./4.)
2037 A(1,2)=-HH/2.*omega*(1./4.)
2038 B(1,29)=(HH/2.)*(3./4.)
2039 A(1,29)=(HH/2.)*(1./4.)
2040 B(1,37)=-(HH/2.)*(3./4.)-(H/2.)*(3./4.)
2041 A(1,37)=-(HH/2.)*(1./4.)
2042 D(1,37)=-(H/2.)*(1./4.)
2043
2044 G(2)=-HH/2.*omega*(C1(1,J-1)+3.*C1(1,J))/4.
2045 1 -H/2.*omega*(C1(1,J+1)+3.*C1(1,J))/4.
2046 2 +DGLM(1)*(C1(2,J+1)-C1(2,J))/H
2047 3 -DGOX(1)*(C1(2,J)-C1(2,J-1))/HH
2048 4 -(HH/2.)*(RXN1(2,J-1)+3.*RXN1(2,J))/4.
2049 5 +(H/2.)*(RXN5(2,J+1)+3.*RXN5(2,J))/4.
2050 6 +(HH/2.)*(RXN5(2,J-1)+3.*RXN5(2,J))/4.
2051 B(2,2)=DGLM(1)/HH+DGOX(1)/HH
2052 D(2,2)=-DGLM(1)/H
2053 A(2,2)=-DGOX(1)/HH
2054 B(2,1)=+HH/2.*omega*(3./4.)+H/2.*omega*(3./4.)
2055 D(2,1)=+H/2.*omega*(1./4.)
2056 A(2,1)=+HH/2.*omega*(1./4.)
2057 B(2,30)=(HH/2.)*(3./4.)
2058 A(2,30)=(HH/2.)*(1./4.)
2059 B(2,38)=-(HH/2.)*(3./4.)-(H/2.)*(3./4.)
2060 A(2,38)=-(HH/2.)*(1./4.)
2061 D(2,38)=-(H/2.)*(1./4.)
2062
2063 C For GOx and H+GOx enzyme,
2064 G(3)=omega*C2(2,J)+omega*C13(2,J)
2065 1 -RXN1(1,J)
2066 2 +RXN4(1,J)
2067 B(3,4)=-omega
2068 B(3,26)=-omega
2069 B(3,29)=+1.
2070 B(3,35)=-1.
2071
2072 G(4)=-omega*C2(1,J)-omega*C13(1,J)
2073 1 -RXN1(2,J)

```

```

2074      2      +RXN4(2 ,J)
2075      B(4 ,3)=omega
2076      B(4 ,25)=omega
2077      B(4 ,30)=+1.
2078      B(4 ,36)=-1.
2079
2080 C   For flux of Gluconic Acid and Gluconate ion ,
2081      G(5)=HH/2.*omega*(C3(2 ,J-1)+3.*C3(2 ,J))/4.
2082      1      +H/2.*omega*(C3(2 ,J+1)+3.*C3(2 ,J))/4.
2083      2      +DGLM(3)*(C3(1 ,J+1)-C3(1 ,J))/H
2084      3      -DGOX(3)*(C3(1 ,J)-C3(1 ,J-1))/HH
2085      4      +HH/2.*omega*(C12(2 ,J-1)+3.*C12(2 ,J))/4.
2086      5      +H/2.*omega*(C12(2 ,J+1)+3.*C12(2 ,J))/4.
2087      6      +DGLM(11)*(C12(1 ,J+1)-C12(1 ,J))/H
2088      7      -DGOX(11)*(C12(1 ,J)-C12(1 ,J-1))/HH
2089      8      +(HH/2.)*(RXN2(1 ,J-1)+3.*RXN2(1 ,J))/4.
2090      B(5 ,5)=DGLM(3)/H+DGOX(3)/HH
2091      D(5 ,5)=-DGLM(3)/H
2092      A(5 ,5)=-DGOX(3)/HH
2093      B(5 ,6)=-HH/2.*omega*(3./4.)-H/2.*omega*(3./4.)
2094      D(5 ,6)=-H/2.*omega*(1./4.)
2095      A(5 ,6)=-HH/2.*omega*(1./4.)
2096      B(5 ,23)=DGLM(11)/H+DGOX(11)/HH
2097      D(5 ,23)=-DGLM(11)/H
2098      A(5 ,23)=-DGOX(11)/HH
2099      B(5 ,24)=-HH/2.*omega*(3./4.)-H/2.*omega*(3./4.)
2100      D(5 ,24)=-H/2.*omega*(1./4.)
2101      A(5 ,24)=-HH/2.*omega*(1./4.)
2102      B(5 ,31)=-(HH/2.)*(3./4.)
2103      A(5 ,31)=-(HH/2.)*(1./4.)
2104
2105      G(6)=-HH/2.*omega*(C3(1 ,J-1)+3.*C3(1 ,J))/4.
2106      1      -H/2.*omega*(C3(1 ,J+1)+3.*C3(1 ,J))/4.
2107      2      +DGLM(3)*(C3(2 ,J+1)-C3(2 ,J))/H
2108      3      -DGOX(3)*(C3(2 ,J)-C3(2 ,J-1))/HH
2109      4      -HH/2.*omega*(C12(1 ,J-1)+3.*C12(1 ,J))/4.
2110      5      -H/2.*omega*(C12(1 ,J+1)+3.*C12(1 ,J))/4.
2111      6      +DGLM(11)*(C12(2 ,J+1)-C12(2 ,J))/H
2112      7      -DGOX(11)*(C12(2 ,J)-C12(2 ,J-1))/HH
2113      8      +(HH/2.)*(RXN2(2 ,J-1)+3.*RXN2(2 ,J))/4.
2114      B(6 ,6)=DGLM(3)/H+DGOX(3)/HH
2115      D(6 ,6)=-DGLM(3)/H
2116      A(6 ,6)=-DGOX(3)/HH
2117      B(6 ,5)=+HH/2.*omega*(3./4.)+H/2.*omega*(3./4.)
2118      D(6 ,5)=+H/2.*omega*(1./4.)
2119      A(6 ,5)=+HH/2.*omega*(1./4.)
2120      B(6 ,24)=DGLM(11)/H+DGOX(11)/HH
2121      D(6 ,24)=-DGLM(11)/H
2122      A(6 ,24)=-DGOX(11)/HH
2123      B(6 ,23)=+HH/2.*omega*(3./4.)+H/2.*omega*(3./4.)
2124      D(6 ,23)=+H/2.*omega*(1./4.)
2125      A(6 ,23)=+HH/2.*omega*(1./4.)
2126      B(6 ,32)=-(HH/2.)*(3./4.)
2127      A(6 ,32)=-(HH/2.)*(1./4.)
2128
2129 C   For GOx2 and GOx-(red .) enzyme complex ,
2130      G(7)=omega*C4(2 ,J)+omega*C14(2 ,J)
2131      1      +RXN2(1 ,J)

```

```

2132      2      -RXN3(1 ,J)
2133      B(7 ,8)=-omega
2134      B(7 ,28)=-omega
2135      B(7 ,31)=-1.
2136      B(7 ,33)=+1.
2137
2138      G(8)=-omega*C4(1 ,J)-omega*C14(1 ,J)
2139      1      +RXN2(2 ,J)
2140      2      -RXN3(2 ,J)
2141      B(8 ,7)=omega
2142      B(8 ,27)=omega
2143      B(8 ,32)=-1.
2144      B(8 ,34)=+1.
2145
2146 C   For O2, being consumed only
2147      G(9)=HH/2.*omega*(C5(2 ,J-1)+3.*C5(2 ,J))/4.
2148      1      +H/2.*omega*(C5(2 ,J+1)+3.*C5(2 ,J))/4.
2149      2      +DGLM(5)*(C5(1 ,J+1)-C5(1 ,J))/H
2150      3      -DGOX(5)*(C5(1 ,J)-C5(1 ,J-1))/HH
2151      4      -(HH/2.)*(RXN3(1 ,J-1)+3.*RXN3(1 ,J))/4.
2152      B(9 ,9)=DGLM(5)/H+DGOX(5)/HH
2153      D(9 ,9)=-DGLM(5)/H
2154      A(9 ,9)=-DGOX(5)/HH
2155      B(9 ,10)=-HH/2.*omega*(3./4.)-H/2.*omega*(3./4.)
2156      D(9 ,10)=-H/2.*omega*(1./4.)
2157      A(9 ,10)=-HH/2.*omega*(1./4.)
2158      B(9 ,33)=(HH/2.)*(3./4.)
2159      A(9 ,33)=(HH/2.)*(1./4.)
2160
2161      G(10)=-HH/2.*omega*(C5(1 ,J-1)+3.*C5(1 ,J))/4.
2162      1      -H/2.*omega*(C5(1 ,J+1)+3.*C5(1 ,J))/4.
2163      2      +DGLM(5)*(C5(2 ,J+1)-C5(2 ,J))/H
2164      3      -DGOX(5)*(C5(2 ,J)-C5(2 ,J-1))/HH
2165      4      -(HH/2.)*(RXN3(2 ,J-1)+3.*RXN3(2 ,J))/4.
2166      B(10 ,10)=DGLM(5)/H+DGOX(5)/HH
2167      D(10 ,10)=-DGLM(5)/H
2168      A(10 ,10)=-DGOX(5)/HH
2169      B(10 ,9)=-HH/2.*omega*(3./4.)+H/2.*omega*(3./4.)
2170      D(10 ,9)=+H/2.*omega*(1./4.)
2171      A(10 ,9)=+HH/2.*omega*(1./4.)
2172      B(10 ,34)=(HH/2.)*(3./4.)
2173      A(10 ,34)=(HH/2.)*(1./4.)
2174
2175 C   For H2O2, reacting species
2176      G(11)=HH/2.*omega*(C6(2 ,J-1)+3.*C6(2 ,J))/4.
2177      1      +H/2.*omega*(C6(2 ,J+1)+3.*C6(2 ,J))/4.
2178      2      +DGLM(6)*(C6(1 ,J+1)-C6(1 ,J))/H
2179      3      -DGOX(6)*(C6(1 ,J)-C6(1 ,J-1))/HH
2180      5      +(HH/2.)*(RXN4(1 ,J-1)+3.*RXN4(1 ,J))/4.
2181      B(11 ,11)=DGLM(6)/H+DGOX(6)/HH
2182      D(11 ,11)=-DGLM(6)/H
2183      A(11 ,11)=-DGOX(6)/HH
2184      B(11 ,12)=-HH/2.*omega*(3./4.)-H/2.*omega*(3./4.)
2185      D(11 ,12)=-H/2.*omega*(1./4.)
2186      A(11 ,12)=-HH/2.*omega*(1./4.)
2187      B(11 ,35)=-(HH/2.)*(3./4.)
2188      A(11 ,35)=-(HH/2.)*(1./4.)
2189

```

```

2190 G(12)=-HH/2.*omega*(C6(1,J-1)+3.*C6(1,J))/4.
2191 1 -H/2.*omega*(C6(1,J+1)+3.*C6(1,J))/4.
2192 2 +DGLM(6)*(C6(2,J+1)-C6(2,J))/H
2193 3 -DGOX(6)*(C6(2,J)-C6(2,J-1))/HH
2194 5 +(HH/2.)*(RXN4(2,J-1)+3.*RXN4(2,J))/4.
2195 B(12,12)=DGLM(6)/H+DGOX(6)/HH
2196 D(12,12)=-DGLM(6)/H
2197 A(12,12)=-DGOX(6)/HH
2198 B(12,11)=-HH/2.*omega*(3./4.)+H/2.*omega*(3./4.)
2199 D(12,11)=-H/2.*omega*(1./4.)
2200 A(12,11)=-HH/2.*omega*(1./4.)
2201 B(12,36)=- $(\text{HH}/2.) * (3./4.)$ 
2202 A(12,36)=- $(\text{HH}/2.) * (1./4.)$ 
2203
2204 C For CX-GOx2, enzyme
2205 G(13)=omega*C7(2,J)
2206 1 +RXN1(1,J)
2207 2 -RXN2(1,J)
2208 B(13,14)=-omega
2209 B(13,29)=-1.
2210 B(13,31)=+1.
2211
2212 G(14)=-omega*C7(1,J)
2213 1 +RXN1(2,J)
2214 2 -RXN2(2,J)
2215 B(14,13)=omega
2216 B(14,30)=-1.
2217 B(14,32)=+1.
2218
2219 C For CX-GOx2, enzyme
2220 G(15)=omega*C8(2,J)
2221 1 +RXN3(1,J)
2222 2 -RXN4(1,J)
2223 B(15,16)=-omega
2224 B(15,33)=-1.
2225 B(15,35)=+1.
2226
2227 G(16)=-omega*C8(1,J)
2228 1 +RXN3(2,J)
2229 2 -RXN4(2,J)
2230 B(16,15)=omega
2231 B(16,34)=-1.
2232 B(16,36)=+1.
2233
2234 C For ALPHA-Glucose, being consumed only
2235 G(17)=H/2.*omega*(C9(2,J+1)+3.*C9(2,J))/4.
2236 1 +HH/2.*omega*(C9(2,J-1)+3.*C9(2,J))/4.
2237 2 +DGLM(1)*(C9(1,J+1)-C9(1,J))/H
2238 3 -DGOX(1)*(C9(1,J)-C9(1,J-1))/HH
2239 4 -(H/2.)*(RXN5(1,J+1)+3.*RXN5(1,J))/4.
2240 5 -(HH/2.)*(RXN5(1,J-1)+3.*RXN5(1,J))/4.
2241 B(17,17)=DGLM(1)/H+DGOX(1)/HH
2242 D(17,17)=-DGLM(1)/H
2243 A(17,17)=-DGOX(1)/HH
2244 B(17,18)=-HH/2.*omega*(3./4.)-H/2.*omega*(3./4.)
2245 D(17,18)=-H/2.*omega*(1./4.)
2246 A(17,18)=-HH/2.*omega*(1./4.)
2247 B(17,37)=(HH/2.)*(3./4.)+(H/2.)*(3./4.)

```

```

2248 A(17,37)=(HH/2.)*(1./4.)
2249 D(17,37)=(H/2.)*(1./4.)
2250
2251 G(18)=-HH/2.*omega*(C9(1,J-1)+3.*C9(1,J))/4.
2252 1 -H/2.*omega*(C9(1,J+1)+3.*C9(1,J))/4.
2253 2 +DGML(1)*(C9(2,J+1)-C9(2,J))/H
2254 3 -DGOX(1)*(C9(2,J)-C9(2,J-1))/HH
2255 4 -(H/2.)*(RXN5(2,J+1)+3.*RXN5(2,J))/4.
2256 5 -(HH/2.)*(RXN5(2,J-1)+3.*RXN5(2,J))/4.
2257 B(18,18)=DGML(1)/H+DGOX(1)/HH
2258 D(18,18)=-DGML(1)/H
2259 A(18,18)=-DGOX(1)/HH
2260 B(18,17)=-HH/2.*omega*(3./4.)+H/2.*omega*(3./4.)
2261 D(18,17)=-H/2.*omega*(1./4.)
2262 A(18,17)=-HH/2.*omega*(1./4.)
2263 B(18,38)=(HH/2.)*(3./4.)+(H/2.)*(3./4.)
2264 A(18,38)=(HH/2.)*(1./4.)
2265 D(18,38)=(H/2.)*(1./4.)
2266
2267 C For H+ ions , OH- ions , gluconate ions and complex enzyme
2268 G(19)=HH/2.*omega*(C10(2,J-1)+3.*C10(2,J))/4.
2269 1 +H/2.*omega*(C10(2,J+1)+3.*C10(2,J))/4.
2270 2 +DGML(9)*(C10(1,J+1)-C10(1,J))/H
2271 3 -DGOX(9)*(C10(1,J)-C10(1,J-1))/HH
2272 4 -HH/2.*omega*(C11(2,J-1)+3.*C11(2,J))/4.
2273 5 -H/2.*omega*(C11(2,J+1)+3.*C11(2,J))/4.
2274 6 -DGML(10)*(C11(1,J+1)-C11(1,J))/H
2275 7 +DGOX(10)*(C11(1,J)-C11(1,J-1))/HH
2276 8 -HH/2.*omega*(C12(2,J-1)+3.*C12(2,J))/4.
2277 9 -H/2.*omega*(C12(2,J+1)+3.*C12(2,J))/4.
2278 1 -DGML(11)*(C12(1,J+1)-C12(1,J))/H
2279 2 +DGOX(11)*(C12(1,J)-C12(1,J-1))/HH
2280 3 +HH/2.*omega*(C13(2,J-1)+3.*C13(2,J))/4.
2281 4 -HH/2.*omega*(C14(2,J-1)+3.*C14(2,J))/4.
2282 B(19,19)=DGML(9)/H+DGOX(9)/HH
2283 D(19,19)=-DGML(9)/H
2284 A(19,19)=-DGOX(9)/HH
2285 B(19,20)=-HH/2.*omega*(3./4.)-H/2.*omega*(3./4.)
2286 D(19,20)=-H/2.*omega*(1./4.)
2287 A(19,20)=-HH/2.*omega*(1./4.)
2288 B(19,21)=-DGML(10)/H-DGOX(10)/HH
2289 D(19,21)=DGML(10)/H
2290 A(19,21)=DGOX(10)/HH
2291 B(19,22)=HH/2.*omega*(3./4.)+H/2.*omega*(3./4.)
2292 D(19,22)=H/2.*omega*(1./4.)
2293 A(19,22)=HH/2.*omega*(1./4.)
2294 B(19,23)=-DGML(11)/H-DGOX(11)/HH
2295 D(19,23)=DGML(11)/H
2296 A(19,23)=DGOX(11)/HH
2297 B(19,24)=HH/2.*omega*(3./4.)+H/2.*omega*(3./4.)
2298 D(19,24)=H/2.*omega*(1./4.)
2299 A(19,24)=HH/2.*omega*(1./4.)
2300 B(19,26)=-HH/2.*omega*(3./4.)
2301 A(19,26)=-HH/2.*omega*(1./4.)
2302 B(19,28)=HH/2.*omega*(3./4.)
2303 A(19,28)=HH/2.*omega*(1./4.)
2304
2305 G(20)=-HH/2.*omega*(C10(1,J-1)+3.*C10(1,J))/4.

```

```

2306   1      -H/2.*omega*(C10(1,J+1)+3.*C10(1,J))/4.
2307   2      +DGLM(9)*(C10(2,J+1)-C10(2,J))/H
2308   3      -DGOX(9)*(C10(2,J)-C10(2,J-1))/HH
2309   4      +HH/2.*omega*(C11(1,J-1)+3.*C11(1,J))/4.
2310   5      +H/2.*omega*(C11(1,J+1)+3.*C11(1,J))/4.
2311   6      -DGLM(10)*(C11(2,J+1)-C11(2,J))/H
2312   7      +DGOX(10)*(C11(2,J)-C11(2,J-1))/HH
2313   8      +HH/2.*omega*(C12(1,J-1)+3.*C12(1,J))/4.
2314   9      +H/2.*omega*(C12(1,J+1)+3.*C12(1,J))/4.
2315  1      -DGLM(11)*(C12(2,J+1)-C12(2,J))/H
2316  2      +DGOX(11)*(C12(2,J)-C12(2,J-1))/HH
2317  3      -HH/2.*omega*(C13(1,J-1)+3.*C13(1,J))/4.
2318  4      +HH/2.*omega*(C14(1,J-1)+3.*C14(1,J))/4.
2319 B(20,20)=DGLM(9)/H+DGOX(9)/HH
2320 D(20,20)=-DGLM(9)/H
2321 A(20,20)=-DGOX(9)/HH
2322 B(20,19)=HH/2.*omega*(3./4.)+H/2.*omega*(3./4.)
2323 D(20,19)=H/2.*omega*(1./4.)
2324 A(20,19)=HH/2.*omega*(1./4.)
2325 B(20,22)=-DGLM(10)/H-DGOX(10)/HH
2326 D(20,22)=DGLM(10)/H
2327 A(20,22)=DGOX(10)/HH
2328 B(20,21)=-HH/2.*omega*(3./4.)-H/2.*omega*(3./4.)
2329 D(20,21)=-H/2.*omega*(1./4.)
2330 A(20,21)=-HH/2.*omega*(1./4.)
2331 B(20,24)=-DGLM(11)/H-DGOX(11)/HH
2332 D(20,24)=DGLM(11)/H
2333 A(20,24)=DGOX(11)/HH
2334 B(20,23)=-HH/2.*omega*(3./4.)-H/2.*omega*(3./4.)
2335 D(20,23)=-H/2.*omega*(1./4.)
2336 A(20,23)=-HH/2.*omega*(1./4.)
2337 B(20,25)=HH/2.*omega*(3./4.)
2338 A(20,25)=HH/2.*omega*(1./4.)
2339 B(20,27)=-HH/2.*omega*(3./4.)
2340 A(20,27)=-HH/2.*omega*(1./4.)
2341
2342 C FOR H+ AND OH- ION EQUILIBRIUM,
2343 G(21)=-CONCSS(10,J)*C11(1,J)-CONCSS(11,J)*C10(1,J)
2344
2345 B(21,19)=CONCSS(11,J)
2346 B(21,21)=CONCSS(10,J)
2347
2348 G(22)=-CONCSS(10,J)*C11(2,J)-CONCSS(11,J)*C10(2,J)
2349 B(22,20)=CONCSS(11,J)
2350 B(22,22)=CONCSS(10,J)
2351
2352 C For gluconic acid dissociation ,
2353 G(23)=equilib7*C3(1,J)-CONCSS(10,J)*C12(1,J)-CONCSS(12,J)*C10(1,J)
2354
2355 B(23,5)=-equilib7
2356 B(23,23)=CONCSS(10,J)
2357 B(23,19)=CONCSS(12,J)
2358
2359 G(24)=equilib7*C3(2,J)-CONCSS(10,J)*C12(2,J)-CONCSS(12,J)*C10(2,J)
2360 B(24,6)=-equilib7
2361 B(24,24)=CONCSS(10,J)
2362 B(24,20)=CONCSS(12,J)
2363

```

```

2364 C For H+GOx dissociation into H+ and GOx(ox.) ,
2365 G(25)=equilib8*C13(1,J)-CONCSS(10,J)*C2(1,J)-CONCSS(2,J)*C10(1,J)
2366 B(25,25)=-equilib8
2367 B(25,3)=CONCSS(10,J)
2368 B(25,19)=CONCSS(2,J)
2369
2370 G(26)=equilib8*C13(2,J)-CONCSS(10,J)*C2(2,J)-CONCSS(2,J)*C10(2,J)
2371 B(26,26)=-equilib8
2372 B(26,4)=CONCSS(10,J)
2373 B(26,20)=CONCSS(2,J)
2374
2375 C For GOx(red.) dissociation into H+ and GOx-(red.) ,
2376 G(27)=equilib9*C4(1,J)-CONCSS(10,J)*C14(1,J)-CONCSS(14,J)*C10(1,J)
2377 B(27,7)=-equilib9
2378 B(27,27)=CONCSS(10,J)
2379 B(27,19)=CONCSS(14,J)
2380
2381 G(28)=equilib9*C4(2,J)-CONCSS(10,J)*C14(2,J)-CONCSS(14,J)*C10(2,J)
2382 B(28,8)=-equilib9
2383 B(28,28)=CONCSS(10,J)
2384 B(28,20)=CONCSS(14,J)
2385
2386 C REACTION1
2387 G(29)=-RXN1(1,J)+ratef1*CONCSS(2,J)*C1(1,J)
2388 1 +ratef1*CONCSS(1,J)*C2(1,J)
2389 2 -C7(1,J)*ratef1/equilib1
2390 B(29,1)=-ratef1*CONCSS(2,J)
2391 B(29,3)=-ratef1*CONCSS(1,J)
2392 B(29,13)=+ratef1/equilib1
2393 B(29,29)=+1.
2394
2395 G(30)=-RXN1(2,J)+ratef1*CONCSS(2,J)*C1(2,J)
2396 1 +ratef1*CONCSS(1,J)*C2(2,J)
2397 2 -C7(2,J)*ratef1/equilib1
2398 B(30,2)=-ratef1*CONCSS(2,J)
2399 B(30,4)=-ratef1*CONCSS(1,J)
2400 B(30,14)=+ratef1/equilib1
2401 B(30,30)=+1.
2402
2403 C REACTION2
2404 G(31)=-RXN2(1,J)+ratef2*C7(1,J)
2405 B(31,13)=-ratef2
2406 B(31,31)=+1.
2407
2408 G(32)=-RXN2(2,J)+ratef2*C7(2,J)
2409 B(32,14)=-ratef2
2410 B(32,32)=+1.
2411
2412 C REACTION3
2413 G(33)=-RXN3(1,J)+ratef3*CONCSS(4,J)*C5(1,J)
2414 1 +ratef3*CONCSS(5,J)*C4(1,J)
2415 2 -C8(1,J)*ratef3/equilib3
2416 B(33,7)=-ratef3*CONCSS(5,J)
2417 B(33,9)=-ratef3*CONCSS(4,J)
2418 B(33,15)=+ratef3/equilib3
2419 B(33,33)=+1.
2420
2421 G(34)=-RXN3(2,J)+ratef3*CONCSS(4,J)*C5(2,J)

```

```

2422      1      +ratef3 *CONCSS(5 ,J )*C4(2 ,J )
2423      2      -C8(2 ,J )*ratef3 /equilib3
2424      B(34 ,8)=-ratef3 *CONCSS(5 ,J )
2425      B(34 ,10)=-ratef3 *CONCSS(4 ,J )
2426      B(34 ,16)=+ratef3 /equilib3
2427      B(34 ,34)=+1.
2428
2429 C   REACTION4
2430 G(35)=-RXN4(1 ,J )+ratef4 *C8(1 ,J )
2431 B(35 ,15)=-ratef4
2432 B(35 ,35)=+1.
2433
2434 G(36)=-RXN4(2 ,J )+ratef4 *C8(2 ,J )
2435 B(36 ,16)=-ratef4
2436 B(36 ,36)=+1.
2437
2438 C   REACTION5
2439 G(37)=-RXN5(1 ,J )+ratef5 *C9(1 ,J )-ratef5 /equilib5 *C1(1 ,J )
2440 B(37 ,17)=-ratef5
2441 B(37 ,1)=ratef5 /equilib5
2442 B(37 ,37)=+1.
2443
2444 G(38)=-RXN5(2 ,J )+ratef5 *C9(2 ,J )-ratef5 /equilib5 *C1(2 ,J )
2445 B(38 ,18)=-ratef5
2446 B(38 ,2)=ratef5 /equilib5
2447 B(38 ,38)=+1.
2448
2449 WRITE(14 ,301) J , (G(K) ,K=1,N)
2450
2451 RETURN
2452 END
2453
2454 SUBROUTINE OUTER(J)
2455 IMPLICIT DOUBLE PRECISION (A-H, O-Z)
2456 COMMON/BAT/ A(38 ,38) ,B(38 ,38) ,C(38 ,10001) ,D(38 ,77) ,G(38) ,
2457 1      X(38 ,38) ,Y(38 ,38)
2458 COMMON/NST/ N, NJ
2459 COMMON/VAR/ CONCSS(14 ,10001) ,RXNSS(7 ,10001)
2460 COMMON/VARR/ COEFFMT(13) ,HHH, KJ
2461 COMMON/CON/ C1(2 ,10001) ,C2(2 ,10001) ,C3(2 ,10001) ,C4(2 ,10001) ,
2462 1      C5(2 ,10001) ,C6(2 ,10001) ,C7(2 ,10001) ,C8(2 ,10001) ,C9(2 ,10001) ,
2463 2      C10(2 ,10001) ,C11(2 ,10001) ,C12(2 ,10001) ,C13(2 ,10001) ,
2464 2      C14(2 ,10001) ,RXN1(2 ,10001) ,RXN2(2 ,10001) ,RXN3(2 ,10001) ,
2465 3      RXN4(2 ,10001) ,RXN5(2 ,10001)
2466 COMMON/RTE/ ratef1 ,equilib1 ,ratef2 ,ratef3 ,equilib3 ,ratef4 ,ratef5 ,
2467 1      equilib5 ,ratef6 ,equilib6 ,equilib7 ,equilib8 ,equilib9
2468 COMMON/OTH/ H,EBIG,HH, IJ
2469 COMMON/POR/ DGOX(17) ,DGLM(17) ,DBULK(17)
2470 COMMON/BCI/ FLUXF,FLUXB,FLUXR,FLUXH,omega
2471 COMMON/BUL/ CBULK(13) ,PARH2O2,PAR02,PARGLUCOSE,PARION,SOLO2,JCOUNT
2472 COMMON/DELT/ DELTA1, DELTA2, FREQ(400) ,CH2O2(1000 ,10001) ,
2473 1      CO2(1000 ,10001) ,CH(1000 ,10001)
2474 COMMON/POT/ VTILDE
2475
2476 301 FORMAT (5x, 'J=' I5 , 38E15.6E3)
2477
2478 C   For BETA-Glucose , being consumed only
2479 G(1)=omega*C1(2 ,J )

```

```

2480      1      +DGLM(1)*(C1(1,J+1)-2.*C1(1,J)+C1(1,J-1))/H**2.
2481      2      +RXN5(1,J)
2482      B(1,1)=2.*DGLM(1)/H**2.
2483      A(1,1)=-DGLM(1)/H**2.
2484      D(1,1)=-DGLM(1)/H**2.
2485      B(1,2)=-omega
2486      B(1,37)=-1.
2487
2488      G(2)=-omega*C1(1,J)
2489      1      +DGLM(1)*(C1(2,J+1)-2.*C1(2,J)+C1(2,J-1))/H**2.
2490      2      +RXN5(2,J)
2491      B(2,2)=2.*DGLM(1)/H**2.
2492      A(2,2)=-DGLM(1)/H**2.
2493      D(2,2)=-DGLM(1)/H**2.
2494      B(2,1)=omega
2495      B(2,38)=-1.
2496
2497 C   For GOx, enzyme
2498 G(3)=C2(1,J)
2499 B(3,3)=-1.
2500
2501 G(4)=C2(2,J)
2502 B(4,4)=-1.
2503
2504 C   For flux of Gluconic Acid and Gluconate ion ,
2505 G(5)=omega*C3(2,J)+omega*C12(2,J)
2506 1      +DGLM(3)*(C3(1,J+1)-2.*C3(1,J)+C3(1,J-1))/H**2.
2507 2      +DGLM(11)*(C12(1,J+1)-2.*C12(1,J)+C12(1,J-1))/H**2.
2508 B(5,5)=2.*DGLM(3)/H**2.
2509 A(5,5)=-DGLM(3)/H**2.
2510 D(5,5)=-DGLM(3)/H**2.
2511 B(5,6)=-omega
2512 B(5,23)=2.*DGLM(11)/H**2.
2513 A(5,23)=-DGLM(11)/H**2.
2514 D(5,23)=-DGLM(11)/H**2.
2515 B(5,24)=-omega
2516
2517 G(6)=-omega*C3(1,J)-omega*C12(1,J)
2518 1      +DGLM(3)*(C3(2,J+1)-2.*C3(2,J)+C3(2,J-1))/H**2.
2519 2      +DGLM(11)*(C12(2,J+1)-2.*C12(2,J)+C12(2,J-1))/H**2.
2520 B(6,6)=2.*DGLM(3)/H**2.
2521 A(6,6)=-DGLM(3)/H**2.
2522 D(6,6)=-DGLM(3)/H**2.
2523 B(6,5)=omega
2524 B(6,24)=2.*DGLM(11)/H**2.
2525 A(6,24)=-DGLM(11)/H**2.
2526 D(6,24)=-DGLM(11)/H**2.
2527 B(6,23)=omega
2528
2529 C   For GOx2, enzyme
2530 G(7)=C4(1,J)
2531 B(7,7)=-1.
2532
2533 G(8)=C4(2,J)
2534 B(8,8)=-1.
2535
2536 C   For O2, being consumed only
2537 G(9)=omega*C5(2,J)

```

```

2538 1      +DGLM(5)*(C5(1,J+1)-2.*C5(1,J)+C5(1,J-1))/H**2.
2539 B(9,9)=2.*DGLM(5)/H**2.
2540 A(9,9)=-DGLM(5)/H**2.
2541 D(9,9)=-DGLM(5)/H**2.
2542 B(9,10)=-omega
2543
2544 G(10)=-omega*C5(1,J)
2545 1      +DGLM(5)*(C5(2,J+1)-2.*C5(2,J)+C5(2,J-1))/H**2.
2546 B(10,10)=2.*DGLM(5)/H**2.
2547 A(10,10)=-DGLM(5)/H**2.
2548 D(10,10)=-DGLM(5)/H**2.
2549 B(10,9)=omega
2550
2551 C   For H2O2, reacting species
2552 G(11)=omega*C6(2,J)
2553 1      +DGLM(6)*(C6(1,J+1)-2.*C6(1,J)+C6(1,J-1))/H**2.
2554 B(11,11)=2.*DGLM(6)/H**2.
2555 A(11,11)=-DGLM(6)/H**2.
2556 D(11,11)=-DGLM(6)/H**2.
2557 B(11,12)=-omega
2558
2559 G(12)=-omega*C6(1,J)
2560 1      +DGLM(6)*(C6(2,J+1)-2.*C6(2,J)+C6(2,J-1))/H**2.
2561 B(12,12)=2.*DGLM(6)/H**2.
2562 A(12,12)=-DGLM(6)/H**2.
2563 D(12,12)=-DGLM(6)/H**2.
2564 B(12,11)=omega
2565
2566 C   For CX-GOx2, enzyme
2567 G(13)=C7(1,J)
2568 B(13,13)=-1.
2569
2570 G(14)=C7(2,J)
2571 B(14,14)=-1.
2572
2573 C   For CX-GOx, enzyme
2574 G(15)=C8(1,J)
2575 B(15,15)=-1.
2576
2577 G(16)=C8(2,J)
2578 B(16,16)=-1.
2579
2580 C   For ALPHA-Glucose , being consumed only
2581 G(17)=omega*C9(2,J)
2582 1      +DGLM(1)*(C9(1,J+1)-2.*C9(1,J)+C9(1,J-1))/H**2.
2583 2      -RXN5(1,J)
2584 B(17,17)=2.*DGLM(1)/H**2.
2585 A(17,17)=-DGLM(1)/H**2.
2586 D(17,17)=-DGLM(1)/H**2.
2587 B(17,18)=-omega
2588 B(17,37)=+1.
2589
2590 G(18)=-omega*C9(1,J)
2591 1      +DGLM(1)*(C9(2,J+1)-2.*C9(2,J)+C9(2,J-1))/H**2.
2592 2      -RXN5(2,J)
2593 B(18,18)=2.*DGLM(1)/H**2.
2594 A(18,18)=-DGLM(1)/H**2.
2595 D(18,18)=-DGLM(1)/H**2.

```

```

2596 B(18,17)=omega
2597 B(18,38)=+1.
2598
2599 C For H+ ions , OH- ions , gluconate ions
2600 G(19)=omega*C10(2,J)-omega*C11(2,J)-omega*C12(2,J)
2601 1 +DGLM(9)*(C10(1,J+1)-2.*C10(1,J)+C10(1,J-1))/H**2.
2602 2 -DGLM(10)*(C11(1,J+1)-2.*C11(1,J)+C11(1,J-1))/H**2.
2603 3 -DGLM(11)*(C12(1,J+1)-2.*C12(1,J)+C12(1,J-1))/H**2.
2604 B(19,20)=-omega
2605 B(19,22)=omega
2606 B(19,24)=omega
2607 B(19,19)=2.*DGLM(9)/H**2.
2608 A(19,19)=-DGLM(9)/H**2.
2609 D(19,19)=-DGLM(9)/H**2.
2610 B(19,21)=-2.*DGLM(10)/H**2.
2611 A(19,21)=DGLM(10)/H**2.
2612 D(19,21)=DGLM(10)/H**2.
2613 B(19,23)=-2.*DGLM(11)/H**2.
2614 A(19,23)=DGLM(11)/H**2.
2615 D(19,23)=DGLM(11)/H**2.
2616
2617 G(20)=-omega*C10(1,J)+omega*C11(1,J)+omega*C12(1,J)
2618 1 +DGLM(9)*(C10(2,J+1)-2.*C10(2,J)+C10(2,J-1))/H**2.
2619 2 -DGLM(10)*(C11(2,J+1)-2.*C11(2,J)+C11(2,J-1))/H**2.
2620 3 -DGLM(11)*(C12(2,J+1)-2.*C12(2,J)+C12(2,J-1))/H**2.
2621 B(20,19)=omega
2622 B(20,21)=-omega
2623 B(20,23)=-omega
2624 B(20,20)=2.*DGLM(9)/H**2.
2625 A(20,20)=-DGLM(9)/H**2.
2626 D(20,20)=-DGLM(9)/H**2.
2627 B(20,22)=-2.*DGLM(10)/H**2.
2628 A(20,22)=DGLM(10)/H**2.
2629 D(20,22)=DGLM(10)/H**2.
2630 B(20,24)=-2.*DGLM(11)/H**2.
2631 A(20,24)=DGLM(11)/H**2.
2632 D(20,24)=DGLM(11)/H**2.
2633
2634 C For H+ and OH- ions equilibrium ,
2635 G(21)=-CONCSS(10,J)*C11(1,J)-CONCSS(11,J)*C10(1,J)
2636
2637 B(21,19)=CONCSS(11,J)
2638 B(21,21)=CONCSS(10,J)
2639
2640 G(22)=-CONCSS(10,J)*C11(2,J)-CONCSS(11,J)*C10(2,J)
2641 B(22,20)=CONCSS(11,J)
2642 B(22,22)=CONCSS(10,J)
2643
2644
2645 C For gluconic acid dissociation ,
2646 G(23)=equilib7*C3(1,J)-CONCSS(10,J)*C12(1,J)-CONCSS(12,J)*C10(1,J)
2647
2648 B(23,5)=-equilib7
2649 B(23,23)=CONCSS(10,J)
2650 B(23,19)=CONCSS(12,J)
2651
2652 G(24)=equilib7*C3(2,J)-CONCSS(10,J)*C12(2,J)-CONCSS(12,J)*C10(2,J)
2653 B(24,6)=-equilib7

```

```

2654      B(24,24)=CONCSS(10,J)
2655      B(24,20)=CONCSS(12,J)
2656 C    For H+GOx(ox),
2657      G(25)=C13(1,J)
2658      B(25,25)=-1.
2659
2660      G(26)=C13(2,J)
2661      B(26,26)=-1.
2662
2663 C    For GOx-(red),
2664      G(27)=C14(1,J)
2665      B(27,27)=-1.
2666
2667      G(28)=C14(2,J)
2668      B(28,28)=-1.
2669
2670 C    REACTION1
2671      G(29)=-RXN1(1,J)
2672      B(29,29)=+1.
2673
2674      G(30)=-RXN1(2,J)
2675      B(30,30)=+1.
2676
2677 C    REACTION2
2678      G(31)=-RXN2(1,J)
2679      B(31,31)=+1.
2680
2681      G(32)=-RXN2(2,J)
2682      B(32,32)=+1.
2683
2684 C    REACTION3
2685      G(33)=-RXN3(1,J)
2686      B(33,33)=+1.
2687
2688      G(34)=-RXN3(2,J)
2689      B(34,34)=+1.
2690
2691 C    REACTION4
2692      G(35)=-RXN4(1,J)
2693      B(35,35)=+1.
2694
2695      G(36)=-RXN4(2,J)
2696      B(36,36)=+1.
2697
2698 C    REACTION5
2699      G(37)=-RXN5(1,J)+ratef5*C9(1,J)-ratef5/equilib5*C1(1,J)
2700      B(37,17)=-ratef5
2701      B(37,1)=ratef5/equilib5
2702      B(37,37)=+1.
2703
2704      G(38)=-RXN5(2,J)+ratef5*C9(2,J)-ratef5/equilib5*C1(2,J)
2705      B(38,18)=-ratef5
2706      B(38,2)=ratef5/equilib5
2707      B(38,38)=+1.
2708
2709 c    SAVE G OUT DATA
2710      IF (J.EQ.(IJ+(NJ-IJ)/2)) THEN
2711      WRITE(14,301) J, (G(K),K=1,N)

```

```

2712 ELSE IF (J.EQ.(NJ-1)) THEN
2713 WRITE(14,301) J, (G(K),K=1,N)
2714 END IF
2715
2716 RETURN
2717 END
2718
2719 SUBROUTINE BCNJ(J)
2720 IMPLICIT DOUBLE PRECISION (A-H, O-Z)
2721 COMMON/BAT/ A(38,38),B(38,38),C(38,10001),D(38,77),G(38),
2722 1 X(38,38),Y(38,38)
2723 COMMON/NST/ N, NJ
2724 COMMON/VAR/ CONCSS(14,10001),RXNSS(7,10001)
2725 COMMON/VARR/ COEFFMT(13),HHH, KJ
2726 COMMON/CON/ C1(2,10001),C2(2,10001),C3(2,10001),C4(2,10001),
2727 1 C5(2,10001),C6(2,10001),C7(2,10001),C8(2,10001),C9(2,10001),
2728 2 C10(2,10001),C11(2,10001),C12(2,10001),C13(2,10001),
2729 2 C14(2,10001),RXN1(2,10001),RXN2(2,10001),RXN3(2,10001),
2730 3 RXN4(2,10001),RXN5(2,10001)
2731 COMMON/RTE/ ratef1, equilib1, ratef2, ratef3, equilib3, ratef4, ratef5,
2732 1 equilib5, ratef6, equilib6, equilib7, equilib8, equilib9
2733 COMMON/OTH/ H, EBIG, HH, IJ
2734 COMMON/POR/ DGOX(17),DGLM(17),DBULK(17)
2735 COMMON/BCI/ FLUXF,FLUXB,FLUXR,FLUXH,omega
2736 COMMON/BUL/ CBULK(13),PARH2O2,PAR02,PARGLUCOSE,PARION,SOLO2,JCOUNT
2737 COMMON/DELT/ DELTA1, DELTA2, FREQ(400),CH2O2(1000,10001),
2738 1 CO2(1000,10001),CH(1000,10001)
2739 COMMON/POT/ VTILDE
2740
2741 301 FORMAT (5x,'J=' I5, 38E15.6E3)
2742
2743 DO 42 I=1,2
2744 C For beta-Glucose, being consumed only
2745 G(I)=C1(I,J)
2746 B(I,I)=-1.
2747 C For GOx, enzyme
2748 G(2+I)=C2(I,J)
2749 B(2+I,2+I)=-1.
2750 C For Gluconic Acid, being produced only
2751 G(4+I)=C3(I,J)
2752 B(4+I,4+I)=-1.
2753 C For GOx2, enzyme
2754 G(6+I)=C4(I,J)
2755 B(6+I,6+I)=-1.
2756 C For O2, being consumed only
2757 G(8+I)=C5(I,J)
2758 B(8+I,8+I)=-1.
2759 C For H2O2, reacting species
2760 G(10+I)=C6(I,J)
2761 B(10+I,10+I)=-1.
2762 C For CX-GOx2, enzyme
2763 G(12+I)=C7(I,J)
2764 B(12+I,12+I)=-1.
2765 C For CX-GOx, enzyme
2766 G(14+I)=C8(I,J)
2767 B(14+I,14+I)=-1.
2768 C For Alpha-Glucose, being consumed only
2769 G(16+I)=C9(I,J)

```

```

2770      B(16+I,16+I)=-1.
2771 C      For H+ ion
2772      G(18+I)=C10(I,J)
2773      B(18+I,18+I)=-1.
2774 C      For OH- ion
2775      G(20+I)=C11(I,J)
2776      B(20+I,20+I)=-1.
2777 C      For gluconate ion ,
2778      G(22+I)=C12(I,J)
2779      B(22+I,22+I)=-1.
2780 C      For H+GOx(ox.) ,
2781      G(24+I)=C13(I,J)
2782      B(24+I,24+I)=-1.
2783 C      For GOx-(red.) ,
2784      G(26+I)=C14(I,J)
2785        42 B(26+I,26+I)=-1.
2786 C      REACTION1
2787      G(29)=-RXN1(1,J)
2788      B(29,29)=+1.
2789
2790      G(30)=-RXN1(2,J)
2791      B(30,30)=+1.
2792
2793 C      REACTION2
2794      G(31)=-RXN2(1,J)
2795      B(31,31)=+1.
2796
2797      G(32)=-RXN2(2,J)
2798      B(32,32)=+1.
2799
2800 C      REACTION3
2801      G(33)=-RXN3(1,J)
2802      B(33,33)=+1.
2803
2804      G(34)=-RXN3(2,J)
2805      B(34,34)=+1.
2806
2807 C      REACTION4
2808      G(35)=-RXN4(1,J)
2809      B(35,35)=+1.
2810
2811      G(36)=-RXN4(2,J)
2812      B(36,36)=+1.
2813
2814 C      REACTION5
2815      G(37)=-RXN5(1,J)+ratef5*C9(1,J)-ratef5/equilib5*C1(1,J)
2816      B(37,17)=-ratef5
2817      B(37,1)=ratef5/equilib5
2818      B(37,37)=+1.
2819
2820      G(38)=-RXN5(2,J)+ratef5*C9(2,J)-ratef5/equilib5*C1(2,J)
2821      B(38,18)=-ratef5
2822      B(38,2)=ratef5/equilib5
2823      B(38,38)=+1.
2824
2825      WRITE(14,301) J, (G(K),K=1,N)
2826
2827      RETURN

```

```

2828      END
2829
2830 C   Subroutine MATINV
2831 SUBROUTINE MATINV(N,M,DETERM)
2832 IMPLICIT DOUBLE PRECISION (A-H,O-Z)
2833 COMMON/BAT/ A(38,38),B(38,38),C(38,10001),D(38,77),G(38),
2834          1 X(38,38),Y(38,38)
2835 COMMON/NST/ NTEMP, NJ
2836 DIMENSION ID(38)
2837 DETERM=1.01
2838 DO 1 I=1,N
2839 1 ID(I)=0
2840 DO 18 NN=1,N
2841 BMAX=1.1
2842 DO 6 I=1,N
2843 IF (ID(I).NE.0) GO TO 6
2844 BNEXT=0.0
2845 BTRY=0.0
2846 DO 5 J=1,N
2847 IF (ID(J).NE.0) GO TO 5
2848 IF (DABS(B(I,J)).LE.BNEXT) GO TO 5
2849 BNEXT=DABS(B(I,J))
2850 IF (BNEXT.LE.BTRY) GO TO 5
2851 BNEXT=BTRY
2852 BTRY=DABS(B(I,J))
2853 JC=J
2854 5 CONTINUE
2855 IF (BNEXT.GE.BMAX*BTRY) GO TO 6
2856 BMAX=BNEXT/BTRY
2857 IROW=I
2858 JCOL=JC
2859 6 CONTINUE
2860 IF (ID(JC).EQ.0) GO TO 8
2861 DETERM=0.0
2862 RETURN
2863 8 ID(JCOL)=1
2864 IF (JCOL.EQ.IROW) GO TO 12
2865 DO 10 J=1,N
2866 SAVE=B(IROW,J)
2867 B(IROW,J)=B(JCOL,J)
2868 10 B(JCOL,J)=SAVE
2869 DO 11 K=1,M
2870 SAVE=D(IROW,K)
2871 D(IROW,K)=D(JCOL,K)
2872 11 D(JCOL,K)=SAVE
2873 12 F=1.0/B(JCOL,JCOL)
2874 DO 13 J=1,N
2875 13 B(JCOL,J)=B(JCOL,J)*F
2876 DO 14 K=1,M
2877 14 D(JCOL,K)=D(JCOL,K)*F
2878 DO 18 I=1,N
2879 IF (I.EQ.JCOL) GO TO 18
2880 F=B(I,JCOL)
2881 DO 16 J=1,N
2882 16 B(I,J)=B(I,J)-F*B(JCOL,J)
2883 DO 17 K=1,M
2884 17 D(I,K)=D(I,K)-F*D(JCOL,K)
2885 18 CONTINUE

```

```

2886      RETURN
2887      END
2888
2889 C      SUBROUTINE BAND(J)
2890      SUBROUTINE BAND(J)
2891      IMPLICIT DOUBLE PRECISION (A-H,O-Z)
2892      DIMENSION E(38,39,10001)
2893      COMMON/BAT/ A(38,38),B(38,38),C(38,10001),D(38,77),G(38),
2894      1 X(38,38),Y(38,38)
2895      COMMON/NST/ N,NJ
2896      SAVE E, NP1
2897 101      FORMAT(15H DETERM=0 AT J=,I5)
2898      IF (J-2) 1,6,8
2899      1 NP1=N+1
2900      DO 2 I=1,N
2901      D(I,2*N+1)=G(I)
2902      DO 2 L=1,N
2903      LPN=L+N
2904      2 D(I,LPN)=X(I,L)
2905      CALL MATINV(N, 2*N+1,DETERM)
2906      IF (DETERM) 4,3,4
2907      3 PRINT 101,J
2908      4 DO 5 K=1,N
2909      E(K,NP1,1)=D(K,2*N+1)
2910      DO 5 L=1,N
2911      E(K,L,1)=-D(K,L)
2912      LPN=L+N
2913      5 X(K,L)=-D(K,LPN)
2914      RETURN
2915      6 DO 7 I=1,N
2916      DO 7 K=1,N
2917      DO 7 L=1,N
2918      7 D(I,K)=D(I,K)+A(I,L)*X(L,K)
2919      8 IF (J-NJ) 11,9,9
2920      9 DO 10 I=1,N
2921      DO 10 L=1,N
2922      G(I)=G(I)-Y(I,L)*E(L,NP1,J-2)
2923      DO 10 M=1,N
2924      10 A(I,L)=A(I,L)+Y(I,M)*E(M,L,J-2)
2925      11 DO 12 I=1,N
2926      D(I,NP1)=-G(I)
2927      DO 12 L=1,N
2928      D(I,NP1)=D(I,NP1)+A(I,L)*E(L,NP1,J-1)
2929      DO 12 K=1,N
2930      12 B(I,K)=B(I,K)+A(I,L)*E(L,K,J-1)
2931      CALL MATINV(N,NP1,DETERM)
2932      IF (DETERM) 14, 13, 14
2933      13 PRINT 101,J
2934      14 DO 15 K=1,N
2935      DO 15 M=1,NP1
2936      15 E(K,M,J)=-D(K,M)
2937      IF (J-NJ) 20,16,16
2938      16 DO 17 K=1,N
2939      17 C(K,J)=E(K,NP1,J)
2940      DO 18 JJ=2,NJ
2941      M=NJ-JJ+1
2942      DO 18 K=1,N
2943      C(K,M)=E(K,NP1,M)

```

```
2944      DO 18 L=1,N  
2945 18   C(K,M)=C(K,M)+E(K,L,M)*C(L,M+1)  
2946      DO 19 L=1,N  
2947      DO 19 K=1,N  
2948 19   C(K,1)=C(K,1)+X(K,L)*C(L,3)  
2949 20   RETURN  
2950      END
```

Code A.7. Matlab code to plot impedance response from impedance calculations

```

1 %Inserting concentration data from Fortran
2
3 clc; close all; clear all;
4 format longE;
5 %input parameters for CPE
6 a = 0.85;
7 Q = 2.61E-5;
8 %Read the unsteady state data at each frequency
9 H2O2 = dlmread( 'cdhgox_H2O2_out.txt' );
10
11 O2 = dlmread( 'cdhgox_O2_out.txt' );
12
13 Hion = dlmread( 'cdhgox_H_ion_out.txt' );
14
15 Bss1 = dlmread( 'cdhgox_out.txt' );
16 Bss=Bss1(:,6);
17
18 %Read constant values used in the Fortran code
19 M = dlmread( 'cdhgox_values_out.txt' );
20
21 N=M(1);
22 NJ=M(2);
23 IJ=M(3);
24 KJ=M(4);
25 H=M(5);
26 HH=M(6);
27 HHH=M(7);
28 V=M(8);
29 AKF=M(9);
30 AKB=M(10);
31 AK2=M(11);
32 AKH=M(12);
33 BBA=M(13);
34 BBC=M(14);
35 BB2=M(15);
36 BBH=M(16);
37 DGOX_H2O2=M(17);
38 DGOX_O2=M(18);
39 DGOX_H=M(19);
40 RTB=M(20);
41 nf=M(21);
42
43 %Read frequency points, Kw=omega, KK=K
44 Kw = dlmread( 'kgox_values_out.txt' );
45
46
47 %deltan=gamma(4/3)*delta;
48
49 %Read the steady state values for CB
50 Css = dlmread( 'cdhgox_os_out.txt' );
51
52 %Other constants
53 F=96487;
54
55 %Create y values for plotting
56 y=zeros(NJ,1);

```

```

57
58 far=HHH*(KJ-1);
59 y1=0:HHH:far;
60
61 far1=HH*(IJ-KJ);
62 y2=y1(KJ):HH:y1(KJ)+far1;
63
64 far2=H*(NJ-IJ);
65 y3=y2(IJ-KJ+1):H:y2(IJ-KJ+1)+far2;
66
67 for k=1:KJ-1
68 y(k)=y1(k);
69 end
70 for k=KJ:IJ-1
71 y(k)=y2(k-KJ+1);
72 end
73 for k=IJ:NJ
74 y(k)=y3(k-IJ+1);
75 end
76
77 %Create complex numbers from unsteady state data
78 CH2O2=rand(NJ,nf);
79 CO2=rand(NJ,nf);
80 CH=rand(NJ,nf);
81 for n=1:nf
82 for k=1:NJ
83 CH2O2(k,n)=complex(H2O2(k,2*n-1),H2O2(k,2*n));
84 CO2(k,n)=complex(O2(k,2*n-1),O2(k,2*n));
85 CH(k,n)=complex(Hion(k,2*n-1),Hion(k,2*n));
86 end
87 end
88 % for n=1:nf
89 % for k=1:NJ
90 % CO2(k,n)=complex(O2(k,2*n-1),O2(k,2*n));
91 % end
92 % end
93
94 % figure(1)
95 % plot(CB,Css(:,1),'-b'); hold on;
96 % figure(2)
97 % plot(CO2,Css(:,1),'-b'); hold on;
98
99 %Calculate the dimensionless diffusion impedance
100 Zdd_H2O2=zeros(1,nf);
101 Zdd_O2=zeros(1,nf);
102 Zdd_H=zeros(1,nf);
103 for k=1:nf
104 Zdd_H2O2(k)=(-CH2O2(1,k)/((-CH2O2(3,k)+4*CH2O2(2,k)-3*CH2O2(1,k))/(2*HHH)))/((far+far1));
105 Zdd_O2(k)=(-CO2(1,k)/((-CO2(3,k)+4*CO2(2,k)-3*CO2(1,k))/(2*HHH)))/((far+far1));
106 Zdd_H(k)=(-CH(1,k)/((-CH(3,k)+4*CH(2,k)-3*CH(1,k))/(2*HHH)))/((far+far1));
107 end
108 %Calculate the ratio factor
109 F_H2O2=zeros(1,nf);
110 F_O2=zeros(1,nf);
111 F_H=zeros(1,nf);
112 for k=1:nf

```

```

113 F_H2O2(k)=((-CH2O2(3,k)+4*CH2O2(2,k)-3*CH2O2(1,k))/(2*HHH)) / ...
114   ((-CH(3,k)+4*CH(2,k)-3*CH(1,k))/(2*HHH));
115 F_O2(k)=((-CO2(3,k)+4*CO2(2,k)-3*CO2(1,k))/(2*HHH)) / ...
116   ((-CH(3,k)+4*CH(2,k)-3*CH(1,k))/(2*HHH));
117 F_H(k)=1;
118 end
119 %Calculate the diffusion impedance
120 Zdfront_H2O2=(RTB*(-AKF*exp(BBA*V)+AK2*(Bss1(1,10)^2)*exp(-BB2*V))) / ...
121   (F*DGOX_H);
122 Zdfront_O2=(RTB*AKB*(Bss1(1,10)^2)*exp(-BBC*V))/(F*DGOX_H);
123 Zdfront_H=(RTB*(2*AKB*Bss1(1,10)*Bss1(1,5)*exp(-BBC*V) + ...
124   2*AK2*Bss1(1,10)*Bss1(1,6)*exp(-BB2*V)+2*AKH*Bss1(1,10)*exp(-BBH*V)))/(F* ...
125   DGOX_H);
125 Zd_H2O2=zeros(1,nf);
126 Zd_O2=zeros(1,nf);
127 Zd_H=zeros(1,nf);
128 Zd=zeros(1,nf);
129 DCH2O2=zeros(1,nf);
130 DCO2=zeros(1,nf);
131 DCH=zeros(1,nf);
132 for k=1:nf
133 Zd_H2O2(k)=Zdfront_H2O2*F_H2O2(k) * ...
134   (-CH2O2(1,k)/((-CH2O2(3,k)+4*CH2O2(2,k)-3*CH2O2(1,k))/(2*HHH)));
135 DCH2O2(k)=(-CH2O2(3,k)+4*CH2O2(2,k)-3*CH2O2(1,k))/(2*HHH);
136 Zd_O2(k)=Zdfront_O2*F_O2(k) * ...
137   (-CO2(1,k)/((-CO2(3,k)+4*CO2(2,k)-3*CO2(1,k))/(2*HHH)));
138 DCO2(k)=((-CO2(3,k)+4*CO2(2,k)-3*CO2(1,k))/(2*HHH));
139 Zd_H(k)=Zdfront_H*F_H(k) * ...
140   (-CH(1,k)/((-CH(3,k)+4*CH(2,k)-3*CH(1,k))/(2*HHH)));
141 Zd(k)=Zd_H2O2(k)+Zd_O2(k)+Zd_H(k);
142 DCH(k)=((-CH(3,k)+4*CH(2,k)-3*CH(1,k))/(2*HHH));
143 end
144
145 %Calculate the faradic impedance
146 Zf=zeros(1,nf);
147 for k=1:nf
148 Zf(k)=RTB+Zd(k);
149 end
150 %Calculate the overall impedance
151 Zo=zeros(1,nf);
152 for n=1:nf
153   Zo(n)=10+Zf(n)/(1+(1i*Kw(n))^a*Q*Zf(n));
154 end
155
156 %Oscillating concentration
157 o=[1 2 3 4];
158 ci1_H2O2=zeros(NJ,length(o));
159 ci2_H2O2=zeros(NJ,length(o));
160 ci3_H2O2=zeros(NJ,length(o));
161 ci1_O2=zeros(NJ,length(o));
162 ci2_O2=zeros(NJ,length(o));
163 ci3_O2=zeros(NJ,length(o));
164 dimfreq=[61 101 144 181];
165 for k=1:NJ
166   for l=1:length(o)
167     t(l)=o(l)*pi/2;
168     ci1_H2O2(k,l)=real(CH2O2(k,141)*exp(1i*t(l)));
169     ci2_H2O2(k,l)=real(CH2O2(k,101)*exp(1i*t(l)));

```

```

170 ci3_H2O2(k,1)=real(CH2O2(k,61)*exp(1i*t(1)));  

171 ci1_O2(k,1)=real(CO2(k,141)*exp(1i*t(1)));  

172 ci2_O2(k,1)=real(CO2(k,101)*exp(1i*t(1)));  

173 ci3_O2(k,1)=real(CO2(k,61)*exp(1i*t(1)));  

174  

175 end  

176 end  

177  

178  

179  

180 % figure(1)  

181 % plot(y,Css(:,1),'-b'); hold on;  

182 % plot(y,Css(:,6),'-r');  

183 % plot(y,Css(:,5),'-m');  

184 % plot(y,Css(:,2),'-k');  

185 % %axis([0 0.1 5e-5 10.1e-5]);  

186 % legend('SS C Glucose','SS C H2O2','SS C O2','SS C GOX');  

187 % title('Steady State Concentration away from Electrode Surface');  

188 % xlabel('Length, cm');  

189 % ylabel('Concentration, moles/cm3');  

190  

191 % figure(6)  

192 % plot(y,Css(:,6),'-r');  

193  

194 figure(1)  

195 Zdreal=real(Zd);  

196 Zdimag=imag(Zd);  

197 plot(Zdreal,-Zdimag,'-ks');hold on; axis equal;  

198 title('Diffusion Impedance Nyquist plot');  

199 step1=10;  

200 step2=1000;  

201 index1=1:step1:70;  

202 index2=71:step2:241;  

203  

204 for i=1:length(index1)  

205 DFreq(i)=Kw(index1(i));  

206 labelreald(i)=Zdreal(index1(i));  

207 labelimagd(i)=Zdimag(index1(i));  

208 end  

209 for k=1:length(index2)  

210 DFreq(i+k)=Kw(index2(k));  

211 labelreald(i+k)=Zdreal(index2(k));  

212 labelimagd(i+k)=Zdimag(index2(k));  

213 end  

214 s = num2str(DFreq','%2.1e');  

215 labels = cellstr(s);  

216 text(labelreald,-labelimagd,labels,'FontSize',12,'Color','blue','  

    HorizontalAlignment','right');  

217 xlabel('Real part of Diffusion Impedance');  

218 ylabel('Imaginary part of Diffusion Impedance');  

219  

220 Zfreal=real(Zf);  

221 Zfimag=imag(Zf);  

222  

223 Zoreal=real(Zo);  

224 Zoimag=imag(Zo);  

225  

226 figure(2)

```

```

227 plot(Zfreal,-Zfimag,'-ks'); hold on; axis equal;
228 %legend('MatLab Data','Finite Film Thickness tanh(sqrt(j*K))/sqrt(j*K)');
229 title('Faradaic Impedance Nyquist plot');
230
231 figure(3)
232 plot(Zoreal,-Zoimag,'-ks'); hold on; axis equal;
233 %legend('MatLab Data','Finite Film Thickness tanh(sqrt(j*K))/sqrt(j*K)');
234 title('Overall Impedance Nyquist plot');
235
236
237 impedancef=zeros(nf,2);
238 impedancef(:,1)=Zfreal';
239 impedancef(:,2)=Zfimag';
240
241 impedanceo=zeros(nf,2);
242 impedanceo(:,1)=Zoreal';
243 impedanceo(:,2)=Zoimag';
244
245 impedanced=zeros(nf,2);
246 impedanced(:,1)=Zdreal';
247 impedanced(:,2)=Zdimag';
248
249 impedancedd_H2O2=zeros(nf,2);
250 impedancedd_H2O2(:,1)=real(Zdd_H2O2);
251 impedancedd_H2O2(:,2)=imag(Zdd_H2O2);
252
253 impedancedd_O2=zeros(nf,2);
254 impedancedd_O2(:,1)=real(Zdd_O2);
255 impedancedd_O2(:,2)=imag(Zdd_O2);
256
257 impedancedd_H=zeros(nf,2);
258 impedancedd_H(:,1)=real(Zdd_H);
259 impedancedd_H(:,2)=imag(Zdd_H);
260
261 impedanced_H2O2=zeros(nf,2);
262 impedanced_H2O2(:,1)=real(Zd_H2O2);
263 impedanced_H2O2(:,2)=imag(Zd_H2O2);
264
265 impedanced_O2=zeros(nf,2);
266 impedanced_O2(:,1)=real(Zd_O2);
267 impedanced_O2(:,2)=imag(Zd_O2);
268
269 impedanced_H=zeros(nf,2);
270 impedanced_H(:,1)=real(Zd_H);
271 impedanced_H(:,2)=imag(Zd_H);
272
273 figure(4)
274 plot(impedancedd_H2O2(:,1),-impedancedd_H2O2(:,2),'-ks'); hold on; axis equal;
275 title('Dimensionless Diffusion Impedance Nyquist plot of H2O2');
276
277 figure(5)
278 plot(impedancedd_O2(:,1),-impedancedd_O2(:,2),'-ks'); hold on; axis equal;
279 title('Dimensionless Diffusion Impedance Nyquist plot of O2');
280
281 figure(6)
282 plot(impedancedd_H(:,1),-impedancedd_H(:,2),'-ks'); hold on; axis equal;
283 title('Dimensionless Diffusion Impedance Nyquist plot of H ion');
284

```

```

285 figure(7)
286 plot(impedanced_H2O2(:,1),-impedanced_H2O2(:,2),'ks');hold on; axis equal;
287 title('Diffusion Impedance Nyquist plot of H2O2');
288
289 figure(8)
290 plot(impedanced_O2(:,1),-impedanced_O2(:,2),'ks');hold on; axis equal;
291 title('Diffusion Impedance Nyquist plot of O2');
292
293 figure(9)
294 plot(impedanced_H(:,1),-impedanced_H(:,2),'ks');hold on; axis equal;
295 title('Diffusion Impedance Nyquist plot of H ion');
296
297 % figure(23)
298 % plot(y,ci1_H2O2(:,1),'k'); hold on;
299 % plot(y,ci1_H2O2(:,2),'r'); hold on;
300 % plot(y,ci1_H2O2(:,3),'m'); hold on;
301 % plot(y,ci1_H2O2(:,4),'b'); hold on;
302 % title('Oscillating concentration of peroxide for K=100');
303 % legend('t1','t2','t3','t4');
304 %
305 % figure(24)
306 % plot(y,ci2_H2O2(:,1),'k'); hold on;
307 % plot(y,ci2_H2O2(:,2),'r'); hold on;
308 % plot(y,ci2_H2O2(:,3),'m'); hold on;
309 % plot(y,ci2_H2O2(:,4),'b'); hold on;
310 % title('Oscillating concentration of peroxide for K=1');
311 % legend('t1','t2','t3','t4');
312 %
313 % figure(25)
314 % plot(y,ci3_H2O2(:,1),'k'); hold on;
315 % plot(y,ci3_H2O2(:,2),'r'); hold on;
316 % plot(y,ci3_H2O2(:,3),'m'); hold on;
317 % plot(y,ci3_H2O2(:,4),'b'); hold on;
318 % title('Oscillating concentration of peroxide for K=0.01');
319 % legend('t1','t2','t3','t4');
320 %
321 % figure(26)
322 % plot(y,ci1_O2(:,1),'k'); hold on;
323 % plot(y,ci1_O2(:,2),'r'); hold on;
324 % plot(y,ci1_O2(:,3),'m'); hold on;
325 % plot(y,ci1_O2(:,4),'b'); hold on;
326 % title('Oscillating concentration of oxygen for K=100');
327 % legend('t1','t2','t2','t2');
328 %
329 % figure(27)
330 % plot(y,ci2_O2(:,1),'k'); hold on;
331 % plot(y,ci2_O2(:,2),'r'); hold on;
332 % plot(y,ci2_O2(:,3),'m'); hold on;
333 % plot(y,ci2_O2(:,4),'b'); hold on;
334 % title('Oscillating concentration of oxygen for K=1');
335 % legend('t1','t2','t2','t2');
336 %
337 % figure(28)
338 % plot(y,ci3_O2(:,1),'k'); hold on;
339 % plot(y,ci3_O2(:,2),'r'); hold on;
340 % plot(y,ci3_O2(:,3),'m'); hold on;
341 % plot(y,ci3_O2(:,4),'b'); hold on;
342 % title('Oscillating concentration of oxygen for K=0.01');

```

```

343 % legend ('t1 ','t2 ','t2 ','t2 ');
344
345 F_Hreal=real(F_H);
346 F_Himag=imag(F_H);
347 F_H2O2real=real(F_H2O2);
348 F_H2O2imag=imag(F_H2O2);
349 F_O2real=real(F_O2);
350 F_O2imag=imag(F_O2);
351 F_Hreal=F_Hreal';
352 F_H2O2real=F_H2O2real';
353 F_O2real=F_O2real';
354 F_H2O2imag=F_H2O2imag';
355 F_O2imag=F_O2imag';
356 F_Himag=F_Himag';
357
358 Zfreal=real(Zf);
359 Zfimag=imag(Zf);
360 Zfreal=Zfreal';
361 Zfimag=Zfimag';
362
363 DCH2O2REAL=real(DCH2O2);
364 DCH2O2imag=imag(DCH2O2);
365 DCH2O2REAL=DCH2O2REAL';
366 DCH2O2imag=DCH2O2imag';
367
368 DCO2REAL=real(DCO2);
369 DCO2imag=imag(DCO2);
370 DCO2REAL=DCO2REAL';
371 DCO2imag=DCO2imag';
372
373 DCHREAL=real(DCH);
374 DCHimag=imag(DCH);
375 DCHREAL=DCHREAL';
376 DCHimag=DCHimag';
377
378 % figure(31)
379 % plot(DCH2O2REAL(:,1),-DCH2O2imag(:,1),'-ks');hold on; axis equal;
380 % figure(32)
381 % plot(DCO2REAL(:,1),-DCO2imag(:,1),'-ks');hold on; axis equal;
382 % figure(33)
383 % plot(DCHREAL(:,1),-DCHimag(:,1),'-ks');hold on; axis equal;n; axis equal;
384 figure(10)
385 plot(Zoreal(1,57:241),-Zoimag(1,57:241),'-ks');hold on; axis equal;
386 title('Overall Impedance Nyquist plot from 1mHz to 100kHz');

```

APPENDIX B MATLAB® GRAPHICAL USER INTERFACE

A graphical user interface was written in Matlab® with Fortran executables. The program contains the three major models (Basic model without buffer, model with PBS buffer and model with BBS buffer) with featured reactions as optional choice. The program grants the users to design input parameters, run the simulations, generate visual figures and save out results for further analysis. The simulations include polarization curve, steady-state profiles, impedance response and oxygen curve.

B.1 Main Console

The program is delivered in .zip file. To start, un-zip the file and run the file named CGM_GUI.m. It shows the main console, as shown in Figure B-1. On the main console, there are three tabs corresponding to the three major models for continuous glucose sensor. **Basic Model** is the mathematical model for continuous glucose sensor without any buffer, which is introduced in Chapter 3. **Model with PBS Buffer** is the mathematical model for continuous glucose sensor in phosphate buffer saline, which is introduced in Chapter 4. **Model with BBS Buffer** is the mathematical model for continuous glucose sensor in bicarbonate buffer saline, which is introduced in Chapter 5.

The tab **[?]** opens a pdf file for a brief introduction of the homogeneous reactions, heterogeneous reactions and the current density considered in the model. An example of the brief guide of the program is shown in Figure B-2.

After clicking the tab of the model, for example **[Model with BBS Buffer]**, the interface changes to Figure B-3. Each model contains three sub models, Base Model, Effective Diffusion Model and Hydrogen Evolution Model. In the Base Model, the diffusion coefficients of species in the GOx and GLM layers are modified by the porosity factor of the biofilm based on Bruggeman Equation. The porosity factors are set and different for large species, such as glucose, and small species such as oxygen. It doesn't have the capability to study the diffusion coefficients separately. This was improved in

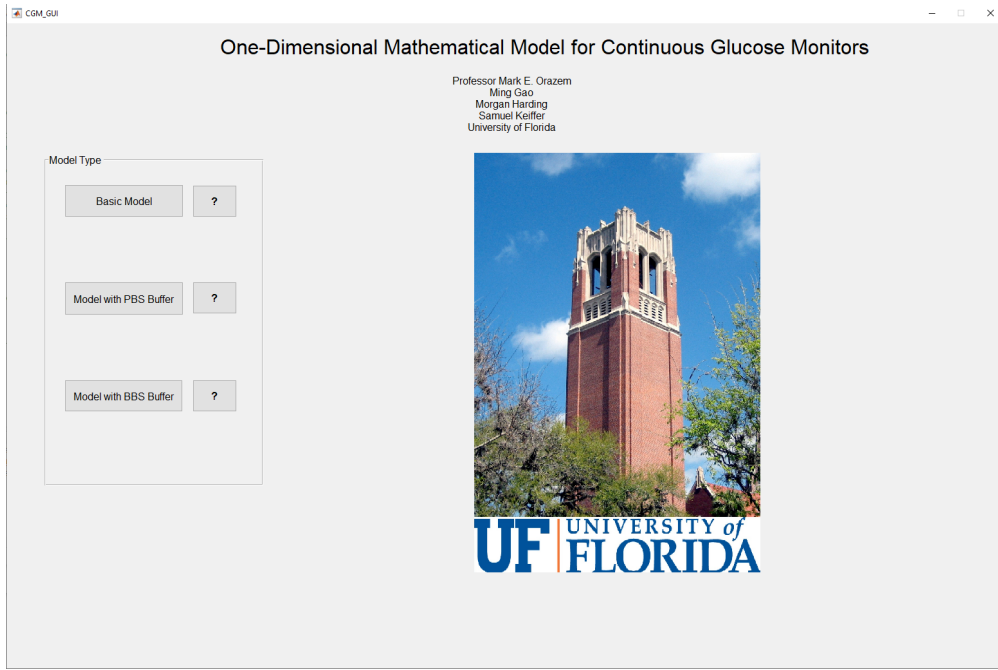


Figure B-1. The initial program layout of the graphical user interface in Matlab®. The three tabs on the left-hand side are corresponding to the three models for continuous glucose sensors.

Effective Diffusion Model, in which the diffusion coefficients of each species in various layers are all input parameters. The hydrogen evolution reaction only contributes to the cathodic current at low applied potentials. Therefore, it is an optional feature, which is included in Hydrogen Evolution Model.

B.2 Sub Console for the Specific Model

For the programs of different models, the layouts are similar. An example of the sub console for the Model with BBS Buffer is shown in Figure B-4.

B.2.1 Control Panel

The control panel of the program is on the left-hand side of the program, as shown in Figure B-4. It allows the users to choose to change the input parameters by Change Input Parameters, recover all the input parameters to the default values by Recover Input Parameters and run various simulations by Run Polarization curve, Run Steady-State Simulation, Run Impedance Simulation and Run Oxygen Curve.

Homogeneous Reactions

$$\beta\text{-D-glucose} + \text{GOx}_{\text{OX}} \xrightleftharpoons[k_{b1}]{k_{f1}} \text{GOx-GA} \xrightarrow{k_{l2}} \text{GA} + \text{GOx}_{\text{RED}} \quad (1)$$

$$\text{GOx}_{\text{RED}} + \text{O}_2 \xrightleftharpoons[k_{b3}]{k_{f3}} \text{GOx-H}_2\text{O}_2 \xrightarrow{k_{f4}} \text{GOx}_{\text{OX}} + \text{H}_2\text{O}_2 \quad (2)$$

$$\alpha\text{-D-glucose} \xrightleftharpoons[k_{b5}]{k_{f5}} \beta\text{-D-glucose} \quad (3)$$

$$\text{H}_2\text{O} \xrightleftharpoons[k_{b6}]{k_{f6}} \text{H}^+ + \text{OH}^- \quad (4)$$

$$\text{GA} \xrightleftharpoons[k_{b7}]{k_{f7}} \text{H}^+ + \text{GA}^- \quad (5)$$

$$\text{H}^+ \text{GOx}_{\text{OX}} \xrightleftharpoons[k_{b8}]{k_{f8}} \text{H}^+ + \text{GOx}_{\text{OX}} \quad (6)$$

$$\text{GOx}_{\text{RED}} \xrightleftharpoons[k_{b9}]{k_{f9}} \text{H}^+ + \text{GOx}_{\text{RED}}^- \quad (7)$$

Heterogeneous Reactions

$$\text{H}_2\text{O}_2 \xrightleftharpoons[K_{\text{O}_2}]{K_{\text{H}_2\text{O}_2}} 2\text{H}^+ + \text{O}_2 + 2\text{e}^- \quad (8)$$

$$\text{H}_2\text{O}_2 + 2\text{H}^+ + 2\text{e}^- \xrightarrow{K_{\text{red}}} 2\text{H}_2\text{O} \quad (9)$$

Therefore, the corresponding total faradaic current for all the heterogeneous reactions included was expressed as

$$i_F = K_{\text{H}_2\text{O}_2} c_{\text{H}_2\text{O}_2}(0) \exp(b_{\text{H}_2\text{O}_2} V) - K_{\text{O}_2} c_{\text{O}_2}(0) \exp(-b_{\text{O}_2} V) - K_{\text{red}} c_{\text{H}_2\text{O}_2}(0) \exp(-b_{\text{red}} V) \quad (10)$$

where $K_{\text{H}_2\text{O}_2}$, K_{O_2} and K_{red} are the effective heterogeneous rate constants.

Figure B-2. An example of the brief guide of the Basic Model opened by the tab [?].

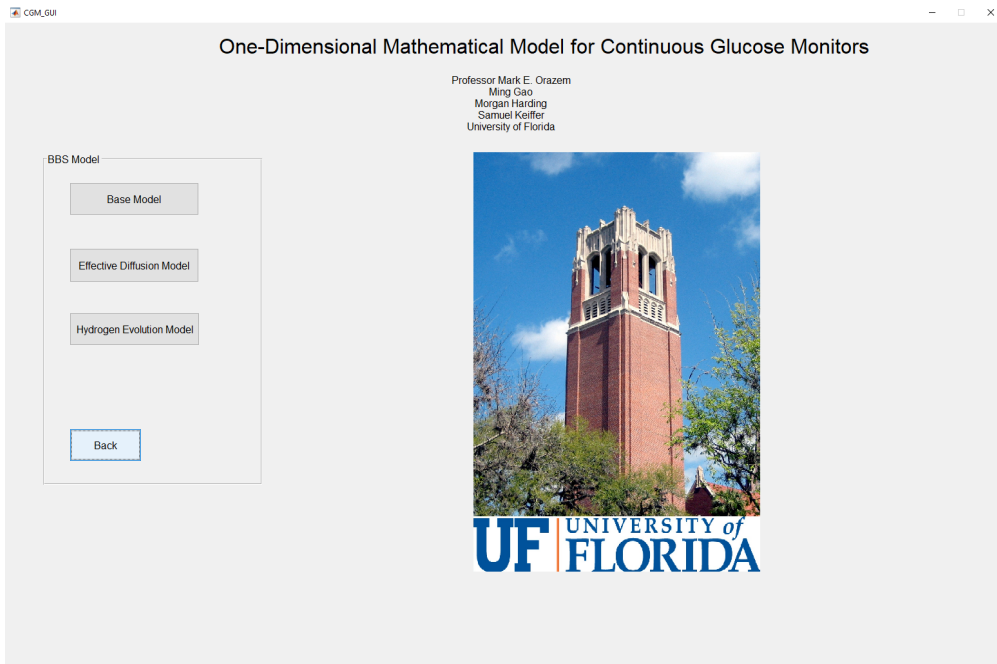


Figure B-3. The layout of the program after clicking the tab **Model with BBS Buffer** on the main console. Each model contains three sub models, **Base Model**, **Effective Diffusion Model** and **Hydrogen Evolution Model**.

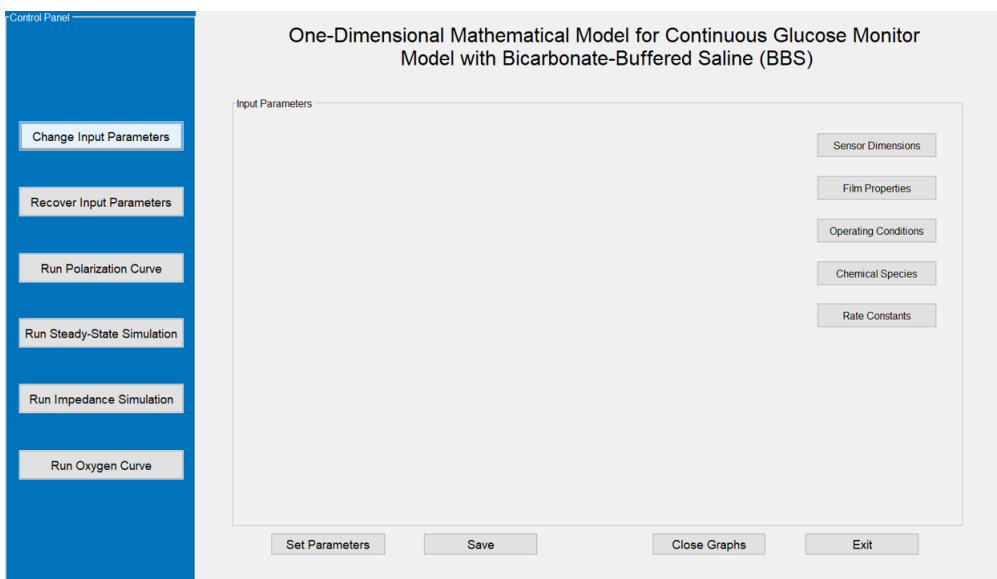


Figure B-4. The program layout for a specific model.

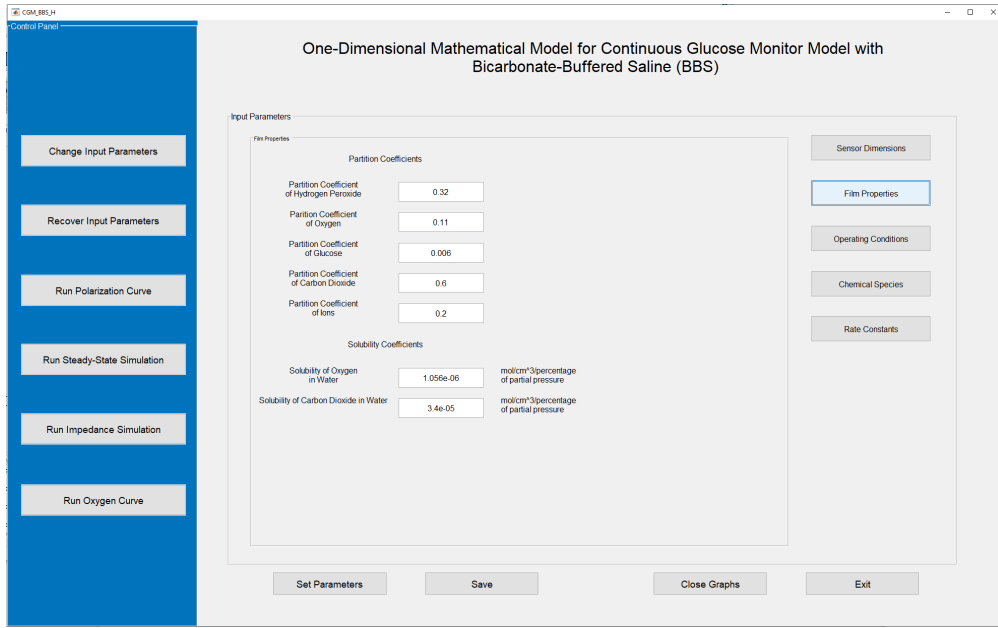


Figure B-5. The program layout of changing input parameters.

B.2.2 Input Parameters

The input parameters are very essential to the simulations. The physical meaning of the parameters are introduced in Section 7.1. In the program, the parameters are characterized into five tabs, **Sensor Dimensions**, **Film Properties**, **Operation Conditions**, **Chemical Species** and **Rate Constants**. An example is shown in Figure B-5. After changing the input values of the parameters, it is necessary to click the tab **Set Parameters** on the bottom to load the changes to the program.

B.2.3 Other Functions

The tabs on the bottom of Figure B-5 provides other functions. **Save** allows the users to save out the current simulation results to a directory in the computer. The file is auto-named by types of simulation, date and time. **Close Graphs** closes all the generated figures. **Exit** closes the current sub console and goes to the main console of the program.

REFERENCES

- [1] M. Gao, M. S. Hazelbaker, R. Kong, M. E. Orazem, Mathematical model for the electrochemical impedance response of a continuous glucose monitor, *Electrochimica Acta* 275 (2018) 119–132.
- [2] G. Roglic, et al., Who global report on diabetes: A summary, *International Journal of Noncommunicable Diseases* 1 (1) (2016) 3.
- [3] L. C. Clark, C. Lyons, Electrode systems for continuous monitoring in cardiovascular surgery, *Annals of the New York Academy of sciences* 102 (1) (1962) 29–45.
- [4] S. Updike, G. Hicks, The enzyme electrode, *Nature* 214 (5092) (1967) 986–988.
- [5] G. Guilbault, G. Lubrano, An enzyme electrode for the amperometric determination of glucose, *Analytica Chimica Acta* 64 (3) (1973) 439–455.
- [6] A. E. Cass, G. Davis, G. D. Francis, H. A. O. Hill, W. J. Aston, I. J. Higgins, E. V. Plotkin, L. D. Scott, A. P. Turner, Ferrocene-mediated enzyme electrode for amperometric determination of glucose, *Analytical chemistry* 56 (4) (1984) 667–671.
- [7] J. E. Frew, H. A. O. Hill, Electrochemical biosensors, *Analytical chemistry* 59 (15) (1987) 933A–944A.
- [8] M. Shichiri, Y. Yamasaki, R. Kawamori, N. Hakui, H. Abe, Wearable artificial endocrine pancreas with needle-type glucose sensor, *The Lancet* 320 (8308) (1982) 1129–1131.
- [9] Y. Degani, A. Heller, Direct electrical communication between chemically modified enzymes and metal electrodes. i. electron transfer from glucose oxidase to metal electrodes via electron relays, bound covalently to the enzyme, *The Journal of Physical Chemistry* 91 (6) (1987) 1285–1289.
- [10] P. Das, M. Das, S. R. Chinnadayyala, I. M. Singha, P. Goswami, Recent advances on developing 3rd generation enzyme electrode for biosensor applications, *Biosensors and Bioelectronics* 79 (2016) 386 – 397.
- [11] S. Demin, E. A. Hall, Breaking the barrier to fast electron transfer, *Bioelectrochemistry* 76 (1) (2009) 19 – 27, advanced design of electron-transfer pathways across biomolecular interfaces, Dedicated to Professor Lo Gorton.
- [12] O. Courjean, F. Gao, N. Mano, Deglycosylation of glucose oxidase for direct and efficient glucose electrooxidation on a glassy carbon electrode, *Angewandte Chemie* 121 (32) (2009) 6011–6013.
- [13] W. Grosse, J. Champavert, S. Gambhir, G. G. Wallace, S. E. Moulton, Aqueous dispersions of reduced graphene oxide and multi wall carbon nanotubes for enhanced glucose oxidase bioelectrode performance, *Carbon* 61 (2013) 467 – 475.

- [14] G. S. Wilson, Native glucose oxidase does not undergo direct electron transfer, *Biosensors and Bioelectronics* 82 (2016) vii – viii.
- [15] P. N. Bartlett, F. A. Al-Lolage, There is no evidence to support literature claims of direct electron transfer (det) for native glucose oxidase (gox) at carbon nanotubes or graphene, *Journal of Electroanalytical Chemistry*.
- [16] E.-H. Yoo, S.-Y. Lee, Glucose biosensors: An overview of use in clinical practice, *Sensors* 10 (5) (2010) 4558–4576.
- [17] D. Müller, Studies on the new enzyme glucoseoxidase, *Biochem. Z* 199 (236).
- [18] Q. H. Gibson, B. E. P. Swoboda, V. Massey, Kinetics and mechanism of action of glucose oxidase, *The Journal of Biological Chemistry* 239 (11) (1964) 3927.
- [19] C. R. Bertozzi, D. Rabuka, Structural basis of glycan diversity (2009).
- [20] T. Nakamura, Y. Ogura, Kinetic studies on the action of glucose oxidase, *The Journal of Biochemistry* 52 (3) (1962) 214.
- [21] H. Bright, Q. Gibson, The oxidation of 1-deuterated glucose by glucose oxidase, *The Journal of Biological Chemistry* 242 (5) (1967) 994–1003.
- [22] H. J. Bright, M. Appleby, The ph dependence of the individual steps in the glucose oxidase reaction, *The Journal of Biological Chemistry* 244 (13) (1969) 3625–3634.
- [23] R. Wilson, A. Turner, Glucose oxidase: An ideal enzyme, *Biosensors and Bioelectronics* 7 (3) (1992) 165 – 185.
- [24] P. Bartlett, R. Whitaker, Electrochemical immobilisation of enzymes: Part i. theory, *Journal of Electroanalytical Chemistry and Interfacial Electrochemistry* 224 (1) (1987) 27 – 35.
- [25] W. Albery, P. N. Bartlett, B. J. Driscoll, R. Lennox, Amperometric enzyme electrodes: Part 5. the homogeneous mediated mechanism, *Journal of Electroanalytical Chemistry* 323 (1) (1992) 77 – 102, an International Journal Devoted to all Aspects of Electrode Kinetics, Interfacial Structure, Properties of Electrolytes, Colloid and Biological Electrochemistry.
- [26] P. Bartlett, K. Pratt, Modelling of processes in enzyme electrodes, *Biosensors and Bioelectronics* 8 (9) (1993) 451 – 462.
- [27] J. Galceran, S. Taylor, P. Bartlett, Modelling the steady-state current at the inlaid disc microelectrode for homogeneous mediated enzyme catalysed reactions, *Journal of Electroanalytical Chemistry* 506 (2) (2001) 65 – 81.
- [28] J. W. Parker, C. S. Schwartz, Modeling the kinetics of immobilized glucose oxidase, *Biotechnology and Bioengineering* 30 (6) (1987) 724–735.

- [29] J. J. Gooding, E. A. H. Hall, Parameters in the design of oxygen detecting oxidase enzyme electrodes, *Electroanalysis* 8 (5) (1996) 407–413.
- [30] L. Michaelis, M. L. Menten, Die kinetik der invertinwirkung, Universitätsbibliothek Johann Christian Senckenberg, 2007.
- [31] G. E. Briggs, J. B. S. Haldane, A note on the kinetics of enzyme action, *Biochemical journal* 19 (2) (1925) 338.
- [32] L. D. Mell, J. Maloy, Model for the amperometric enzyme electrode obtained through digital simulation and applied to the immobilized glucose oxidase system, *Analytical Chemistry* 47 (2) (1975) 299–307.
- [33] J. K. Leypoldt, D. A. Gough, Model of a two-substrate enzyme electrode for glucose, *Analytical Chemistry* 56 (14) (1984) 2896–2904, pMID: 6524662. [arXiv:
<https://doi.org/10.1021/ac00278a063>](https://doi.org/10.1021/ac00278a063)
- [34] D. A. Gough, J. Y. Lucisano, P. H. S. Tse, Two-dimensional enzyme electrode sensor for glucose, *Analytical Chemistry* 57 (12) (1985) 2351–2357, pMID: 4061843. [arXiv:
<https://doi.org/10.1021/ac00289a042>](https://doi.org/10.1021/ac00289a042)
- [35] M. Abdekhodaie, X. Wu, Modeling of a cationic glucose-sensitive membrane with consideration of oxygen limitation, *Journal of membrane science* 254 (1-2) (2005) 119–127.
- [36] A. M. Albisser, B. S. Leibel, T. G. Ewart, Z. Davidovac, C. K. Botz, W. Zingg, H. Schipper, R. Gander, Clinical control of diabetes by the artificial pancreas, *Diabetes* 23 (5) (1974) 397–404. [arXiv:
\[http://diabetes.diabetesjournals.org/
content/23/5/397.full.pdf\]\(http://diabetes.diabetesjournals.org/content/23/5/397.full.pdf\)](http://diabetes.diabetesjournals.org/content/23/5/397.full.pdf)
- [37] M. Shichiri, Y. Yamasaki, R. Kawamori, N. Hakui, H. Abe, Wearable artificial endocrine pancreas with needle-type glucose sensor, *The Lancet* 320 (8308) (1982) 1129 – 1131, originally published as Volume 2, Issue 8308.
- [38] U. Hoss, E. S. Budiman, H. Liu, M. P. Christiansen, Continuous glucose monitoring in the subcutaneous tissue over a 14-day sensor wear period, *Journal of Diabetes Science and Technology* 7 (5) (2013) 1210–1219.
- [39] J. J. Chamberlain, D. Small, Case study: Successful use of a single subcutaneous continuous glucose monitor sensor for 28 days in a patient with type 1 diabetes, *Clin. Diabetes* 26 (2008) 138–139.
- [40] C. Zhao, Y. Fu, Statistical analysis based online sensor failure detection for continuous glucose monitoring in type i diabetes, *Chemometrics and Intelligent Laboratory Systems* 144 (2015) 128 – 137.
- [41] U. Klueh, J. Frailey, Y. Qiao, O. Antar, D. L. Kreutzer, Cell based metabolic barriers to glucose diffusion: Macrophages and continuous glucose monitoring, *Biomaterials* 35 (2014) 3145–3153.

- [42] M. T. Novak, F. Yuan, W. M. Reichert, Modeling the relative impact of capsular tissue effects on implanted glucose sensor time lag and signal attenuation, *Anal. Bioanal. Chem.* 398 (2010) 1695–1705.
- [43] E. Katz, I. Willner, Probing biomolecular interactions at conductive and semiconductive surfaces by impedance spectroscopy: Routes to impedimetric immunosensors, dna-sensors, and enzyme biosensors. *Electroanalysis, Electroanalisis* 15 (11) (2003) 913–947.
- [44] K. J. Otto, M. D. Johnson, D. R. Kipke, Voltage pulses change neural interface properties and improve unit recordings with chronically implanted microelectrodes, *IEEE Transactions on Biomedical Engineering* 53 (2) (2006) 333–340.
- [45] V. Sankar, E. Patrick, R. Dieme, J. C. Sanchez, A. Prasad, T. Nishida, Electrode impedance analysis of chronic tungsten microwire neural implants: understanding abiotic vs. biotic contributions, *Frontiers in Neuroengineering* 7 (13) (2014) 1.
- [46] P. Agarwal, M. E. Orazem, L. H. García-Rubio, Measurement models for electrochemical impedance spectroscopy: 1. Demonstration of applicability, *Journal of the Electrochemical Society* 139 (1992) 1917–1927.
- [47] P. Agarwal, O. D. Crisalle, M. E. Orazem, L. H. García-Rubio, Measurement models for electrochemical impedance spectroscopy: 2. Determination of the stochastic contribution to the error structure, *Journal of the Electrochemical Society* 142 (1995) 4149–4158.
- [48] P. Agarwal, M. E. Orazem, L. H. García-Rubio, Measurement models for electrochemical impedance spectroscopy: 3. Evaluation of consistency with the kramers-kronig relations, *Journal of the Electrochemical Society* 142 (1995) 4159–4168.
- [49] M. E. Orazem, B. Tribollet, *Electrochemical Impedance Spectroscopy*, 2nd Edition, John Wiley & Sons, Hoboken, 2017.
- [50] J. S. Newman, Numerical solution of coupled, ordinary differential equations, *Industrial and Engineering Chemistry Fundamentals* 7 (3) (1968) 514–517.
- [51] M. T. T. Tran, B. Tribollet, V. Vivier, M. E. Orazem, On the impedance response of reactions influenced by mass transfer, *Russian Journal of Electrochemistry* (2017) in press.
- [52] J. S. Newman, K. E. Thomas-Alyea, *Electrochemical Systems*, 3rd Edition, John Wiley & Sons, Hoboken, 2004.
- [53] W. Watson, M. Orazem, A python-based measurement model toolbox for impedance spectroscopy, Tech. rep., Tech. rep., University of Florida (2020).

- [54] M. E. Orazem, B. Tribollet, Problem Solving in Electrochemical Impedance Spectroscopy: Methods, Data Analysis and Case Studies, WILEY, in preparation, 2023.
- [55] R. Baronas, F. Ivanauskas, J. Kulys, Mathematical modeling of biosensors: an introduction for chemists and mathematicians, Vol. 9, Springer Science & Business Media, 2009.
- [56] M. K. Weibel, H. J. Bright, Insolubilized enzymes. kinetic behaviour of glucose oxidase bound to porous glass particles, *Biochemical Journal* 124 (4) (1971) 801–807.
- [57] F. R. Duke, M. Weibel, D. Page, V. Bulgrin, J. Luthy, Glucose oxidase mechanism. enzyme activation by substrate, *Journal of the American Chemical Society* 91 (14) (1969) 3904–3909.
- [58] B. Atkinson, D. Lester, An enzyme rate equation for the overall rate of reaction of gel-immobilized glucose oxidase particles under buffered conditions. i. pseudo-one substrate conditions, *Biotechnology and Bioengineering* 16 (10) (1974) 1299–1320.
- [59] B. Atkinson, D. Lester, An enzyme rate equation for the overall rate of reaction of gel-immobilized glucose oxidase particles under buffered conditions. ii. two limiting substrates, *Biotechnology and bioengineering* 16 (10) (1974) 1321–1343.
- [60] A. Gómez-Marín, K. Schouten, M. Koper, J. Feliu, Interaction of hydrogen peroxide with a pt (111) electrode, *Electrochemistry communications* 22 (2012) 153–156.
- [61] J. Wang, N. Markovic, R. Adzic, Kinetic analysis of oxygen reduction on pt (111) in acid solutions: intrinsic kinetic parameters and anion adsorption effects, *The Journal of Physical Chemistry B* 108 (13) (2004) 4127–4133.
- [62] E. Skúlason, V. Tripkovic, M. E. Björketun, S. Guðmundsdóttir, G. Karlberg, J. Rossmeisl, T. Bligaard, H. Jónsson, J. K. Nørskov, Modeling the electrochemical hydrogen oxidation and evolution reactions on the basis of density functional theory calculations, *The Journal of Physical Chemistry C* 114 (42) (2010) 18182–18197.
- [63] N. Marković, B. Grgur, P. N. Ross, Temperature-dependent hydrogen electrochemistry on platinum low-index single-crystal surfaces in acid solutions, *The Journal of Physical Chemistry B* 101 (27) (1997) 5405–5413.
- [64] J. Newman, Numerical solution of coupled, ordinary differential equations, *Industrial & Engineering Chemistry Fundamentals* 7 (3) (1968) 514–517.
- [65] D. A. G. Bruggeman, Berechnung verschiedener physikalischer konstanten von heterogenen substanzen. i. dielektrizitätskonstanten und leitfähigkeiten der mischkörper aus isotropen substanzen, *Annals of Physics* 416 (1935) 636–664.
- [66] J. H. Sluyters, On the impedance of galvanic cells I. theory, *Recueil des Travaux Chimiques des Pays-Bas Journal of the Royal Netherlands Chemical Society* 79 (1960) 1092–1100.

- [67] P. Delahay, Electrode processes without a priori separation of double-layer charging, *Journal of Physical Chemistry* 70 (7) (1966) 2373–2379.
- [68] P. Delahay, G. G. Susbielle, Double-layer impedance of electrodes with charge-transfer reaction, *Journal of Physical Chemistry* 70 (10) (1966) 3150–3157.
- [69] P. Delahay, K. Holub, G. G. Susbielle, G. Tessari, Double-layer perturbation without equilibrium between concentrations and potential, *Journal of Physical Chemistry* 71 (3) (1967) 779–780.
- [70] K. Nisancioglu, J. S. Newman, Separation of double-layer charging and faradaic processes at electrodes, *Journal of the Electrochemical Society* 159 (2012) E59–E61.
- [71] S.-L. Wu, M. E. Orazem, B. Tribollet, V. Vivier, The influence of coupled faradaic and charging currents on impedance spectroscopy, *Electrochimica Acta* 131 (2014) 3–12.
- [72] M. Harding, Mathematical models for impedance spectroscopy, Ph.D. thesis, University of Florida, Gainesville, FL (2017).

BIOGRAPHICAL SKETCH

Ming Gao received her B.S. degree in chemistry from Nanjing University (Nanjing, China) in 2014 and her Master of Science degree in chemistry from the University of Florida in 2016. She is a PhD candidate in Professor Mark Orazem's group studying the modeling of electrochemical impedance spectroscopy problems. Ms. Gao is a member of the International Society of Electrochemistry (ISE) and the Electrochemistry Society (ECS). She served as Academic Chair of the Graduate Association of Chemical Engineers (GRACE), Vice President of Electrochemical Society Student Chapter, and Chemical Engineering departmental representative to the Engineering Graduate Student Council (EGSC) at the University of Florida. Ms. Gao also served as the safety manager for the Orazem group and served as the group representative to the Chemical Engineering Student Safety Council.